The role of ms1 in cardiac physiology and disease

Thesis submitted for the degree of

Doctor of Philosophy

at the University of Leicester

by

Andrea Louise Koekemoer

Department of Cardiovascular Sciences

University of Leicester

March 2008

ProQuest LLC
789 East Eisenhower Parkway
P.O. Box 1346
Ann Arbor, MI 48106-1346

Acknowledgements

I would like to thank my supervisors Professor Nilesh Samani and Dr Nelson Chong for giving me the opportunity to undertake a Ph.D. in Cardiology. Their advice, guidance and encouragement throughout the duration of this project have been greatly appreciated.

Many thanks to Dr Catrin Pritchard and Sarah Munson of the Biochemistry Department for their guidance and expertise in mouse genetics and transgenics.

Thanks to all the staff of the Biomedical Services Division, especially to Jane Brown, Anthony Oakden, Lin Scrimshire, Ken White and Aimee Craighead who have been a great help.

Thanks to Professor Alison Goodall and Tina James for their help and expertise in flow cytometry.

I would like to thank the members of staff and students of the Division of Cardiology, Division of Cardiac Surgery, Department of Biochemistry and Department of Respiratory Medicine for the useful help, advice and friendship over the years.

I would also like to thank the Thomas Herbert Wathes Centenary Scholarship and the British Heart Foundation for funding my Ph.D. studentship.

Many thanks to Mum, Dad and Paul for all their love, support and encouragement throughout my studies.

Finally, sincere thanks to my husband Gerrit for his love, patience, support and influence throughout the last few years.

AL Koekemoer
University of Leicester

The role of msl in cardiac physiology and disease

Abstract

Left ventricular hypertrophy (LVH) is an adaptive response to increased workload, stress or injury. Initially this adaptation is beneficial but sustained hypertrophy is a predisposing risk factor for cardiac morbidity and death. Many signalling pathways regulate hypertrophy but the molecular controllers that sense pressure overload and initiate hypertrophy are unclear.

Previous work in the group identified a novel gene, designated myocyte stress 1 (msl), which is up-regulated within 1 hour in the left ventricle following aortic banding in the rat, suggesting a possible role for msl in the initial signalling of the hypertrophic response. msl is also expressed during cardiac development and is transiently up-regulated during ischaemia-reperfusion *in vitro*. This suggests that msl may play a more widespread role in cardiac physiology.

The aim of the work in this thesis was to better understand the role of msl in cardiac physiology and disease through a combination of *in vitro* and *in vivo* approaches. It was demonstrated that transient over-expression of a c-Myc-msl fusion protein into a heart-derived rat cell line, H9c2, colocalised with actin and altered expression of known hypertrophic and cardioprotective target genes of the myocardin-related transcription factor (MRTF)/serum response factor (SRF) transcriptional pathway. The size of cells over-expressing msl significantly increased by 47% compared to untransfected cells and over-expression of msl markedly inhibited staurosporine-induced apoptosis by 88%. A Cre/*loxP* system based construct was developed to assess the *in vivo* effects of increased msl expression and was confirmed to work in a cell-based system. However, two independent attempts to make a transgenic mouse over-expressing msl were unsuccessful despite successful integration of the transgene.

Overall the findings suggest that msl induces a hypertrophic response and provides cardioprotection via a MRTF-SRF signalling mechanism. The findings provide for the first time direct evidence of the involvement of msl in hypertrophy and cardioprotection.

Contents

Abbreviations

ABLIM	actin-binding LIM
α-MHC	α-myosin heavy chain
ANP	atrial natriuetic peptide
AMPK	adenosine monophosphate-activated protein kinase
AR	adrenergic receptor
ARC	apoptosis repressor with caspase recruitment domain
AT	angiotensin II receptor
A-V	atrioventricular
β-MHC	β-myosin heavy chain
BNP	brain natriuretic peptide
BSA	bovine serum albumin
cDNA	complementary deoxyribonucleic acid
CMV	cytomegalo virus
Ct	threshold cycle
dH_2O	distilled water
DMSO	dimethyl sulfoxide
DNA	deoxyribonucleic acid
DNase I	deoxyribonuclease I
dNTP	deoxyribonucleotide 5' triphosphate
DTT	dithiothreitol
E	embryonic day
ECL	enhanced chemiluminescence
EDTA	Ethylenediaminetetraacetic acid
EGF	epidermal growth factor
EGFP	enhanced green fluorescent protein
ERKs	extracellular regulated kinases
ES	embryonic stem
Et	endothelin receptor
FISH	fluorescence in situ hybridisation
FITC	fluorescein isothiocyanate
Fra-1	fos-related antigen-1
GFP	green fluorescent protein

gp130	glycoprotein 130
GPCRs	G protein-coupled receptors
GSK-3β	glycogen synthase-3β
HATs	histone acetyltransferases
HBSS	Hanks' balanced salt solution
HDACs	histone deacetylases
hpf	hours post fertilisation
HRP	horseradish peroxidase
IGF1	insulin-like growth factor 1
IL-2	interleukin 2
IL-6	interleukin 6
IMS	industrial methylated spirit
IRES	internal ribosome entry site
JAK-STAT	janus kinase-signal transducer and activator of transcription
JNKs	C-Jun N-terminal kinases
LA	left atrium
LB	luria broth
LIF	leukemia inhibitory factor
LPA	lysophosphatidic acid
LV	left ventricle
LVH	left ventricular hypertrophy
MADS	Mcm 1 and Arg80 in yeast, Agamous and Deficiens in plants, and SRF in animals
MAP	mitogen-activated protein
MAPK	mitogen-activated protein kinase
MAPKs	mitogen-activated protein kinases
MAPKKs	mitogen-activated protein kinase kinases
MAPKKKs	mitogen-activated protein kinase kinase kinases
MEF2	myocyte enhancer factor 2
MEF2C	myocyte enhancer factor 2C
MI	myocardial infarction
MKP-1	MAPK phosphatase-1
MLC2a	myosin light chain 2 atrial
MLC2v	myosin light chain 2 ventricular

mRNA	messenger ribonucleic acid
MRTFs	myocardin-related transcription factors
msl	myocyte stress 1
NFAT	nuclear factor of activated T cells
PARP	poly(ADP-ribose) polymerase
PBS	phosphate buffered saline
PCR	polymerase chain reaction
PDK1	phosphatidylinositol 3,4,5-trisphosphate-dependent protein kinase
PEG	polyethylene glycol
PI3K	phosphoinositide 3-OH kinase
$p70^{s6k}$	p70 ribosomal s6 kinase
Ptd $InsP_3$	phosphatidylinositol 3,4,5-trisphosphate
RA	right atrium
RM1	rat and mouse no. 1 maintenance
RNA	ribonucleic acid
ROCK	rho-associated kinase
RPL32	ribosomal protein L32
RT	reverse transcription
RTKs	receptor tyrosine kinases
RT-PCR	reverse transcription polymerase chain reaction
RV	right ventricle
S-A	sinoatrial
SAPKs	stress-activated protein kinases
SEM	standard error of mean
SD	standard deviation
SDS	sodium dodecyl sulphate
SiRNA	small interfering RNA
SRF	serum response factor
SSC	sodium saturated citrate
STARS	striated muscle activator of rho signalling
TAE	tris-acetate ethylenediaminetetraacetic acid
TBP	tata-binding protein
TCF	ternary complex factor
TPA	12-*O*-tetradecanoly-phorbol-13-acetate

TSS	transcriptional start site
TUNEL	terminal deoxynucleotidyl transferase biotin-dUTP nick end labelling

Chapter 1

Introduction

1.1 Development of the vertebrate heart

The first organ to form in the embryo is the heart (Olson, 2004; Olson and Schneider, 2003). In response to an axial signalling system, differentiated cardiac myocytes become organised into a linear heart tube that undergoes rightward looping and forms asymmetry across the left-right axis of the embryo (Kelly and Buckingham, 2002; Olson, 2004). Growth of the looped heart tube and septation forms the multichambered heart (Olson, 2004). This is shown in figure 1.1. In order for blood to be delivered to and from the lungs and body, the right (pulmonary) and left (systemic) ventricular and atrial chambers of the heart are separated by an interventricular and interatrial septum. The sinoatrial node (pacemaker) controls each heart beat and a synchronised round of cardiac contraction and relaxation. The cardiac conduction system and direct cell-cell coupling of cardiac myocytes propagates electrical impulses through the heart (Olson, 2004).

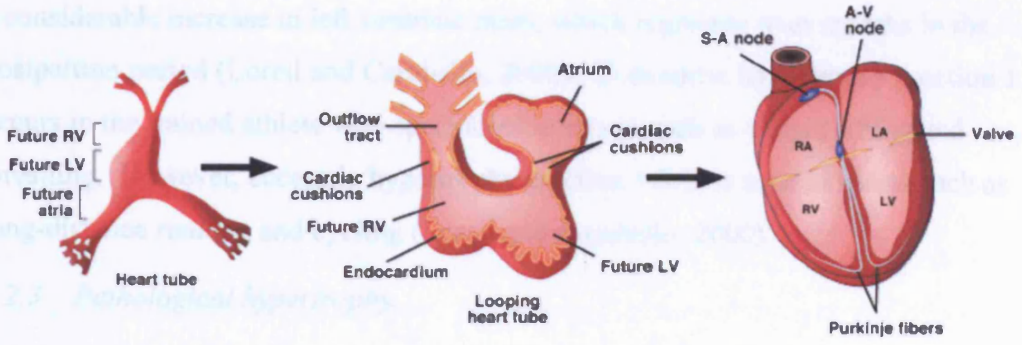

Figure 1.1. Heart development (Olson, 2004).

Progenitors of the cardiogenic mesoderm form the linear heart tube and ultimately the four chambers of the heart. The cardiac conduction system components within the multichambered heart are shown. A-V, atrioventricular; LA, Left atrium; LV, Left ventricle; RA, Right atrium; RV, Right ventricle; S-A, sinoatrial.

1.2 Cardiac hypertrophy

1.2.1 Definition

Growth of the heart during embryogenesis occurs primarily through proliferation of cardiac myocytes (hyperplasia). However, after birth, the general consensus is that the cardiac myocytes withdraw from the cell cycle and subsequent growth of the heart occurs predominantly through hypertrophy (increase in cell size) rather than myocyte hyperplasia (increase in cell number). In broad terms there are two forms of cardiac hypertrophy, physiological and pathological (Olson and Schneider, 2003).

1.2.2 Physiological hypertrophy

In physiological hypertrophy growth of the heart occurs in the following 3 situations: during normal postnatal development, in pregnancy and in response to exercise (Chien and Olson, 2002; Lorell and Carabello, 2000), see figure 1.2. In humans the heart grows in proportion to the growth of the body where the left ventricle weight in grams is 3 to 4 times the body weight in kilograms. The 10-fold increase in left ventricle mass that occurs from childhood to adulthood is essential and not harmful. The requirement for an increased stroke volume and cardiac output during pregnancy is accompanied by a considerable increase in left ventricle mass, which regresses over months in the postpartum period (Lorell and Carabello, 2000). Concentric hypertrophy (section 1.3.1) occurs in the trained athlete who specialises in sports such as weight lifting and wrestling. However, eccentric hypertrophy (section 1.3.1) is seen in sports such as long-distance running and cycling (Lorell and Carabello, 2000).

1.2.3 Pathological hypertrophy

Pathological hypertrophy occurs in response to stress signals, which include hypertension, pressure or volume overload, endocrine disorders, myocardial infarction, and contractile dysfunction from inherited mutations in sarcomeric or cytoskeletal proteins (Olson and Schneider, 2003). This is shown in figure 1.2. In pressure overload hypertrophy such as aortic stenosis or hypertension, concentric hypertrophy (section 1.3.1) occurs which increases in wall thickness (Lorell and Carabello, 2000). In valvular disease and mitral regurgitation eccentric hypertrophy (section 1.3.1) occurs (Lorell and Carabello, 2000; Sugden and Clerk, 1998).

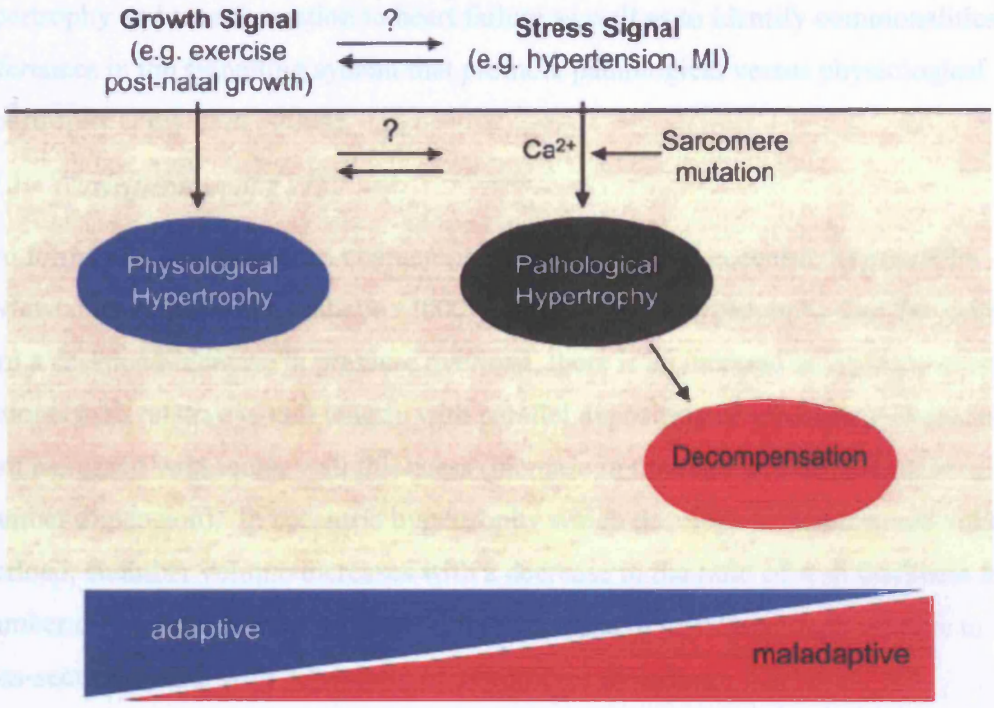

Figure 1.2. Physiological versus Pathological hypertrophy (Frey *et al.*, 2004).
Physiological hypertrophy occurs in response to growth signals such as exercise and post-natal growth. Stress signals that induce pathological hypertrophy include hypertension and myocardial infarction (MI). Little is known whether each form of hypertrophy derives from unique signals or whether overstimulation evokes a pathological response.

1.3 Importance of pathological hypertrophy

One of the most important contributions to heart disease leading to heart failure and cardiac death is cardiac hypertrophy. Hypertrophy of the left or right ventricles is an adaptation of the heart in response to variety of biochemical, hemodynamic and hormonal stimuli (Pokharel *et al.*, 2003). The primary inducing stimulus for left ventricular hypertrophy (LVH) is an increase in hemodynamic load (pressure or volume overload) and the heart adapts to accommodate this extra workload by increasing muscle mass. This adaptation of the heart is initially beneficial but in the long term LVH is an important independent risk factor for cardiovascular morbidity and mortality (Hunter and Chien, 1999; Pokharel *et al.*, 2003). Pathological hypertrophy may be associated with an absence of symptoms for many years before the development of heart failure and sudden death (Lorell and Carabello, 2000). Thus it is important to recognise molecular mechanisms involved in the hypertrophic development of

hypertrophy and transformation to heart failure as well as to identify commonalities and differences in the signalling system that promote pathological versus physiological hypertrophy (Frey *et al.*, 2004).

1.3.1 Classification of LVH

Two forms of LVH have been characterised, concentric and eccentric hypertrophy (reviewed by Lorell and Carabello (2000)). In concentric hypertrophy that develops from a sustained increase in pressure overload, there is an increase in myocyte cross-sectional area relative to cell length, with parallel deposition of sarcomeres that results in an increased ventricular wall thickness (increase in the ratio of wall thickness to chamber dimension). In eccentric hypertrophy which develops from sustained volume overload, chamber volume increases with a decrease in the ratio of wall thickness to chamber dimension. It is associated with an increase in myocyte length relative to cross-sectional area, with deposition of sarcomeres in series.

1.3.2 Diagnosis of LVH

The absence of symptoms associated with the development of LVH, means that detection is reliant on non-invasive techniques. Echocardiography provides an accurate non-invasive means of estimation of LV mass that is more sensitive and specific than previous routine methods of the electrocardiogram for detecting LVH (Reichek and Devereux, 1981). The detection of LVH requires adjustments for sex, height and body mass. The echocardiographic criteria for LVH was identified from analysis of healthy men and women within the large original cohort and offspring subjects (n = 6148) of the Framingham Heart Study (Levy *et al.*, 1987). The normal mean values and normal upper limit criteria for LVH based on mean plus 2 standard deviation for LV mass, LV mass corrected for body surface area and LV mass corrected for height are, respectively, 294 g, 150 g/m^2 and 164 g/m in men and 198 g, 120 g/m^2 and 121 g/m in women (Levy *et al.*, 1987).

Analysis from the Framingham Heart Study demonstrated that echocardiographic LVH identifies subjects with an increased risk for cardiovascular disease. Subjects with LVH are older, more obese, have higher blood pressures and are more likely to have pre-existing coronary disease and depressed LV systolic function (ejection fraction) (Levy *et al.*, 1992). Increased LV mass determined echocardiographically also predicts an increased risk of cardiovascular morbidity and mortality, even after adjustment for other

major risk factors such as age, blood pressure, pulse pressure, treatment for hypertension, smoking, diabetes, obesity, cholesterol profile and electrocardiographic evidence for LVH. In addition, Haider *et al.* (1998) reported increased LV mass and hypertrophy are associated with increased risk for sudden death after accounting for known risk factors. Collectively these findings suggest that echocardiographically detected LVH is of prognostic value for cardiovascular morbidity and mortality.

1.4 Molecular changes in LVH

The cellular hallmark of hypertrophy is an increase in size of the cardiac myocyte, enhanced protein synthesis and a re-organisation of contractile elements from a series to a parallel arrangement. These changes in cellular phenotype are usually accompanied by complex changes in gene reprogramming. These changes include an induction of transcription factor-coding early genes such as the proto-oncogenes c-myc, c-jun and c-fos. This is followed by re-expression of atrial natriuetic peptide (ANP) and brain natriuetic peptide (BNP) that are only otherwise expressed during foetal development. Skeletal muscle α-actin and β-myosin heavy chain (β-MHC) expression are also up-regulated. Constitutively expressed contractile protein genes (cardiac muscle α-actin and myosin light chain 2 ventricular (MLC2v)) are up-regulated in the longer term (Chien *et al.*, 1991; Finn *et al.*, 1999; Sugden and Clerk, 1998). In addition, there is a modification of intracellular ion homeostasis, for example, down regulation of sarcoplasmic reticulum calcium ATPase with variable up-regulation of the Na^{+}/Ca^{2+} exchanger, and down regulation of parasympathetic and sympathetic receptors (for example down regulation of [beta]1 –adrenergic receptors and M2 muscarinic receptors) (Lorell and Carabello, 2000).

The molecular mechanisms that lead to cardiac hypertrophy are not fully understood. Much effort has concentrated on identifying the signals that mediate the pathways that are associated with hypertrophy and subsequently heart failure. A number of signalling pathways involving downstream molecules (figure 1.3) have been implicated such as G proteins, protein kinase C, small G proteins, members of the mitogen-activated protein kinase (MAPK) family and calcineurin. Transcription factors such as GATA 4 and myocyte enhancer factor 2C (MEF2C) have also been implicated (Molkentin and Dorn II, 2001). No single pathway regulates cardiac hypertrophy independently, but instead each pathway works together to regulate cardiac hypertrophy (Frey and Olson, 2003), see figure 1.3.

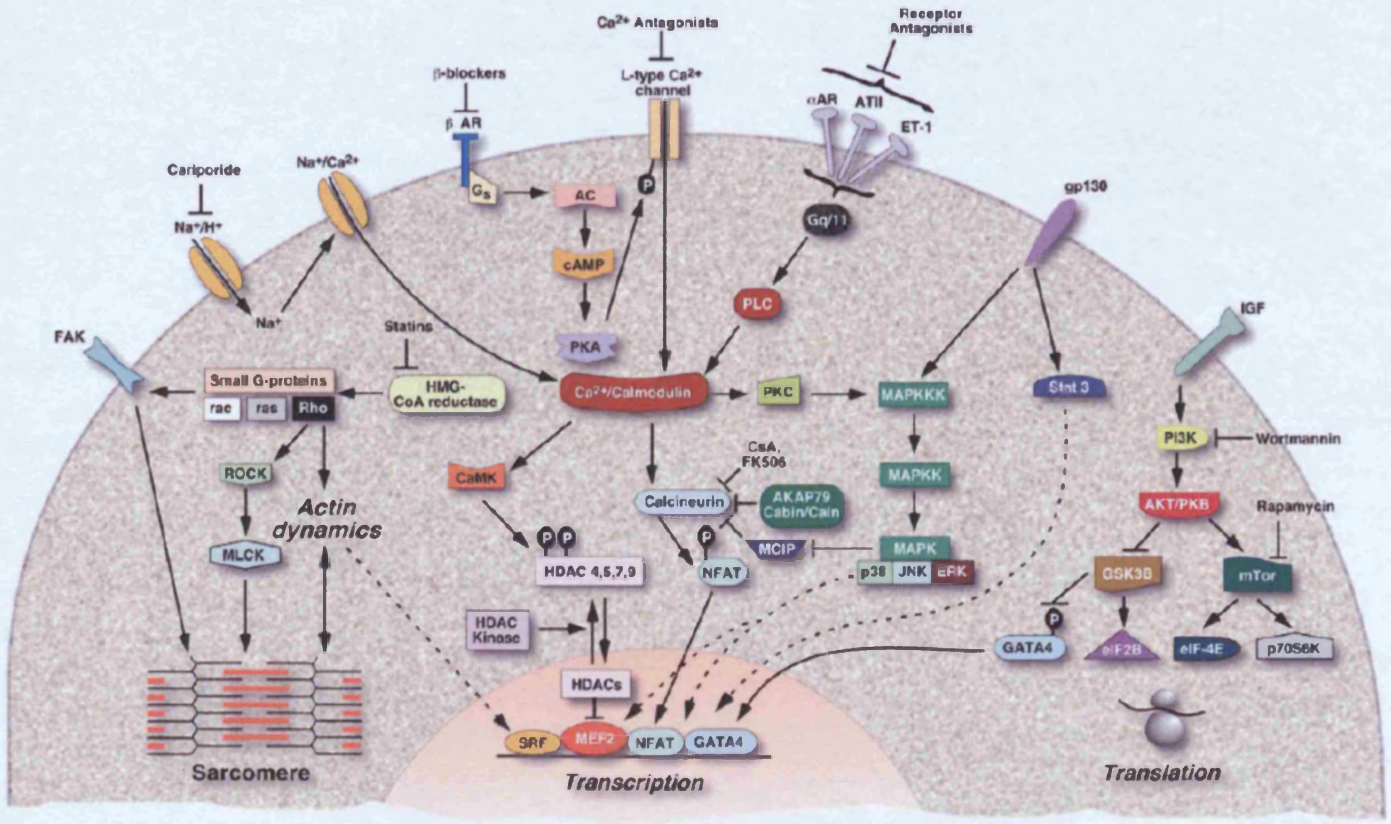

Figure 1.3. Signalling pathways implicated in cardiac hypertrophy (Frey and Olson, 2003).

The main hypertrophic signalling pathways include small GTP-binding proteins and sarcomeric signalling, calcineurin-nuclear factor of activated T cells (NFAT) signalling, mitogen-activated protein kinase (MAPK) pathways and phosphoinositide 3-OH kinase (PI3K)/Akt/glycogen synthase-3 (GSK-3)-dependent signalling. Hypertrophic pathways ultimately converge on common downstream targets such as the transcription factors serum response factor (SRF), myocyte enhancer factor 2 (MEF2), NFAT and GATA 4.

1.5 Signalling pathways

Several signalling pathways have been implicated in cardiac hypertrophy where the G protein-coupled receptors (GPCRs), small G proteins, MAPKs, Akt, calcineurin and the transcription factors SRF, GATA 4 and MEF2C are considered the most important molecules (figure 1.3).

1.5.1 G protein-coupled receptors

Three functional classes of G protein-coupled receptors correspond to the three major classes of G proteins within the cardiovascular system. All G proteins consist of separate Gα and Gβγ subunits and are classified according to their α subunits into subfamilies, for example Gαs, Gαi and Gαq. β-adrenergic receptors couple primarily to Gαs and mediate heart rate and myocardial contractility in response to epinephrine and norepinephrine stimulation. Cholinergic receptors couple to Gαi, which are activated by acetylcholine. Angiotensin II, endothelin, and α-adrenergic receptors are the third class of receptors that couple to Gαq/ Gα11 and have been studied and implicated in cardiac hypertrophy (reviewed by Molkentin and Dorn (2001)). For example, over-expression of Gαq/ Gα11 in transgenic models resulted in cardiac hypertrophy (Molkentin and Dorn II, 2001). Cardiac-specific ablation of Gα11/ Gαq in an adult animal model of aortic banding resulted in a lack of cardiac hypertrophy. Also over-expression of a dominant-negative mutant of Gαq in hearts of transgenic mice blunts pressure overload hypertrophy (Frey *et al.*, 2004). These studies demonstrate that Gαq/ Gα11 are both essential for mediating cardiac hypertrophy.

1.5.2 Small G proteins

Small G proteins play an important role in sarcomeric and cytoskeletal organisation, hallmark features of the hypertrophic phentotype (Frey *et al.*, 2004). They have been characterised into five subfamilies (Ras, Rho, ADP ribosylation factors, Rab and Ran), each consisting of multiple members. Ras and Rho subfamilies have been mainly studied in the heart (Clerk and Sugden, 2000).

Ras induced a significant increase in cardiac mass when a constitutively active mutant was over-expressed in transgenic mouse hearts. This Ras mutant expressed in neonatal rat cardiac myocytes also resulted in hypertrophic gene expression (Frey *et al.*, 2004).

The Rho family of small G proteins, consists of RhoA, Rac, and cdc42 subfamilies (Frey *et al.*, 2004). Transfection of cardiac myocytes with Rac increased ANF and BNP expression and promotes morphological changes associated with myocyte hypertrophy (Clerk and Sugden, 2000). Constitutive activation of Rac in cardiac myocytes *in vitro* and *in vivo* leads to hypertrophy linked with alterations in focal adhesions (Frey *et al.*, 2004).

Rho plays an important role in a variety of cytoskeletal-dependent cell functions that include actin polymerisation, f-actin bundling, myosin-based contractility and focal adhesion formation (Yanazume *et al.*, 2002). Activated Rho induced myofibrillar organisation and stimulated the expression of ANP in cardiac myocytes (Hoshijima *et al.*, 1998). RhoA activates several protein kinases, specifically Rho-associated kinase (ROCK). The Rho/ROCK pathway has been linked to GATA 4 transcriptional activity during hypertrophy in neonatal rat cardiac myocytes (Yanazume *et al.*, 2002). There is evidence that Rho activates transcription via serum response factor (SRF) (Hill *et al.*, 1995). SRF regulates serum-inducible genes and genes expressed in skeletal, smooth and cardiac muscle such as ANP and α-skeletal actin. SRF is a MADS (Mcm 1 and Arg80 in yeast, Agamous and Deficiens in plants, and SRF in animals) box transcription factor and regulates these genes by binding to a DNA sequence ($CC[A/T]_6GG$) known as the CArG box elements in their promoter/enhancer sequences (Frey and Olson, 2003; Sotiropoulos *et al.*, 1999). Current evidence suggest that Rho activates transcription via SRF through a mechanism mediated by changes in actin treadmilling (Hill *et al.*, 1995; Sotiropoulos *et al.*, 1999). These results implicate Rho, Rac and Ras in cardiac hypertrophy; however, the precise signalling pathways are still unclear (Clerk and Sugden, 2000).

1.5.3 Mitogen-activated protein kinases

Mitogen-activated protein kinases (MAPKs) have been implicated as mediators of the hypertrophic response. MAPKs are classified into three major phosphorylation cascades, the extracellular regulated kinases (ERKs), C-Jun N-terminal kinases (JNKs) and the p38MAPKs (see figure 1.4). The latter two are termed the stress-activated MAPKs. ERKs are activated by classical hypertrophic agonists such as phenylephrine and endothelin-1, whereas the stress-activated MAPKs are activated more strongly by cell stresses such as ischaemia or cytotoxic agents (Finn *et al.*, 1999; Wang *et al.*, 1998b). MAPKs have been well established as transducers of growth and stress

responses in many cell types. However, considerable controversy exists concerning their importance as mediators of cardiomyocyte hypertrophy. A number of studies have demonstrated roles for ERKs, p38MAPKs or JNKs as hypertrophic mediators but an almost equal number of studies have not found MAPKs involved in mediating hypertrophy (Bueno *et al.*, 2001). The evidence for whether MAPKs play a role in mediating cardiac hypertrophy is discussed in the following sections.

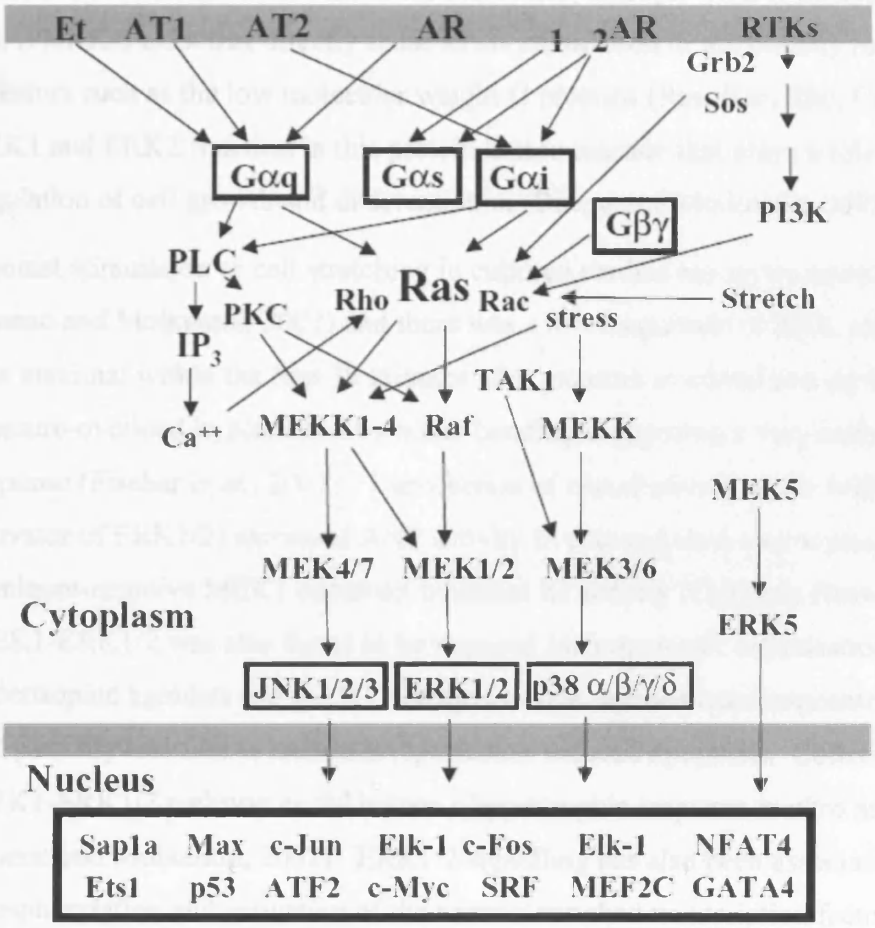

Figure 1.4. MAPK signalling pathways (Liang and Molkentin, 2003).

G protein-coupled receptors (endothelin receptor (Et), angiotensin II receptor (AT), adrenergic receptor (AR) and receptor tyrosine kinases (RTKs) initiate signalling through G proteins that promote small G proteins. These upstream events promote activation of MAPK kinase kinases (MAPKKKs), which in turn regulate the MAPK kinases (MAPKKs), resulting in activation of JNKs, ERKs and p38 MAPKs and phosphorylation of transcription factors within the nucleus.

1.5.3.1 ERKs

Evidence that hypertrophic agonists activate ERKs initially implicated the ERK cascade in the hypertrophic response (Sugden and Clerk, 1998). There are at least five different ERK proteins that have been identified in mammalian cells named ERK1 to 5. The first MAPKs to be identified and the most highly studied and abundantly expressed are ERK1 and ERK2 (also known as p44 and p42 respectively). These are directly regulated by two MAPK kinases (MAPKKs), MEK1 and MEK2 (also referred to as MKK1 and MKK2). Upstream of the MAPKKs, multiple MAPK kinase kinases (MAPKKKs) exist that directly sense stress stimulation or are directly regulated by effectors such as the low molecular weight G proteins (Ras, Rac, Rho, Cdc42 etc). Both ERK1 and ERK2 function in this protein kinase cascade that plays a role in the regulation of cell growth and differentiation (Bueno and Molkentin, 2002).

Agonist stimulation or cell stretching in cultured cardiac myocytes activated ERK1/2 (Bueno and Molkentin, 2002) and there was a low magnitude of ERK activation that was maximal within the first 30 minutes after pressure overload in a rat model of pressure-overload hypertrophy by aortic banding, suggesting a very early and transient response (Fischer *et al.*, 2001). Transfection of constitutively active MEK1 (upstream activator of ERK1/2) increased ANP activity in cultured cardiomyocytes, whereas a dominant-negative MEK1 construct inhibited its activity (Gillespie-Brown *et al.*, 1995). MEK1-ERK1/2 was also found to be required for sarcomeric organisation induced by hypertrophic agonists and MEK1 transgenic mice demonstrated concentric hypertrophy and partially resistant to ischemia/reperfusion-induced apoptosis. Collectively the MEK1-ERK1/2 pathway could induce a hypertrophic response *in vitro* and *in vivo* (Bueno and Molkentin, 2002). ERK1/2 signalling has also been associated with phosphorylation and activation of the cardiac-enriched transcription factor GATA 4. GATA 4 is a critical regulator of most cardiac-expressed structural genes and hypertrophy responsive genes (Bueno and Molkentin, 2002). ERKs along with the JNKs and p38MAPKs can phosphorylate and activate the ternary complex factors Elk1 and SAP1a, which act at the serum response element in conjunction with SRF to up-regulate c-fos expression (early hallmark of the hypertrophic response) (Sugden and Clerk, 1998).

All these observations have implicated ERKs as regulators of cardiac hypertrophy but there are studies that do not support this. For example, stimulated ERK activation was

completely normalised or desensitised within 1-2 hours despite the continued presence of the agonists (Liang and Molkentin, 2003). However, other studies have observed transient ERK activation during an acute or initiation phase of long term stimulation that otherwise produces hypertrophic growth (Hoshijima and Chien, 2002). A number of negative regulators of cardiac signalling have been described. One is of a negative feedback system for the cardiac MAPK signalling cascade in which forced expression of MAPK phosphatase-1 (MKP-1) negatively regulates the cardiac hypertrophic response by down regulating ERK1/2 (Bueno *et al.*, 2001). Other studies have also found ERK1/2 to be down regulated through MKP-1 and attenuate or decrease hypertrophy (Andersson *et al.*, 1998; Black *et al.*, 2002; Bueno *et al.*, 2001; Takahashi *et al.*, 2003). Recently ERK deactivation has also been found via adenosine monophosphate-activated protein kinase (AMPK). AMPK is a stress activated protein kinase that is involved in regulating energy and metabolic homeostasis. AMPK is increase during acute and chronic stresses such as hypoxia, ischaemia and cardiac hypertrophy (Shibata *et al.*, 2004). Researchers investigated the role of adiponectin (circulating adipose-derived cytokine that is down regulated in cardiovascular disease) in regulating cardiac hypertrophy. They found that in cultures of cardiac myocytes, adiponectin activated AMPK and inhibited agonist stimulated hypertrophy and ERK activation. Also the effects were reversed when a dominant-negative form of AMPK was used (Shibata *et al.*, 2004).

Finally studies have shown that ERK could be cardiomyocyte protective as inhibition of ERK caused increased hydrogen peroxide-induced apoptosis (Turner *et al.*, 1998) and increased daunomycin-induced apoptosis (Bueno and Molkentin, 2002) in cardiomyocytes. Also ERK activation attenuated the amount of apoptosis subsequent to reperfusion injury (Bueno and Molkentin, 2002).

1.5.3.2 p38MAPKs

p38MAPKs are activated by a wide range of stress stimuli including chemical stress, physical stress, osmolar stress, radiation stress and G protein-coupled receptor activation. Four separate p38MAPK isoforms have been described including p38α, p38β, p38γ and p38δ. p38α and p38β are expressed in the human heart and thought to be the most important isoforms whereas p38γ and p38δ are undetectable in the heart (Molkentin and Dorn II, 2001). The upstream activators of p38MAPK are MEK3 and MEK6 (also referred to as MKK3 and MKK6) but less is known of the MAPKKK

factors which lie upstream of MEK3 and MEK6 (Molkentin and Dorn II, 2001; Sugden and Clerk, 1998). p38MAPK can phosphorylate and activate the transcription factors ATF-2 and MEF2C. MEF2C may regulate expression of c-jun (an early response to hypertrophic stimulation or cell stress) and other genes (Sugden and Clerk, 1998). p38MAPK can also phosphorylate and activate other protein kinases which in turn phosphorylate the small heat shock protein 25/27 which may increase its cytoprotective ability and maybe important in cell survival (Sugden and Clerk, 1998). As observed for ERK, an increase in p38MAPK was found in a rat model of pressure overload hypertrophy by aortic banding. This was a very early and transient response as it reached maximal activation within the first 30 minutes after pressure overload (Fischer *et al.*, 2001). Activated MEK3/6 over-expression induced hypertrophy and ANP expression in neonatal cardiomyocytes (Wang *et al.*, 1998a; Zechner *et al.*, 1997). Inhibitors of p38MAPK were found to block agonist-stimulated cardiomyocyte hypertrophy in culture (Zechner *et al.*, 1997). In addition, the hypertrophic response in neonatal cardiomyocytes was blunted in response to adenovirus-mediated gene transfer of a dominant negative p38βMAPK (Wang *et al.*, 1998b).

p38MAPK signalling has also been indicated to not function as a forward regulator of the hypertrophic response. For example as found for ERK activation, p38MAPK activation has only been transiently observed during an acute or initiation phase of long term stimulation that otherwise produces hypertrophic growth (Hoshijima and Chien, 2002). In contrast to the study discussed earlier where over-expression of MEK3/6 induced hypertrophy (Wang *et al.*, 1998a; Zechner *et al.*, 1997) another study found that over-expression of MEK3/6 in the heart did not induce hypertrophic growth (Liao *et al.*, 2001). As observed for ERK, transgenic mice expressing MKP-1 in the heart caused reduced p38MAPK and attenuated cardiac hypertrophy in response to aortic banding (Bueno *et al.*, 2001). Another study concluded that p38 MAPK plays an essential role in the cardiomyocyte survival pathway but not in cardiac hypertrophy in response to pressure overload (Nishida *et al.*, 2004). p38MAPKs are known to regulate cell viability; however, it is still unknown whether p38MAPKs are cytoprotective or pro-apoptotic. The majority of evidence suggests that p38MAPK signalling serves a pro-apoptotic role in the heart (reviewed by Baines and Molkentin) (Baines and Molkentin, 2005).

1.5.3.3 JNKs

The JNKs which are also known as the stress-activated protein kinases (SAPKs) are involved in cellular responses to pathological stresses and cytotoxic agents (Sugden and Clerk, 1998). MEK4 and MEK7 (also known as MKK4 and MKK7) appear to be upstream activators of JNKs and in turn are activated by MEKK1 or MEKK2. The MAPKKKs upstream of MEKK1 and MEKK2 include other protein kinases such as PAKs, GCKs and MLKs and members of the low-molecular-weight G proteins (Ras) (Molkentin and Dorn II, 2001). Phosphorylation of the transcription factors c-jun and ATF-2 are mediated by JNKs and this has been demonstrated in ventricular myocytes in response to hypertrophic agonists or cellular stresses (Sugden and Clerk, 1998). JNKs have been found to be activated in myocytes by cellular stresses such as hyperosmotic shock and by hypertrophic interventions such as stretch and Angiotensin II (Sugden and Clerk, 1998). These findings suggest the role for JNKs in the hypertrophic response. Also a marked transient increase in JNK (also observed for p38MAPK) was observed in a rat model of pressure overload hypertrophy by aortic banding (Fischer *et al.*, 2001). It has been suggested that the α_1-adrenergic receptor mediates ANP gene expression through a Ras-MEKK-JNK pathway and that elevated JNK activity is important in the development of hypertrophy *in vitro* and *in vivo* (Ramirez *et al.*, 1997). Over-expression of MEK1 or MEK7, upstream activators of the JNK pathway, induced transcriptional and morphological features of the hypertrophic response (Bogoyevitch *et al.*, 1996; Wang *et al.*, 1998b). Adenovirus-mediated gene transfer of a dominant-negative MEK4 factor attenuated agonist-induced cardiomyocyte hypertrophy *in vitro* and reduced hypertrophy in hearts of aortic-banded rats (Molkentin and Dorn II, 2001).

JNK signalling has also been suggested not to function as a positive regulator of hypertrophy just like ERK and p38MAPK. As observed for ERK and p38MAPK, a transient activation of JNK was found during the initial phase of a long-term stimulation that otherwise produces a hypertrophic growth response (Hoshijima and Chien, 2002) and transgenic mice over-expressing MKP-1 in the heart, had reduced JNK and attenuated cardiac hypertrophy in response to aortic banding (Bueno *et al.*, 2001). In contrast to researchers showing that a dominant negative MEKK1 attenuated ANP activity (Ramirez *et al.*, 1997), transfection of MEKK1 was reported to attenuate sarcomeric organisation, suggesting an antihypertrophic effect of the JNK signalling pathway (Thorburn *et al.*, 1997). Also in contrast to over-expression of MEK7 inducing

features of hypertrophy (Wang *et al.*, 1998b), over-expression of activated MEK7 in transgenic mice did not cause hypertrophy (Liang and Molkentin, 2003).

JNKs (along with p38MAPK signalling), have been shown to regulate cell viability through cytoprotective and proapoptotic effects, with the majority of evidence suggesting a pro-apoptotic regulatory role for JNK signalling in the heart (Baines and Molkentin, 2005).

However, that ERK, p38MAPK, and JNK may not positively regulate cardiac hypertrophy does not exclude their potential importance in modulating the hypertrophic response or the transition towards heart failure in concert with other signalling pathways (Molkentin, 2004).

1.5.4 Akt

Akt (also known as protein kinase B) regulates cellular processes associated with growth (e.g. protein synthesis), survival (e.g. apoptosis), and carbohydrate metabolism (e.g, glycogenesis and possibly glycolytic flux and glucose uptake). Akt is also important in insulin and insulin-like growth factor 1 (IGF1) signalling (Sugden, 2003). It is activated though the phosphoinositide 3-OH kinase (PI3K) pathway. PI3K is activated by receptor protein tyrosine kinases or by G protein-coupled receptors and catalyses the conversion of phosphatidylinositol 4,5-bisphosphate to phosphatidylinositol 3,4,5-trisphosphate (Ptd $InsP_3$). PDK1 (Ptd $InsP_3$-dependent protein kinase) is then activated which causes phosphorylation and activation of Akt (Clerk *et al.*, 2003). Phosphorylation and activation of Akt has been observed at 15 minutes and 1 day after aortic banding in rabbits prior to morphological changes and downstream targets of Akt, glycogen synthase-3β (GSK-3β) and p70 ribosomal s6 kinase ($p70^{s6k}$) was observed at 15 minutes after pressure overload (Miyamoto *et al.*, 2004). Prolonged (6 weeks) activation of Akt in the adult mouse heart resulted in cardiac hypertrophy, severe defects in contractility and massive fibrosis (Schiekofer *et al.*, 2006). However, there was no hypertrophy observed by another study expressing Akt in the mouse heart (Tsujita *et al.*, 2006). In most systems, Akt activation occurs downstream of PI3K and the PI3K-Akt pathway has been implicated as regulating body/organ size, growth and apoptosis (Burgering and Coffer, 1995; Franke *et al.*, 1995; Shioi *et al.*, 2000). PI3K has emerged as being involved in membrane trafficking, cytoskeletal organisation, cell growth and apoptosis (Van Empel and De Windt, 2004).

Expression of constitutively active or dominant negative mutants of PI3K in the heart resulted in mice with larger or smaller hearts, respectively (Shioi *et al.*, 2000). Transgenic over-expression of Akt caused cardiac hypertrophy in mice (Frey and Olson, 2003). In contrast, over-expression of GSK-3β (a downstream target of Akt) in transgenic mouse hearts inhibited hypertrophy by aortic banding and partially prevented cardiac hypertrophy caused by an activated form of calcineurin, suggesting an important role of GSK-3β in regulating cardiac hypertrophy (Antos *et al.*, 2002).

Akt is also known to mediate cell survival by inhibiting apoptosis through phosphorylation of Bad and tethers Bad in the cytoplasm, thereby diminishing its pro-apoptotic ability (Sugden, 2003). Over-expression of PI3K or Akt provides protection against myocyte apoptosis induced by doxorubicin, hypoxia or serum deprivation in cultured cells. Over-expression of Akt also protected against myocyte apoptosis resulting from ischaemia-reperfusion *in vivo* (Clerk *et al.*, 2003). The PI3K/Akt pathway has been shown to be required for protein synthesis in cardiac myocytes, both in the basal state or due to hypertrophic stimulation, but signalling through this pathway also has clear cytoprotective effects. Over-expression of the phosphatase PTEN, which dephosphorylates Ptd $InsP_3$ to inactivate the pathway, causes myocyte apoptosis. Thus, a basal PI3K/Akt signal may be required for cardiac myocyte protection (Clerk *et al.*, 2003). Akt activation was also shown to promote cardiomyocyte viability in another study; however, its role in hypertrophy was not reported (Molkentin and Dorn II, 2001).

Taken together, these results suggest that the Akt pathway plays a dual role in producing the hypertrophic response of the heart and also in modulating cell survival (Van Empel and De Windt, 2004).

1.5.5 Calcineurin

Intense research has focused on the calcium-dependent signalling pathways implicated in cardiac hypertrophy (Olson, 2004) (figure 1.5). One such pathway involves calcineurin, a calcium calmodulin-dependent phosphatase. Calcineurin is activated by a rise of intracellular calcium and dephosphorylates a range of cellular substrates including the nuclear factor of activated T cells (NFAT) transcription factor, facilitating translocation of NFAT to the nucleus where it can mediate expression of pro-hypertrophic genes (Molkentin *et al.*, 1998; Olson, 2004).

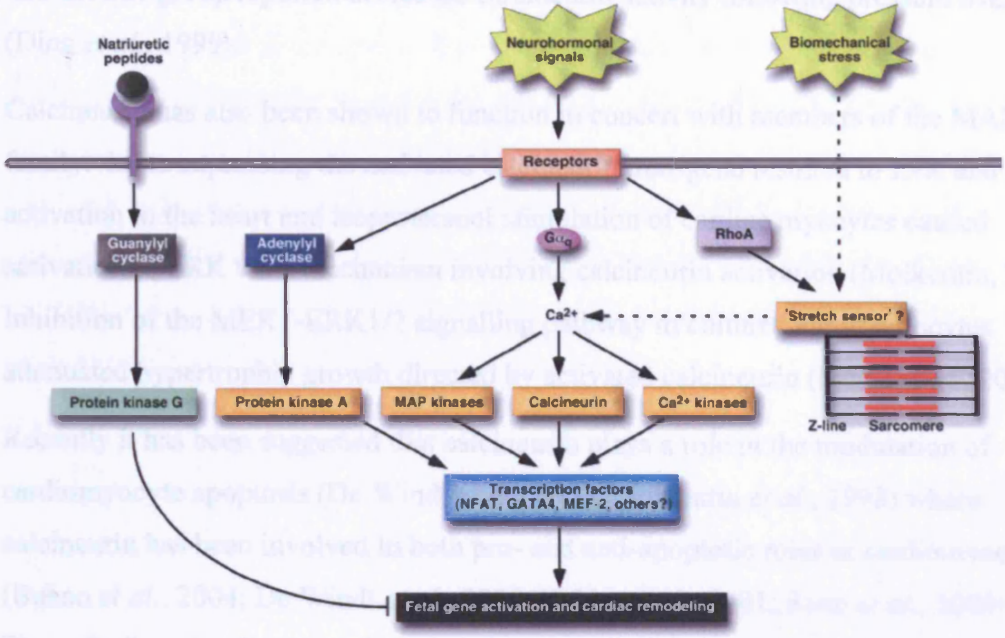

Figure 1.5. Calcium-dependent signalling pathways implicated in the hypertrophic growth of the adult heart (Olson, 2004).

The calcineurin phosphatase is activated by sustained elevation of intracellular calcium and dephosphorylates a range of cellular substrates including the nuclear factor of activated T cells (NFAT) transcription factor to induce hypertrophy, characterised by fetal gene activation and remodelling. The calcineurin pathway is integrated with other pathways such as the stress-responsive MAPKs.

Transgenic mice that over-express these components of the calcineurin signalling pathway developed hypertrophy that lead to heart failure and cyclosporine, an inhibitor of calcineurin, was found to suppress hypertrophy (Molkentin *et al.*, 1998). However, calcineurin inhibitors failed to suppress experimental hypertrophy in several animal models (Ding *et al.*, 1999; Zhang *et al.*, 1999). *In vitro*, activated calcineurin expression in cardiomyocytes resulted in hypertrophy (De Windt *et al.*, 2000) and a number of groups have reported elevated calcineurin activity in hypertrophic hearts induced by aortic banding in rats or mice (De Windt *et al.*, 2001; Eto *et al.*, 2000; Lim *et al.*, 2000; Saito *et al.*, 2003; Shimoyama *et al.*, 1999; Zou *et al.*, 2001). A significant increase in calcineurin activity was also observed in patients with cardiac hypertrophy (Ritter *et al.*, 2002). There are a few studies that do not implicate that calcineurin is activated in the hypertrophic heart. For example one group found no change in calcineurin activity in response to pressure overload stimulation (Zhang *et al.*, 1999)

and another group reported decreased calcineurin activity following pressure overload (Ding *et al.*, 1999).

Calcineurin has also been shown to function in concert with members of the MAPK family. Mice expressing the activated calcineurin transgene resulted in JNK and ERK activation in the heart and isoproterenol stimulation of cardiac myocytes caused activation of ERK via a mechanism involving calcineurin activation (Molkentin, 2004). Inhibition of the MEK1-ERK1/2 signalling pathway in cultured cardiomyocytes attenuated hypertrophic growth directed by activated calcineurin (Sanna *et al.*, 2005).

Recently it has been suggested that calcineurin plays a role in the modulation of cardiomyocyte apoptosis (De Windt *et al.*, 2000; Molkentin *et al.*, 1998) where calcineurin has been involved in both pro- and anti-apoptotic roles in cardiomyocytes (Bueno *et al.*, 2004; De Windt *et al.*, 2000; Kakita *et al.*, 2001; Saito *et al.*, 2000). These findings implicate calcineurin in both cardiac hypertrophy and apoptosis.

1.5.6 SRF

Expression of SRF in the adult mouse is high in skeletal and cardiac muscle, but low in the liver, lung and spleen tissues (Belaguli *et al.*, 1997). During embryogenesis, SRF is expressed preferentially in differentiating cardiac and skeletal muscle cells (Zhang *et al.*, 2001). Certain muscle-specific genes containing mutations in CArG boxes in their promoters lead to a loss of their expression in cardiac muscle cells (Zhang *et al.*, 2001). Inactivation of SRF in cardiac/smooth muscle cells resulted in embryonic lethality at approximately embryonic day 11.5 (E11.5). SRF deficient mice display defects in sarcomeric assembly and absence of smooth muscle cell actin/intermediate filament bundles (Miano *et al.*, 2004). In another study, Tamoxifen-inducible Cre recombinase was used to disrupt SRF in the hearts of mice. This caused impaired left ventricular function with reduced contractility, leading to dilated cardiomyopathy and subsequent death from heart failure (Parlakian *et al.*, 2005). Taken together these studies indicate that SRF is involved in the organisation of cytoskeletal functions of cardiomyocytes and vascular smooth muscle cells.

The majority of SRF target genes identified in a genome-wide (*in silico*) screen were experimentally validated to be involved in cell growth, migration, cytoskeletal organisation, and myogenesis (Sun *et al.*, 2006) suggesting a role for SRF in the regulation of genes responsible for cardiac structure and function.

SRF has also been implicated as a potential regulator of cardiac gene expression in response to hypertrophic signals. Transgenic mice that over-express SRF in the heart displayed massive cardiac hypertrophy and subsequently died within a few weeks after birth (Zhang *et al.*, 2001). In hypertrophy transgenic hearts, SRF was found required for the induction of a range of genes such as ANP, c-fos, BNP, α-actin, and β-MHC (Nelson *et al.*, 2005). Together these findings suggest a role for SRF in cardiac hypertrophy but the mechanisms that connect SRF to hypertrophic signalling remains unknown.

1.5.7 GATA 4

The family of GATA transcription factors consists of six proteins (GATA 1-6) that regulate differentiation, growth and survival of a wide range of cell types (Pikkarainen *et al.*, 2004). GATA 4 is one of the earliest transcription factors expressed in the developing mouse heart. GATA 4 mRNA is detected as early as at 7.0-7.5 days postcoitum in the precardiac mesoderm and is expressed during formation of the heart tube at 8.0 days postcoitum (Heikinheimo *et al.*, 1994). GATA 4 mRNA is expressed in cardiac myocytes through to adulthood and in the mouse GATA 4 is expressed in the gut, gonads, liver, visceral endoderm and parietal endoderm (Arceci *et al.*, 1993; Laverriere *et al.*, 1994). After initial studies identified GATA 4 as a major GATA-binding factor in the heart, its role in development has emerged. Increased differentiation of beating hearts was observed in PI9 embryonal carcinoma cells when over-expressing GATA 4, while inhibition of GATA 4 prevents cardiomyocyte differentiation and triggers apoptosis (Pikkarainen *et al.*, 2004). Inactivation of GATA 4 in transgenic mice causes death during embryonic development (Kuo *et al.*, 1997; Molkentin *et al.*, 1997).

GATA 4 is one of the targets of hypertrophic signals that mediate transcriptional activity of genes encoding α- and β-MHC, angiotensin II type 1 receptor, ANP, BNP, and endothelin-1 (Molkentin, 2000; Pikkarainen *et al.*, 2004). GATA 4 also regulates cardiac transcription factors such as Nkx2.5, Hand2 and MEF2C (myocyte enhancer factor 2C) (Pikkarainen *et al.*, 2004; Xin *et al.*, 2006).

The DNA binding activity of GATA 4 was found to increase during the hypertrophic process (Yanazume *et al.*, 2002). Binding is rapid in pressure-overloaded rat hearts and peaks at 30 minutes, which is similar to endothelin-1 stimulated neonatal rat cardiac

myocytes (Pikkarainen *et al.*, 2004). Cardiac hypertrophy was observed when GATA 4 was over-expressed in cultured cardiomyocytes and transgenic mice (Liang *et al.*, 2001) and features of cardiomyocyte hypertrophy induced by phenylephrine and endothelin-1 in culture were diminished when a dominant negative GATA 4 or antisense GATA 4 mRNA were used (Charron *et al.*, 2001; Liang *et al.*, 2001). Mice heterozygous for deletion of the second exon of GATA 4 (G4D) resulted in mild systolic and diastolic dysfunction with reduced heart weight and cardiomyocyte apoptosis. G4D mice developed overt heart failure and eccentric cardiac hypertrophy associated with significant increased fibrosis and cardiomyocyte apoptosis following pressure overload (Bisping *et al.*, 2006). Another group (Oka *et al.*, 2006) who used a Cre/*loxP* system to ablate GATA 4 in cardiomyocytes also observed cardiomyocyte apoptosis at baseline and after pressure overload. However, they found that hypertrophy was blunted after pressure overload. Taken together, these findings suggest that GATA 4 plays important roles in cardiac development, differentiation, growth and survival.

1.5.8 Members of the myocyte enhancer factor 2 (MEF2) family

The MEF2 family of transcription factors control cardiomyocyte differentiation, myofibrillogenesis and muscle metabolism (Olson and Schneider, 2003). Members of the MEF2 family like SRF contain a MADS domain; however, MEF2 and SRF bind only to their respective sites. MEF2 activates transcription by binding to the consensus sequence, called the MEF2-binding site $CTA(A/T)_4TAG$, which is found in the promoter regions of numerous muscle specific genes (Black and Olson, 1998). In vertebrates there are four MEF2 genes, MEF2A, MEF2B, MEF2C, and MEF2D. Mice lacking in MEF2C die around E9.5 by improper development of the heart (Lin *et al.*, 1997) and transgenic expression of a dominant-negative mutant of MEF2 in mouse hearts results in impaired growth of the myocardium (Kolodziejczyk *et al.*, 1999).

The MEF2 transcription factor appears to be a critical target for hypertrophic signals (Chien and Olson, 2002). MEF2 activity is controlled by direct association with Class II histone deacetylases (HDACs). HDACs deacetylate nucleosomal histones, thus promoting chromatin condensation and transcriptional repression of MEF2 target genes. HDAC activity is opposed by histone acetyltransferases (HATs), which activate target genes by acetylating nucleosomal histones, thereby relaxing chromatin (Frey and Olson, 2003). It has been proposed that HDACs associate with MEF2 and repress hypertrophy and the fetal gene programme. Hypertrophic signals cause activation of a cardiac

HDAC kinase that phosphorylates the serine sites in HDACs. When phosphorylated, HDACs dissociate from MEF2 and are exported from the nucleus. Upon release of HDACs, MEF2 can associate with HATs and activate downstream target genes that govern a hypertrophic response (Zhang *et al.*, 2002). Therefore to inhibit the HDAC kinase could be therapeutically beneficial to prevent cardiac hypertrophy.

The various intracellular signalling pathways discussed in this section have been implicated as important pathways of the hypertrophic response but the key regulatory molecules involved and there interactions are still unknown. Until these findings are discovered, the molecular mechanisms of LVH remain unclear.

1.6 Myocyte stress 1 (ms1)

Previous work in the group applied a molecular indexing approach (Mahadeva *et al.*, 1998) to identify genes that are regulated during the early stages of pressure-induced LVH in a rat model of aortic banding. This approach for the isolation of differentially expressed genes involves digestion of cDNA pools from different samples with class II restriction endonucleases that generates fragments with non-identical cohesive ends. The ligation of adapters with perfectly complementary overhangs, partitions the cDNA fragments into non-overlapping subpopulations. These internal cDNA restriction fragments are then exponentially amplified by adapter primer PCR and visualised by non-denaturing polyacrylamide gel electrophoresis (Mahadeva *et al.*, 1998). Using the molecular indexing approach to identify genes that are differentially expressed in the early stages of aortic banding in the rat, a model of pressure-induced LVH, led to the identification and characterisation of a novel gene, myocyte stress 1 (ms1). ms1 was up-regulated within 1 hour in the left ventricle following aortic banding in the rat, with a peak expression before 1 day at 4 hours, well before any detectable increase in LV mass suggesting a possible role for ms1 in the initial signalling of the hypertrophic response (Mahadeva *et al.*, 2002). Interestingly ms1 is preferentially expressed in striated muscle as ms1 mRNA was found expressed at high levels in the adult heart and skeletal muscle of the rat. ms1 mRNA expression was observed in the rat left ventricle during embryogenesis and was found to be regulated post-natally through to adulthood. The rat ms1 gene is located on chromosome 7 and its full-length transcript size is approximately 1.3 kb. ms1 has a relatively simple genomic organisation of two exons and one intron. ms1 is a 375-amino acid protein and BLAST searches revealed that ms1 full-length cDNA and putative protein show no significant homology to any known

genes at date of submission. However, there is significant identity of specific regions that are well conserved between species implying evolutionary conservation and thus functional importance (Mahadeva *et al.*, 2002).

At the same time the mouse homologue of msl termed STARS (striated muscle activator of Rho signalling) was identified in the early embryonic heart (E8.25) and shown to be a sarcomeric actin-binding protein which stimulates SRF-dependent transcription through a mechanism involving RhoA signalling and actin polymerisation (Arai *et al.*, 2002). The molecular mechanism by which STARS activates SRF-dependent transcription was discovered a few years later and during the time of our own investigations into identifying the downstream targets of msl. Kuwahara *et al.* (2005) have shown that STARS activates SRF-dependent transcription by inducing the nuclear accumulation of the SRF co-factors, myocardin-related transcription factors (MRTFs) MRTF-A and MRTF-B through a mechanism dependent on RhoA and actin polymerisation. MRTF-A (MAL/MKL-1) and MRTF-B (MKL-2) are expressed in a wide range of embryonic and adult tissues (Wang *et al.*, 2002). MRTFs, like myocardin (belongs to a family of nuclear proteins that plays a role in cardiac gene expression and is a master regulator of smooth muscle development (Li *et al.*, 2003)), enhance the transcriptional activity of SRF by forming a stable ternary complex on CArG boxes by associating with SRF and providing their powerful transcription activation domains (Wang *et al.*, 2001b; Wang *et al.*, 2002). MRTFs also convey stimulatory signals to SRF from Rho GTPase and the actin cytoskeleton by the use of their regulated translocation into the nucleus (Cen *et al.*, 2003; Du *et al.*, 2003; Miralles *et al.*, 2003). Kuwahara *et al.* (2005) propose that STARS binds to actin and promotes actin polymerisation in the presence of Rho activity, which releases MRTFs from the inhibitory influence of G-actin, allowing the nuclear import of MRTFs and stimulation of SRF dependent gene activation (figure 1.6) (Kuwahara *et al.*, 2005).

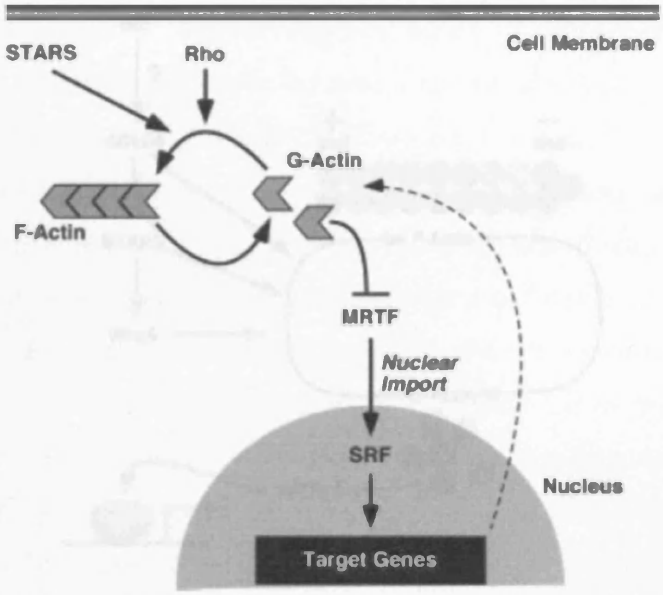

Figure 1.6. The proposed mechanism by which STARS activates SRF-dependent transcription via MRTFs and Rho-actin signalling (Kuwahara *et al.*, 2005).

STARS stimulates SRF-dependent transcription by binding to G-Actin and promoting actin polymerisation in the presence of basal Rho activity, thereby allowing the nuclear accumulation of MRTFs and subsequent SRF-dependent gene activation. Actin itself is regulated via SRF thus generating a negative feedback loop.

More recently it has emerged that members of the actin-binding LIM (ABLIM) protein family interact with STARS, bind to actin and positively modulate STARS dependent activation of SRF transcriptional activity (figure 1.7) (Barrientos *et al.*, 2007). The novel ABLIM proteins, ABLIM-2 and ABLIM-3 were identified to interact with STARS by performing a yeast-two hybrid screen of a human skeletal muscle cDNA library using STARS as bait and by co-immunoprecipitation. Another member of the ABLIM protein family, ABLIM-1 was also found to interact with STARS. ABLIM-1 is expressed in the retina, brain and muscle tissue and postulated to regulate actin dependent signalling. ABLIM-2 is highly expressed in skeletal muscle and not in the heart whereas ABLIM-3 is predominantly expressed in the heart. These ABLIM proteins bind to actin, are localised to the sarcomere in striated muscle and enhance STARS-dependent SRF-activation. Moreover, knockdown of ABLIM-1, -2 and -3 inhibited STARS-mediated SRF-activation, further supporting a role for ABLIM proteins to modulate actin-dependent SRF activity via binding of STARS (Barrientos *et al.*, 2007).

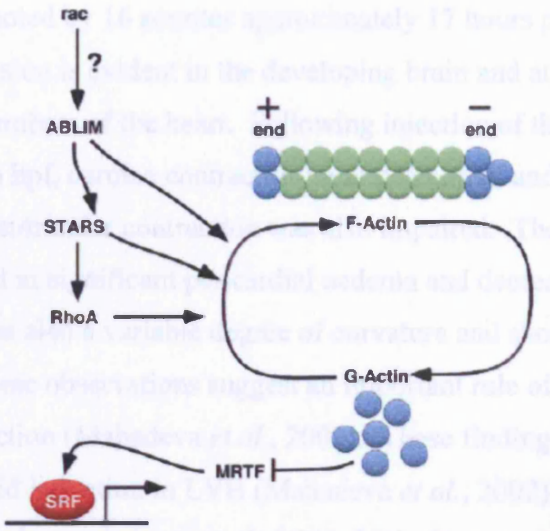

Figure 1.7. ABLIM proteins associate with STARS and regulate STARS mediated activation of SRF transcription (Barrientos *et al.*, 2007).
ABLIM proteins can augment STARS-dependent SRF-activation and are likely to serve as a scaffold to integrate signals from small G proteins via STARS towards the actin cytoskeleton.

As discussed earlier in section 1.5.2 Rho has been demonstrated to play a critical role in hypertrophy and Rho activates transcription via SRF, whereby the mechanism involves alterations in actin dynamics. Actin itself is regulated via SRF thus generating a negative feedback loop. Members of the ABLIM protein family are expressed in striated muscle tissue and localised to the sarcomere. ms1 is also a striated muscle specific protein and its mRNA increased markedly in the left ventricle of the rat from embryo to adulthood. ms1 expression was found to be up-regulated in a model of pressure-induced hypertrophy (Mahadeva *et al.*, 2002) and as sacromeric and cytoskeletal organisation are hallmarks of the hypertrophic phenotype these findings, along with others (Arai *et al.*, 2002; Barrientos *et al.*, 2007; Kuwahara *et al.*, 2005), suggest that the ABLIM proteins and the ms1-MRTF/SRF pathway may play an important role in the aetiology of certain heart disease.

In subsequent work our group has identified that ms1 is transiently up-regulated during simulated ischaemia and reperfusion in a heart-derived rat cell line, H9c2. Ischaemia alone had no effect on ms1 mRNA expression. However, ms1 mRNA is up-regulated following 1 hour to 2 hours of reperfusion and then returns to basal levels by 4 hours (Chong, unpublished results). Furthermore, the role of ms1 in cardiac development was

investigated in the zebrafish. The earliest site of msl expression is the somites, where strong expression is noted by 16 somites approximately 17 hours post fertilisation (hpf). At 24 hpf msl expression is evident in the developing brain and at 48 hpf expression is detectable in both chambers of the heart. Following injection of the msl antisense morpholino, by 48-56 hpf, cardiac contractility was decreased, and the atrium was markedly enlarged; ventricular contraction was also impaired. These cardiac abnormalities resulted in significant pericardial oedema and decreased or absent circulation. There was also a variable degree of curvature and shortening of the longitudinal axis. These observations suggest an important role of msl in cardiac development and function (Mahadeva *et al.*, 2007). These findings coupled with other findings of msl's rapid induction in LVH (Mahadeva *et al.*, 2002), expression of msl during embryonic development (Arai *et al.*, 2002; Mahadeva *et al.*, 2002), its transient up-regulation during ischaemia-reperfusion and that msl is a striated muscle specific protein (Arai *et al.*, 2002; Mahadeva *et al.*, 2002) suggests that msl plays an important widespread role in cardiac development and physiology.

1.7 Aims

Multiple signalling pathways have been shown to regulate hypertrophy; however, the molecular controllers that sense pressure overload and initiate hypertrophy are unclear. The determinants of progression from cardiac hypertrophy to failure are not fully understood either and may be a consequence of alterations in specific signalling molecules and their downstream pathways. Cardiac hypertrophy is one of the most important causes of heart disease leading to heart failure, an increase risk of arrhythmia and sudden death; therefore, it is essential to identify the molecular events involved whose actions could be interrupted thereby halting or perhaps reversing clinical deterioration.

The novel gene msl, may play a role in the initial signalling of the hypertrophic response and an important role in cardiac physiology and disease. This study proposes to further examine the function of msl in cardiac physiology and disease by using a combination of *in vitro* and *in vivo* approaches:

1. To identify putative target genes and downstream pathways of msl by over-expressing a c-Myc-msl fusion protein *in vitro* and examining altered mRNA and protein expression.

2. To examine the cellular consequences following over-expression of msl *in vitro*.
3. To investigate the physiological and pathophysiological consequences of msl over-expression *in vivo*.

Chapter 2

Materials and Methods

In this chapter the materials and methods used in this thesis will be presented, starting with the materials and general methods of DNA, RNA and protein manipulation, followed by specific methods of cell culture, flow cytometry and genetic manipulation. Other specific methods are detailed in individual chapters where relevant.

2.1 Materials

2.1.1 Reagents

All chemicals were obtained from Sigma or Fisher unless otherwise stated. Antibiotics and X-Gal were purchased from Melford Laboratories. Plasmid preparation, DNA purification and RNeasy kits were purchased from Qiagen. TRIzol was purchased from Invitrogen and genomic DNA extraction kits (GenElute Mammalian Genomic DNA Miniprep) were bought from Sigma. M-PER Mammalian Protein Extraction reagent was bought from Pierce. DNA markers were purchased from Promega. Restriction enzymes, enzymes for reverse transcription (Superscript II enzyme) and synthetic oligonucleotides were obtained from Invitrogen. Enzymes for polymerase chain reaction (PCR) were purchased from Abgene, Qiagen (HotStarTaq DNA polymerase) or Roche (Expand High Fidelity PCR System). T4 ligase used for DNA ligations was bought from Promega. Positively charged nylon membranes used for Southern blot analysis were purchased from Amersham. α^{32}P dCTP was obtained from MP Biomedicals. Radioactive labelling of DNA was performed using the RadPrime DNA Labeling System bought from Invitrogen. Cells were fixed and permeabilised prior to flow cytometry and microscopy using Leucoperm purchased from Serotec. Vybrant DyeCycle Violet Stain to stain DNA, Alexa fluor 350 phalloidin and Prolong Gold Antifade were purchased from Invitrogen. For sodium dodecyl sulphate (SDS) polyacrylamide protein gel electrophoresis 30% (w/v) acrylamide: 0.8% (w/v) bis acrylamide solution was bought from Flowgen. Protein markers (SeeBlue Plus2 pre-stained standard) were obtained from Invitrogen and nitrocellulose membranes (Protran) for immunoblots were purchased from Schleicher and Schuell Bioscience. Enhanced chemiluminescence (ECL) was performed using ECL Advanced Western blotting detection kit and the luminescent signal was detected on Hyperfilm ECL, both purchased from Amersham.

2.1.2 Antibodies

The α-tubulin (Tu-02) mouse monoclonal antibody and c-Myc (9E10) mouse monoclonal antibody were purchased from Santa Cruz Biotechnology Inc. Phospho-Akt (Ser473) (193H12) rabbit monoclonal, phospho-p44/42 MAPK (Thr202/Tyr204) (197G2) rabbit monoclonal and Akt2 (5B5) rabbit monoclonal antibodies were all purchased from Cell Signalling Technology Inc. Anti c-Myc fluorescein isothiocyanate (FITC) antibody was bought from Serotec and rabbit GFP polyclonal antibody was purchased from Molecular Probes. Rabbit polyclonal antisera (C-48) raised against msl (immunising peptide was GRPKEGSKTAERAKRAEEHI) was produced at Pepceuticals Ltd. Biotinylated swine anti-rabbit antibody was obtained from DakoCytomation. Anti-rabbit and anti-mouse horseradish peroxidase (HRP) conjugates were purchased from Amersham.

2.1.3 Mammalian cell culture and reagents

The H9c2 cell line derived from the embryonic rat ventricle was obtained from the European Collection of Cell Cultures and NIH3T3 cells (murine embryonic fibroblasts) were purchased from the American Type Culture Collection.

Dulbecco's Modified Eagle's Medium, fetal bovine serum, penicillin and streptomycin were all purchased from Invitrogen. Trypsin-Ethylene diamine tetraacetic acid (EDTA) was bought from BioWhittaker and JetPEI cationic transfection reagent was purchased from Qbiogene.

2.1.4 Plasmids

pAlpha-MHCpromoter-msl sense (mouse) was provided by H Mahadeva. pGEM-T Easy vector was purchased from Promega. The mammalian expression vector pcDNA3.1(+) was kindly given by Professor G Brooks. The transgenic vector PCCALL2-IRES-EGFP/anton (pi Z/EG) was kindly provided by C Lobe and the pCre-Pac vector was a generous gift from C Pritchard.

All vector maps are shown in appendix 1 (section 2.8) and shown in figure 2.1 is how these plasmids were experimentally used.

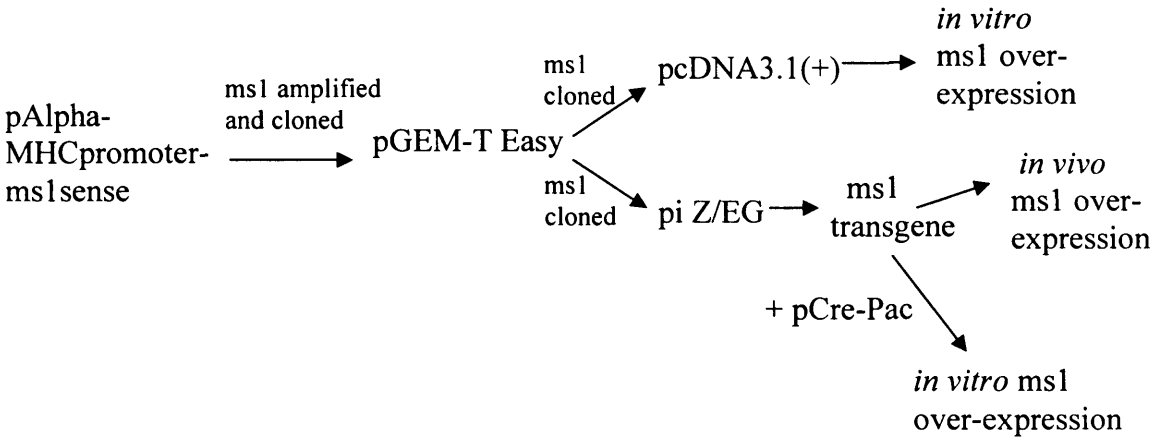

Figure 2.1. A diagram to show the plasmids involved to generate an expression vector to over-express ms1 *in vitro* and a ms1 transgene for *in vitro* and *in vivo* ms1 over-expression.

2.2 DNA Manipulation

2.2.1 High Fidelity Polymerase Chain Reaction (PCR)

The full-length coding sequence of mouse ms1 was amplified using the Roche Expand High Fidelity PCR System (a mixture of Taq DNA polymerase plus another proof reading polymerase). 5 ng of a plasmid containing mouse ms1 termed pAlpha-MHCpromoter-ms1sense (mouse) provided by H Mahadeva was PCR-amplified using forward

*Bgl*II site
| | | c-myc | mouse ms1 |
(5′-ccagatct**atg**gagcagaagctcatcagcgaggaggacctggctccaggagaaagggaaagggag-3′)

*Xho*I site
| | mouse ms1 |
and reverse (5′-cgcctcgag**tta**ctcaacgagagtaatcacaacatg-3′) primers.

Multiple reactions were performed in a master mix. A typical 50 µl reaction would contain the following:

5 ng	Template DNA
2.5 µl	10 µM Forward Primer (final concentration of 0.5 µM)
2.5 µl	10 µM Reverse Primer (final concentration of 0.5 µM)
5 µl	10 × Expand High Fidelity PCR buffer with M_gCl_2
5 µl	2 mM dNTP mix (final concentration of 0.2 mM)
3.5 U/µl	Expand High Fidelity PCR System
dH_2O to a final volume of 50 µl	

Oil (2 drops) was then placed on the top of each reaction and the tubes were placed in a Techne Techgene thermal cycler. The thermocycling parameters were 1 cycle of 94°C , 2 minutes; 30 cycles of 94°C, 45 seconds; 59°C, 45 seconds; 72°C, 1 minute 10 seconds; a final extension step was performed at 72°C for 5 minutes. The PCR product was then ran alongside a 1 kb marker on a 1% (w/v) agarose gel as described in section 2.2.2. When the correct sized fragment for msl (approximately 1.3 kb) was obtained by electrophoresis the band was cut from the agarose gel and extracted and purified using the QIAquick Gel Extraction Kit (Qiagen) as stated by the manufacturer's protocol.

2.2.2 Agarose gel electrophoresis

The appropriate volume of 6 × loading buffer (40% (v/v) glycerol, 60% (v/v) TE buffer (Tris Ethylene diamine tetraacetic acid (EDTA), 10 mM Tris-HCl, 1 mM EDTA, pH 8.0), and very small amount of bromophenol blue) was added to the sample. Samples were centrifuged for 1 minute at 13,000 rpm, loaded onto the appropriate percentage agarose gel in 1 × Tris-Acetate EDTA (TAE) buffer (40 mM Tris-HCl, 20 mM Glacial Acetic Acid, 0.1 mM EDTA, pH 8.0) and run alongside an appropriate sized marker (Promega). Ethidium bromide was present in the gel at a concentration of 0.035 µg/ml. The gel was electrophoresed in 1 × TAE buffer at a constant 80 V for 1 hour. The bands were visualised on ultraviolet light.

2.2.3 Extraction and purification of DNA from an agarose gel

When the correct sized fragment was obtained by electrophoresis the band was cut from the agarose gel and extracted and purified using the QIAquick Gel Extraction Kit

(Qiagen). The method was followed as stated in the QIAquick Spin Handbook (Qiagen). The DNA was stored at -20°C until required.

2.2.4 Quantification of DNA

The concentration of DNA was determined by diluting the DNA 1:50 with dH_2O. The absorbance was read in a spectrophotometer at wavelengths of 260 nm and 280 nm. An A_{260} of 1 was equivalent to 50 µg DNA/ml. The concentration of DNA in ng/µl was calculated as follows:

50 µg/ml × A_{260} × dilution factor

2.2.5 Ligation of DNA from PCR product or Plasmid into Vector

This method was based on the pGEM-T and pGEM-T Easy Vector Systems for cloning of PCR products (Promega). 100 ng of vector was placed into the ligation reaction with an appropriate amount of DNA (insert) calculated so there was 3 × insert : 1 × vector ratio as follows:
(ng of vector × kb size of insert) ÷ kb size of vector × insert:vector ratio = ng of insert.

The total reaction volume was 10 µl and to this 3 U of T4 ligase, T4 DNA ligation buffer (10 ×) and H_2O (to make final volume) was added. A control was also performed where the insert was omitted; this indicated the presence of re-circularised vector plasmid. The reactions were incubated overnight at 4°C.

2.2.6 Transformation of bacteria with DNA from PCR product or Plasmid

Half the ligation reaction was added to 100 µl DH5α chemically competent cells (Invitrogen), mixed gently by tapping and incubated on ice for 30 minutes. The reaction was then heat shocked for exactly 45 seconds at 37°C using a water bath. Next the reaction was placed on ice for 2 minutes and then 400 µl pre-warmed SOC was added. The reaction was then incubated at 37°C for exactly 1 hour at 225 rpm in a shaking incubator. Following the incubation, half the reaction was spread onto Luria Broth (LB) agar plates containing ampicillin (100 µg/ml) for selection of the transformed cells. Where possible, 40 µl X-Gal (20 mg/ml) was added to the LB agar plates containing the appropriate antibiotic to enable blue/white selection of transformants. The plates were inverted and incubated at 37°C overnight.

Single putative transformant colonies were isolated and grown in approximately 10 ml of LB (containing the appropriate antibiotic) at 37°C overnight at 225 rpm in a shaking incubator. 6 ml of these cultures were used to extract plasmid DNA using QIAprep Spin Miniprep kit (Qiagen) when DNA was needed to digest with appropriate restriction enzymes to allow identification of the plasmids containing the insert. The method for extracting DNA for this purpose was followed as stated in the QIAprep Spin Miniprep kit protocol. If a positive clone was obtained the remaining 4 ml culture was used to make a 20% (v/v) glycerol stock for long-term storage at -80°C and the rest was used to set up more culture (approximately 10 ml) to extract plasmid DNA using Qiagen-tip 20 Plasmid Mini Kit when DNA was to be cloned, sequenced or transfected. The method for extracting plasmid DNA for these purposes was followed as stated in the Qiagen-tip 20 Plasmid Mini Kit protocol. When DNA was used to be injected into mouse oocytes the remaining 4 ml culture was used to make a 20% (v/v) glycerol stock for long-term storage at -80°C and the rest was used to set up more culture (approximately 250 ml) to extract plasmid DNA using the Qiagen Endofree Maxi Kit by following the manufacturer's instructions.

2.2.7 Restriction digest of DNA

To allow identification of the plasmid containing the PCR fragment (insert), the required amount of DNA was added with the restriction enzyme (or enzymes) (Invitrogen) of choice in a reaction volume containing the appropriate amount of reaction buffer (Invitrogen) at the optimum temperature for the enzyme(s) to work. This reaction was incubated overnight and the total reaction volume was then run out on an appropriate percentage agarose gel as described in section 2.2.2 to check that the enzyme had cut the DNA. If a restriction digest was performed to isolate a band of DNA from, for example a plasmid, then the digest reaction was incubated for a maximum of 2 hours, run out on an appropriate percentage agarose gel as described in section 2.2.2 and the correct sized band was cut from the agarose gel and extracted and purified as already described in section 2.2.3. All cloned PCR fragments were sequenced using the automated sequencing facility at the University of Leicester PNACL.

2.3 RNA Manipulation

2.3.1 RNA extraction from tissue and cells

RNA was extracted from tissue using the RNeasy Maxi kit (Qiagen) by following the manufacturer's protocol.

Cell culture media was removed and total RNA was extracted using TRIzol (Invitrogen) by following the manufacturer's protocol.

Quantification of RNA was performed as described in section 2.2.4 except that an A_{260} of 1 was equivalent to 40 μg RNA/ml. The concentration of RNA in ng/μl was calculated as follows:

40 μg/ml × A_{260} × dilution factor

2.3.2 Deoxyribonuclease I (DNase I) treatment of RNA

1 μg total RNA was DNase I (Sigma) treated following the manufacturer's protocol and then cDNA synthesis by Reverse Transcription (RT) was performed as stated below.

2.3.3 cDNA synthesis by Reverse Transcription (RT)

1 μl oligo dT (0.5 μg) and 1 μl of a 10 mM dNTP mix (final concentration of 0.5 mM each) was added to the DNase I treated RNA and placed in a Perkin Elmer Cetus DNA thermal cycler at 70°C for 10 minutes. The reaction was then placed on ice for 1 minute and briefly centrifuged (pulse spin) to remove condensation. To the reaction, 4 μl of 5 × First strand buffer (Invitrogen), 2 μl of 0.1 M DTT (Invitrogen, final concentration of 10 mM) and 1 μl Superscript II enzyme (Invitrogen, 200 U) was added giving a total reaction volume of 20 μl. Controls (minus RT) were also included that contained 1 μl dH_2O instead of the 1 μl Superscript II enzyme (200 U). The reaction was then placed back in the thermal cycler for 42°C, 55 minutes; 70°C, 10 minutes; and then back on ice.

2.3.4 Semi-quantitative RT-PCR

The cDNA synthesised by RT was diluted 1:5 with dH_2O prior to semi-quantitative RT-PCR. Multiple reactions were performed in a master mix. A typical 20 µl reaction would contain the following:

1 µl	Template cDNA
1 µl	10 µM Forward Primer (final concentration of 0.5 µM)
1 µl	10 µM Reverse Primer (final concentration of 0.5 µM)
2 µl	Abgene 10 × buffer (final concentration in the reaction was 1 ×)
1.2 µl	Abgene 25 mM M_gCl_2 (final concentration of 1.5 mM)
2 µl	2 mM dNTP mix (final concentration of 0.2 mM)
0.3 µl	Abgene Taq polymerase (final concentration of 1.25 U)
dH_2O to a final volume of 20 µl	

A no template control was also included which contained 1 µl dH_2O instead of 1 µl template DNA. Ribosomal Protein L32 (RPL32) was used as a loading control. Oil (2 drops) was then placed on the top of each reaction and the tubes were placed in a Techne Techgene thermal cycler. The genes, ms1, GATA 4, ARC, myocardin, SRF, BNP, calcineurin, MEF2C, cardiac α-actin, and the loading control RPL32 were PCR-amplified using the forward and reverse primers shown in table 2.1. The thermocycling parameters were 1 cycle of 94°C, 2 minutes; see table 2.1 for the number of cycles of 94°C, 45 seconds; 59°C, 45 seconds; 72°C, 45 seconds; a final extension step was performed at 72°C for 5 minutes.

Primer	Sequence 5′ to 3′	Cycle Number
ms1 Forward Primer	GTGACAGCATAGACACAGAGGAC	
ms1 Reverse Primer	CACTGCTGCCACCTGCCTT	28
GATA-4 Forward Primer	CTGCGGCCTCTACATGAAGC	
GATA-4 Reverse Primer	CTGAATGTCTGGGACATGGA	29
ARC Forward Primer	CACTGGGCCTGAGTATGAAGC	
ARC Reverse Primer	CTGAACTGGGTGCCTCTGG	29
Myocardin Forward Primer	CCATCGCCTAACAACCATTACT	
Myocardin Reverse Primer	TCTGGCCTCCCGAAGATGC	26
SRF Forward Primer	GCATTCACAGTCACCAACCTGC	
SRF Reverse Primer	TCATTCACTCTTGGTGCTGTGGG	26
BNP Forward Primer	CACGATGCAGAAGCTGCTGG	
BNP Reverse Primer	ACAACCTCTGCCCGTCACA	32
Calcineurin Forward Primer	GGATACCCAGGGTTGATGTT	
Calcineurin Reverse Primer	CTCTCAGAAGGAATAATGTGCT	29
MEF2C Forward Primer	AGATAGTGTCATGTTGCAGGTTCA	
MEF2C Reverse Primer	CTCATGGCTTAGGGATGTGCTTTC	26
Cardiac α-actin Forward Primer	CACCACCGCTGAACGTGAAAT	
Cardiac α-actin Reverse Primer	GGAGCAATAATCTTAATCTTCAT	29
RPL32 Forward Primer	GTGAAGCCCAAGATCGTC	
RPL32 Reverse Primer	GAACACAAAACAGGCACAC	19

Table 2.1. Primer Sequences and optimised cycle number for each gene.

Samples were electrophoresed as described earlier in section 2.2.2.

Gel images were documented directly onto a PC and relative mRNA expression was analysed by band quantification (using gene tools from Syngene software) and corrected for RPL32.

2.3.4.1 Statistical analysis

Statistical analysis was carried out using a Student's *t* test. A P value < 0.05 was considered to be significant.

2.3.5 Real-time quantitative RT-PCR

Real-time quantitative RT-PCR was performed using either TaqMan® Gene Expression Assays (Applied Biosystems) and analysed using the comparative ($\Delta\Delta C_T$) method or using SYBR® Green with custom designed primers and analysed using the Pfaffl method.

2.3.5.1 Real-time quantitative RT-PCR using TaqMan® Gene Expression Assays and analysed using the comparative ($\Delta\Delta C_T$) method

The cDNA synthesised by RT (as described in section 2.3.3) was diluted 1:5 with dH_2O prior to real-time RT-PCR. Multiple reactions were performed in a master mix. A typical 20 µl reaction would contain the following:

1-2 µl Template cDNA

1 µl 20 × Pre-formulated assay mix (Applied Biosystems) containing:
2 unlabeled PCR primers (900 nM final concentration)
1 FAM™ dye-labeled TaqMan® MGB probe (250 nM final concentration). Final concentration in the reaction was 1 ×

10 µl 2 x TaqMan® Universal PCR Master Mix, No AmpErase® UNG (Applied Biosystems, final concentration in the reaction was 1 ×)

dH_2O to a final volume of 20 µl

Tata-binding protein (TBP) was used as a reference gene to normalise mRNA levels between different samples.

The reaction was carried out using the ABI Prism® 7900 HT sequence detection system. The thermal cycling conditions were set at 50°C for 2 minutes (hold step), 95°C for 10 minutes (hold step) and then the reaction ran for 40 cycles at 95°C for 15 seconds (denature) and 60°C for 1 minute (anneal/extend).

The data was analysed using the comparative ($\Delta\Delta C_T$) method (Livak and Schmittgen, 2001) using the formula:

Fold induction = $2^{-\Delta\Delta Ct}$

ΔC_T = mean $C_T^{(\text{gene of interest})}$ – mean $C_T^{(\text{reference gene})}$

$\Delta\Delta C_T = \Delta C_T^{(\text{unknown})} - \Delta C_T^{(\text{calibrator})}$

The calibrator sample (e.g. nontreated control sample) allows corrections to be made for inter-assay variation and represents 1 × expression of the gene of interest.

The formula is based on the assumption that the efficiency of the PCR for both the gene of interest and reference gene is identical with a doubling of product every cycle.

2.3.5.2 Real- time quantitative RT-PCR using SYBR® Green and analysed using the Pfaffl method

Relative mRNA quantification in real-time RT-PCR was analysed using the Pfaffl method (Pfaffl, 2001). The cDNA synthesised by RT (as described in section 2.3.3) was diluted 1:5 with dH_2O prior to real-time RT-PCR. Multiple reactions were performed in a master mix. A typical 25 µl reaction would contain the following:

0.01-3 µl	Template cDNA
0.5 µl	10 µM Forward Primer (final concentration of 0.2 µM)
0.5 µl	10 µM Reverse Primer (final concentration of 0.2 µM)
12.5 µl	2 × Power SYBR® Green PCR Master Mix, (Applied Biosystems, final concentration in the reaction was 1 ×)

dH_2O to a final volume of 25 µl

RPL32 was used as a reference gene to normalise mRNA levels between different samples.

The reaction was carried out using the ABI Prism® 7900 HT sequence detection system. The thermal cycling conditions were set at 95°C for 10 minutes (hold step) and then the reaction ran for 40 cycles at 95°C for 45 seconds, 59/62°C for 45 seconds, 72°C for 45 seconds and then a final step at 95°C for 15 seconds and 60°C for 1 minute. The primer sequences for the reference gene and genes of interest are given in table 2.2.

Primer	Sequence 5′ to 3′	Annealing Temperature (°C)
Interleukin 6 Forward Primer	TCAACTCCATCTGCCCTTCAG	59
Interleukin 6 Reverse Primer	AAGGCAACTGGCTGGAAGTCT	59
Coagulation factor III Forward Primer	CTTGGAGTGGCAACCGAAACC	59
Coagulation factor III Reverse Primer	GGTTCCTCCCCATGAGTTCCA	59
Adrenomedullin Forward Primer	AGAAGTGGAATAAGTGGGCGCT	62
Adrenomedullin Reverse Primer	ATGCCGTCCTTGTCTTTGTCTG	62
Leukemia inhibitory factor Forward Primer	GGATTGTGCCCCTAGTGCT	59
Leukemia inhibitory factor Reverse Primer	GGCAGTGGGGTTGAGGTTTT	59
Jun-B Forward Primer	ATCAGACACAGGCGCATCTC	59
Jun-B Reverse Primer	TCTTGTGCAGGTCGTCCAG	59
Fos-like antigen I Forward Primer	CAGGCGGAGACCGACAAGTT	59
Fos-like antigen I Reverse Primer	TGCAGTGCTTCCGGTTCAA	59
RPL32 Forward Primer	GTGAAGCCCAAGATCGTC	59
RPL32 Reverse Primer	GAACACAAAACAGGCACAC	59

Table 2.2. Primer Sequences and annealing temperature for each gene.

A series of cDNA dilutions were first generated to obtain a standard curve for the reference gene and gene of interest by plotting log of input cDNA verse C_T. From this the efficiency (E) was calculated according to the equation:

$E = 10^{[-1/slope]}$

The efficiency of the reference gene and gene of interest do not have to be equal, but are incorporated into the analysis, resulting in increased accuracy. Thus the relative expression ratio (fold change) is calculated as follows:

1. mean C_T values are determined for calibrator (e.g. nontreated control sample) and samples for the reference gene and gene of interest
2. gene of interest ΔC_p = mean gene of interest.C_T (calibrator) – mean gene of interest.C_T (sample)

3. reference gene ΔC_p = mean reference gene.C_T (calibrator) – mean reference gene.C_T (sample)

4. the values for efficiency of each gene is then raised to the power of the respective ΔC_p , and the ratio of gene of interest:reference gene is calculated using the formula:

$$\text{Ratio (fold change)} = \frac{\text{Efficiency (gene of interest)}^{\Delta Cp\ (\text{gene of interest})}}{\text{Efficiency (reference gene)}^{\Delta Cp\ (\text{reference gene})}}$$

The formula makes the assumption that while the efficiencies of the reference gene and gene of interest may differ, the efficiency of amplification for each sample within a PCR reaction is the same.

2.3.5.3 Statistical analysis

Statistical analysis was carried out using a Student's *t* test. A P value < 0.05 was considered to be significant.

2.4 Protein Manipulation

2.4.1 Extraction of proteins from cultured mammalian cells

M-PER Mammalian Protein Extraction reagent (Pierce) was used to extract proteins from H9c2 cells following transfection as described following the manufacturers instructions. 1 × Complete mini protease inhibitor cocktail (Roche) was added to the reagent before proceeding with the cell lysis to inhibit proteases to ensure that the protein of interest remains intact.

2.4.2 Quantification of Protein

Protein was quantified using the Bio-Rad Protein Assay (Bio-Rad) as instructed by the manufacturer. The protein standard used was bovine serum albumin (BSA) at concentrations of 0.2 μg/μl, 0.4 μg/μl, 0.6 μg/μl, 0.8 μg/μl and 1.0 μg/μl. The total volume used for each standard and sample was 20 μl. The amount of diluted dye reagent added to each was 1 ml.

2.4.3 Western blotting

This method was based on a previous method described (Bollag *et al.*, 1996; Sambrook *et al.*, 1989). To 15 μg protein, a half volume of 3 × loading buffer (188 mM Tris-HCl

(pH 6.8), 6% (v/v) Sodium dodecyl sulfate (SDS), 30% (v/v) Glycerol, 15% (v/v) β-mercaptoethanol, 0.03% (w/v) bromophenol blue) was added. Samples were then boiled (100°C) for 5 minutes prior to loading onto an appropriate percentage SDS-Polyacrylamide gel. Samples were run alongside a SeeBlue Plus2 pre-stained standard (Invitogen) in gel running buffer (25 mM Tris, 250 mM Glycine, 0.1% (v/v) SDS) at a constant current of 10 mA overnight.

When the SDS-polyacrylamide gel had run to completion the proteins were transferred from the gel to a Protran nitrocellulose transfer membrane (Schleicher and Schuell BioScience) at a constant current of 400 mA for 3 hours using a wet module system (Bio-rad trans-blot cell) containing transfer buffer (48 mM Tris, 39 mM Glycine, 0.0375% (v/v) SDS, 20% Methanol) that was surrounded by ice. Membranes were stored dry until ready to process further.

Ponceau S solution (enough to just cover the membrane, Sigma) was used to stain the membrane to check there was protein on the membrane. This solution was washed off prior to blocking the membrane with three 5 minute washes in TBS-T pH 7.6 (20 mM Tris, 137 mM NaCl, 0.1% (v/v) Tween-20). The membrane was then blocked for 1 hour at room temperature with shaking in TBS-MT (TBS-T, 5% (w/v) skimmed milk powder (Somerfield)). Next the membrane was incubated with the primary antibody diluted in TBS-MT at 4°C overnight with shaking. After this three 5 minute washes in TBS-T were carried out at room temperature with shaking prior to incubation with the secondary antibody (carrying a horseradish peroxidase (HRP) conjugate, Amersham) for 1 hour at 4°C with shaking. A further three 5 minute washes in TBS-T at room temperature with shaking were carried out and then enhanced chemiluminescence (ECL) was performed using an ECL Advanced Western blotting detection kit (Amersham) as stated by the manufacturer's instructions. The luminescent signal created was detected on Hyperfilm ECL (Amersham).

Developed films were scanned into a PC and relative protein expression was analysed by band quantification (using gene tools from Syngene software) and corrected for α-tubulin.

The primary antibodies used were the loading control α-tubulin (Tu-02) mouse monoclonal (1:1000, Santa Cruz Biotechnology Inc.), msl (rabbit C-48 polyclonal, 1:250, Pepceuticals Ltd), c-Myc (9E10) mouse monoclonal (1:200, Santa Cruz

Biotechnology Inc.), phospho-Akt (Ser473) (193H12) rabbit monoclonal (1:1000, Cell Signalling Technology Inc.), phospho-p44/42 MAPK (Thr202/Tyr204) (197G2) rabbit monoclonal (1:1000, Cell Signalling Technology Inc.) and Akt2 (5B5) rabbit monoclonal (1:1000, Cell Signalling Technology Inc.).

2.4.3.1 Statistical analysis

Statistical analysis was carried out using a Student's *t* test. A P value < 0.05 was considered to be significant.

2.4.4 Immunofluorescence

Approximately 40,000 H9c2 cells/well of a 6 well plate were plated out onto ethanol treated coverslips. Cells were left for 48 hours to attach onto the coverslips and then transfected as described in section 2.5.2. Cells were left for 24 or 72 hours and then fixed and permeabilised using a Leucoperm kit (Serotec) by following the manufacturer's protocol. During permeabilisation mouse anti c-Myc fluorescein isothiocyanate (FITC) (Serotec) was added at a 1:10 dilution in phosphate buffered saline (PBS) and left for 30 minutes at room temperature in the dark. After this three 5 minute washes in PBS at room temperature were carried out and then Alexa fluor 350 phalloidin (Invitrogen) was added at a 1:40 dilution in 1% BSA (in PBS) and left for 20 minutes at room temperature in the dark. Following this three 5 minute washes in PBS at room temperature were carried out. Coverslips were mounted onto slides using Prolong Gold Antifade (Invitrogen). Images were captured using a Nikon Eclipse TE2000-E microscope and processed using Volocity 4 software (Improvision).

2.4.5 LacZ expression in mammalian cells by histochemical staining

NIH3T3 cells were left untransfected or transfected as described in section 2.5.2 with 1 μg of the empty vector (pi Z/EG) or the ms1 transgene (pi Z/EG-ms1). Staining of transiently transfected cells began following 48 hours of transfection using the BetaBlue Staining Kit (Novagen) by following the manufacturer's instructions. Images were viewed using an Olympus CKX41 microscope and photographed using a Nikon MXA 5400 digital camera.

2.4.6 GFP Visualisation in mammalian cells

NIH3T3 cells were left untransfected, transfected as described in section 2.5.2 with 1 μg of the empty vector (pi Z/EG) or the ms1 transgene (pi Z/EG-ms1) or the pCre-Pac

vector (Taniguchi *et al.*, 1998) (appendix 1) or co-transfected with 1 μg of the empty vector (pi Z/EG) and 1 μg of the pCre-Pac vector or with 1 μg of the ms1 transgene (pi Z/EG-ms1) and 1 μg of the pCre-Pac vector. GFP fluorescence was observed following 48 hours of transfection via a FITC filter, using a Zeiss Axiovert 135 microscope. Images were captured using a C14 digital camera.

2.5 Cell Culture

2.5.1 Cell Maintenance

The H9c2 cell line derived from the embryonic rat ventricle was obtained from the European Collection of Cell Cultures and NIH3T3 cells (murine embryonic fibroblasts) were purchased from the American Type Culture Collection and cultured in Dulbecco's Modified Eagle's Medium (Invitrogen) supplemented with 10% fetal bovine serum (Invitrogen), 100 U/ml penicillin (Invitrogen) and 100 μg/ml streptomycin (Invitrogen). Cells were grown and passaged regularly in a tissue culture 80 cm^2 filter cap flask (Nunc) in an atmosphere of 5% CO_2/95% humidified air at 37°C.

2.5.2 Transfection

Approximately 40,000 H9c2 cells/well or 20,000 NIH3T3 cells/well of a 6 well plate were plated out so that cells were about 50% confluent 48 hours later for transfection. 1 μg DNA of pcDNA3.1(+) containing c-Myc tagged ms1 (pcDNA3.1(+) + ms1) or the empty expression vector control (pcDNA3.1(+)) was transfected using the JetPEI Cationic Transfection Reagent (Qbiogene) as stated by the manufacturer's protocol.

2.6 Flow cytometric analysis

2.6.1 Cell size

H9c2 cells were left untransfected or transfected as stated in section 2.5.2 except that approximately 100,000 cells/25 cm^2 filter cap flask were plated to obtain cells that were about 50% confluent 48 hours later for transfection using 3 μg DNA. Cells were left for 24 or 72 hours following transfection and then cells were washed once with trypsin-EDTA (0.05% trypsin, 0.53 mM EDTA (BioWhittaker)), incubated with trypsin-EDTA for a few minutes and subjected to gentle agitation to detach cells from the flask. 2.5 ml Dulbecco's Modified Eagle's Medium (Invitrogen) supplemented with 10% fetal bovine serum (Invitrogen), 100 U/ml penicillin (Invitrogen) and 100 μg/ml streptomycin (Invitrogen) was then added and the cells were collected into a 20 ml sterilin. Cells

were then centrifuged at 1200 rpm for 5 minutes at room temperature. Following centrifugation the supernatant was removed, cells were washed with PBS and then centrifuged at 1200 rpm for 5 minutes at room temperature. The supernatant was removed and cells were re-suspended in 1 ml PBSA (PBS containing 0.03% (w/v) Sodium Azide and 0.2% (w/v) BSA). Viable cells were counted using 0.4% Trypan blue solution (Sigma) and a haemocytometer chamber where 10 µl of cells were added to 10 µl of Tryphan blue, this was mixed and 10 µl of this cell suspension was added to the haemocytometer. Cells that were live appeared translucent and dead cells appeared blue. Cells were counted in the four 0.1 mm^3 corner squares of the haemocytometer, averaged, multiplied by 2 and then multiplied by 10^4 to give the number of cells per ml. Cells were adjusted to have at least 1×10^5 cells in 100 µl PBSA.

Next cells were fixed and permeabilised using a Leucoperm kit (Serotec) by following the manufacturer's protocol. During permeabilisation mouse anti c-Myc fluorescein isothiocyanate (FITC) antibody (Serotec) was added at a 1:10 dilution in PBS and left for 30 minutes at room temperature in the dark.

Cells were analysed using a Beckman Coulter Epics XL·MCL flow cytometer and System II software. Cells were passed through a laser beam where the emission wavelength is 488 nm and analysed for size (forward scatter) and granularity (side scatter). The c-Myc FITC fluorescence of individual cells was measured and the data were registered on a logarithmic scale. This gave two cell populations comprising of cells that were and were not green. The total number of cells, the number of cells that were not green and the number of cells that were green were counted and presented as percentages. From these two populations cell size (forward scatter) of individual cells was measured and the data were registered on a linear scale and presented as the median thus allowing the median cell size of untransfected cells (not green) versus ms1 transfected cells (green) to be compared.

2.6.1.1 Statistical analysis

Statistical analysis was carried out using a Student's *t* test. A P value < 0.05 was considered to be significant.

2.6.2 Detection of DNA fragmentation (apoptosis)

The assay was based on a method previously described using propidium iodide (Nicoletti *et al.*, 1991). Cells were transfected as described in section 2.6.1 and

following transfection for 24 hours, cells were treated with 5 nM staurosporine (Sigma) for 24 hours and then collected, fixed and permeabilised as described in section 2.6.1 except that Hanks' balanced salt solution (HBSS (Invitrogen)) was used instead of PBS. Following permeabilisation and addition of the mouse anti c-Myc FITC antibody, cells were washed in HBSS and centrifuged at 1200 rpm for 5 minutes at room temperature. The supernatant was then removed and cells were re-suspended in 900 µl HBSS. To a 900 µl cell sample 100 µl RNAse (1 mg/ml, Sigma) and 1 µl Vybrant DyeCycle Violet Stain (Invitrogen) was added. The sample was gently mixed and incubated in the dark at 37°C for 30 minutes.

Cells were measured using a DakoCytomation CyAn ADP flow cytometer and analysed using Summit v4.3 software. Cells were analysed as described in section 2.6.1 except that the violet fluorescence of individual cells was also measured in addition to the c-Myc FITC fluorescence of individual cells. The violet fluorescence was collected due to violet staining of DNA content and the data were registered on a linear scale. Cell cycle analysis based on measurements on DNA content generates a clear distribution where normal populations of growing cells have either one set of paired chromosomes per cell (G_0/G_1 phase of cell cycle), an intermediate amount of DNA, DNA synthesis (S phase), or two sets of paired chromosomes per cell, prior to cell division (G_2/M phase). During apoptosis the DNA of the cell fragments and following fixation and permeabilisation, the low molecular weight DNA inside the cytoplasm of apoptotic cells elutes during the wash procedure. Therefore, following staining with the violet dye, cells with lower DNA content contain less DNA stained and thus cells with lower DNA staining than that of G_1 cells show a sub-G_1 peak and are considered apoptotic (Nicoletti *et al.*, 1991; Telford *et al.*, 1991; Telford *et al.*, 1992). The percentage of apoptotic cells was determined on the basis of the number in the sub-G_1 peak in the DNA violet fluorescence histogram thus allowing the percentage of apoptotic untransfected cells (not green) versus the percentage of apoptotic ms1 transfected cells (green) to be compared.

2.6.2.1 Statistical analysis

Statistical analysis was carried out using a Student's *t* test. A P value < 0.05 was considered to be significant.

2.7 Genetic Manipulation

2.7.1 Pronuclear microinjection

Prior to pronuclear microinjection the ms1 transgene was linearised at the *Sfi*I and *Sca*I sites by restriction digest to remove the plasmid back bone. The linearised plasmid DNA (ms1 transgene) was electroeluted, precipitated and purified through 2 clean up columns, QIAquick Nucleotide Removal Column (Qiagen) and Bio-Spin P-30 Column (Bio-Rad). The DNA was finally eluted in Injection Buffer (5 mM Tris-HCl pH 7.4, 0.1 mM EDTA) made with embryo grade solutions. These procedures were performed by S Munson at the Embryonic Stem Cell Facility, University of Leicester.

The ms1 transgene was then injected into the pronucleus of day 1 post-fertilisation oocytes by a continuous flow method of injection using the Eppendorff Femtojet system until pronuclear swelling was observed. Surviving oocytes were reimplanted into the oviducts of pseudopregnant females. This was performed by J Brown at the University of Leicester transgenic unit.

2.7.2 Animal husbandry

Mice were housed in internationally ventilated cages (Allentown). Bedding was aspen and sizzle nest and environmental enrichment products were mouse corner houses and fun tunnels. Water and diets were given ad lib. Diets were supplied by Special Diets Services. Mice were routinely maintained on Rat and Mouse No. 1 Maintenance (RM1) which contains 0.25% sodium, corresponding to approximately 0.7% sodium chloride. Lactating females were maintained on a higher protein diet (RM3).

2.7.3 Generation and identification of ms1 transgenic mice by PCR and Southern blotting

2.7.3.1 PCR analysis

For PCR analysis, at 4-6 weeks (following weaning) genomic DNA was extracted from an ear punch of the mouse (or yolk sac when staining embryos for lacZ) using the GenElute Mammalian Genomic DNA Miniprep kit (Sigma) as stated by the manufacturer's protocol. The mice were screened to assess inheritance of the ms1 transgene by PCR using lacZ and GFP vector specific primers. Interleukin 2 (IL-2) was used as an internal control.

The PCR reaction using the lacZ primers would contain the following:

2 µl Template DNA

2 µl 10 µM Forward Primer (final concentration of 1 µM)

2 µl 10 µM Reverse Primer (final concentration of 1 µM)

2 µl Qiagen 10 × buffer including 15mM $MgCl_2$ (final concentration in the reaction was 1 × buffer including 1.5mM $MgCl_2$)

2 µl 2 mM dNTP mix (final concentration of 0.2 mM)

0.1 µl 5 Uµl Qiagen HotStarTaq DNA Polymerase (final concentration of 0.5 U)

dH_2O to a final volume of 20 µl

Oil (2 drops) was then placed on the top of each reaction and the tubes were placed in a Techne Techgene thermal cycler. The thermocycling parameters were 1 cycle of 96°C , 15 minutes; 35 cycles of 96°C, 30 seconds; 59°C, 1 minute; 72°C, 1 minute; a final extension step was performed at 72°C for 5 minutes.

The PCR reaction using the GFP primers would contain the following:

2 µl Template DNA

1 µl 10 µM Forward Primer (final concentration of 0.5 µM)

1 µl 10 µM Reverse Primer (final concentration of 0.5 µM)

2 µl Qiagen 10 × buffer including 15mM $MgCl_2$ (final concentration in the reaction was 1 × buffer including 1.5mM $MgCl_2$)

2 µl 2 mM dNTP mix (final concentration of 0.2 mM)

0.2 µl 5 U/µl Qiagen HotStarTaq DNA Polymerase (final concentration of 1 U)

1 µl Dimethyl sulfoxide (DMSO) (final concentration of 5%)

dH_2O to a final volume of 20 µl

Oil (2 drops) was then placed on the top of each reaction and the tubes were placed in a Techne Techgene thermal cycler. The thermocycling parameters were 1 cycle of 96°C , 15 minutes; 35 cycles of 96°C, 45 seconds; 57°C, 1 minute; 72°C, 1 minute; a final extension step was performed at 72°C for 5 minutes.

The PCR reaction using the IL-2 primers contained the following:

0.5 µl Template cDNA

1 µl 10 µM Forward Primer (final concentration of 0.5 µM)

1 µl 10 µM Reverse Primer (final concentration of 0.5 µM)

2 µl Abgene 10 × buffer (final concentration in the reaction was 1 ×)

1.2 µl Abgene 25 mM M_gCl_2 (final concentration of 1.5 mM)

2 µl 2 mM dNTP mix (final concentration of 0.2 mM)

0.3 µl Abgene *Taq* polymerase (final concentration of 1.25 U)

dH_2O to a final volume of 20 µl

Oil (2 drops) was then placed on the top of each reaction and the tubes were placed in a Techne Techgene thermal cycler. The thermocycling parameters were 1 cycle of 94°C , 1.5 minutes; 35 cycles of 94°C, 30 seconds; 60°C, 1 minute; 72°C, 1 minute; a final extension step was performed at 72°C for 2 minutes.

A no template control was included with all PCR reactions which contained 1 µl dH_2O instead of 1 µl template DNA. DNA from a mouse known to inherit the transgene was included as a positive control and DNA from a mouse known not to carry the transgene was used as a negative control.

All samples were electrophoresed as described earlier in section 2.2.2.

The primer sequences used are listed below in table 2.3.

Primer	**Sequence 5′ to 3′**
LacZ Forward Primer	ACTCTGGCTCACAGTACGCGT
LacZ Reverse Primer	CAGCGTTCGACCCAGGCGT
GFP Forward Primer	CCTACGGCAAGCTGACCCTGA
GFP Reverse Primer	ACGCTGCCGTCCTCGATGT
IL-2 Forward Primer	CTAGGCCACAGAATTGAAAGATCT
IL-2 Reverse Primer	GTAGGTGGAAATTCTAGCATCATCC

Table 2.3. Primer Sequences.

2.7.3.2 Southern blot analysis

For Southern blot analysis (Southern, 1975), 10 µg genomic DNA was extracted from mouse liver tissue using the GenElute Mammalian Genomic DNA Miniprep kit (Sigma)

as stated by the manufacturer's protocol. Genomic DNA (10 μg) was digested with *Sst*I or *Eco*RV and separated on a 0.6% agarose gel in 1 × TAE (Invitrogen) at 100 V for 30 minutes, 30 V overnight. After electrophoresis, agarose gels were depurinated for 10 minutes at room temperature with gentle agitation in 0.25 M HCl, denatured for 30 minutes at room temperature with gentle agitation in denaturisation solution (0.5 M NaOH, 1.5 M NaCl) and neutralised for 30 minutes at room temperature with gentle agitation in neutralisation solution (0.5 M Tris-HCl, 3 M NaCl, pH 7.5). DNA was then transferred from the agarose gel onto Hybond N membrane (Amersham) in 10 × Sodium saturated citrate (SSC), 1.5 M NaCl, 0.15 M Sodium citrate, pH 7 for approximately 24 hours. Membranes were then cross linked for 1 minute in a UV cross linker (120,000 microjoules/cm^2) and rinsed briefly in 2 × SSC.

The ^{32}P-labelled probe was a 655 bp *Not*I-*Bam*HI fragment generated by restriction digest (section 2.2.7) that includes the rabbit β-globin polyadenylation sequence of the pi Z/EG vector. 20 ng of probe DNA was labelled with approximately 50 μCi [α^{32}P]dCTP using the RadPrime DNA Labeling System (Invitrogen) following the manufacturer's instructions. Unincorporated nucleotides were removed using the Qiagen Nucleotide removal kit as stated by the manufacturer's protocol. Hybridisation was carried out in a Hybaid oven using Hybaid bottles and wire meshes. Membranes were placed onto the wire meshes (DNA facing upwards) and rolled up and placed into the Hybaid bottles. Membranes were pre-hybridised for 1 hour at 42°C in hybridisation buffer (0.5% (w/v) milk powder, 60 mg/ml Polyethylene glycol (PEG), 1 × SSPE (0.15 M NaCl, 0.2 mM Na_2PO_4, 1 mM EDTA, pH 7.4), 1% SDS) with gentle rotation and then the labelled probe was added to fresh hybridisation buffer, added to the membrane and left rotating overnight at 42°C.

After hybridisation the membranes were washed in 5 x SSC at 42°C for 10 minutes. The Geiger counter was used to assess if further washes were required to remove excess radioactivity. If further washes were require to remove excess radioactivity the membranes were washed in 3 x SSC at 42°C for 10 minutes.

The membrane was then left exposed to film (Kodak) overnight at -80°C and then developed.

2.7.4 ms1 breeding colony

Positive founder mice that were identified to have inherited the ms1 transgene (ms1 transgenic) by PCR and Southern blotting were then bred with C57BL6 mice to establish a breeding colony. Lines that showed successful germ-line transmission of the ms1 transgene were chosen to cross further to create more breeding lines so enough mice were available for subsequent experiments. Positive offspring were identified using PCR analysis as discussed above.

2.7.5 LacZ expression in embryos/tissues by histochemical staining and semi-quantitative RT-PCR

Embryos at E10.5 were rinsed in PBS and then fixed for 8 minutes in lacZ fix (2% (w/v) paraformaldehyde and 0.2% (v/v) glutaraldehyde in PBS). Following fix, embryos were washed three times for 5 minutes in lacZ wash buffer (0.1% (v/v) sodium deoxycholate, 0.02% (v/v) nonidet-P40, 2 mM M_gCl_2 in 100 mM sodium phosphate, pH 7.3). Staining was carried out in 1 mg/ml X-gal, 6 mM potassium ferrocyanide, 5 mM potassium ferricyanide in lacZ wash buffer at 37°C overnight with protection from light. After completion of staining, embryos were washed twice for 5 minutes in PBS, fixed in lacZ fix for 15 minutes and stored in 70% ethanol at 4°C.

ms1 transgenic mice (F_2) at approximately 8 weeks of age from each line were visualised for lacZ expression in tissue slices of the liver, kidney and heart compared to a littermate wild type control by using the BetaBlue Staining Kit (Novagen). For those embryos and tissues expressing high levels of lacZ, a cytoplasmic blue colour appeared which determined expression of the ms1 transgene. Embryos and tissues were viewed using a LEICA M216F dissection microscope and photographed using a Nikon DXM1200 digital camera. ms1 transgenic mice from each line were also analysed for lacZ mRNA expression in the kidney of F_2 animals at approximately 8 weeks of age compared to a littermate wild type control by semi-quantitative RT-PCR using the lacZ PCR conditions as stated in section 2.7.3. RPL32 was used as an internal control. Primers used were RPL32 forward (5′GTGAAGCCCAAGATCGTC-3′) and RPL32 reverse (5′CATCAGCAGCACCTCCAGC-3′). PCR conditions used are as stated in section 2.3.4.

2.7.6 MLC2v Cre breeding colony

The MLC2v Cre mouse breeding colony was already established at the University of Leicester transgenic unit and was initially obtained from K R Chien (Chen *et al.*, 1998b). Mice at generation 18 were bred with C57BL6 mice to carry on the breeding line and create our own breeding colony to use to cross with the ms1 transgenic line.

2.7.7 Identification of MLC2v Cre positive mice

DNA was extracted from an ear punch of the mouse at 4-6 weeks following weaning using the GenElute Mammalian Genomic DNA Miniprep kit (Sigma) as stated by the manufacturer's protocol. Cre positive mice were identified by PCR. Primers used were Cre forward (5'GTTCGCAAGAACATGATGGACA-3') and Cre reverse (5'CTAGAGCCTGTTTTGCACGTTC-3') (Chen *et al.*, 1998b).

The PCR reaction contained the following:

2 µl Template DNA

1 µl 10 µM Forward Primer (final concentration of 1 µM)

1 µl 10 µM Reverse Primer (final concentration of 1 µM)

2 µl Qiagen 10 × buffer including 15mM $MgCl_2$ (final concentration in the reaction was 1 × buffer including 1.5mM $MgCl_2$)

2 µl 2 mM dNTP mix (final concentration of 0.2 mM)

0.1 µl 5 Uµl Qiagen HotStarTaq DNA Polymerase (final concentration of 0.5 U)

dH_2O to a final volume of 20 µl

A no template control was included with all PCR reactions which contained 1 µl dH_2O instead of 1 µl template DNA. DNA from a mouse known to carry the Cre locus was included as a positive control and DNA from a mouse known not to carry the Cre locus was used as a negative control.

Oil (2 drops) was then placed on the top of each reaction and the tubes were placed in a Techne Techgene thermal cycler. The thermocycling parameters were 1 cycle of 95°C, 15 minutes; 35 cycles of 94°C, 30 seconds; 66°C, 1 minute; 72°C, 1 minute; a final extension step was performed at 72°C for 10 minutes.

IL-2 was used as an internal control and the primer sequences and thermocycling parameters for IL-2 are stated in section 2.7.3.1

All samples were electrophoresed as described earlier in section 2.2.2.

2.7.8 Identification of double transgenic mice carrying the msl transgene and Cre locus

The two lines of transgenic mice (msl and MLC2v Cre) were mated to generate selective expression of msl in the heart. At 4-6 weeks following weaning DNA was extracted from an ear punch of the mouse using the GenElute Mammalian Genomic DNA Miniprep kit (Sigma) by following the manufacturer's instructions. Mice carrying the msl transgene and the Cre locus were identified by PCR using GFP primers (section 2.7.3.1) and Cre primers (section 2.7.7) respectively.

2.7.9 Cardiac over-expression of msl detected by semi-quantitative RT-PCR and GFP Immunostaining

Positive founder mice that were identified to have inherited the msl transgene and Cre locus (double transgenics) by PCR were then analysed by semi-quantitative RT-PCR for msl over-expression (section 2.3.4) and GFP expression (section 2.7.3.1) in the heart compared to littermate wild type and msl transgenic (transgenic mouse that carries the msl transgene) controls. RPL32 was used as an internal control. Primers used were RPL32 forward (5′GTGAAGCCCAAGATCGTC-3′) and RPL32 reverse (5′CATCAGCAGCACCTCCAGC-3′). PCR conditions used are as stated in section 2.3.4.

GFP Immunostaining was performed on hearts from mice that were identified to have inherited the msl transgene and Cre locus (double transgenics) compared to a transgenic mouse that carries the msl transgene (msl transgenic) that acts as a control. Hearts were rinsed in PBS and fixed in 4% (w/v) paraformaldehyde at room temperature with shaking overnight and then stored in 70% ethanol at 4°C until ready to process in paraffin wax.

Paraffin wax processing was performed by J Edwards, MRC Toxicology Unit, University of Leicester where the tissue was processed through a series of steps to dehydrate, clear and to wax impregnate the tissue. This was carried out using a Shandon Citadel 2000 where the tissue was in 70% Industrial Methylated Spirit (IMS) for 2 hours, 90% IMS for 2 hours, 100% IMS for 2 hours, 100% IMS for 2 hours, 100% IMS

for 2 hours, 100% IMS for 1 hour, 100% IMS for 1 hour, chloroform for 2 hours, chloroform for 2 hours, chloroform for 2 hours, wax for 2 hours and wax for 2 hours. Next the tissue was embedded in paraffin wax, cooled and stored at 4°C until ready to section.

Sections were cut at 5 microns using the LEICA RM 2135 microtome. Paraffin sections were then stained for GFP which included an extra section per sample to act as a 2°ry antibody only control (not incubated with the 1°ry antibody) and a section known to stain positive for GFP to act as a positive control. The paraffin wax was removed by submerging the sections twice in xylene for 10 minutes and then by removing the xylene by placing the sections twice in 100% ethanol for 10 minutes. Endogenous peroxidase was blocked by placing the sections in 0.18% (v/v) hydrogen peroxide in methanol for 10 minutes and then placed into dH_2O. Next antigen retrieval was carried out by placing the sections into pre-heated 0.01 M citrate buffer pH 6 in a pressure cooker and boiling for 15 minutes using a microwave. After the antigen retrieval sections were placed into dH_2O.

Sections were next incubated in 100 µl swine blocking serum (1:25, DakoCytomation) in PBS for 1 hour at room temperature in a humidifying chamber. The blocking serum was then removed from each section (except for the 2°ry antibody only control) and the sections were incubated in 100 µl of 1:200 1°ry antibody (rabbit GFP polyclonal antibody, Molecular Probes) in swine blocking serum at 4°C overnight in a humidifying chamber. Next the 1°ry antibody was removed from the sections and after this three 10 minute washes in PBS were carried out. The sections were then incubated in 100 µl of 1:500 biotinylated 2°ry swine anti-rabbit antibody (DakoCytomation) in PBS for 1 hour at room temperature in a humidifying chamber. Next the 2°ry antibody was removed from the sections and after this three 10 minute washes in PBS were carried out. The sections were then incubated in 100 µl of 1:500 streptavidin-HRP (DakoCytomation) in PBS for 45 minutes at room temperature in a humidifying chamber. Following this the strepdavidin-HRP was removed from the sections and after this three 10 minute washes in PBS were performed. Next PBS was removed from the sections and the sections were incubated in DAB peroxidase substrate (Vector Laboratories) for 2 minutes at room temperature and then the sections were place in dH_2O to wash. The sections were then dehydrated by placing the sections in 90% ethanol for 10 minutes, 100% ethanol

for 10 minutes and then sections were cleared in xylene and mounted using distrene-tri cresyl phosphate in xylene (DPX-type mountant).

For each sample a section was also stained for Haematoxylin and Eosin to show staining of nucleic acids and basic components in the cytoplasm. This was carried out by J Edwards, MRC Toxicology Unit, University of Leicester using a slide staining machine (Shandon Varistain 24-4) where the sections were incubated in xylene for 2 minutes, xylene for 3 minutes, IMS for 1 minute, IMS for 1 minute, 70% IMS for 1 minute, dH_2O for 1 minute, haematoxylin for 15 minutes, dH_2O for 1 minute, 1% acid alcohol for 25 seconds, dH_2O for 6 minutes, dH_2O for 1 minute, dH_2O for 2 minutes, 1% aqueous eosin for 3 minutes, dH_2O for 2 minutes, 70% IMS for 1 minute, IMS for 1 minute, IMS for 1 minute, IMS for 1 minute, IMS for 1 minute, xylene for 2 minutes and xylene for 5 minutes.

Sections were then mounted in DPX-type mountant. All sections were viewed using an Olympus CKX41 microscope and photographed using a Nikon MXA 5400 digital camera.

2.8 Appendix 1

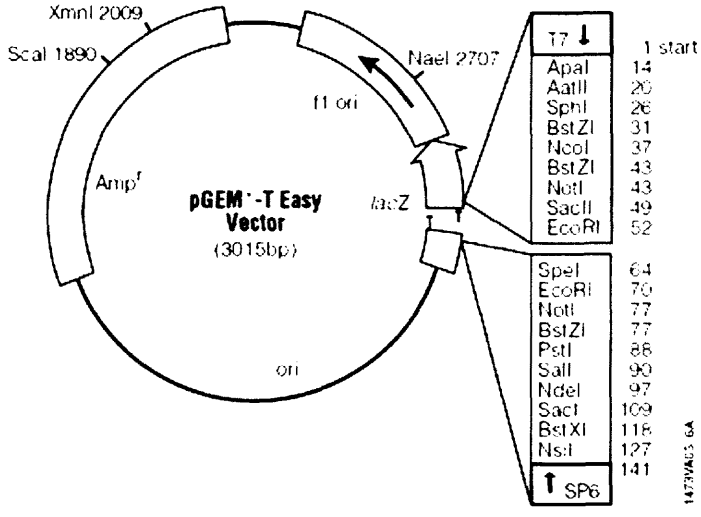

Figure 2.2. The main features of the pGEM-T Easy vector (Promega) used for the TA cloning of PCR amplification products.

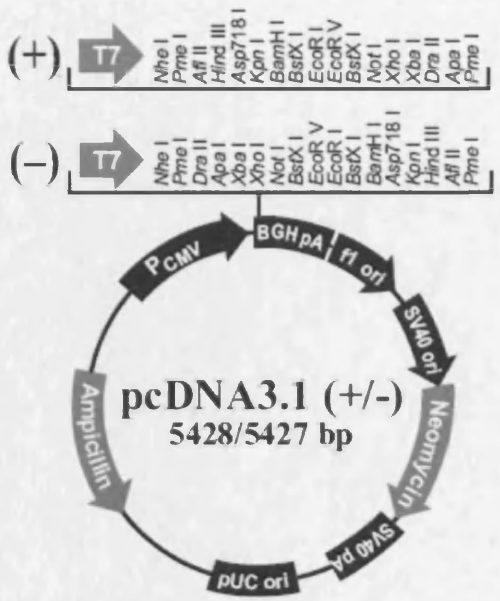

Figure 2.3. The main features of the expression vector pcDNA3.1(+) (Invitrogen) used to over-express ms1.

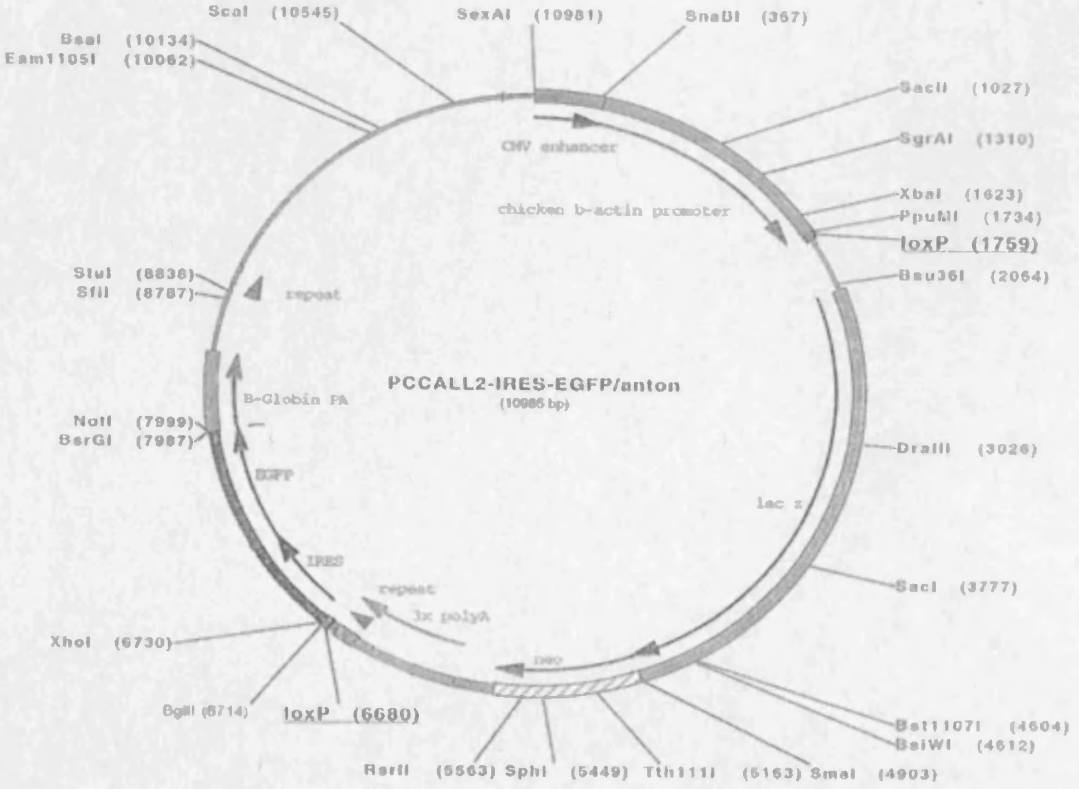

Figure 2.4. The pi Z/EG transgenic vector.

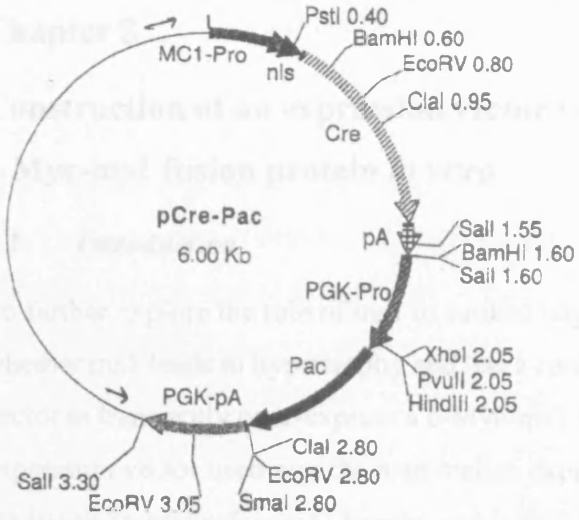

Figure 2.5. The pCre-Pac vector.

Chapter 3

Construction of an expression vector to transiently over-express a c-Myc-ms1 fusion protein *in vitro*

3.1 Introduction

To further explore the role of ms1 in cardiac physiology and disease, in particular whether ms1 leads to hypertrophy and has a cardioprotective role *in vitro*, an expression vector to transiently over-express a c-Myc-ms1 fusion protein was first generated. The expression vector used was the mammalian expression vector pcDNA3.1(+) that was kindly given by Professor G Brooks and is widely used for over-expression studies (Ekhterae *et al.*, 1999; Turner *et al.*, 1998). This vector is shown in appendix 1 of chapter 2. To generate an ms1 expression construct, the full-length coding sequence of mouse ms1 was amplified by PCR and cloned into the mammalian expression vector pcDNA3.1(+). A c-Myc tag is situated in the N-terminus before the coding sequence of ms1 and this modification has been previously used by others (Arai *et al.*, 2002; Barrientos *et al.*, 2007; Kuwahara *et al.*, 2005). The c-Myc tag allows ms1 expression to be detected by western blotting and immunocytochemical approaches using antibodies for the c-Myc tag.

The ms1 expression construct was transiently transfected *in vitro*, in a heart-derived rat cell line, H9c2 and ms1 mRNA and ms1 protein over-expression was examined by semi-quantitative RT-PCR and western blotting, respectively, to confirm that the ms1 expression construct generated worked and cells over-expressed a c-Myc-ms1 fusion protein. Transient ms1 over-expression in cells was also analysed by immunofluorescence using a fluorescent labelled antibody for the c-Myc tag.

The heart-derived rat cell line, H9c2, was chosen as an *in vitro* model system as this cell line has been widely used by others to investigate hypertrophy (Brostrom *et al.*, 2000; Huang *et al.*, 2004; Hwang *et al.*, 2006; Laufs *et al.*, 2002; Liu *et al.*, 2008) or cell death (Bonavita *et al.*, 2003; Chen *et al.*, 2000; Ekhterae *et al.*, 1999; Gustafsson *et al.*, 2004; Han *et al.*, 2004; Pesant *et al.*, 2006; Tanaka *et al.*, 2003; Turner *et al.*, 1998). The H9c2 cell line was established by the researchers, Kimes and Brandt (Kimes and Brandt, 1976) and is an immortalised cell line capable of proliferation and differentiation. Another *in vitro* model system would be the use of neonatal or adult mammalian cardiomyocytes in primary culture. Neonatal cardiac muscle cells can

divide in cell culture for a short period of time, but they ultimately withdraw permanently from the cell cycle, and adult cardiomyocytes can not divide and eventually die. Cardiomyocytes have been derived from embryonic stem cells (Doetschman *et al.*, 1985), P19 cells (Edwards *et al.*, 1983), and bone marrow stromal cells (Makino *et al.*, 1999) to establish cardiac muscle cell lines; however, these cells differentiated into different cell types in culture and therefore were not a homogenous cell population. Other cell lines such as the H9c2 cell line derived from rat embryonic heart tissue, has the ability to retain the properties of muscle cells. The H9c2 cells are strictly mononucleated myoblasts that resemble both skeletal and cardiac muscle myoblasts. At the myoblast stage, H9c2 cells express both myosin light chain 2 atrial (MLC2a) and MLC2v cardiac markers that are also expressed in newborn rat cardiac myocytes in primary culture (Menard *et al.*, 1999; Rybkin *et al.*, 2003). Upon reaching confluence they begin to form multinucleated tubular structures. Also the H9c2 cells adopted features of skeletal muscle because the cells expressed nicotinic receptors and synthesised a muscle-specific creatine phosphokinase isoenzyme when the mononucleated myoblasts fused. The lengths, diameter and arrangement into sarcomeres observed in myotubes of H9c2 have also been observed in the developing skeletal and heart muscle and the ability to generate action potentials and to contract in response to electrical stimulation is more evidence to suggest that H9c2 resemble skeletal and heart muscle cells and can serve as a model system for a variety of investigations (Kimes and Brandt, 1976).

The aim of the work presented in this chapter was to construct an expression vector to transiently over-express a c-Myc-msl fusion protein *in vitro* and to confirm msl over-expression by semi-quantitative RT-PCR, western blotting and immunofluorescence microscopy.

3.2 Results

3.2.1 Construction of an expression vector to transiently over-express a c-Myc-msl fusion protein

To generate a msl expression construct, firstly the full-length coding sequence of mouse msl was amplified by PCR from a plasmid termed pAlpha-MHCpromoter-msl sense (mouse) that was previously generated by H Mahadeva where restriction sites (*Bgl*II and *Xho*I) were included in the primers to allow cloning into the mammalian

expression vector pcDNA3.1(+). A c-Myc tag comprising of 30 nucleotide sequences corresponding to the 10 amino acid sequence, EQKLISEEDL was added to the N-terminus of the ms1 coding sequence by oligonucleotide-mediated mutagenesis with PCR where the c-Myc tag codon sequences were incorporated into the primers. This c-Myc tag was added to allow ms1 expression to be detected by using antibodies for the c-Myc tag. The amplified full-length ms1 coding sequence (figure 3.1) was then cloned into the pGEM-T Easy vector because this is one of the most convenient systems for cloning of PCR products.

Figure 3.1. The full-length ms1 coding sequence amplified by PCR.

Single putative transformant colonies were isolated, extracted for DNA and restriction digest confirmed that the pGEM-T Easy vector contained ms1 by producing the correct sized fragment for ms1 (approximately 1.3 kb) and correct sized band for the pGEM-T Easy vector (approximately 3 kb) which is shown in figure 3.2. Sequencing confirmed ms1 to be cloned into the pGEM-T Easy vector.

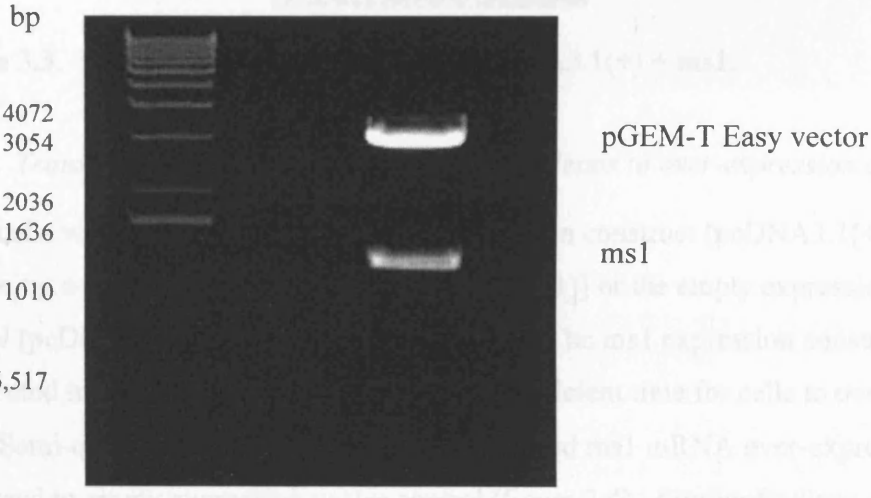

Figure 3.2. Restriction digest analysis of pGEM-T Easy + ms1.

The mammalian expression vector pcDNA3.1(+) and the pGEM-T Easy vector were both cut by the same restriction enzymes, *EcoR*I and *Xho*I. The full-length ms1 fragment (approximately 1.3 kb) was released from the pGEM-T Easy vector (approximately 3 kb) following the digest. The ms1 fragment and the pcDNA3.1(+) expression vector (approximately 5.4 kb) were agarose gel extracted and checked for DNA purity on an agarose gel before ligation of ms1 into pcDNA3.1(+). The purified ms1 fragment was then cloned into the gel extracted and purified mammalian expression vector pcDNA3.1(+).

Restriction digest confirmed that the pcDNA3.1(+) vector contained ms1 by producing the correct approximate 1.3 kb fragment for ms1 and approximately 5.4 kb for pcDNA3.1(+) which is shown in figure 3.3. Sequencing was also performed to verify that ms1 was cloned into the pcDNA3.1(+) vector.

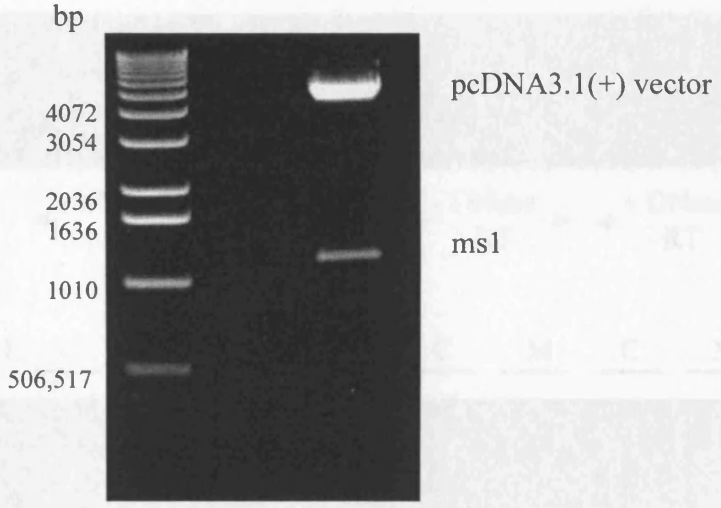

Figure 3.3. Restriction digest analysis of pcDNA3.1(+) + ms1.

3.2.2 Transient transfection for 24 and 72 hours leads to over-expression of ms1

H9c2 cells were transfected with the ms1 expression construct [pcDNA3.1(+) containing c-Myc tagged ms1 (pcDNA3.1(+) + ms1)] or the empty expression vector control (pcDNA3.1(+)) for either 24 or 72 hours. The ms1 expression construct was transfected in H9c2 cells for 72 hours to allow sufficient time for cells to over-express ms1. Semi-quantitative RT-PCR analysis confirmed ms1 mRNA over-expression compared to empty expression vector control (figure 3.4). Similar findings of ms1 mRNA over-expression were observed following transient transfection for 24 and 72

hours, where an example of this at 24 hours is shown in figure 3.4. Low ms1 expression was observed in the empty expression vector control samples (can not see this clearly on the image in figure 3.4) and ms1 was clearly over-expressed when compared to the empty expression vector control. RNA was DNase treated prior to cDNA synthesis and the reverse transcription enzyme was excluded during cDNA synthesis in order to separate ms1 mRNA from ms1 plasmid DNA. As shown in figure 3.4, there was no ms1 expression detected when the RNA was DNase treated and the enzyme was excluded. This suggests that DNase treatment of the RNA removed plasmid DNA contamination and confirms that the ms1 expression detected was ms1 mRNA over-expression and not from the ms1 expression plasmid. There was no RPL32 (internal control) expression when the reverse transcription enzyme was excluded, suggesting that genomic DNA contamination was not present in the RNA.

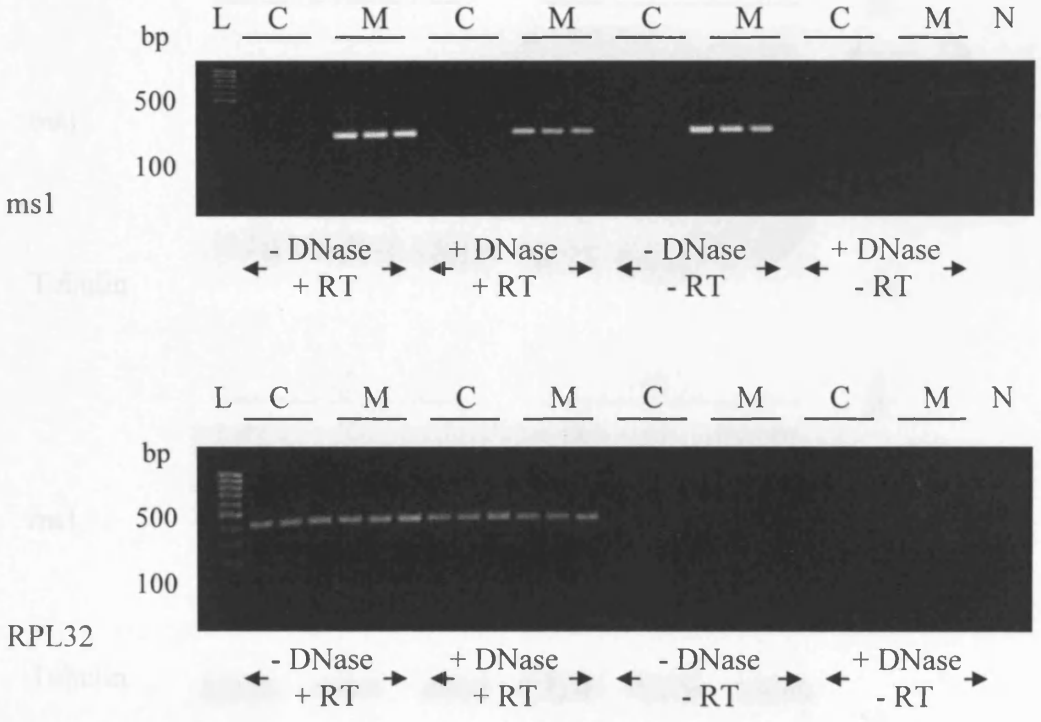

Figure 3.4. ms1 mRNA over-expression in H9c2 cells.

Semi-quantitative RT-PCR analysis of ms1 mRNA. RPL32 was used as an internal control for inaccuracies in initial RNA levels. C refers to the empty vector control (pcDNA3.1(+)) and M refers to the ms1 expression vector (pcDNA3.1(+) + ms1), n = 3. N refers to the no template control, L refers to the 100 bp DNA ladder and the band sizes (bp) are given. - DNase indicates that the RNA was not DNase treated prior to reverse transcription (RT), + DNase indicates that the RNA was DNase treated prior to RT, + RT indicates that the RT enzyme was present during cDNA synthesis and - RT indicates that the RT enzyme was omitted.

Western blot analysis using the ms1 and c-Myc antibodies confirmed ms1 protein over-expression compared to empty expression vector control following transient transfection for 24 hours (figure 3.5 (a) and 3.6 (a)) and 72 hours (figure 3.5 (b) and 3.6 (b)). The ms1 protein (approximately 45 kDa) appeared as a doublet on the blot consisting of two separate bands referred to as the top and bottom band of the doublet. When this doublet was detected using the ms1 antibody (figure 3.5 (a) and (b)), ms1 protein expression was observed in the empty vector controls (endogenous ms1 in H9c2 cells) for the top band of the doublet but not for the bottom band of the doublet and for the ms1 over-expression samples for the top and bottom bands of the doublet. This finding was apparent following transient transfection for both 24 and 72 hours.

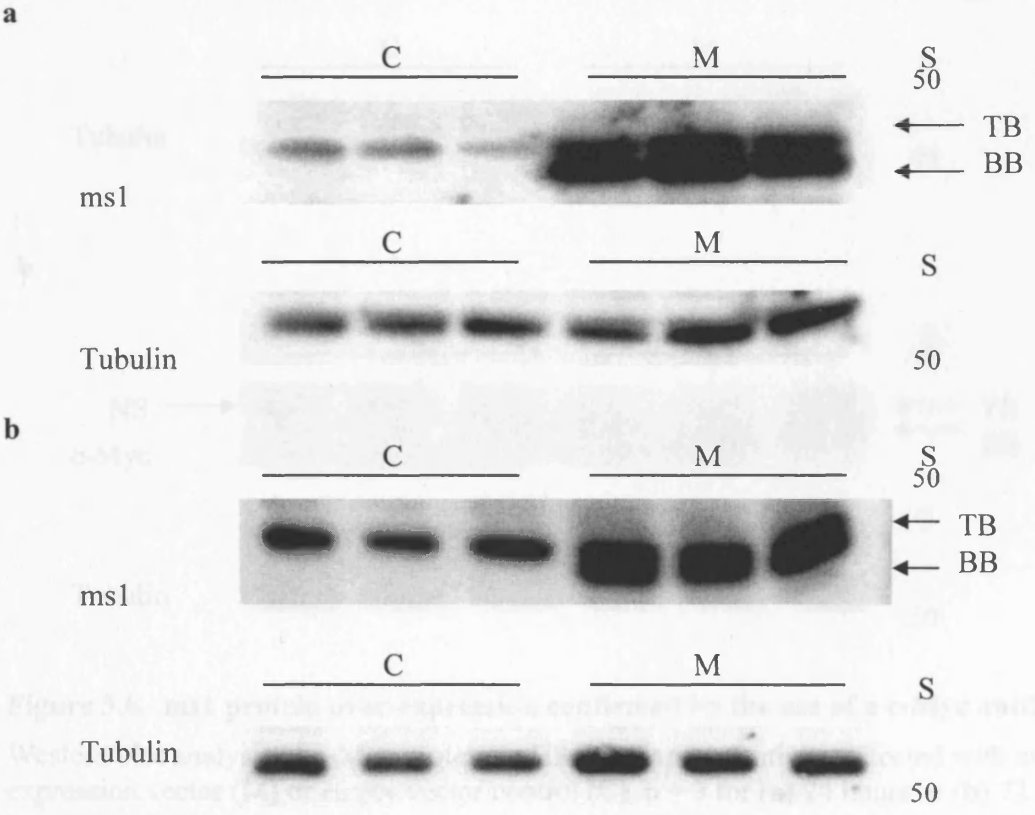

Figure 3.5. ms1 protein over-expression in H9c2 cells.

Western blot analysis confirms ms1 protein over-expression following **(a)** 24 hours and **(b)** 72 hours of transient transfection. α-tubulin was used as an internal control for inaccuracies in initial protein levels, C refers to the empty expression vector control (pcDNA3.1(+)) and M refers to the ms1 expression vector (pcDNA3.1(+) + ms1), n = 3. S refers to the SeeBlue Plus2 pre-stained standard and the molecular weights (kDa) are given to the right. TB refers to the top band of the doublet and BB refers to the bottom band of the doublet.

When the c-Myc antibody was used to confirm ms1 over-expression, c-Myc protein expression was not found in the empty vector controls but was for the ms1 over-expression samples for the top and bottom bands of the doublet indicating ms1 over-expression (figure 3.6). There was a faint band observed in the empty vector expression control samples from a 72 hour transfection that could be a non-specific band rather than the top band of the c-Myc protein doublet.

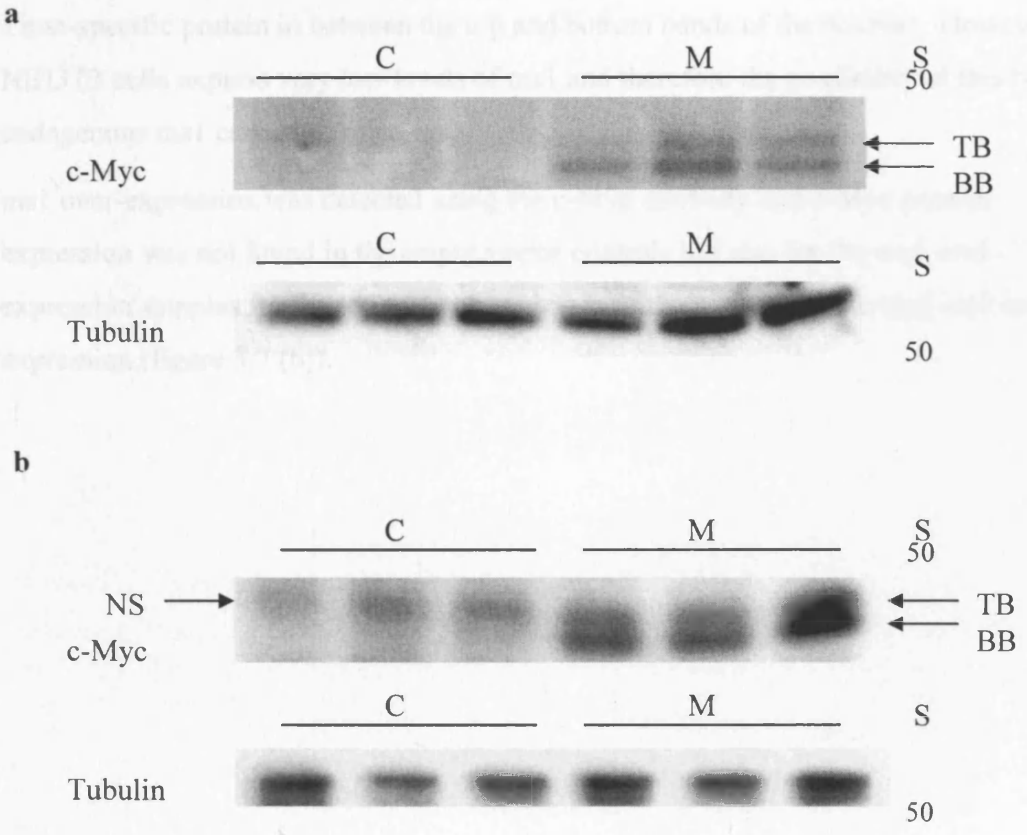

Figure 3.6. ms1 protein over-expression confirmed by the use of a c-Myc antibody. Western blot analysis of c-Myc protein in H9c2 cells transiently transfected with an ms1 expression vector (M) or empty vector control (C), n = 3 for (**a**) 24 hours or (**b**) 72 hours. α-tubulin was used as an internal control for inaccuracies in initial protein levels. S refers to the SeeBlue Plus2 pre-stained standard and the molecular weights (kDa) are given to the right. NS refers to non-specific bands, TB refers to the top band of the doublet and BB refers to the bottom band of the doublet.

To confirm the ms1 protein doublet, the ms1 expression construct was transfected into another cell line, NIH3T3, for 72 hours. ms1 is expressed at much lower levels in NIH3T3 cells (murine embryonic fibroblasts) than H9c2 cells (Ounzain, personal

communication). msl protein over-expression in NIH3T3 cells was detected by western blotting using both the msl and c-Myc antibodies (figure 3.7) and the msl protein appeared as a doublet on the blot as previously observed in H9c2 cells (figure 3.5 and 3.6). msl protein expression was not clearly identified in the empty vector controls but was for the msl over-expression samples for the top and bottom bands of the doublet when the msl antibody was used indicating msl over-expression (figure 3.7 (a)). There was a band observed in the empty expression control samples detected by the msl antibody and was thought not to be the top band of the msl protein doublet but a non-specific protein in between the top and bottom bands of the doublet. However, NIH3T3 cells express very low levels of msl and therefore the possibility of this being endogenous msl cannot be ruled out.

msl over-expression was detected using the c-Myc antibody and c-Myc protein expression was not found in the empty vector controls but was for the msl over-expression samples for the top and bottom bands of the doublet confirming msl over-expression (figure 3.7 (b)).

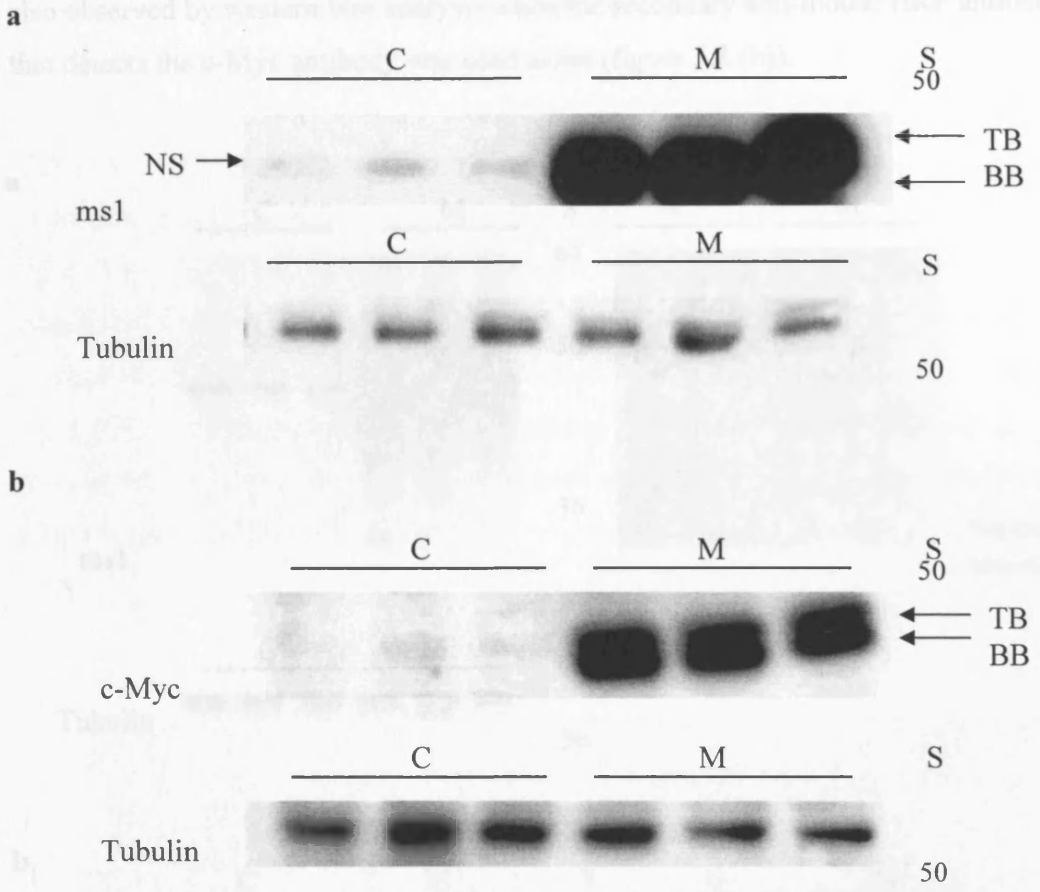

Figure 3.7. ms1 protein over-expression in NIH3T3 cells.

Western blot analysis using (**a**) ms1 and (**b**) c-Myc antibodies confirms ms1 protein over-expression in NIH3T3 cells. α-tubulin was used as an internal control for inaccuracies in initial protein levels. C refers to the empty expression vector control (pcDNA3.1(+)) and M refers to the ms1 expression vector (pcDNA3.1(+) + ms1), n = 3. S refers to the SeeBlue Plus2 pre-stained standard and the molecular weights (kDa) are given to the right. NS indicates a non-specific band, TB refers to the top band of the doublet and BB refers to the bottom band of the doublet.

The empty expression vector protein samples and the ms1 over-expression protein samples from the 72 hour transfection in NIH3T3 cells were analysed again by western blotting but immunoblotted for just the secondary antibodies used to detect ms1 and c-Myc primary antibodies. This was done to confirm that the ms1 protein doublet was real and that one of the doublet bands was not due to the secondary antibody. Western blot analysis using just the secondary anti-rabbit HRP antibody (detects the ms1 primary antibody) confirmed that the ms1 protein doublet was real as no protein bands appeared that resembled the ms1 protein doublet (figure 3.8 (a)). The same result was

also observed by western blot analysis when the secondary anti-mouse HRP antibody that detects the c-Myc antibody was used alone (figure 3.8 (b)).

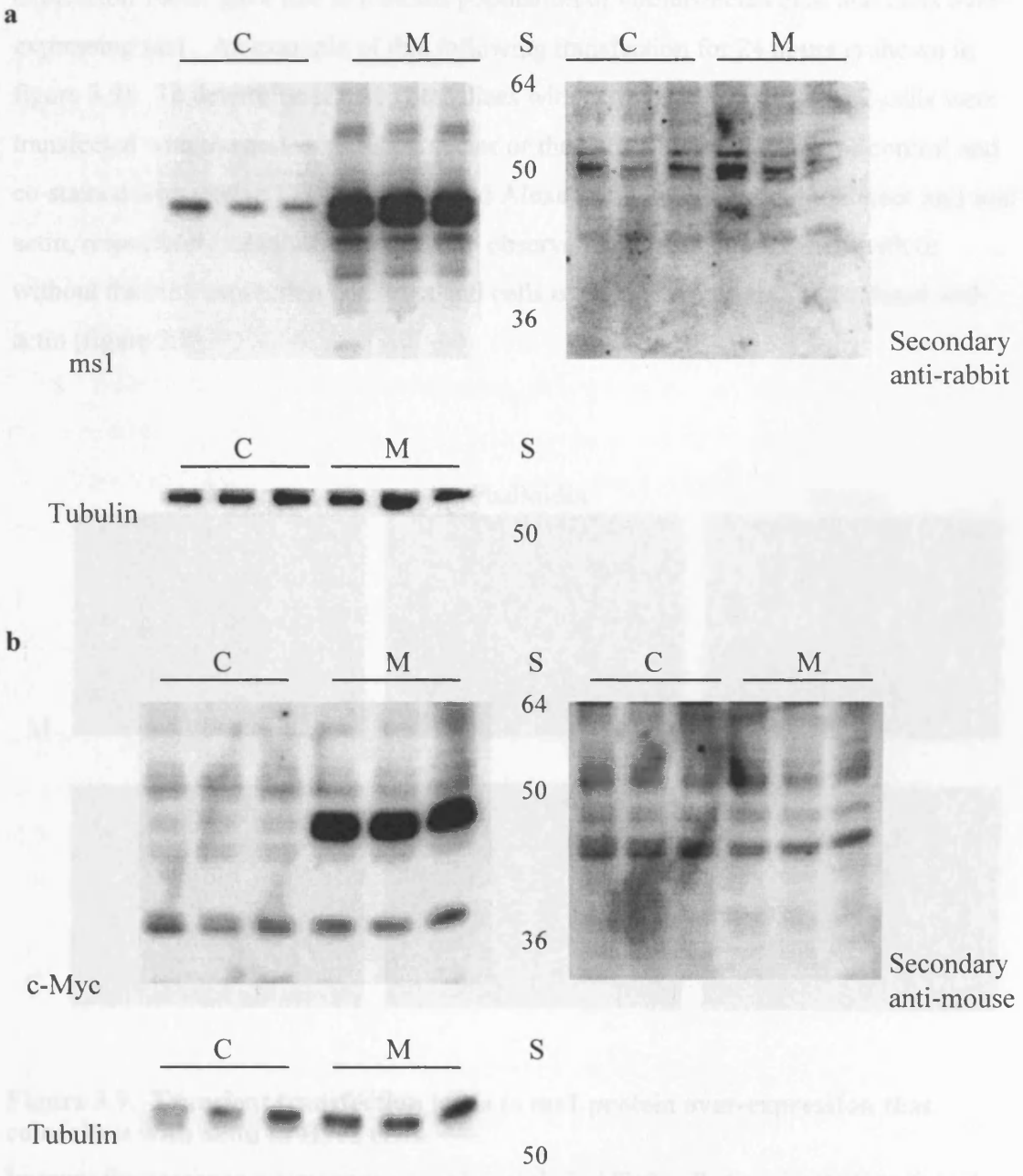

Figure 3.8. ms1 over-expression protein doublet is not due to the secondary antibody.

Western blot analysis using (**a**) secondary anti-rabbit HRP antibody and (**b**) secondary anti-mouse HRP antibody confirms that the ms1 protein doublet was present. α-tubulin was used as an internal control for inaccuracies in initial protein levels. C refers to the empty expression vector control (pcDNA3.1(+)) and M refers to the ms1 expression vector (pcDNA3.1(+) + ms1), n = 3. S refers to the SeeBlue Plus2 pre-stained standard and the molecular weights (kDa) are given.

Immunofluorescence microscopy using a c-Myc FITC antibody confirmed that H9c2 cells over-expressed c-Myc-ms1 and hence were successfully transfected with the ms1 expression vector (figure 3.9). Transient transfection (24 and 72 hours) of the ms1 expression vector gave rise to a mixed population of untransfected cells and cells over-expressing ms1. An example of this following transfection for 24 hours is shown in figure 3.9). To determine if ms1 colocalises with actin in H9c2 cells, H9c2 cells were transfected with the ms1 expression vector or the empty expression vector control and co-stained with c-Myc FITC antibody and Alexa fluor 350 phalloidin to detect ms1 and actin, respectively. Actin filaments were observed in all cells transfected with or without the ms1 expression construct and cells over-expressing ms1 colocalised with actin (figure 3.9).

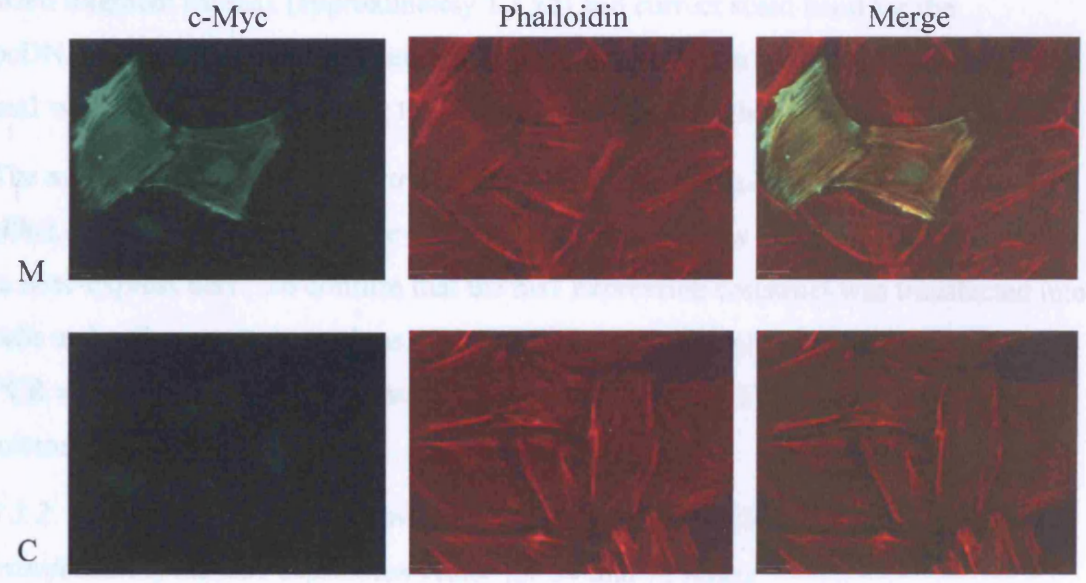

Figure 3.9. Transient transfection leads to ms1 protein over-expression that colocalises with actin in H9c2 cells.

Immunofluorescence microscopy of ms1 protein in H9c2 cells transiently transfected with an ms1 expression vector (M) or empty vector control (C), n = 3. Cells were co-stained with c-Myc FITC antibody and Alexa fluor 350 phalloidin to detect ms1 and actin, respectively. Merge image shows ms1 colocalisation with actin in ms1 transfected cells. Bar = 20 μm. Magnification 40×.

3.3 Discussion

In order to explore the role of msl in cardiac hypertrophy and cell survival *in vitro* an expression vector to transiently over-express a c-Myc-msl fusion protein was first constructed. Semi-quantitative RT-PCR was used to confirm msl mRNA over-expression and western blotting and immunofluorescence microscopy were used to confirm msl protein over-expression.

3.3.1 Successful cloning of msl into the pcDNA3.1(+) vector to construct a msl expression vector

The full-length coding sequence of mouse msl was amplified by PCR (figure 3.1), and then cloned into the pGEM-T Easy vector (figure 3.2). msl was then moved from the pGEM-T Easy vector into the mammalian expression vector pcDNA3.1(+). Restriction digest confirmed that the pcDNA3.1(+) vector contained msl by producing the correct sized fragment for msl (approximately 1.3 kb) and correct sized band for the pcDNA3.1(+) vector (approximately 5.4 kb) which is shown in figure 3.3. In addition, msl was verified by sequencing to be cloned in frame into the pcDNA3.1(+) vector.

The msl expression vector was transiently transfected into a heart-derived rat cell line, H9c2, for 24 and 72 hours where 72 hours was used to allow enough time for the cells to over-express msl. To confirm that the msl expression construct was transfected into cells and cells over-expressed msl, msl mRNA was analysed by semi-quantitative RT-PCR and msl protein was analysed by western blotting and immunofluorescence microscopy.

3.3.2 msl mRNA and protein over-expression in vitro confirms successful transient transfection of the msl expression vector for 24 and 72 hours

Semi-quantitative RT-PCR analysis confirmed transient (24 and 72 hours) msl mRNA over-expression compared to empty expression vector control (figure 3.4). msl protein over-expression was confirmed by western blotting using the msl and c-Myc antibodies (figure 3.5 and 3.6). When the msl antibody was used to detect msl protein, msl protein appeared on the western blot as a doublet (figure 3.5). This was observed following transient transfection for 24 and 72 hours. There was much more msl protein detected in the msl over-expression samples compared to the empty vector control samples for the bottom band of the doublet. This suggests that the top band of the protein doublet could be non-specific and the actual msl protein was the bottom band of

the doublet. However, H9c2 cells express msl and there was no endogenous msl protein (bottom band of the doublet) detected in cells transfected with the empty vector control. To verify this, the c-Myc antibody was used to detect c-Myc protein and hence confirm msl over-expression as the c-Myc antibody detects the c-Myc tag situated in the N-terminus before the coding sequence of msl. The c-Myc protein also appeared on the western blot as a doublet and msl was over-expressed compared to empty vector control for both bands of the doublet following transfection for 24 and 72 hours (figure 3.6). A faint protein band was observed in each of the empty expression vector control samples from a 72 hour transfection that were thought to be non-specific bands. However, this band could be a non-specific top band of the c-Myc protein and again raised the possibility that the bottom band was the real c-Myc-msl protein. This suggestion was an unlikely explanation because these non-specific bands were not observed following transfection for 24 hours and when the msl antibody was used there was no basal msl protein expression (bottom band of the doublet) detected and endogenous msl should have been detected as H9c2 cells express msl.

To further investigate this protein doublet, the msl expression vector was transiently transfected in another cell line, NIH3T3. msl and c-Myc protein again appeared on the western blot as a doublet in cells transfected with the msl expression construct and msl protein (detected by both msl and c-Myc antibodies) was over-expressed compared to empty vector control for both bands of the doublet (figure 3.7). Western blot analysis using the msl antibody detected a protein band in cells transfected with empty vector control. This could be a non-specific band in between the top and bottom bands of the msl doublet rather than the top band of the msl protein doublet. It is feasible that this was endogenous msl (top band of the doublet) as NIH3T3 cells express low levels of msl and therefore this possibility cannot be disregarded. When the c-Myc antibody was used no protein bands were detected in cells transfected with empty vector control and the c-Myc protein doublet was observed in cells transfected with msl, verifying the msl protein doublet was real.

One of the msl protein doublet bands could be due to the secondary antibodies used to detect msl and c-Myc primary antibodies. Figure 3.8 shows that when secondary antibodies were used alone, no protein bands were present on the western blot that could be the msl or c-Myc protein doublet. These findings suggest that the protein doublet appears to be real. Endogenous msl protein appeared as a single protein band on the

blot when cells were transfected with the empty vector control and ms1 protein was observed as a doublet consisting of two protein bands referred to the top and bottom bands of the doublet in cells over-expressing ms1.

Immunofluorescence microscopy using a c-Myc FITC antibody further confirmed that transient transfection for 24 and 72 hours of the ms1 expression vector leads to ms1 protein over-expression and phalloidin staining showed that ms1 associates with the actin cytoskeleton in transfected H9c2 cells (figure 3.9). This finding further strengthens the role of ms1 as an actin binding protein.

3.3.3 Reasons why the over-expressed ms1 protein appears as a doublet when anaysed by western blotting

The top band of the protein doublet could be endogenous ms1 protein as it was present when cells were transfected with the empty vector control. ms1 protein appears to be mainly in the bottom band of the doublet when cells were transfected with the ms1 expression vector but there was some ms1 protein in the top band of the doublet confirmed by the additional use of a c-Myc antibody, suggesting there was endogenous and over-expressed ms1 protein in the top band. Therefore it appears that some of the over-expressed ms1 protein runs the same as endogenous ms1 protein but most runs lower. This is probably due the c-Myc tag possibly affecting the structure causing the over-expressed ms1 protein to run lower. The much higher levels of ms1 protein when over-expressed could be another reason why most of the over-expressed ms1 protein runs lower than the endogenous ms1 protein. Another explanation is due to secondary structure or post-translational modification of the protein where there is covalent modification that changes the properties of a protein. Examples of post-translational modifications include phosphorylation, glycosylation, acetylation and methylation (Mann and Jensen, 2003). A urea gel that allows much higher denaturation may resolve the doublet to a single band and explain any possible secondary structure. To evaluate the possibility of a post-translational modification for example phosphorylation, treatment with an enzyme such as a phosphatase could be performed.

Although there were two ms1 protein bands they were both definitely ms1 and secondary antibody only controls confirmed this. Immunofluorescence microscopy further confirmed that ms1 protein was over-expressed.

In summary, the main aim was to generate an expression vector to transiently over-express a c-Myc-ms1 fusion protein *in vitro*. It was demonstrated in H9c2 cells that transient transfection of the ms1 expression vector for 24 hours and 72 hours resulted in ms1 mRNA and protein over-expression confirmed by semi-quantitative RT-PCR and western blotting, respectively. ms1 protein over-expression was further confimed by immunofluorescence microscopy and ms1 binds to actin filaments in transfected H9c2 cells further demonstrating that ms1 associates with the actin cytoskeleton. The ms1 expression vector generated leads to ms1 over-expression when transfected into cells and thus this construct can be used *in vitro* to investigate whether ms1 over-expression affects genes involved in hypertrophy and cell survival; therefore, allowing identification of target genes and downstream pathways of ms1 and to examine whether ms1 over-expression increases cell size and can protect against apoptotic cell death to determine if ms1 leads to cardiac hypertrophy and has an anti-apoptotic function.

Chapter 4

Effects of ms1 over-expression *in vitro*

4.1 Introduction

To identify putative target genes and downstream pathways of ms1, in particular ones involved in hypertrophy and cell survival, changes in mRNA and protein expression for a range of genes were examined in H9c2 cells over-expressing ms1. A range of genes were investigated that have been associated with cardiac hypertrophy such as the contractile gene cardiac α-actin, the transcription factor SRF and other known markers of hypertrophy such as BNP, calcineurin, GATA 4, myocardin and MEF2C. Protein kinases that are implicated as mediators of the hypertrophic response and involved in the cell survival pathway such as Akt and ERK1/2 were also examined. In addition, the apoptotic repressor ARC (apoptosis repressor with caspase recruitment domain) was investigated to determine if over-expression of ms1 altered ARC expression.

ms1 has been shown to activate SRF-dependent transcription via a Rho-MRTF pathway (Kuwahara *et al.*, 2005). Microarray experiments using a cell line that expresses dominant negative MRTF-A identified twenty eight genes that were MRTF-dependent and five of these are known SRF target genes (Selvaraj and Prywes, 2004). It is possible that these twenty eight MRTF-dependent genes are putative targets of ms1 and therefore altered mRNA expression of six out of the twenty eight MRTF-dependent genes were analysed in ms1 over-expressing cells. The six genes chosen were adrenomedullin, interleukin-6 (IL-6), coagulation factor III (tissue factor), leukemia inhibitory factor (LIF) and two known SRF target genes, jun-B and fos-related antigen-1 (fra-1). These genes were examined because they have been associated with cardiac diseases such as cardiac hypertrophy, ischaemia/reperfusion injury and heart failure (discussed in section 4.3.3).

Altered mRNA expression of these six MRTF-dependent genes following ms1 over-expression may further support a role for ms1 in cardiac hypertrophy and cardioprotection and would suggest that ms1 regulates MRTF-dependent genes possibly via the Rho-MRTF pathway.

4.2 Results

4.2.1 Altered gene expression following 24 hours of ms1 over-expression

Gene expression changes following 24 hours of ms1 over-expression was examined by semi-quantitative RT-PCR (figure 4.1). RPL32 was used as an internal control. There was no significant change in the contractile gene cardiac α-actin, and markers for hypertrophy such as BNP, calcineurin and MEF2C following ms1 over-expression. Other markers for hypertrophy such as the transcription factors GATA 4 and myocardin were up-regulated approximately 1.4 fold in cells over-expressing ms1 but this fold change was not found to be significant for GATA 4 or myocardin. The transcription factor, SRF, and the apoptotic repressor, ARC, were increased approximately 2 fold in ms1 over-expressing cells. The fold change was significant for SRF ($P < 0.05$) and the approximate 2 fold change in ARC expression was borderline significant ($P = 0.082$). When ARC mRNA was examined in the same cells over-expressing ms1 by real-time quantitative RT-PCR (figure 4.2) using the comparative ($\Delta\Delta C_T$) method, ARC expression was again increased approximately 2 fold and this fold change was borderline significant ($P = 0.048$).

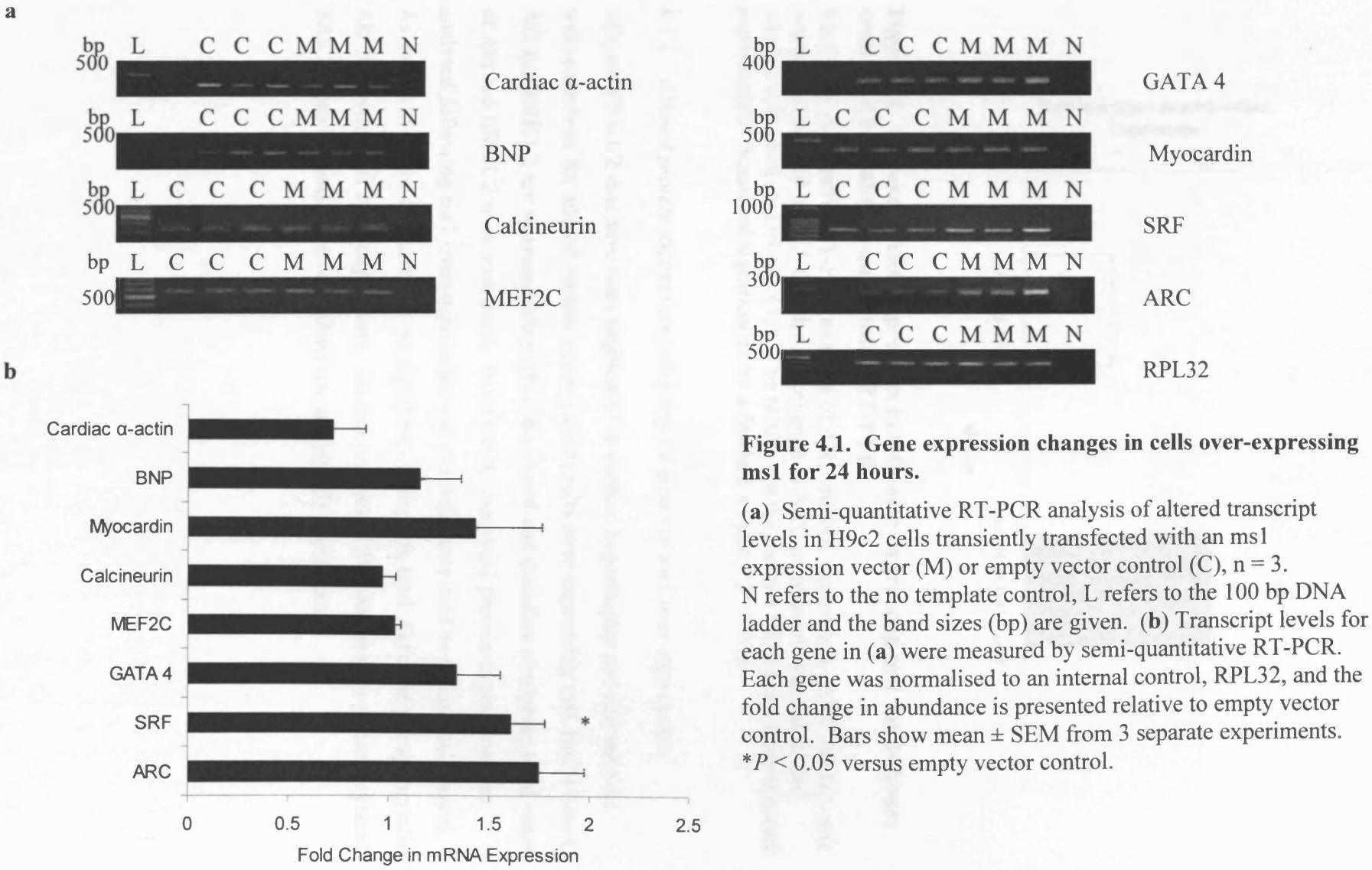

Figure 4.1. Gene expression changes in cells over-expressing ms1 for 24 hours.

(**a**) Semi-quantitative RT-PCR analysis of altered transcript levels in H9c2 cells transiently transfected with an ms1 expression vector (M) or empty vector control (C), n = 3. N refers to the no template control, L refers to the 100 bp DNA ladder and the band sizes (bp) are given. (**b**) Transcript levels for each gene in (**a**) were measured by semi-quantitative RT-PCR. Each gene was normalised to an internal control, RPL32, and the fold change in abundance is presented relative to empty vector control. Bars show mean ± SEM from 3 separate experiments. $^{*}P < 0.05$ versus empty vector control.

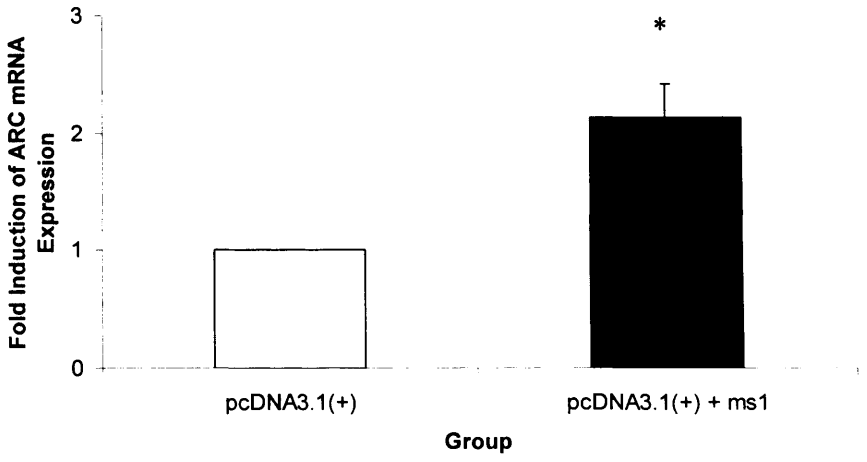

Figure 4.2. Increased ARC expression in cells over-expressing ms1 for 24 hours confirmed by real-time quantitative RT-PCR.

Real-time quantitative RT-PCR analysis of ARC mRNA expression. ARC mRNA was normalised to TBP mRNA and the fold change in ARC expression was calculated relative to control (pcDNA3.1(+)). The results are the mean ± SEM from three separate experiments. Statistical significance by a Student's *t* test: $*P < 0.05$.

4.2.2 Altered protein expression following 24 hours of ms1 over-expression

Akt and ERK1/2 that have been implicated in cardiac hypertrophy and cell survival were examined for altered protein expression in cells over-expressing ms1 for 24 hours. Akt and ERK1/2 are activated when phosphorylated and therefore phosphorylated states of Akt and ERK1/2 were examined. In addition, total Akt2 protein expression was analysed following ms1 over-expression and α-tubulin was used as an internal control. As shown in figure 4.3 there was no significant change in total Akt2 and phosphorylated Akt following ms1 over-expression. An approximate 2 fold decrease in phosphorylated ERK1/2 protein was observed, albeit not statistically significant.

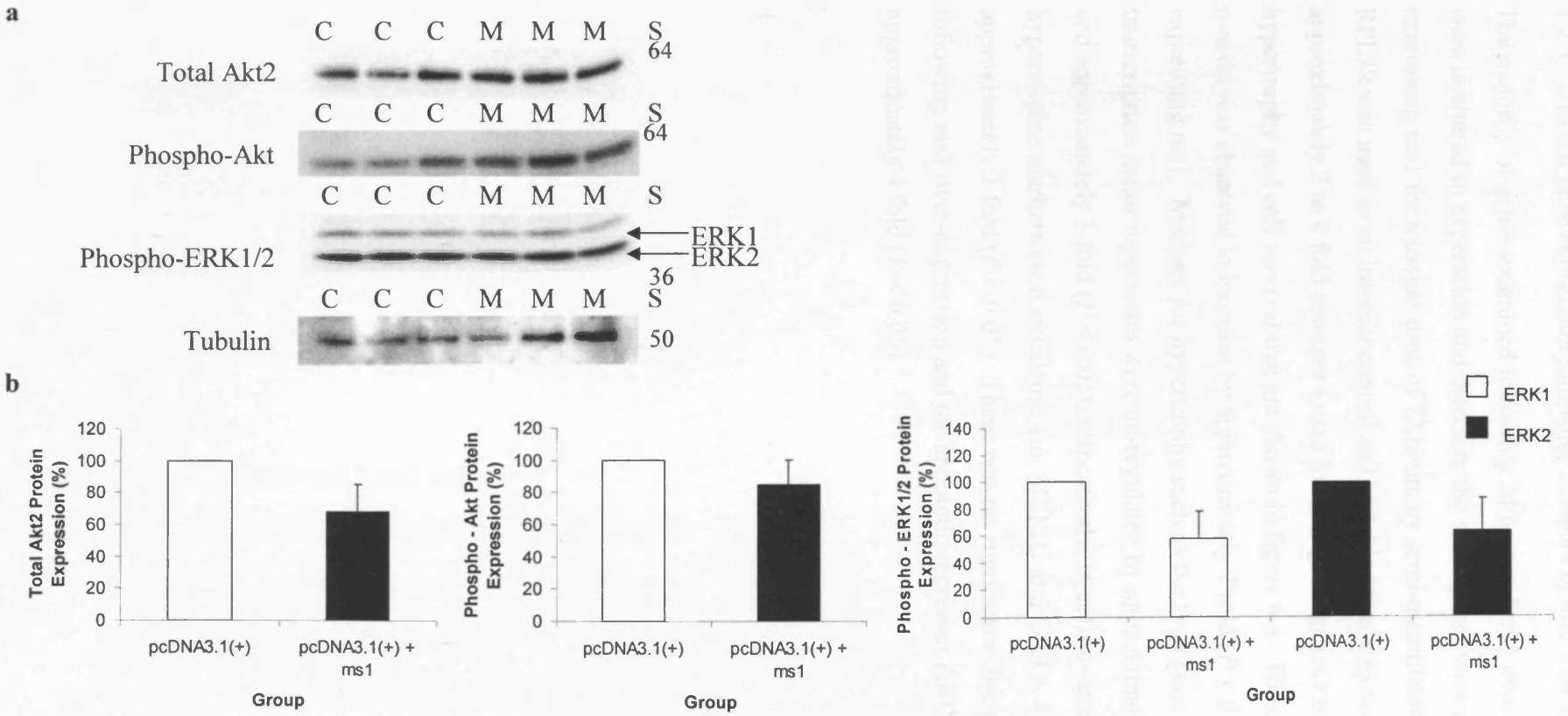

Figure 4.3. Changes in protein expression of kinases in H9c2 cells over-expressing ms1 for 24 hours.

(**a**) Altered protein levels in H9c2 cells transiently transfected with an ms1 expression vector (M) or empty vector control (C), n = 3, analysed by Western blotting. S refers to the SeeBlue Plus2 pre-stained standard and the molecular weights (kDa) are given. (**b**) Densitometric analysis for each protein kinase expression presented in (**a**). The percentage of protein expression is presented relative to empty vector control (pcDNA3.1(+)) after standardisation to α-tubulin as an internal control. Bars show mean ± SEM from 3 separate experiments. $*P < 0.05$ versus empty vector control.

4.2.3 Altered gene expression following 72 hours of msl over-expression

The majority of genes examined following 24 hours of msl over-expression (figure 4.1) were unaltered in expression and therefore the same genes were examined in cells over-expressing msl for a longer time of 72 hours by semi-quantitative RT-PCR. Again RPL32 was used as an internal control and by taking this into account there were approximately 2 to 4 fold changes found for a range of genes known to be involved in hypertrophy and cell survival that are shown in figure 4.4. The contractile gene cardiac α-actin was observed to increase by approximately 2 fold ($P < 0.01$) in cells over-expressing msl. Markers for hypertrophy such as the fetal gene BNP and the transcription factor myocardin were up-regulated by approximately 4 fold ($P < 0.01$) and approximately 3 fold ($P < 0.05$), respectively, in cells over-expressing msl. Other hypertrophic markers such as calcineurin, MEF2C and GATA 4 were increased approximately 2 fold ($P < 0.05$). There was no significant change in SRF expression following msl over-expression and the apoptotic repressor ARC was up-regulated approximately 4 fold ($P < 0.05$).

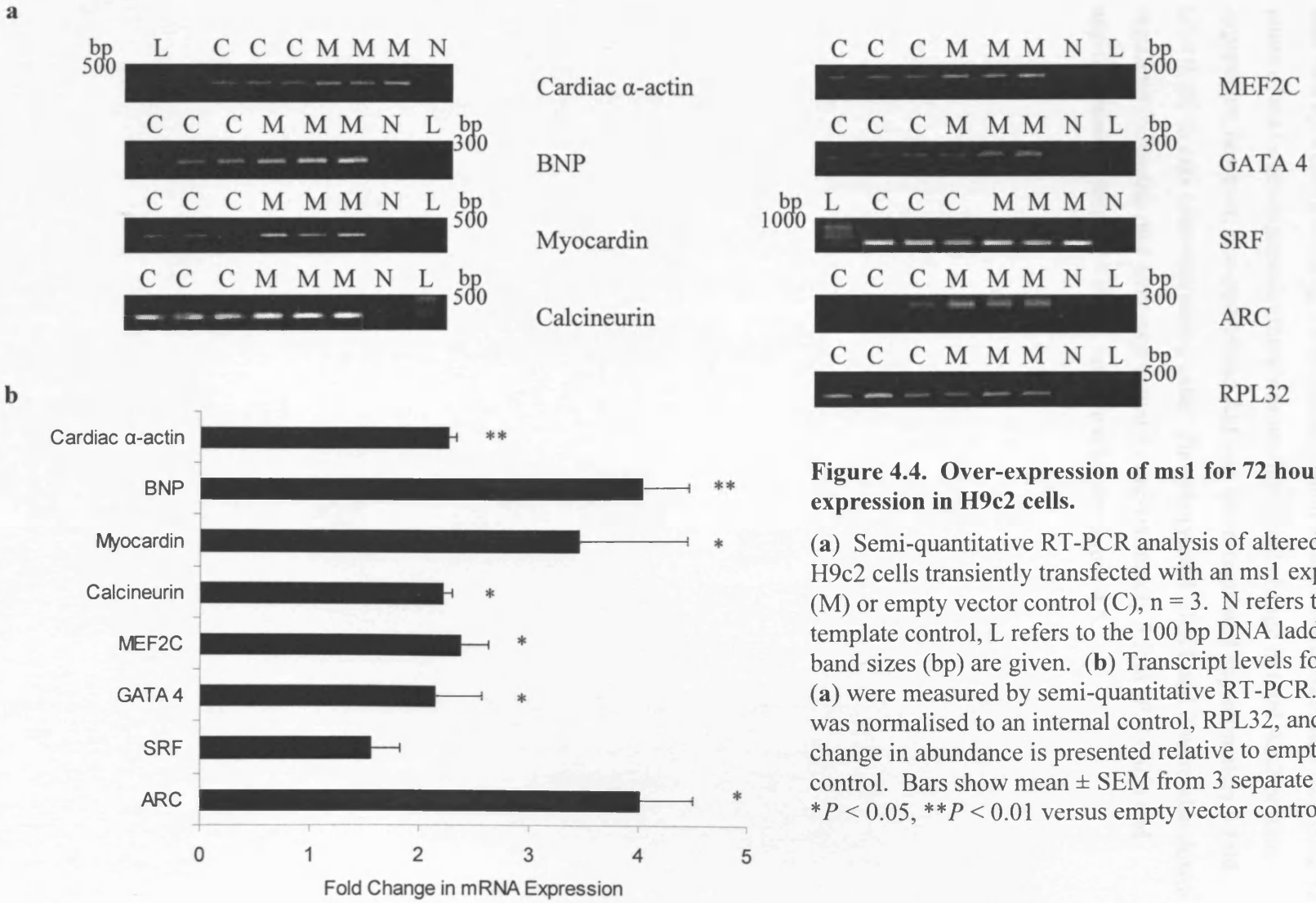

Figure 4.4. Over-expression of ms1 for 72 hours alters gene expression in H9c2 cells.

(**a**) Semi-quantitative RT-PCR analysis of altered mRNA in H9c2 cells transiently transfected with an ms1 expression vector (M) or empty vector control (C), n = 3. N refers to the no template control, L refers to the 100 bp DNA ladder and the band sizes (bp) are given. (**b**) Transcript levels for each gene in (**a**) were measured by semi-quantitative RT-PCR. Each gene was normalised to an internal control, RPL32, and the fold change in abundance is presented relative to empty vector control. Bars show mean ± SEM from 3 separate experiments. $*P < 0.05$, $**P < 0.01$ versus empty vector control.

4.2.4 Altered protein expression following 72 hours of ms1 over-expression

There was no altered protein expression for total Akt2, phosphorylated Akt and phosphorylated ERK1/2 in cells over-expressing ms1 for 24 hours (figure 4.3) when analysed by western blotting. When these protein kinases were examined following 72 hours of ms1 over-expression there was no significant change in total Akt2 protein expression; however, phosphorylated Akt was down-regulated approximately 4 fold ($P < 0.05$) in ms1 over-expressing cells. Phosphorylated ERK1 and 2 were also down-regulated following ms1 over-expression by approximately 5 fold ($P < 0.05$) and approximately 4 fold ($P < 0.05$), respectively, see figure 4.5.

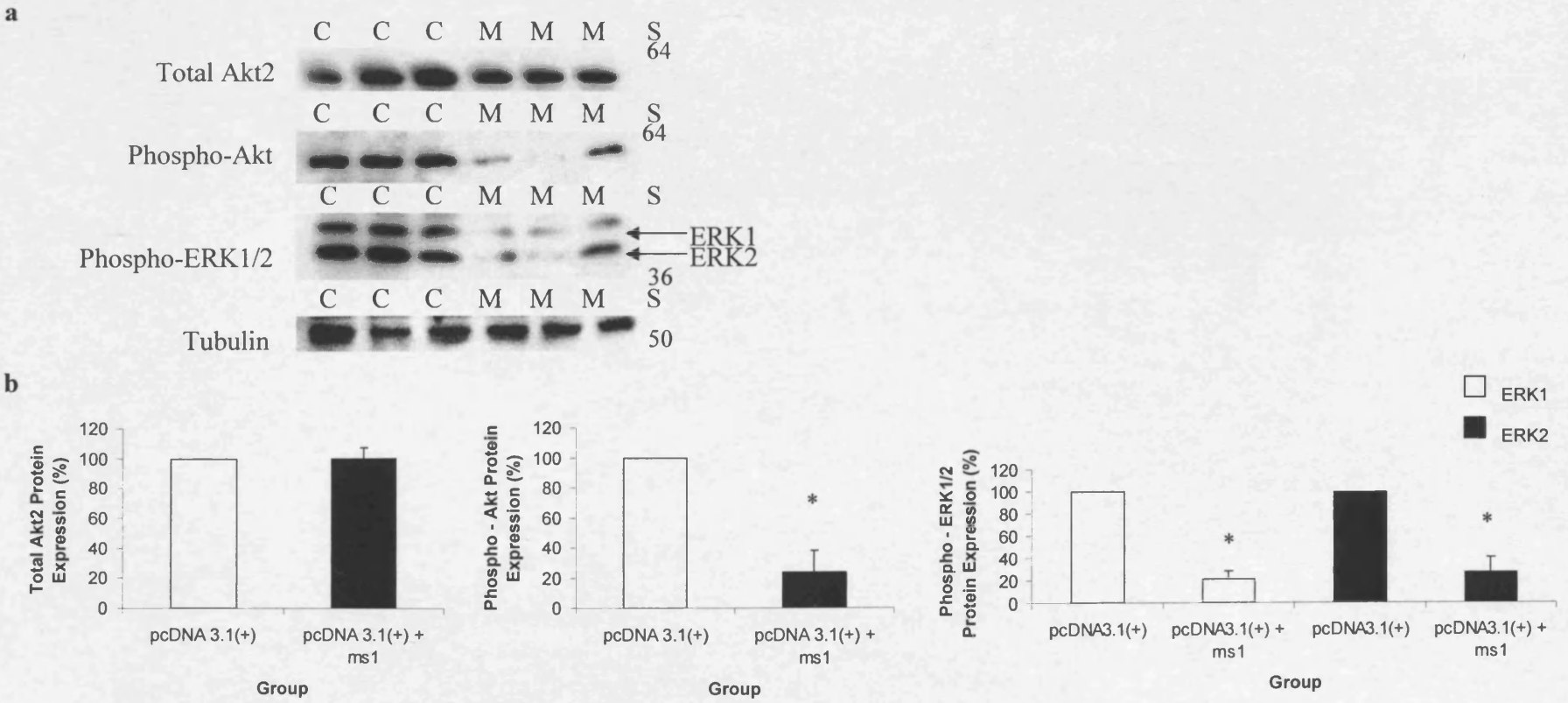

Figure 4.5. Over-expression of ms1 for 72 hours alters protein expression of kinases in H9c2 cells.

(**a**) Western blot analysis of altered protein levels in H9c2 cells transiently transfected with an ms1 expression vector (M) or empty vector control (C), n = 3. S refers to the SeeBlue Plus2 pre-stained standard and the molecular weights (kDa) are given. (**b**) Densitometric analysis for each protein kinase expression presented in (**a**). The percentage of protein expression is presented relative to empty vector control (pcDNA3.1(+)) after standardisation to α-tubulin as an internal control. Bars show mean ± SEM from 3 separate experiments. $*P < 0.05$ versus empty vector control.

4.2.5 Altered gene expression of MRTF-dependent genes in H9c2 cells over-expressing msl

To determine whether MRTF-dependent genes are targets of msl, changes in expression of six known MRTF-dependent genes, adrenomedullin, IL-6, tissue factor, LIF, jun-B and fra-1 following 24 hours of msl over-expression were examined by real-time quantitative RT-PCR using the Pfaffl method (Pfaffl, 2001) as explained in section 2.3.5.2 of the materials and methods chapter. Over-expression of msl significantly induced all the six known MRTF-dependent genes (figure 4.7). The cytokines LIF and IL-6 were up-regulated by approximately 2.5 fold ($P < 0.01$) and 6 fold ($P < 0.01$), respectively, in cells over-expressing msl. An induction of approximately 1.5 fold was observed for tissue factor ($P < 0.01$) and the vasodilating peptide adrenomedullin ($P < 0.05$). The proto-oncogene jun-B and the transcription factor fra-1 were increased approximately 2 fold following msl over-expression. There was strong evidence that this fold change was significant for jun-B ($P < 0.01$) and fra-1 ($P < 0.01$).

MRTF-dependent genes were altered in expression following msl over-expression for 24 hours and therefore were not examined in cells over-expressing msl for 72 hours.

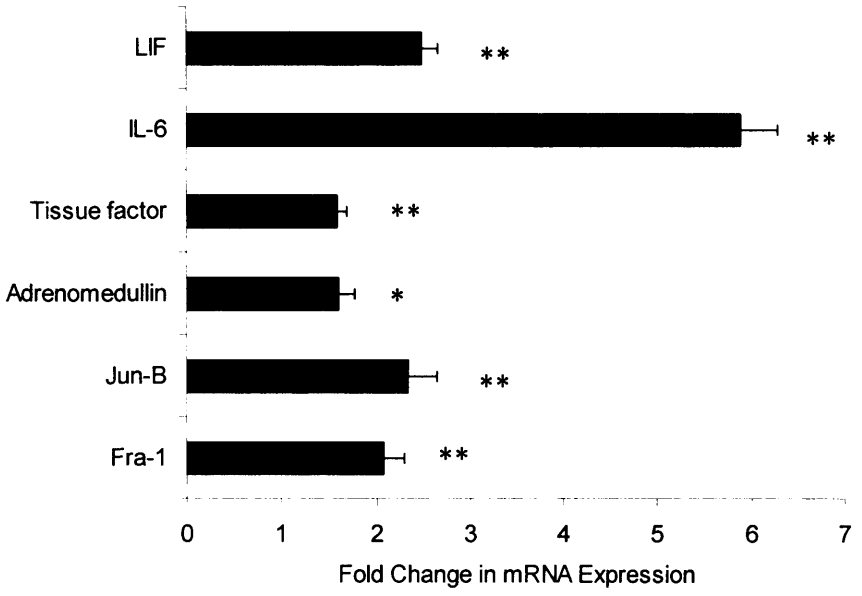

Figure 4.7. Up-regulation of MRTF-dependent genes following msl over-expression.

Over-expression of msl alters transcript levels in H9c2 cells. Transcript levels for each gene were quantified by real-time quantitative RT-PCR. Each gene was normalised to an internal control, RPL32 and the fold change in abundance is presented relative to empty vector control. Bars show mean ± SEM from 6 separate experiments. $^{*}P < 0.05$, $^{**}P < 0.01$ versus empty vector control.

4.2.6 Promoter analysis of msl and msl target genes for SRF binding sites

SRF regulates serum-inducible genes and genes expressed in skeletal, smooth and cardiac muscle by binding to CArG box elements (SRF binding sites) in their promoter sequences (Frey and Olson, 2003; Sotiropoulos *et al.*, 1999). msl is able to stimulate SRF-dependent transcription by inducing the nuclear accumulation of MRTFs where they associate with SRF to activate transcription of genes containing SRF binding sites (Kuwahara *et al.*, 2005). Therefore the promoters of putative target genes of msl were analysed for SRF binding sites to investigate whether msl alters gene expression of SRF target genes which would further support that activation of SRF target genes are mediated by msl via the Rho-MRTF pathway.

The msl promoter and the promoters of all genes examined in sections 4.2.1, 4.2.3 and 4.2.5 that are possible downstream target genes of msl were analysed for CArG box elements (SRF binding sites) using the programme DCODE.org Comparative Genomics Center (www.dcode.org). First the ECR browser in DCODE.org was used to extract the promoter sequences (-4000) and align human, mouse and rat sequences. rVista 2.0 was then used to identify conserved SRF binding sites. Exons and Introns were also analysed for SRF binding sites for certain genes known to have sites in these areas. SRF, cardiac α-actin, BNP, adrenomedullin, myocardin, jun-B and fra-1 are known to contain SRF binding sites (Adiseshaiah *et al.*, 2005; Belaguli *et al.*, 1997; Miano, 2003; Minty and Kedes, 1986; Miwa and Kedes, 1987; Nelson *et al.*, 2005; Selvaraj and Prywes, 2004; Spencer and Misra, 1996; Sun *et al.*, 2006; Wang *et al.*, 2001b) but were analysed using DCODE.org to confirm that the database identified SRF binding sites.

Using published data and DCODE.org (ECR browser and rVista 2.0), conserved SRF binding sites were found in msl and nine out of the fourteen probable msl target genes (table 4.1) which are cardiac α-actin, SRF, BNP, myocardin, MEF2C, adrenomedullin, jun-B, fra-1, and LIF. Calcineurin (mouse) contains a possible SRF binding site but this sequence was not conserved in rat and human. A possible SRF binding site was identified in GATA 4, ARC and IL-6 that was conserved in mouse and rat but not in human. Tissue factor was not found to contain any likely SRF binding sites.

Gene	#CArG	Conserved CArG Sequence[a]	Postion[c]
msl	1	CCT***C***TAAATGG	-303
Cardiac α-actin	5	CCAAACATGG	-1545
		CCCTAT***A***TGG	-239
		CCTTACATGG	-202
		CCA***A***GAATGG	-151
		CCAAATAAGG	-111
SRF	4	CCATATAAGG	-82
		CCATAAAAGG	-62
		CTTTATATGG	-39
		CCATATAAGG	+2800
BNP	1	***T***CTATACAAGG	-276
Myocardin	1	CCAA***A***TTTTG	+6666
Calcineurin	1	CCATTACTGG, **NOT CONSERVED**	-1111
GATA 4	1	***T***CTTTTAT***G***G, **NOT CONSERVED**[b]	-3821
MEF2C	1	CATTTTTTAGG	-245
ARC	1	CCCTTATTGG, **NOT CONSERVED**[b]	-870
Adrenomedullin	1	CCTTATAAGG	-732
Jun-B	1	CCTAATATGG	-1739
Fra-1	1	CCATGTATGG	-74
IL-6	2	CCAATCAAAGG, **NOT CONSERVED**[b]	-2896
		CCATTTATGC, **NOT CONSERVED**[b]	-2768
LIF	1	CCATTTGAGC	+8957
Tissue factor	0		

Table 4.1. Summary of msl and msl possible target genes containing CArG sequences in the mouse genome.

[a]CArG boxes conserved in sequence between mouse, rat and human. Bold and italicised bases represent non-conserved nucleotides (1 or 2 bp tolerable mismatch), e.g. a mouse A might be a T in human or rat. [b]CArG boxes conserved in sequence between mouse and rat but not in human. [c]The position of each CArG element is relative to the transcriptional start site (TSS) according to Ensembl (www.ensembl.org/index.html).

Cardiac α-actin, SRF, BNP, myocardin, adrenomedullin, jun-B and fra-1 have been reported to contain SRF binding sites (Adiseshaiah *et al.*, 2005; Belaguli *et al.*, 1997; Miano, 2003; Minty and Kedes, 1986; Miwa and Kedes, 1987; Nelson *et al.*, 2005; Selvaraj and Prywes, 2004; Spencer and Misra, 1996; Sun *et al.*, 2006; Wang *et al.*, 2001b) with the same sequences shown in table 4.1 which confirms the use of DCODE.org as a tool to search for SRF (transcription factor) binding sites. Out of these seven genes containing SRF binding sites, cardiac α-actin, BNP, adrenomedullin, jun-B

hours. There was a significant induction of BNP (approximately 4 fold) and myocardin (approximately 3 fold) when over-expressing msl. However, SRF transcript levels were not significantly up-regulated following msl over-expression for 72 hours. At 24 hours only SRF was significantly up-regulated and this was by approximately 2 fold when compared to empty vector control. These findings suggest that msl appears to affect genes involved in cardiac hypertrophy and implicates these genes as putative targets of msl and downstream pathways of msl that collectively may be involved in the development of hypertrophy.

Expression of hypertrophic genes was up-regulated following msl over-expression for 72 hours and not following 24 hours. Induction of SRF mRNA was only observed in cells over-expressing msl for 24 hours and not for 72 hours. A possible explanation for this could be time-dependency where SRF was initially up-regulated and then the other hypertrophic genes were up-regulated. The cells were confluent by 72 hours in culture and H9c2 cells when confluent can differentiate into tubular structures (Kimes and Brandt, 1976). Many of these genes implicated in the hypertrophic response also regulate cell differentiation for example myocardin (Du *et al.*, 2003; Wang *et al.*, 2003), MEF2C (Gauthier-Rouviere *et al.*, 1996) and GATA 4 (Pikkarainen *et al.*, 2004) thus msl also appears to affect transcription factors that regulate cardiomyocyte differentiation, suggesting that msl may play a role in differentiation. msl mRNA was found up-regulated when H9c2 cells differentiate (Ounzain, personal communication) thus further supporting a role for msl in cell differentiation.

msl via the Rho-MRTF pathway can stimulate SRF activity by binding to actin, promoting actin polymerisation in the presence of Rho activity which releases MRTFs from the inhibitory influence of G-actin, allowing the nuclear import of MRTFs and stimulation of SRF dependant gene activation (Kuwahara *et al.*, 2005). It is therefore feasible that the identified downstream target genes of msl were up-regulated following msl over-expression via the MRTF-SRF signalling pathway as many of theses genes could be SRF target genes. This will be discussed further in section 4.3.4.

4.3.2 msl appears to affect genes involved in cell survival

To establish if msl affects genes involved in cell survival pathways, transcript levels of the apoptotic repressor, ARC was examined by semi-quantitative RT-PCR and real-time quantitative RT-PCR following msl over-expression for 24 hours and 72 hours. ARC

was investigated because like msl, ARC was found expressed in the heart and skeletal muscle (Koseki *et al.*, 1998). ARC was found to inhibit apoptosis by interacting with caspase 2 and 8 (Koseki *et al.*, 1998), in contrast other studies have shown that inhibition of apoptosis via ARC does not necessarily operate through the caspases. For instance, hypoxia-induced apoptosis was suppressed by ARC inhibition of cytochrome C release from the mitochondria in a caspase-independent manner (Ekhterae *et al.*, 1999). In addition, ARC over-expression inhibited hydrogen peroxide-induced cell death in H9c2 cells mediated totally or part through the blockade of hypoxia-induced cytochrome C release from the mitochondria (Neuss *et al.*, 2001).

ARC has been reported to protect against ischaemia-reperfusion injury by reducing creatine kinase release and infarct size (Gustafsson *et al.*, 2002). ARC and a mutant form of ARC (in the CARD domain) were then investigated in ischaemia-reperfusion injury and hydrogen peroxide-induced cell death and their effect on Bax (a pro-apoptotic Bcl-2 family protein that translocates to the mitochondria in response to death stimuli, causing cytochrome release from the mitochondria). It was found that the mutant form of ARC did not reduce creatine kinase release and infarct size after ischaemia-reperfusion or resulted in protection against hydrogen peroxide-mediated cell death in H9c2 cells. ARC co-immunoprecipitated with Bax and prevented Bax activation and cytochrome release in hydrogen peroxide treated cells but the mutant form of ARC did not. These results demonstrated that the CARD domain is important in mediating the protective effects of ARC and that ARC interacts with Bax which, prevents its activation and release of cytochrome C from the mitochondria (Gustafsson *et al.*, 2004).

These results taken together with other results (Ekhterae *et al.*, 1999; Neuss *et al.*, 2001) suggest that ARC prevents cell death by interacting with multiple pathways (Gustafsson *et al.*, 2004). More recently it was demonstrated that ARC protein levels were down regulated in human failing heart and ARC provided cardioprotection in response to pressure overload and ischaemia (Donath *et al.*, 2006).

ARC expression was significantly up-regulated approximately 4 fold when msl was over-expressed for 72 hours and increased approximately 2 fold following msl over-expression for 24 hours. Therefore the anti-apoptotic factor ARC appears to be a target gene of msl and hence msl may play a role in cell survival via ARC. ARC expression like msl was found increased in differentiated cells (Hunter *et al.*, 2007) and ARC

expression was significantly up-regulated in cells over-expressing msl for 72 hours where the cells were confluent and can start to differentiate further strengthening the role of msl in differentiation.

Subsequent work further investigated the role of msl in cell survival by examining the changes in protein expression of kinases involved in the cell survival pathway such as Akt and ERK1/2. Total Akt2, phosphorylated Akt and phosphorylated ERK1/2 were not significantly altered in their protein expression following msl over-expression for 24 hours. Again total Akt2 protein expression was unaffected in cells over-expressing msl for 72 hours; however, phosphorylated Akt and phosphorylated ERK1/2 were significantly down-regulated. Inhibition of ERK1/2 and Akt caused increased apoptosis (Bueno and Molkentin, 2002; Clerk *et al.*, 2003; Turner *et al.*, 1998; Yasuoka *et al.*, 2004) and it was found that over-expressing msl significantly down-regulated ERK1/2 and Akt but no apoptosis (DNA fragmentation) was observed when analysed by flow cytometry as shown in figure 5.4 and 5.11 of chapter 5. Also msl over-expression caused an induction of the apoptosis repressor ARC; therefore, it is plausible that msl over-expression may provide a protective response against apoptosis and promote cell survival via deactivation of ERK1/2, Akt and activation of ARC.

Calcineurin-mediated NFAT activation has also been suggested to be critical in preventing cardiomyocyte apoptosis (Frey *et al.*, 2004). Recent evidence has also linked a deactivation of Akt with elevated calcium in H9c2 cells and the inactivation of Akt was well correlated with the susceptibility to apoptosis (Yasuoka *et al.*, 2004). The phosphatase, calcineurin is activated by a rise in intracellular calcium (Olson, 2004) and calcineurin also appears to be involved in apoptosis (Klumpp and Krieglstein, 2002). Thus, it is possible that over-expression of msl may also have an anti-apoptotic response via the deactivation of Akt in response to elevated calcium and therefore possible activation of calcineurin.

Taken together all these findings suggest that msl appears to affect genes involved in cell survival and may prevent apoptosis by interacting with multiple cell survival pathways.

It is important to note that numerous studies have implicated ERK1/2 and Akt in producing the hypertrophic response. Phosphorylated ERK1/2 and Akt were significantly down-regulated when msl was over-expressed and down-regulation of

these kinases has been observed to decrease hypertrophy (Andersson *et al.*, 1998; Black *et al.*, 2002; Bueno *et al.*, 2001; Frey and Olson, 2003; Hardt and Sadoshima, 2004; Shibata *et al.*, 2004; Shioi *et al.*, 2000; Takahashi *et al.*, 2003) suggesting that over-expressing ms1 may produce an anti-hypertrophic response via ERK1/2 and Akt deactivation.

SRF regulates immediate early and muscle specific gene expression by binding to the CArG box elements in their promoter/enhancer sequences and this is thought to occur via different signalling pathways that involve MAPK signalling and actin dynamics (figure 4.8).

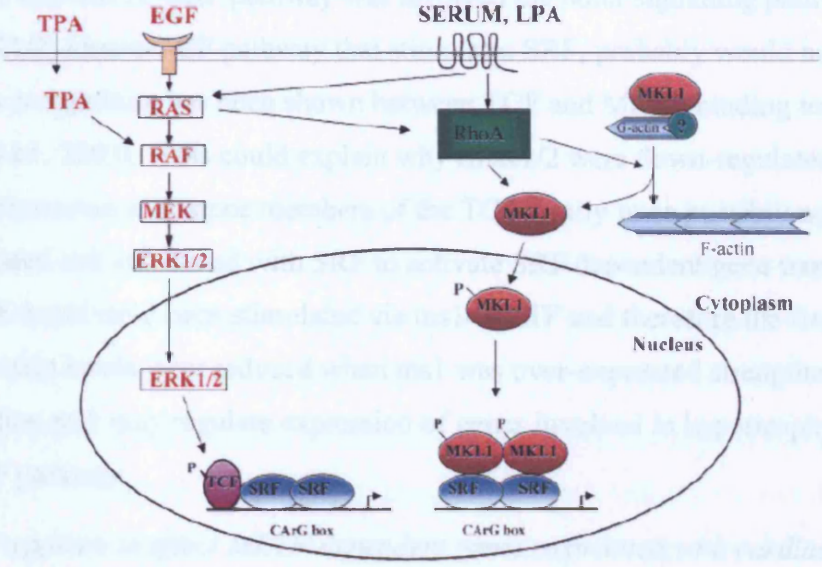

Figure 4.8. The possible mechanism to regulate the transcriptional activity of SRF through two parallel signalling pathways (Cen *et al.*, 2004).

SRF bound to CArG boxes can be activated by either the ternary complex factor (TCF) family or MRTFs (MKL1). TCF is activated by MAPK phosphorylation. MRTFs are sequestered in the cytoplasm by binding to G-actin and are activated when extracellular signals stimulate actin polymerisation via Rho signalling causing MRTF translocation to the nucleus. Additional abbreviations: TPA, 12-*O*-tetradecanoly-phorbol-13-acetate; EGF, epidermal growth factor; LPA, lysophosphatidic acid.

Activation of MAPK pathways leads to phosphorylation of the ternary complex factor (TCF) family which associate with SRF on target genes that contain TCF binding sites (GGAA/T) adjacent to the CArG box (Janknecht *et al.*, 1993). The binding of TCF and myocardin/MRTFs to SRF is in fact mutually exclusive (Wang *et al.*, 2004). The B box of Elk-1 (one member of the TCF family) competes for MRTF binding to SRF, suggesting that they bind to the same region on SRF (Miralles *et al.*, 2003). Signalling

by the Rho family of small GTPases stimulates SRF activity via actin polymerisation, independently of MAPK activation and TCFs (Sotiropoulos *et al.*, 1999). MRTFs are sequestered in the cytoplasm by binding to G-actin monomers via their N-terminal RPEL motif. Extracellular signals stimulate actin polymerisation via Rho signalling and this causes MRTF translocation to the nucleus resulting in activation of SRF (Miralles *et al.*, 2003).

In section 4.2.3 it was demonstrated that msl over-expression for 72 hours up-regulated expression of many known markers of hypertrophy and in section 4.3.1 it was suggested that msl may regulate expression of genes involved in hypertrophy via the MRTF-SRF pathway. If this MRTF-SRF pathway was involved the other signalling pathway, the MAP (ERK1/2) kinase-TCF pathway that stimulates SRF, probably would not be involved as competition has been shown between TCF and MRTF binding to SRF (Miralles *et al.*, 2003). This could explain why ERK1/2 were down-regulated following msl over-expression and hence members of the TCF family were possibly not phosphorylated and associated with SRF to activate SRF dependent gene transcription. Instead SRF could have been stimulated via msl-MRTF and therefore the finding that ERK1/2 protein levels were reduced when msl was over-expressed strengthens the possibility that msl may regulate expression of genes involved in hypertrophy via the MRTF-SRF pathway.

4.3.3 msl appears to affect MRTF-dependent genes associated with cardiac hypertrophy and cell survival

Selvaraj and Prywes used a cell line expressing dominant negative MRTF-A (can block activation by all of the members of the MRTF family) and identified many MRTF-dependent genes where a subset of these genes are known SRF targets (Selvaraj and Prywes, 2004). It has been recently demonstrated that msl via the Rho-MRTF pathway can activate SRF-dependent transcription (Kuwahara *et al.*, 2005) and therefore it was speculated that the MRTF-dependent genes whether SRF target genes or not were putative targets of msl. In order to identify msl target genes that are specifically dependent on the MRTF pathway altered mRNA expression of MRTF-dependent genes published by Selvaraj and Prywes (2004) were analysed in msl over-expressing cells. Adrenomedullin, IL-6, tissue factor, LIF and two known SRF target genes jun-B and fra-1 were examined because they have been associated with cardiac hypertrophy and cell survival. For example numerous studies have shown that the cytokines LIF and

IL-6 can induce cardiac hypertrophy via glycoprotein 130 (gp130) signalling (Casey *et al.*, 2005; Fredj *et al.*, 2005; Hirota *et al.*, 1995; Matsui *et al.*, 1996; Sano *et al.*, 2000) that involves activation of PI3K-Akt-p70s6k pathway (Hiraoka *et al.*, 2003), Janus kinase-signal transducer and activator of transcription (JAK-STAT) pathway (Ancey *et al.*, 2002; Kodama *et al.*, 1997; Kunisada *et al.*, 1996; Kunisada *et al.*, 1998) and MAPK pathways (Ancey *et al.*, 2002; Kunisada *et al.*, 1998). LIF and IL-6 have also been shown to be cardioprotective (Matsushita *et al.*, 2005; Smart *et al.*, 2006; Yasukawa *et al.*, 2001).

Elevated levels of tissue factor, the protease receptor initiating the coagulation cascade, was observed in hearts of rabbits subjected to myocardial ischaemia/reperfusion injury (Chong *et al.*, 2003; Erlich *et al.*, 2000; Golino *et al.*, 1996). Administration of an inhibitory anti-rabbit tissue factor monoclonal antibody reduced infarct size (Chong *et al.*, 2003; Erlich *et al.*, 2000; Golino *et al.*, 1996) suggesting that myocardial ischaemia/reperfusion injury could be decreased using anti-tissue factor therapy. Elevated tissue factor levels have also been found in patients with ischaemic heart disease (Falciani *et al.*, 1998). In addition, tissue factor has been suggested to be involved in the maintenance of cardiac muscle structure (Luther *et al.*, 2000).

Considerable controversy exists in the role that adrenomedullin plays in cardiac hypertrophy. Studies have found that adrenomedullin levels did not increase following aortic banding (Kaiser *et al.*, 1998) and phenylephrine or endothelin-mediated hypertrophy (Autelitano *et al.*, 2001) with many studies suggesting that adrenomedullin has anti-hypertrophic effects (Autelitano *et al.*, 2001; Niu *et al.*, 2004; Wang *et al.*, 2001a; Zhang *et al.*, 2000). However, there are an equal number of studies reporting an increase in adrenomedullin. One group observed this following aortic banding (Morimoto *et al.*, 1999; Nishikimi *et al.*, 2003), another following chronic pressure overload in rats by administrating angiotensin II (Romppanen *et al.*, 1997) and many studies observed increased ventricular adrenomedullin levels in several hypertensive models with cardiac hypertrophy (Ishiyama *et al.*, 1997; Shimokubo *et al.*, 1995; Shimokubo *et al.*, 1996). However, ventricular adrenomedullin gene expression is consistently induced in the failing heart (Jougasaki *et al.*, 1995; Jougasaki *et al.*, 1996; Kaiser *et al.*, 1998; Nishikimi *et al.*, 1997; Oie *et al.*, 2000) and adrenomedullin was shown to inhibit cardiac myocyte apoptosis following doxorubicin (Tokudome *et al.*,

2002) or ischaemia/reperfusion (Okumura *et al.*, 2003; Okumura *et al.*, 2004; Yin *et al.*, 2004).

The proto-oncogene jun-B which is a known SRF target gene is transiently up-regulated after cardiac hypertrophy stimuli (Parker and Schneider, 1991; Ricci *et al.*, 2005; Rockman *et al.*, 1991) and induced in cardiac myocytes exposed to hypoxia (Webster *et al.*, 1993) and ischaemia/reperfusion (Brand *et al.*, 1992). However, there is conflicting data regarding the SRF target gene fra-1 upon cardiac hypertrophy stimuli. One group demonstrated no induction of fra-1 following aortic banding (Rockman *et al.*, 1991) and another study observed both up-regulation and down-regulation of fra-1 expression in cardiomyocytes *in vitro* depending on the stimulus (van Wamel *et al.*, 2000). Fra-1 knockout mice subjected to aortic banding have a normal hypertrophic response whereas over-expression of fra-1 lead to premature heart failure (Ricci *et al.*, 2005).

These MRTF-dependent genes were examined by real-time quantitative RT-PCR following 24 hours of msl over-expression and as shown in figure 4.7 were all significantly up-regulated in H9c2 cells over-expressing msl compared to cells expressing empty vector control. Tissue factor and adrenomedullin were up-regulated by approximately 1.5 fold. Jun-B and fra-1 were increased approximately 2 fold in cells over-expressing msl and LIF and IL-6 were up-regulated by approximately 2.5 fold and 6 fold, respectively, following msl over-expression. These findings demonstrate that msl again appears to affect genes involved in cardiac hypertrophy and cell survival and implicates these MRTF-dependent genes as target genes of msl. It is feasible that msl regulates these genes via endogenous MRTFs possibly present in H9c2 cells. The MRTF-dependent genes jun-B and fra-1 are known SRF target genes and as a result further provides evidence that msl activates SRF-dependent transcription via the Rho-MRTF pathway.

4.3.4 msl appears to affect SRF target genes associated with cardiac hypertrophy and cell survival

The evidence so far suggests that msl affects many genes known to be involved in cardiac hypertrophy and cell survival and msl affects MRTF-dependent genes also known to be involved in hypertrophy and cell survival further supporting a role for msl in cardiac hypertrophy and cardioprotection. msl may regulate these genes via the MRTF-SRF pathway where msl induces the nuclear accumulation of MRTFs and they

al., 2003; Selvaraj and Prywes, 2004) and as shown in figure 4.4 and 4.7 they were up-regulated following msl over-expression. Collectively, these findings suggest that msl may regulate cardiac α-actin, jun-B, fra-1 and adrenomedullin via the MRTF-SRF pathway.

One conserved CArG sequence was found in the msl target gene LIF. This SRF binding site has not been reported elsewhere and therefore was identified as a novel CArG sequence. However, LIF has not been experimentally validated as a SRF target gene and was therefore considered as a probable target of SRF. IL-6 contained two CArG sequences that were conserved in mouse and rat but not in human. LIF and IL-6 were experimentally validated MRTF-dependent genes (Selvaraj and Prywes, 2004) and hence msl may regulate LIF and IL-6 via MRTF that involves an unknown mechanism or via the MRTF-SRF pathway.

BNP and MEF2C both contained one conserved SRF binding site approximately -200 bp from the TSS (according to Ensembl) where the SRF binding site in BNP has been experimentally validated (Nelson *et al.*, 2005). The SRF binding site in MEF2C was a novel finding as this CArG sequence has not been reported to date in the literature and will require experimental validation to confirm that it is a SRF binding site. BNP and MEF2C dependency on MRTFs have not been reported to date. Both BNP and MEF2C were increased in cells over-expressing msl (figure 4.4) and therefore msl could regulate both via SRF especially BNP as BNP is a known SRF target gene (Nelson *et al.*, 2005). This mechanism may or may not involve MRTFs.

The possible msl target gene myocardin contained one conserved SRF binding site when analysed using DCODE.org and this site was observed previously (Miano, 2003; Wang *et al.*, 2001b). This suggests that myocardin may be a target of SRF and hence regulated by the msl-MRTF-SRF pathway. Myocardin like MRTFs strongly associates with SRF to enhance the expression of SRF dependent genes (Wang *et al.*, 2001b). Therefore myocardin is an unlikely target of MRTFs but could be a target of msl-SRF where MRTFs are not involved.

SRF contained four conserved SRF binding sites which have been identified by others (Selvaraj and Prywes, 2004; Sun *et al.*, 2006) and it is possible that SRF may regulate its own expression (Spencer and Misra, 1999). SRF was identified as a MRTF-dependent gene (Selvaraj and Prywes, 2004) and was up-regulated following transient

(24 hours) msl over-expression, suggesting that msl via MRTF-SRF may regulate SRF. msl itself was found to contain a conserved SRF binding site approximately -300 bp relative to the TSS as shown in table 4.1 and it has been demonstrated by chromatin immunoprecipitation assays performed with formaldehyde cross-linked chromatin isolated from feline adult cardiomyocytes that SRF binds to this site in the msl promoter (Ounsain, personnel communication), raising the possibility that msl is a SRF target, thereby creating a feedback loop (figure 4.9).

Many of the putative downstream targets of msl contain SRF binding sites (SRF target genes), were identified as MRTF-dependent genes and are associated with cardiac hypertrophy and cell survival pathways. Therefore msl appears to affect genes involved in cardiac hypertrophy and cell survival suggesting that msl may play a role in the development of hypertrophy and may provide cardioprotection via a MRTF-SRF signalling pathway.

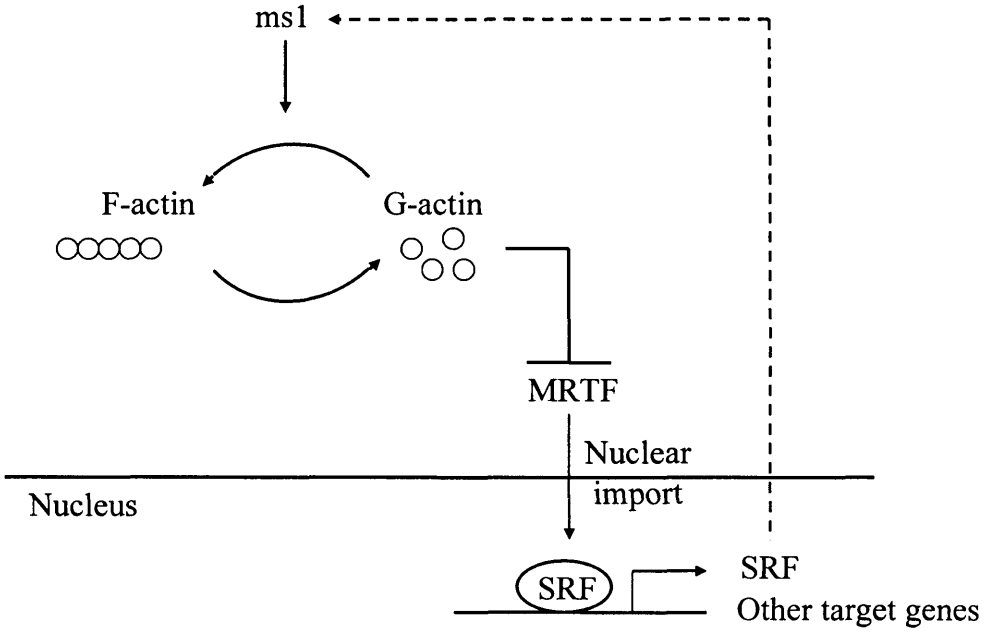

Figure 4.9. A proposed model to describe how msl may regulate MRTF-SRF target genes.

Putative target genes of msl may be regulated via the MRTF-SRF pathway. msl itself could be a SRF target gene, thus creating a feedback mechanism.

Chapter 5

Biological effects of msl over-expression *in vitro*

5.1 Introduction

In chapter 4 it was demonstrated that msl appears to affect genes involved in cardiac hypertrophy and affects genes known to protect against apoptotic cell death which possibly occurs via a MRTF-SRF signalling mechanism. These findings along with other findings of msl's rapid induction in LVH and during ischaemia-reperfusion (discussed in chapter 1) suggest that msl may play a role in the development of hypertrophy and provide cardioprotection. Hence, the work in this chapter directly examined the role of msl in cardiac cellular hypertrophy and cardioprotection *in vitro*.

As explained in chapter 1 cardiac hypertrophy is usually accompanied by complex changes in gene reprogramming. In addition to these changes in the patterns of gene and protein expression, the defining characteristics of hypertrophy are an increase in cell size of cardiac myocytes, enhanced protein synthesis and increased myofibrillar assembly (Frey and Olson, 2003; Sugden and Clerk, 1998). An increase in cell size can be monitored by an enlargement in cell size where the cross-sectional area of the cell is measured (Hunter *et al.*, 1995). Therefore, the first aim of this study was to investigate whether msl leads to hypertrophy by measuring an increase in the size of H9c2 cells following msl over-expression *in vitro*.

The second aim sought to determine whether msl can provide cardioprotection and protect H9c2 cells from apoptotic cell death. Apoptosis was a term first coined by Kerr *et al.* (1972) and proposed as a mechanism of controlled cell deletion, which occurs in two stages. The first is the formation of apoptotic bodies and the second is their phagocytosis and degradation by other cells. Apoptosis is defined as programmed cell death recognised by morphological and biochemical changes distinct from necrosis or accidental cell death (Arends and Wyllie, 1991). In apoptosis because the nucleus and cytoplasm shrink and often fragments, and the cells or fragments are phagocytosed, the contents of the cells do not leak into the extracellular space and therefore there is no inflammation. However, necrosis results from cell injury. The cells swell and lyse and the cell's contents spill into the extracellular space, inducing an inflammatory response (Kerr *et al.*, 1972; Raff, 1992). For cells to survive and not undergo apoptosis continuous signalling by cytokines, cell-cell contacts, cell-matrix interactions, growth

factors and hormones are required. Defects in cell death signalling, in membrane or cytoplasmic receptors or alterations in the genes that govern apoptosis have been implicated in the pathogenesis of cancer and autoimmune, neurodegenerative, and cardiovascular diseases (Thompson, 1995). In the cardiovascular system, apoptosis plays an essential role in homeostasis and development but also in the death of myocytes in animal models of myocardial ischaemia (Gottlieb *et al.*, 1994), in models of pressure overload (Teiger *et al.*, 1996), in aged spontaneously hypertensive rats (Li *et al.*, 1997b), in humans with acute myocardial infarction (Saraste *et al.*, 1997) and in congestive heart failure (Narula *et al.*, 1996).

In summary, the aim of this chapter was to elucidate a role for ms1 in cardiac hypertrophy and cardioprotection by transiently over-expressing ms1 *in vitro* and examining cell size and the ability of ms1 to protect against apoptotic cell death.

5.2 Results

5.2.1 Cell size quantification of ms1 over-expressing cells by microscopy

The cell size of individual H9c2 cells over-expressing ms1 versus untransfected cells (ms1 untransfected cells following transfection of the ms1 expression vector), empty vector transfected cells and untreated cells were initially examined by immunofluorescence microscopy using the software Volocity 4 (Improvision) that allows the cell area of individual cells to be measured. H9c2 cells were left untreated or transfected with the ms1 expression vector or empty vector and co-stained with c-Myc FITC antibody and Alexafluor 350 phalloidin to detect ms1 and actin, respectively. The phalloidin antibody was used so that the whole area of the cell was visualised and hence measured. Transient transfection (72 hours) of the ms1 expression vector gave rise to a mixed population of untransfected cells and cells over-expressing ms1. The software identified c-Myc FITC labelled cells (ms1 transfected cells) that appeared green and calculated the area of each cell also marked by phalloidin (actin) staining versus untransfected cells (not green) marked by phalloidin staining. However, quantification of cell size using this method was problematic because the cells were confluent following 72 hours in culture after the transfection and therefore the software could not accurately measure the area of each individual cell as the cells were in contact with other cells or overlapping each other. Even following 24 hours of ms1 over-expression when the cells were less confluent the cell area was difficult to quantify accurately using

the software because the cells still maintained cell to cell contact. Also the transfection efficiency was low which meant many cells must be counted to obtain accurate numbers and this would be very time consuming. Due to these reasons it was decided to use the flow cytometer which can measure the size of thousands of individual cells on the basis of light scatter parameters where the forward-angle light scatter relates to the cell size (Brown and Wittwer, 2000). Furthermore, the flow cytometer can rapidly analyse multiple characteristics of thousands of single cells, thus overcoming low transfection efficiencies and allowing different parameters to be measured.

5.2.2 Cell size quantification of ms1 over-expressing cells by flow cytometry

H9c2 cells were left untreated or transfected with the ms1 expression vector or the empty vector control for either 24 hours or 72 hours and then collected, fixed, permeabilised and stained with the c-Myc FITC antibody to detect ms1 over-expressing cells. Transient transfection of the ms1 expression vector will give rise to a percentage of cells transfected with the ms1 expression vector (ms1 transfected cells) and a percentage of cells will remain untransfected unlike stable transfections which is the formation of a stable cell line were all clonal descendants express the construct. This will also occur following transient transfection of the empty vector control which will give rise to a population of empty vector transfected cells and untransfected cells. The empty vector (pcDNA3.1(+)) does not contain a c-Myc tag or any other tag to distinguish empty vector transfected cells from untransfected cells and therefore was only included as a control to show there were no cells labelled with the c-Myc FITC antibody and hence over-expressing ms1. Using the flow cytometer the cells were analysed by forward scatter and side scatter parameters and displayed on a histogram as shown in figure 5.1 (a), (e) and (i). The whole cell population was gated (gate A in figure 5.1 (a), (e) and (i)) and the c-Myc FITC fluorescence of individual cells from this population was measured and registered on a logarithmic scale, see figure 5.1 (b), (f) and (j). The histogram displayed a population of cells that were not labelled with the c-Myc FITC antibody and a population of cells that were labelled.

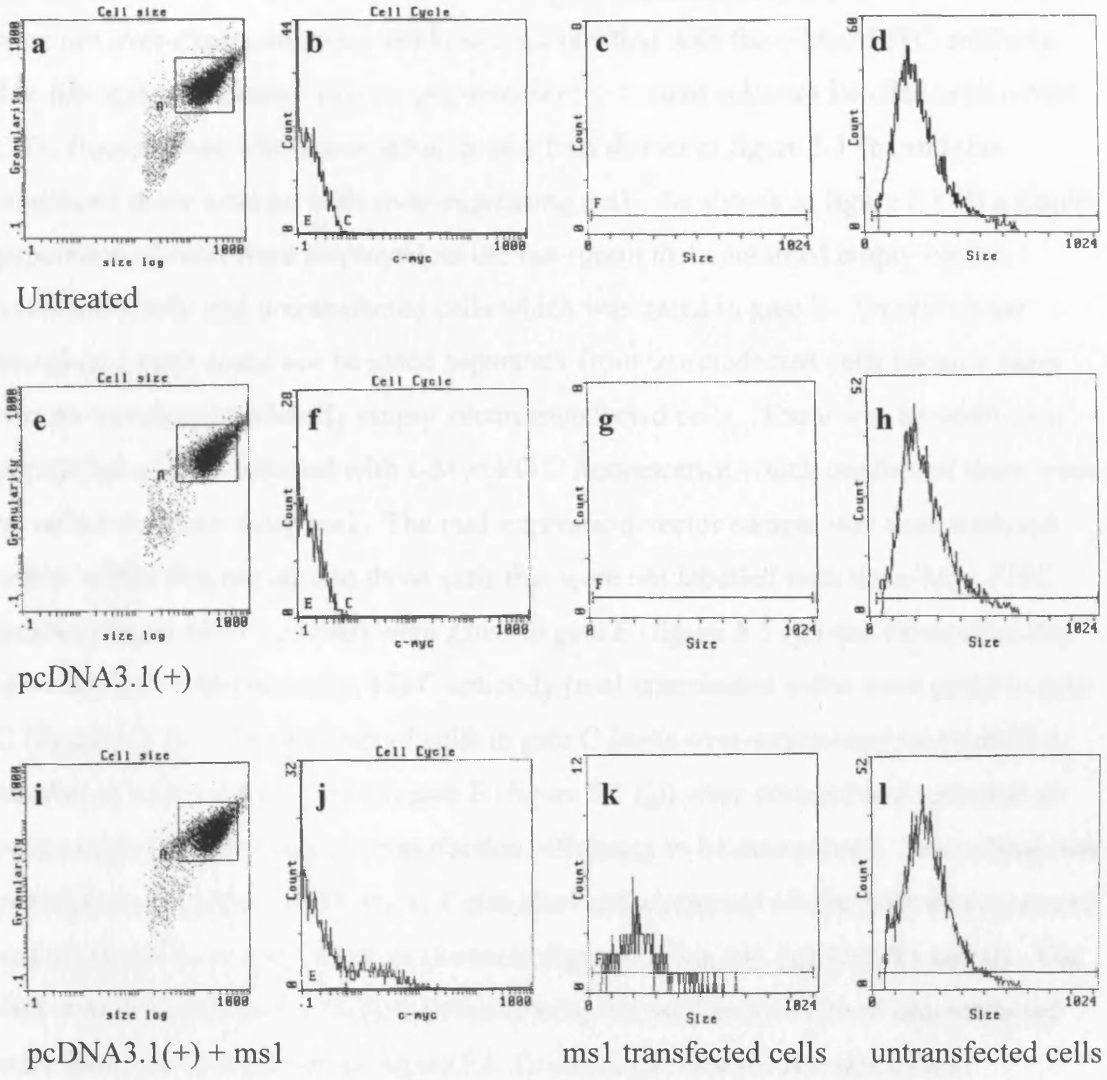

Figure 5.1. Quantification of the size of cells over-expressing ms1 by flow cytometry.

H9c2 cells were left untreated or transiently transfected with the empty vector control (pcDNA3.1(+)) or the ms1 expression vector (pcDNA3.1(+) + ms1), stained with c-Myc FITC antibody to detect ms1 over-expressing cells (gate C in (**b**), (**f**) and (**j**)) and analysed for cell size (gate F in (**c**), (**g**) and (**k**) and gate G in (**d**), (**h**) and (**l**)) by flow cytometry.

The untreated and empty vector control samples were first analysed because these cells were not over-expressing ms1 and hence not labelled with the c-Myc FITC antibody. The histogram displayed a single population of untreated cells not labelled with c-Myc FITC fluorescence which was gated in gate E as shown in figure 5.1 (b) and this confirmed there were no cells over-expressing ms1. As shown in figure 5.1 (f) a single population of cells were displayed on the histogram that contained empty vector transfected cells and untransfected cells which was gated in gate E. Empty vector transfected cells could not be gated separately from untransfected cells because there was no technique to identify empty vector transfected cells. There was no additional population of cells labelled with c-Myc FITC fluorescence which confirmed there were no cells over-expressing ms1. The ms1 expression vector sample was then analysed where within that population those cells that were not labelled with the c-Myc FITC antibody (untransfected cells) were gated in gate E (figure 5.1 (j)) and those cells that were labelled with the c-Myc FITC antibody (ms1 transfected cells) were gated in gate C (figure 5.1 (j)). The number of cells in gate C (cells over-expressing ms1) and the number of untransfected cells in gate E (figure 5.1 (j)) were counted and recorded as percentages thus allowing the transfection efficiency to be determined. From these two populations in gates C and E the cell size (forward scatter) of single cells was measured and displayed on a linear scale as shown in figure 5.1 (c), (d), (g), (h), (k) and (l). The data were recorded as the median thus allowing the median cell size of untransfected cells from gate G as shown in figure 5.1 (l) versus the median cell size of ms1 transfected cells from gate F (figure 5.1 (k)) to be compared.

5.2.3 Cell size analysis following 24 and 72 hours of ms1 over-expression

The cell size of single H9c2 cells following no treatment or transient transfection of the empty vector or the ms1 expression vector for 24 and 72 hours were examined by flow cytometry. As shown in figure 5.2 when cells were transfected with the ms1 expression vector, 13.0% ± 0.5% of cells were positive for c-Myc and hence were ms1 transfected cells that over-expressed ms1 compared to 86.9% ± 0.5% untransfected cells. This finding was similar at both 24 hour and 72 hour transfections. This low transfection efficiency of approximately 13% was observed previously in chapter 3 using immunofluorescence microscopy; however, because approximately 10,000 cells were analysed by flow cytometry, 13% of cells was equivalent to approximately 1300 cells quantified that over-expressed ms1.

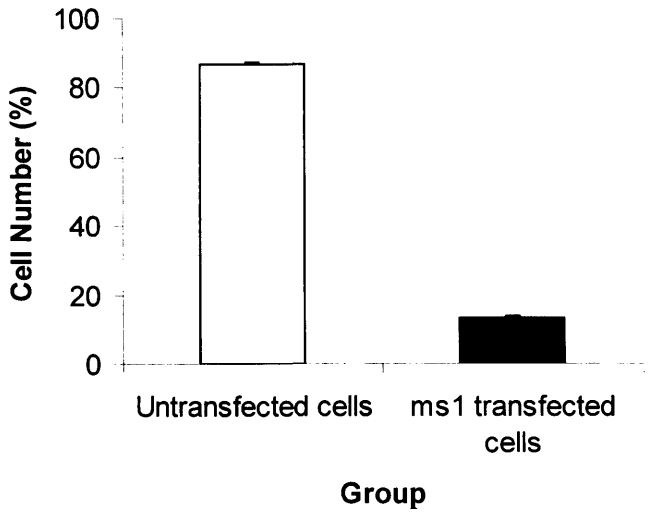

Figure 5.2. 13.0% ± 0.5% of H9c2 cells over-expressed ms1 following transfection for 72 hours when analysed by flow cytometry.

H9c2 cells were transiently transfected with the ms1 expression vector (pcDNA3.1(+) + ms1), stained with c-Myc FITC antibody and analysed using a flow cytometer for the percentage of cells over-expressing ms1 (ms1 transfected cells) detected by c-Myc FITC fluorescence. Bars show median ± SD, n = 4.

There was no change in the size of cells over-expressing ms1 (ms1 transfected cells) compared to untransfected cells, empty vector transfected and untransfected cells (following transfection of the empty vector, pcDNA3.1(+)) or untreated cells following 24 hours (figure 5.3 (a)). Thus, over-expression of ms1 for 24 hours does not appear to alter cell size. However, there was a significant approximate 1.5 fold increase in cell size following 72 hours of ms1 over-expression (in ms1 transfected cells) compared to untransfected cells ($P < 0.01$), empty vector transfected and untransfected cells following transfection of the empty vector, pcDNA3.1(+) ($P < 0.01$) and untreated cells ($P < 0.01$) as shown in figure 5.3 (b). Thus, the size of H9c2 cells appears to increase following 72 hours of ms1 over-expression.

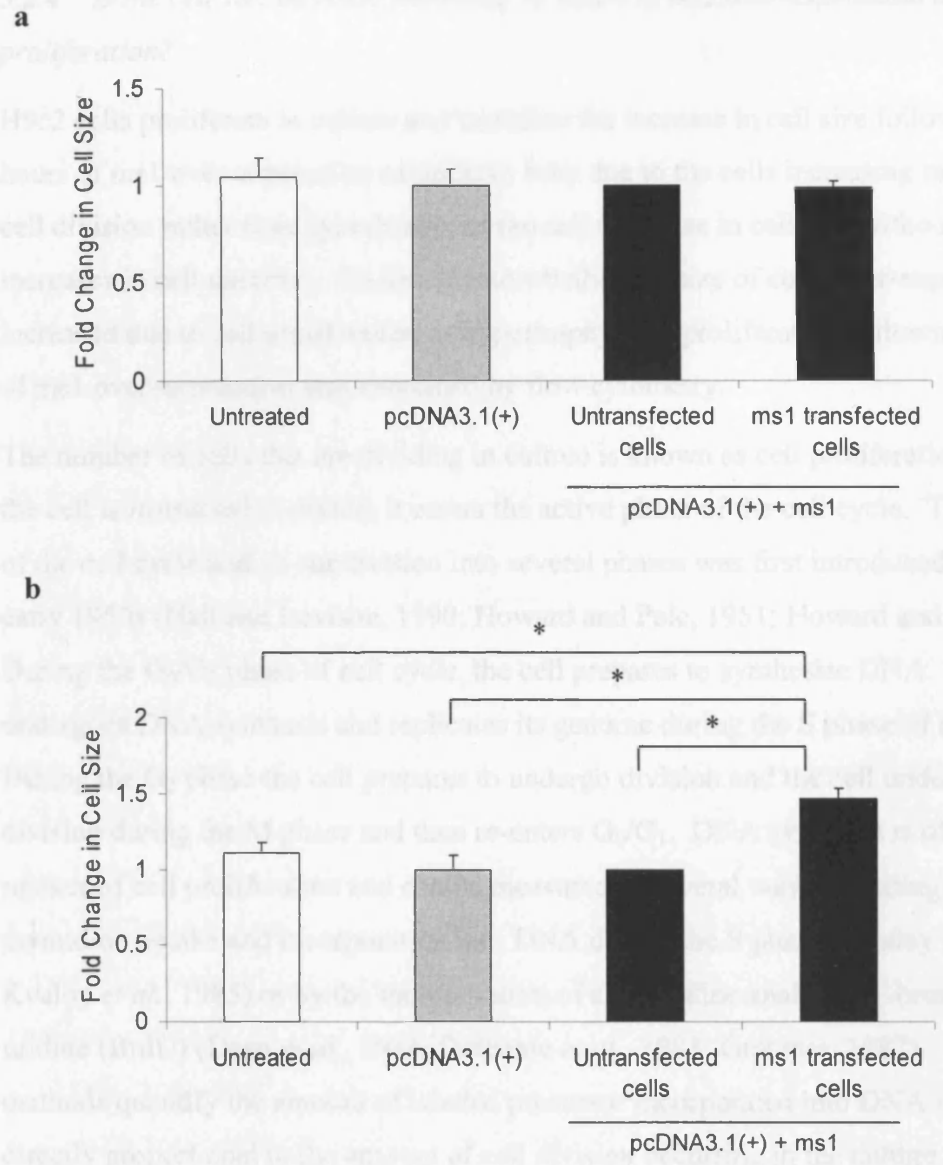

Figure 5.3. Cell size following ms1 over-expression for 24 and 72 hours.

Flow cytometric analysis of the size of cells following no treatment (untreated) or transient transfection of the empty vector (pcDNA3.1(+)) or the ms1 expression vector (pcDNA3.1(+) + ms1) for (**a**) 24 hours and (**b**) 72 hours. The median size of ms1 transfected cells, untransfected cells, empty vector transfected and untransfected cells (pcDNA3.1(+)) and untreated cells were quantified and the fold change in cell size was calculated relative to control (untransfected cells). Bars show mean ± SD from 4 separate experiments. $*P < 0.01$.

5.2.4 Is the cell size increase following 72 hours of ms1 over-expression due to cell proliferation?

H9c2 cells proliferate in culture and therefore the increase in cell size following 72 hours of ms1 over-expression could have been due to the cells increasing in size prior to cell division rather than hypertrophy of the cell (increase in cell size without associated increases in cell number). To investigate whether the size of cells over-expressing ms1 increased due to cell proliferation or hypertrophy, cell proliferation following 72 hours of ms1 over-expression was examined by flow cytometry.

The number of cells that are dividing in culture is known as cell proliferation and once the cell is instructed to divide, it enters the active phase of the cell cycle. The concept of the cell cycle and its subdivision into several phases was first introduced during the early 1950s (Hall and Levison, 1990; Howard and Pelc, 1951; Howard and Pelc, 1953). During the G_0/G_1 phase of cell cycle, the cell prepares to synthesise DNA. The cell undergoes DNA synthesis and replicates its genome during the S phase of the cell cycle. During the G_2 phase the cell prepares to undergo division and the cell undergoes division during the M phase and then re-enters G_0/G_1. DNA synthesis is often used as a marker of cell proliferation and can be measured in several ways including tritiated thymidine uptake and incorporation into DNA during the S phase (Kvaloy *et al.*, 1981; Kvaloy *et al.*, 1985) or by the incorporation of a thymidine analogue 5-bromo-2'-deoxy-uridine (BrdU) (Dean *et al.*, 1984; Dolbeare *et al.*, 1983; Gratzner, 1982). Both methods quantify the amount of labeled precursor incorporated into DNA which is directly proportional to the amount of cell division occurring in the culture. Flow cytometry using dyes that can bind to DNA such as propidium iodide can measure DNA content, thus, allowing the S phase fraction of the cell cycle to be determined (Braylan *et al.*, 1980; Lee *et al.*, 1992; Timm *et al.*, 1998). Cell proliferation can also be measured where molecules that regulate the cell cycle are measured either by their activity for example cdc2 kinases (Draetta *et al.*, 1988; Draetta and Beach, 1988) or by using antibodies that recognise proliferating cells such as ki67 (Gerdes *et al.*, 1983; Gerdes *et al.*, 1984; Verheijen *et al.*, 1989a; Verheijen *et al.*, 1989b). All these methods to assess cell proliferation have their advantages and disadvantages. It was initially decided to use flow cytometry using propidium iodide to measure the fraction of cells with S phase DNA content by DNA distribution analysis as a marker of proliferation in cells over-expressing ms1 versus untransfected cells. This method had advantages over

other methods because thousands of cells can be analysed using the flow cytometer which was required because of the low transfection efficiency. Also propidium iodide can measure apoptosis (sub-G_1) (Nicoletti *et al.*, 1991; Telford *et al.*, 1991; Telford *et al.*, 1992) and all the cell cycle phases at the same time.

H9c2 cells were left untreated or transfected with the ms1 expression vector or empty vector control for 72 hours and then collected, fixed, permeabilised and stained with the c-Myc FITC antibody to detect ms1 over-expressing cells and propidium iodide to stain DNA content. When analysed by the flow cytometer, the cells did not take up propidium iodide. Cells are usually fixed in ice cold 70% ethanol prior to the addition of propidium iodide and when this method was used, the cells did take up propidium iodide. However, in order to detect ms1 over-expressing cells using the c-Myc FITC antibody (that recognises the c-Myc tag on ms1), the cells were fixed and permeabilised prior to the addition of the antibody using a different method to the one used with propidium iodide, where the fixative was formaldehyde based. Although this method detected ms1 over-expressing cells it was not compatible with propidium iodide to stain DNA content. An alternative to propidium iodide is the Vybrant DyeCycle Violet Stain which stains DNA in the same way as propidium iodide. Vybrant DyeCycle Violet Stain can be used on unfixed or fixed cells and was compatible with the fixation and permeabilisation method used to detect ms1 over-expressing cells by the c-Myc FITC antibody. In brief, cells were transfected and following 72 hours the cells were collected, fixed, permeabilised and stained with the c-Myc FITC antibody to detect ms1 over-expressing cells and stained with Vybrant DyeCycle Violet Stain to detect DNA content. The Beckman Coulter Epics XL·MCL flow cytometer that was originally used to measure cell size does not have the correct fluorescence detector to identify the cells stained with the Vybrant DyeCycle Violet Stain and therefore cells were measured using a DakoCytomation CyAn ADP flow cytometer and analysed using Summit v4.3 software in subsequent experiments.

The cells were analysed as described previously in section 5.2.2 except that the whole cell population gated in R1 was also gated through another gate R2 where the R2 gate collected single cells stained with Vybrant DyeCycle Violet Stain (figure 5.4). The c-Myc FITC fluorescence of single cells from cells in gate R2 was measured and displayed on a logarithmic scale as shown in figure 5.4 (c), (g) and (k). Cells that were not over-expressing ms1 and hence not labelled with the c-Myc FITC antibody

(untreated cells, empty vector transfected cells and untransfected cells following transfection of the empty vector and cells exposed to the transfection of the ms1 expression vector but remained untransfected) were gated in gate R8 (figure 5.4 (c), (g) and (k)). Cells over-expressing ms1 and therefore labelled with the c-Myc FITC antibody were gated in gate R9 (figure 5.4 (k)). The cell cycle distribution within these two populations in gates R8 and R9 was measured and displayed on a linear scale as shown in histograms (d), (h), (l) and (m) of figure 5.4. The percentages of cells in each cell cycle phase was recorded where the cells in gate R13/R16 represented the percentage of apoptotic cells (sub-G_1), cells in gate R15/R14 represented cells in G_0/G_1 phase, cells in gate R19/17 represented cells in S phase (DNA synthesis) and the percentage of cells in gate R22/R23 represented cells in G_2/M phase of the cell cycle. Cells that were not exposed to the transfection method (untreated cells) were included as a control to set the gates for each phase of the cell cycle (figure 5.4 (d)). Thus, the percentage of cells in each phase of the cell cycle in particular the S phase (marker of proliferating cells) was compared for those cells that over-expressed ms1 and those cells that did not.

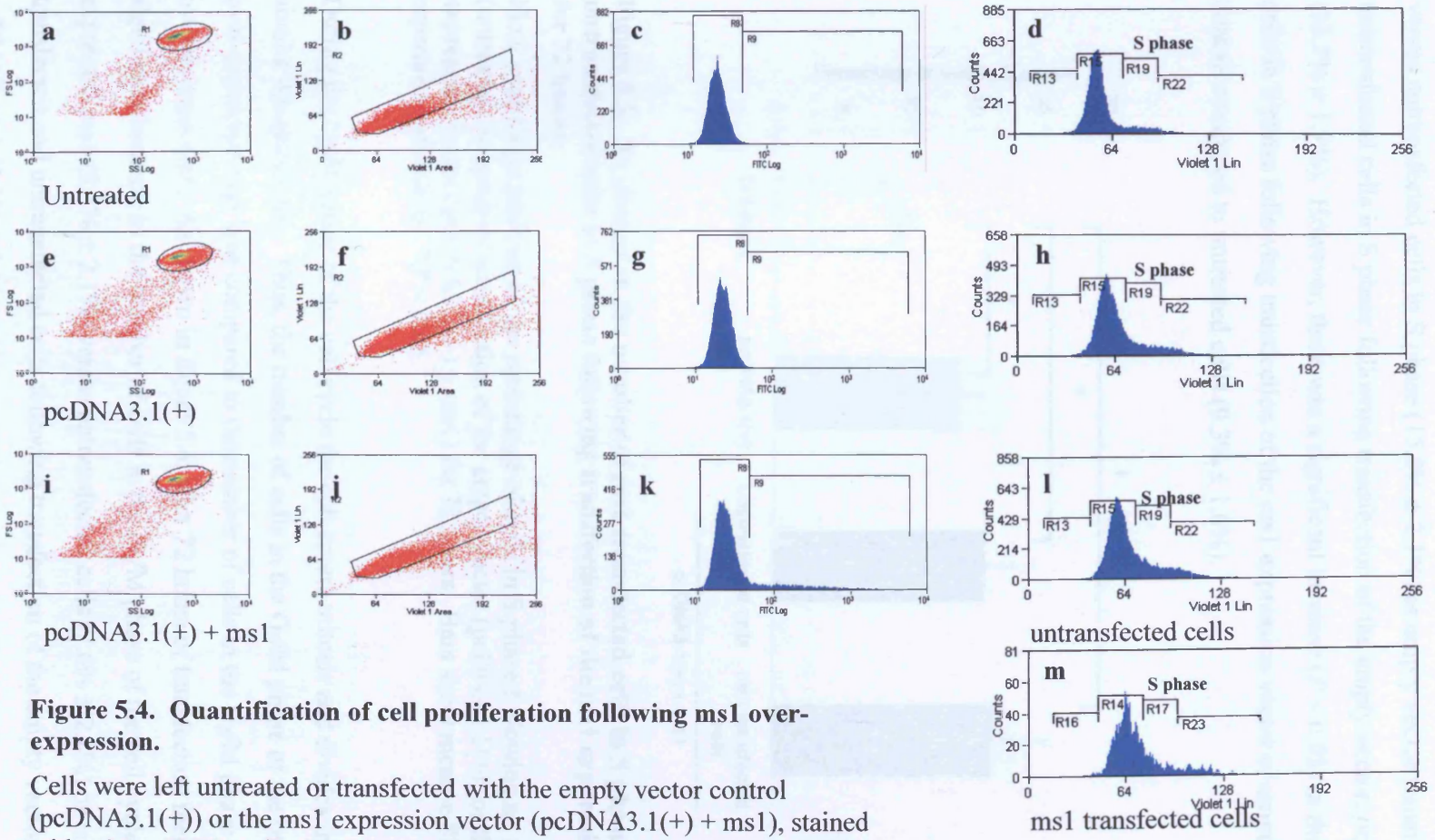

Figure 5.4. Quantification of cell proliferation following ms1 over-expression.

Cells were left untreated or transfected with the empty vector control (pcDNA3.1(+)) or the ms1 expression vector (pcDNA3.1(+) + ms1), stained with c-Myc FITC antibody to detect ms1 over-expressing cells (gate R9 in (**c**), (**g**), (**k**)) and Vybrant DyeCycle Violet Stain, to analyse S phase DNA content as a marker of proliferation ((**d**), (**h**), (**l**), (**m**)) by flow cytometry.

As shown in figure 5.5, after 72 hours of transfection there was no significant change in the number of cells over-expressing ms1 in S phase of the cell cycle (16.4% ± 4.0%) versus untransfected cells in S phase (15.8% ± 2.1%) or empty vector transfected and untransfected cells in S phase following transfection of the empty vector, pcDNA3.1(+) (13.7% ± 1.7%). However, there was a significant increase ($P < 0.05$) in the number of cells in S phase following transfection of the ms1 expression vector or empty vector control compared to untreated cells (9.3% ± 1.0%).

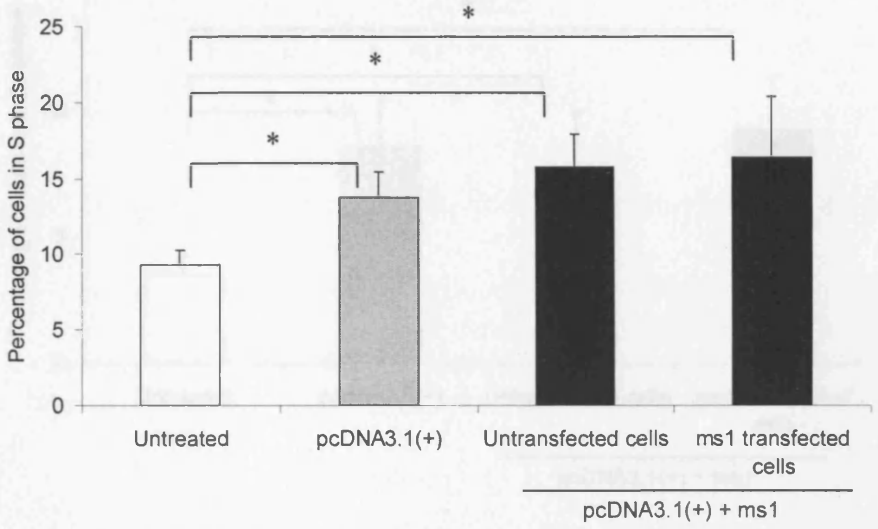

Figure 5.5. No change in the number of ms1 transfected cells in S phase versus untransfected cells in S phase following transfection of the ms1 expression vector for 72 hours.

Flow cytometric analysis of the percentage of cells in S phase following no treatment (untreated) or transient transfection of the empty vector (pcDNA3.1(+)) or the ms1 expression vector (pcDNA3.1(+) + ms1) for 72 hours. Bars show mean ± SD from 4 separate experiments. *$P < 0.05$.

During the G_2/M phase of the cell cycle the cell enters mitosis and divides into two similar daughter cells. Thus, the number of cells in the G_2/M phase of the cell cycle that over-expressed ms1 was compared to the number of cells in the G_2/M phase that did not over-express ms1. As shown in figure 5.6, after 72 hours of transfection there was no significant increase in the number of cells in the G_2/M phase of the cell cycle that over-expressed ms1 (9.3% ± 2.1%) versus untransfected cells (7.6% ± 2.4%) or empty vector transfected and untransfected cells following transfection of the empty vector, pcDNA3.1(+) (8.6% ± 2.1%). However, the number of cells in S phase significantly

increased ($P < 0.05$) following transfection of the ms1 expression vector or empty vector control compared to untreated cells (3.5% ± 0.8%). Thus, it appears that the transfection itself of the empty vector or the ms1 expression vector increases the number of cells in S phase or G_2/M phase but over-expression of ms1 for 72 hours does not appear to alter the number of cells in S phase or G_2/M phase of the cell cycle compared to cells that did not over-express ms1 following transfection.

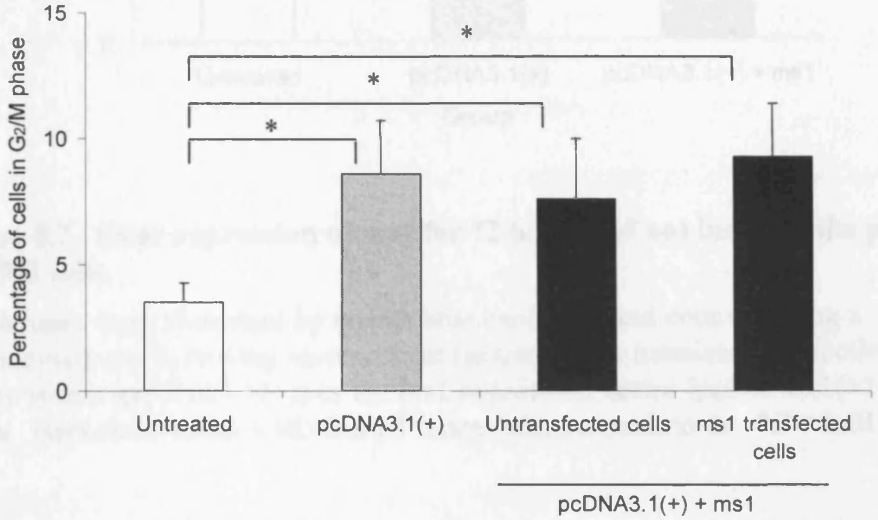

Figure 5.6. The number of ms1 transfected cells in G_2/M phase did not increase compared to the number of untransfected cells in G_2/M phase following transfection of the ms1 expression vector for 72 hours.

The number of H9c2 cells in G_2/M phase following no treatment (untreated) or transient transfection of the empty vector (pcDNA3.1(+)) or the ms1 expression vector (pcDNA3.1(+) + ms1) for 72 hours was examined by flow cytometry. Bars show mean ± SD from 4 separate experiments. $^*P < 0.05$.

In addition, cellular proliferation of cells that over-expressed ms1 compared to those that did not over-express ms1 was quantified by direct cell counting using a haemocytometer. There was no significant difference in the number of cells between the two transfected groups following 72 hours of transfection (figure 5.7). A significantly greater ($P < 0.01$) number of cells in the untreated group were observed probably due to the known cytotoxic effect of the transfection reagent. Therefore, over-expression of ms1 does not appear to increase cell proliferation.

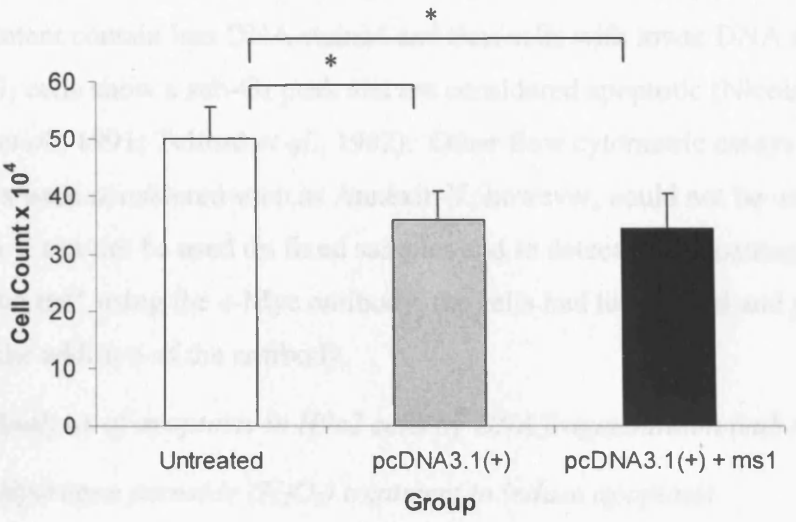

Figure 5.7. Over-expression of ms1 for 72 hours did not increase the proliferation of H9c2 cells.

Viable cells were identified by trypan blue exclusion and counted using a haemocytometer following no treatment (untreated) or transient transfection of the empty vector (pcDNA3.1(+)) or the ms1 expression vector (pcDNA3.1(+) + ms1) for 72 hours. Bars show mean ± SD from 4 independent experiments. $*P < 0.01$.

5.2.5 Detection of apoptosis

As discussed earlier in section 5.1, apoptosis is a distinct form of cell death characterised by a sequence of morphological events that include cell shrinkage, cell shape change, condensation of the cytoplasm, nuclear envelope changes, nuclear fragmentation, formation of apoptotic bodies and eventual cell disintegration (Kerr *et al.*, 1972; Wyllie, 1980). It was discovered that the percentage of cells over-expressing ms1 was low and hence quantification of apoptosis by microscopy would be rather cumbersome. To overcome this, the flow cytometer was used because of the advantage that it can analyse multiple characteristics of many thousands of single cells. As explained in section 5.2.4 it was found that the Vybrant DyeCycle Violet Stain could be used as an alternative to propidium iodide to stain DNA content of cells and therefore flow cytometry using this stain was the method chosen to measure apoptosis. Cell cycle analysis based on measurements on DNA content generates a clear distribution consisting of the G_0/G_1 phase of cell cycle, the S phase and the G_2/M phase. During apoptosis the DNA of the cell fragments and following fixation and permeabilisation, the low molecular weight DNA inside the cytoplasm of apoptotic cells elutes during the

wash procedure. Therefore, following staining with the violet dye, cells with lower DNA content contain less DNA stained and thus cells with lower DNA staining than that of G_1 cells show a sub-G_1 peak and are considered apoptotic (Nicoletti *et al.*, 1991; Telford *et al.*, 1991; Telford *et al.*, 1992). Other flow cytometric assays that measure apoptosis were considered such as Annexin V; however, could not be used because Annexin V can not be used on fixed samples and to detect the percentage of cells over-expressing ms1 using the c-Myc antibody, the cells had to be fixed and permeabilised prior to the addition of the antibody.

5.2.6 Analysis of apoptosis in H9c2 cells by DNA fragmentation (sub-G_1)

5.2.6.1 Hydrogen peroxide (H_2O_2) treatment to induce apoptosis

Apoptosis is increased during oxidative stress and is involved in several cardiovascular diseases (Han *et al.*, 2004). Hydrogen peroxide (H_2O_2) is a well known oxidant that has been used to induce apoptosis in H9c2 cells (Chen *et al.*, 2000; Gupta *et al.*, 2006; Gustafsson *et al.*, 2004; Han *et al.*, 2004; Hou and Hsu, 2005; Neuss *et al.*, 2001; Pesant *et al.*, 2006; Tanaka *et al.*, 2003; Turner *et al.*, 1998; Zhang and Herman, 2006) and was therefore used to induce apoptosis following transfection of the ms1 expression vector or empty vector control in H9c2 cells, to identify whether over-expression of ms1 can protect against H_2O_2 induced apoptosis.

Different concentrations of H_2O_2 (500 μM – 800 μM) was added to H9c2 cells for 24 hours to first determine the amount of H_2O_2 that caused H9c2 cells to undergo apoptosis. Cells were collected, fixed, permeabilised and stained with the c-Myc FITC antibody and Vybrant DyeCycle Violet Stain following 24 hours after H_2O_2 treatment. The cells were analysed using a DakoCytomation CyAn ADP flow cytometer as described previously in section 5.2.4 except that the gates R1, R2, R8 and R9 were extended to collect apoptotic cells, see figure 5.8 (a-c), (e-g) and (i-k).

The percentage of cells in each phase of the cell cycle was recorded where the cells in gate 13 (sub-G_1 phase) represent the percentage of apoptotic cells (figure 5.8 (d), (h) and (l). The percentage of apoptotic H9c2 cells were quantified following treatment with various concentrations of H_2O_2 for 24 hours. As shown in figure 5.9 very few H9c2 cells were apoptotic following treatment with 500 μM (1.5% ± 0.2%) or 600 μM H_2O_2 (4.5% ± 0.6%) for 24 hours. With 700 μM H_2O_2 or more, cells appeared very apoptotic with condensed nuclei; however, cells would not pellet following centrifugation in order

to collect the cells probably because the cells were too fragmented and thus could not be analysed using the flow cytometer. Treatment of H9c2 cells with 500 μM or 600 μM H_2O_2 for 24 hours did not cause a sufficient amount of apoptosis and amounts above 600 μM H_2O_2 caused too much cell fragmentation where the cells could not be collected and therefore H_2O_2 was not used further to study apoptosis.

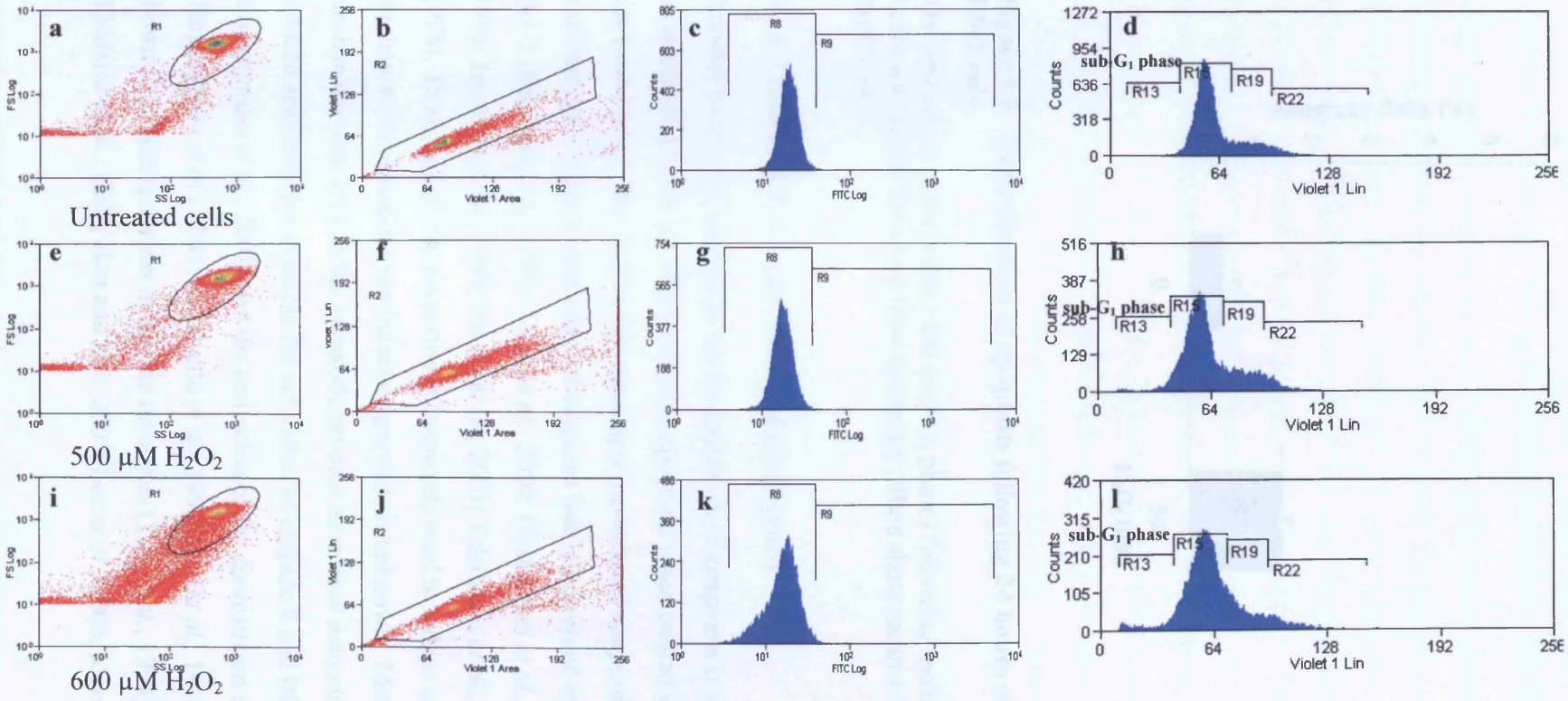

Figure 5.8. Quantification of H_2O_2 induced apoptosis in H9c2 cells by flow cytometry.

Cells were left untreated or treated with 500 μM H_2O_2 or 600 μM H_2O_2 for 24 hours, stained with c-Myc FITC antibody and Vybrant DyeCycle Violet Stain and analysed by flow cytometry for the percentage of apoptotic cells based on the sub-G_1 phase DNA content (gate R13 in (**d**), (**h**) and (**l**)).

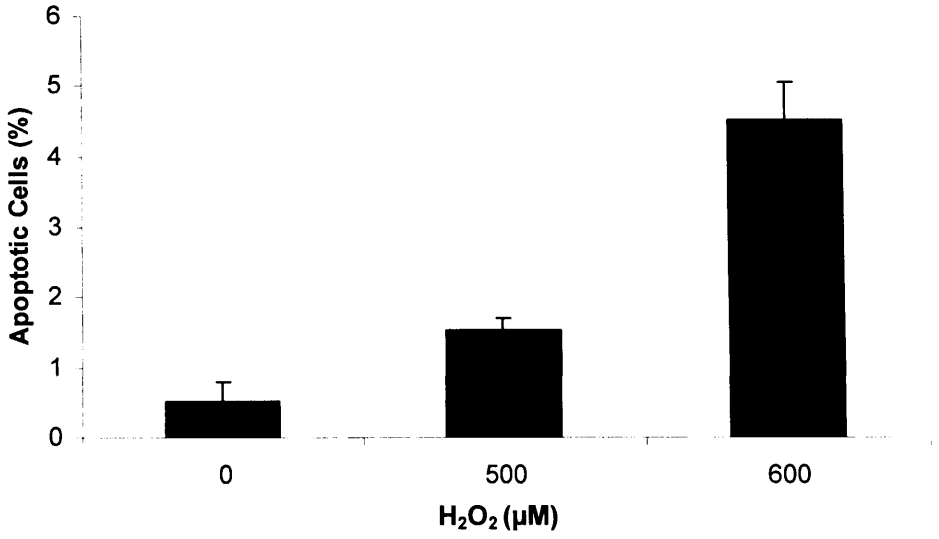

Figure 5.9. Quantification of apoptosis following 24 hours of H_2O_2 treatment in H9c2 cells.

The percentage of apoptotic cells (sub-G_1 phase) following treatment with H_2O_2 for 24 hours was quantified using flow cytometry. Bars show mean ± SD from 3 independent experiments.

5.2.6.2 Staurosporine treatment to induce apoptosis

Another frequently used agent for the induction of apoptosis is staurosporine. Nearly all mammalian cells are able to become apoptotic when treated with staurosporine and it has been consistently shown that staurosporine-induced apoptosis involves cytochrome c release and results in activation of caspases that is prevented by over-expression of Bcl-2 (Bertrand *et al.*, 1994; Chen *et al.*, 2000; Gustafsson *et al.*, 2004; Jacobsen *et al.*, 1996; Jacobson *et al.*, 1994; Neuss *et al.*, 2001; Takahashi *et al.*, 1997; Turner *et al.*, 1998). Even though staurosporine is frequently used to induce apoptosis, the exact mechanism of staurosporine-induced apoptosis is unknown. Many important mechanisms involved in the apoptotic process have been demonstrated in staurosporine-induced apoptosis for example the activation of caspase 8 and Bid cleavage (Stepczynska *et al.*, 2001) and the activation of the downstream effector caspase 3 (Stepczynska *et al.*, 2001; Takahashi *et al.*, 1997; Yue *et al.*, 1998). Staurosporine was shown to induce apoptosis in cardiac myocytes (Yue *et al.*, 1998) and in H9c2 cells (Ekhterae *et al.*, 2003; Hou and Hsu, 2005; Lee *et al.*, 2006; Mao *et al.*, 2004)

demonstrating that staurosporine-induced apoptosis is a useful model to investigate apoptosis in mammalian cells and was therefore used as a substitute for H_2O_2.

H9c2 cells were treated with various concentrations of staurosporine (5 nM - 25 nM) for 24 hours and assayed as described above to quantify the percentage of cells that displayed apoptosis. As shown in figure 5.10 (a) the size of the sub-G_1 peak increased as the amount of staurosporine added to H9c2 cells increased and when the percentage of apoptotic cells under the sub-G_1 peak were quantified the amount of apoptotic cells increased with increasing concentrations of staurosporine. 28.5% ± 1.7% of cells were apoptotic following treatment with 5 nM staurosporine for 24 hours. With 15 nM staurosporine, 39.4% ± 1.1% of cells were apoptotic and just under half of the cells (44.5% ± 2.4%) displayed apoptosis following treatment with 25 nM staurosporine for 24 hours (figure 5.10 (b)). This demonstrated that flow cytometry using the Vybrant DyeCycle Violet Stain to detect DNA fragmentation (apoptotic cells present in the sub-G_1 phase) was a valid assay for detecting apoptosis in H9c2 cells when treated with various concentrations of staurosporine (5 nM - 25 nM) for 24 hours.

a

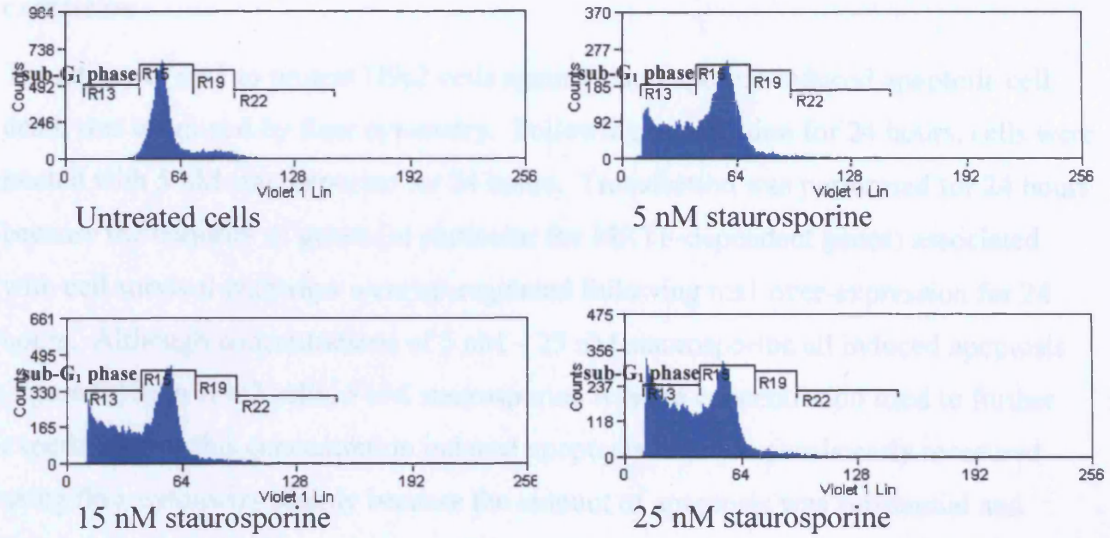

b

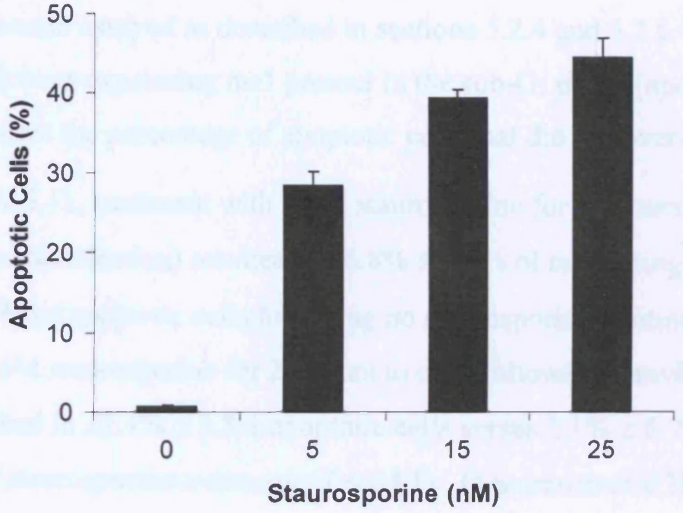

Figure 5.10. Quantification of staurosporine induced apoptosis in H9c2 cells by flow cytometry.

H9c2 cells were left untreated or treated with staurosporine (5 nM - 25 nM) for 24 hours, stained with c-Myc FITC antibody and Vybrant DyeCycle Violet Stain to detect apoptotic cells (sub-G_1 phase) by flow cytometry (**a**). (**b**) The percentage of apoptotic cells based on the sub-G_1 phase DNA content (gate R13 in (**a**)) was quantified. The results are the mean ± SD from 3 independent experiments.

5.2.7 Analysis of staurosporine-induced apoptotic cell death following ms1 over-expression

The ability of ms1 to protect H9c2 cells against staurosporine-induced apoptotic cell death was examined by flow cytometry. Following transfection for 24 hours, cells were treated with 5 nM staurosporine for 24 hours. Transfection was performed for 24 hours because the majority of genes (in particular the MRTF-dependent genes) associated with cell survival pathways were up-regulated following ms1 over-expression for 24 hours. Although concentrations of 5 nM – 25 nM staurosporine all induced apoptosis (figure 5.10) in H9c2 cells, 5 nM staurosporine was the concentration used in further experiments as this concentration induced apoptosis that was consistently measured using flow cytometry mainly because the amount of apoptosis was substantial and hence the sub-G_1 peak was not too large which enabled the amount of apoptosis in this peak to be quantified without difficulty. Following treatment with 5 nM staurosporine for 24 hours, cells were assayed as described in sections 5.2.4 and 5.2.6 where the percentage of cells over-expressing ms1 present in the sub-G_1 phase (apoptotic cells) was compared against the percentage of apoptotic cells that did not over-express ms1.

As shown in figure 5.11, treatment with 5 nM staurosporine for 24 hours to untreated cells (unexposed to transfection) resulted in 26.8% ± 3.5% of cells being apoptotic versus 0.6% ± 0.1% of apoptotic cells following no staurosporine treatment ($P < 0.01$). Treatment with 5 nM staurosporine for 24 hours to cells following transfection with the empty vector resulted in 32.4% ± 3.8% apoptotic cells versus 2.1% ± 0.7% of apoptotic cells following no staurosporine treatment ($P < 0.01$). In untransfected H9c2 cells within the population of cells transfected with the ms1 expression vector, 1.6% ± 0.5% of cells underwent apoptosis under control conditions. Treatment with 5 nM staurosporine for 24 hours markedly increased the percentage of cells undergoing apoptosis to 29.0% ± 2.9% ($P < 0.01$). Less than 1% of ms1 transfected cells (0.7% ± 0.3%) underwent apoptosis following no treatment with staurosporine and this was significantly less than the amount of apoptotic untransfected cells ($P < 0.05$) and apoptotic cells following transfection with the empty vector ($P < 0.05$) when not treated with staurosporine. With 5 nM staurosporine for 24 hours, 3.5% ± 1.0% of ms1 transfected cells were apoptotic and this increase was significant ($P < 0.05$) compared to baseline ms1 transfected cells following no treatment. In contrast to the response of cells left untreated (not exposed to transfection), cells following transfection with the

empty vector and untransfected cells (within the population of cells transfected with the ms1 expression vector) to 5 nM staurosporine for 24 hours, H9c2 cells transfected with ms1 displayed very little apoptosis when exposed to the same conditions. Over-expression of ms1 significantly inhibited staurosporine-induced apoptosis compared with untreated cells (no transfection) ($P < 0.01$), cells following transfection with the empty vector ($P < 0.01$) and untransfected cells ($P < 0.01$). These results suggest that ms1 over-expression prevents staurosporine-induced apoptotic cell death.

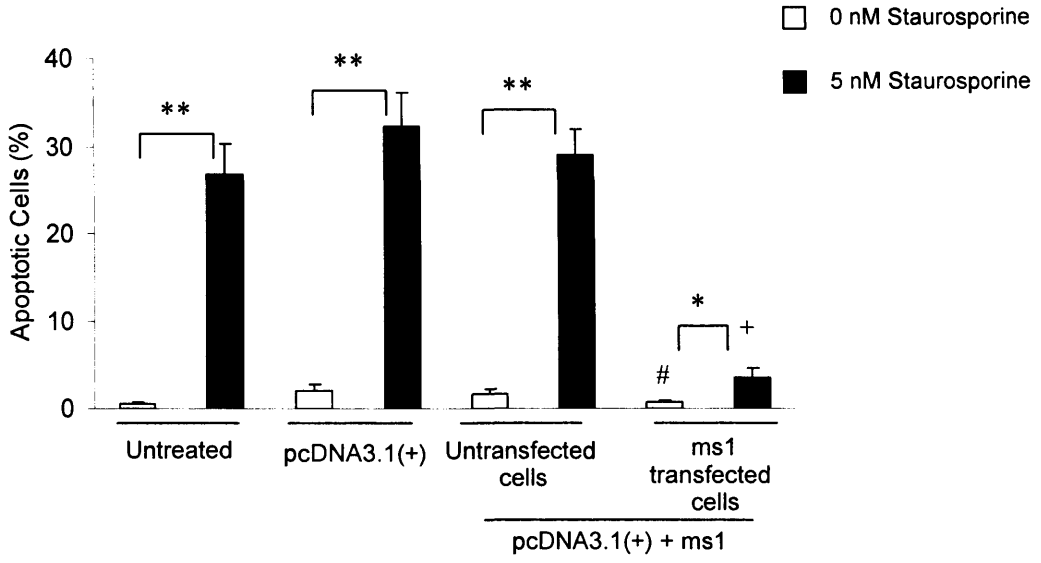

Figure 5.11. ms1 inhibits apoptosis induced by staurosporine in H9c2 cells.

Cells were left untreated or transfected (24 hours) with the empty vector (pcDNA3.1(+)) or ms1 expression vector (pcDNA3.1(+) + ms1) and treated with or without 5 nM staurosporine for 24 hours, stained with c-Myc FITC antibody and Vybrant DyeCycle Violet Stain to detect the percentage of apoptotic cells (sub-G_1 phase) by flow cytometry. The results are the mean ± SD from 4 independent experiments. $*P < 0.05$, $**P < 0.01$, $+P < 0.01$ versus untreated cells, empty vector cells and untransfected cells with staurosporine treatment, $\#P < 0.05$ versus empty vector and untransfected cells without staurosporine treatment.

During apoptosis the cell shrinks and this can be distinguished by flow cytometry on the basis of forward angle light scatter which relates to cell size because they bend less light into the forward scatter detector than a viable cell does. Thus, cells undergoing apoptosis should appear "smaller" than living cells in a flow cytometer. The median size of cells over-expressing ms1 compared to the median size of cells not over

expressing ms1 following treatment with 5 nM staurosporine for 24 hours was also measured.

As shown in figure 5.12, treatment with 5 nM staurosporine for 24 hours to untreated cells (unexposed to transfection) resulted in a significant reduction in cell size ($P < 0.01$). This finding was also observed when cells following transfection with the empty vector and untransfected cells (within the population of cells transfected with the ms1 expression vector) were treated with 5 nM staurosporine for 24 hours. However, the size of cells over-expressing ms1 following staurosporine treatment was similar to the size of cells that over-expressed ms1, the size of untransfected cells, the size of cells following transfection with the empty vector and the size of untreated cells with no staurosporine treatment. Cells over-expressing ms1 were approximately twice as large in cell size compared to untransfected cells ($P < 0.01$), cells following transfection with the empty vector ($P < 0.01$) and untreated cells (not exposed to transfection) ($P < 0.01$), subsequent to treatment with staurosporine. These findings suggest that the size of cells over-expressing ms1 remain unaltered following treatment with staurosporine.

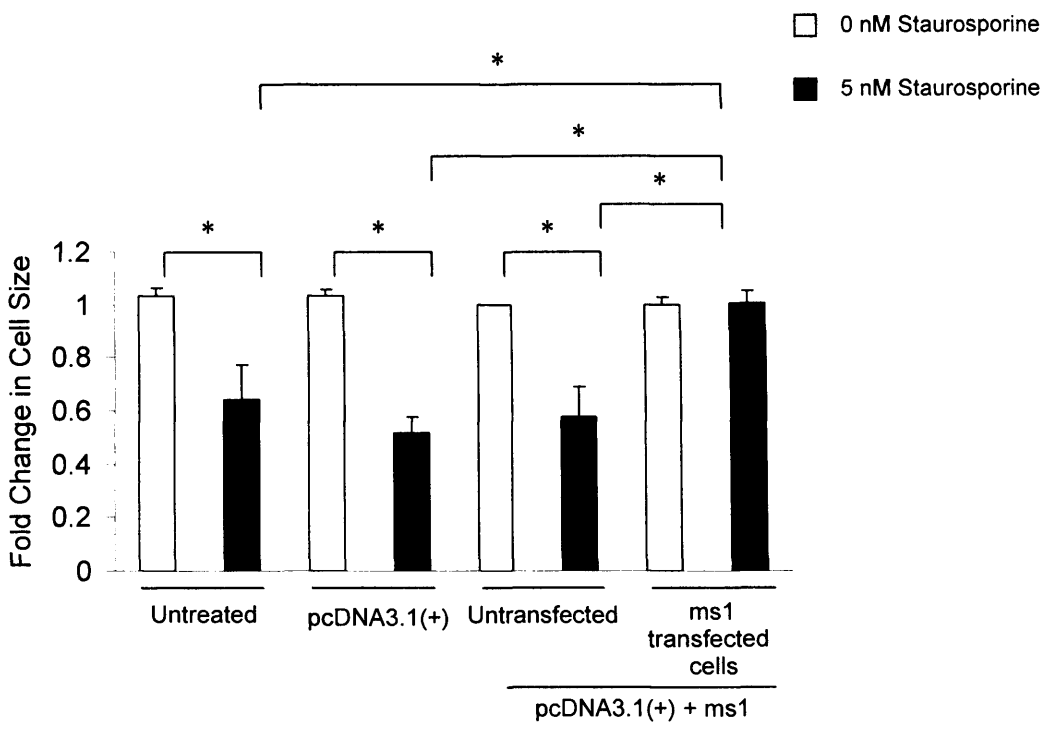

Figure 5.12. ms1 prevents a reduction in the size of H9c2 cells induced by staurosporine.

The size of H9c2 cells was examined by flow cytometry following no treatment (untreated) or transient transfection of the empty vector (pcDNA3.1(+)) or the ms1 expression vector (pcDNA3.1(+) + ms1) for 24 hours with or without 5 nM staurosporine for 24 hours. The median size of ms1 transfected cells, untransfected cells, empty vector transfected and untransfected cells (pcDNA3.1(+)) and untreated cells were quantified and the fold change in cell size was calculated relative to control (non treated untransfected cells). The results are the mean ± SD from 4 independent experiments. $*P < 0.01$.

5.3 Discussion

The main findings were:

1. ms1 increases the size of H9c2 cells without an increase in cell proliferation.
2. ms1 protects H9c2 cells from staurosporine-induced apoptosis.

5.3.1 ms1 increases the size of H9c2 cells without an increase in cell proliferation

In order to investigate the role of ms1 in cardiac hypertrophy, the size of cells over-expressing ms1 versus the size of cells that did not over-express ms1 were initially examined by immunofluorescence microscopy where the cell area of individual cells were measured. H9c2 cells were transfected with the ms1 expression vector and co-

stained with c-Myc FITC antibody and phalloidin to detect msl and actin, respectively. Phalloidin staining enabled the area of each cell to be visualised and hence measured. The transfection efficiency of H9c2 cells transfected with the msl expression vector for 24 hours or 72 hours was low and gave rise to a mixed population of untransfected cells and msl expressing cells. The low transfection efficiency meant quantification of cell size by microscopy would be time consuming. It was also discovered that H9c2 cells were confluent after 72 hours in culture and cells maintained cell to cell contact whether confluent or not, thus accurate measurement of cell size was impossible. To overcome these problems flow cytometry was used which allowed the cell size of many thousands of individual cells to be measured on the basis of light scatter parameters.

Following 24 hours or 72 hours of transfection with the msl expression vector, the transfection efficiency of H9c2 cells transfected with the msl expression vector and hence over-expressing msl was 13.0% ± 0.5% (figure 5.2) and equivalent to approximately a thousand cells that over-expressed msl. Following 72 hours of transfection with the msl expression vector, the size of cells over-expressing msl were significantly increased by approximately 1.5 fold (figure 5.3 (b)) when compared to untransfected cells. However, there was no change in the size of cells over-expressing msl following a 24 hour transfection (figure 5.3 (a)) probably because 24 hours was too early to detect any changes in cell size.

The size of H9c2 cells increased following a longer time (72 hours) of msl over-expression and it was demonstrated in chapter 4 that expression of hypertrophic genes was up-regulated following msl over-expression for 72 hours and not following 24 hours. It was also demonstrated that msl appears to affect genes involved in cardiac hypertrophy that are MRTF-dependent genes and/or SRF target genes. It is therefore interesting to speculate that msl regulates genes associated with cardiac hypertrophy that collectively may promote an increase in cell size i.e. hypertrophy via the MRTF-SRF pathway.

H9c2 cells proliferate in culture and the increase in cell size could have been caused by cell proliferation (the number of dividing cells) rather than hypertrophy. It was investigated whether the increase in size of cells over-expressing msl was caused by cell proliferation by flow cytometry using a dye (Vybrant DyeCycle Violet Stain) that can bind to DNA, allowing the percentage of cells with S phase DNA content (DNA synthesis) by DNA distribution analysis to be measured as a marker of proliferation.

There was no change in the number of cells over-expressing msl in S phase (figure 5.5) or in G_2/M phase (figure 5.6) of the cell cycle compared to the number of cells not over-expressing msl following transfection. In addition, there was no increase in the number of cells following msl over-expression when quantified by direct cell counting (figure 5.7). Therefore, msl does not appear to alter the rate of DNA synthesis and cell division, suggesting that msl does not stimulate proliferation. The increase in cell size following msl over-expression appears not to be due to the cell increasing in size as a result of the cell dividing but likely due to a hypertrophic increase in cell size which is supported by the finding that msl affects genes known to promote hypertrophy.

5.3.2 msl protects H9c2 cells from staurosporine-induced apoptosis

It was demonstrated that even with a low transfection efficiency of H9c2 cells with the msl expression vector, transient over-expression of msl protects H9c2 cells from staurosporine-induced apoptosis (figure 5.11). To confirm this finding, the size of cells over-expressing msl were investigated following staurosporine-induced apoptosis because during apoptosis the cell shrinks and appears smaller in size than viable cells when analysed using flow cytometry. The size of cells over-expressing msl were unaltered in size following staurosporine treatment; however, cells not over-expressing msl were much smaller in size (figure 5.12). Cells over-expressing msl were not smaller in size probably because these cells hardly underwent apoptosis compared to non msl over-expressing cells. These findings suggest that msl has a profound role in protection against staurosporine-induced apoptotic cell death.

Understanding the mechanism(s) through which staurosporine causes apoptosis could provide an insight into the mechanism of msl's protective effects. Unfortunately the exact mechanism by which staurosporine induces apoptosis is unknown. Caspase-3 activation (a critical effector caspase of the apoptotic process) has been observed in staurosporine-induced apoptosis in cardiomyocytes that may be a potential target in the treatment of heart diseases caused by excessive cell death (Yue *et al.*, 1998). Given that msl is expressed in the heart, it is feasible that msl could protect cells from staurosporine-induced apoptosis by preventing caspase-3 activation. However, the experiments in this study were performed in the heart derived H9c2 cells; therefore, additional studies with cardiac myocytes, in culture and *in vivo*, will be necessary to establish how msl prevents staurosporine-induced apoptosis.

The proapoptotic protein Bax of the Bcl-2 family plays an important role in apoptosis (Oltvai *et al.*, 1993). Bax translocates from the cytosol to the mitochondria during apoptosis and is associated with the release of cytochrome c (Manon *et al.*, 1997) and activation of caspases that lead to cell death (Li *et al.*, 1997a). Bax translocation to the mitochondria and release of cytochrome c was observed in H9c2 cells upon induction of apoptosis by staurosporine (Hou and Hsu, 2005). Therefore it is possible that ms1 may protect H9c2 cells against apoptotic cell death by preventing Bax translocation to the mitochondria and subsequent cytochrome c release and activation of caspases. Further work would be required in order to determine which apoptotic pathway ms1 interferes with.

In chapter 4 it was shown that ms1 affects many genes known to be cardioprotective, for example, ARC, calcineurin, LIF, IL-6, tissue factor and adrenomedullin as well as Akt and ERK1/2. Thus ms1 could protect cells against staurosporine-induced apoptosis via one or a collection or all of these anti-apoptotic genes. Interestingly, ARC has been shown to inhibit staurosporine-induced apoptosis (Ekhterae *et al.*, 2003) and ARC was observed to mediate its protective effects by interacting with Bax, preventing Bax activation and release of cytochrome c (Gustafsson *et al.*, 2004); therefore it is reasonable to suggest that ms1 may prevent staurosporine-induced apoptosis via ARC. A combination of a variety of assays will be required to delineate which apoptotic pathway (extrinsic or intrinsic) and which signaling mechanism ms1 interacts with to inhibit apoptotic cell death.

5.3.3 Limitations of the study

There are a number of limitations that require consideration. Even though there was low transfection efficiency, ms1 was discovered to have an anti-apoptotic role. However, this is the first study to demonstrate ms1's protective effects and requires confirmation using other apoptotic assays where many involve microscopy. Therefore it would be necessary to improve the transfection efficiency. It would also be an advantage to have increased transfection efficiency so that ms1's role in hypertrophy could be confirmed by additional assays including measuring cell size using microscopy.

The transfection efficiency can depend on many factors including the quality of plasmid DNA, optimised amounts of transfection reagent and DNA used, the expression vector

and the cell line. Plasmid DNA was extracted using a trasfection-grade plasmid kit (Qiagen) and the purity of plasmid DNA extracted was determined using a 260 nm/280 nm ratio which gave a ratio of approximately 1.8 and therefore the quality of plasmid DNA did not cause low transfection efficiency. The transfection method was optimised and the amounts of transfection reagent (JetPEI) and plasmid DNA was at optimum to give the highest transfection reagent it could without toxicity. The low transfection efficiency could be due to the expression vector or the cell line used or a combination of both. Only one other group has used the JetPEI Cationic transfection reagent for transient transfection with H9c2 cells (Pesant *et al.*, 2006); however, they did not use the same expression vector pcDNA3.1(+). Transient transfection of the expression vector pcDNA3.1(+) in H9c2 cells has only recently been demonstrated and this was with the transfection reagent Lipofectamine (Miyazaki *et al.*, 2006; Zhang and Herman, 2006). Lipofectamine could therefore be used to improve the efficiency of transient transfections. Other ways to improve the transfection efficiency would be to generate a stable cell line over-expressing ms1 and this has previously been successfully achieved using the expression vector pcDNA3.1(+) and the transfection reagent Lipofectamine in H9c2 cells (Ekhterae *et al.*, 1999; Ekhterae *et al.*, 2003; Kageyama *et al.*, 2002; Turner *et al.*, 1998), or to use adenovirus-mediated transduction.

A future consideration would be the use of cardiac myocytes as an alternative to the heart-derived H9c2 cells. Adult cardiac myocytes in culture cease to proliferate unlike H9c2 cells and therefore would be highly beneficial to use instead of H9c2 cells when examining cell size as a marker of hypertrophy. Neonatal cardiomyocytes have been experimentally used to assess hypertrophy by cell size (Hoshijima *et al.*, 1998; Wang *et al.*, 1998a) and successfully transfected with pcDNA3.1(+) DNA constructs (Charron *et al.*, 2001; Liang *et al.*, 2001; Oka *et al.*, 2005; Yanazume *et al.*, 2002).

Although ms1 appears to increase cell size and protect cells from apoptosis, additional controls are necessary to confirm this finding. ms1 increased cell size when compared to untransfected cells (figure 5.3 (b)) and inhibited staurosporine-induced apoptosis when compared to untransfected cells (figure 5.11) where untransfected cells were cells exposed to the transfection of the ms1 expression vector that did not take up the ms1 expression construct. However, it was not known whether ms1 itself increases cell size and prevents apoptosis or the transfection of the plasmid DNA increases cell size and prevents apoptosis. This is because ms1 transfected cells could not be accurately

compared to empty vector transfected cells because when the empty vector was transfected the whole population was analysed and transfection of the empty vector would have resulted in a mixed population of cells that were untansfected and cells that were transfected with the empty vector. Cells transfected with the empty vector should have been analysed but were not because the empty vector (pcDNA3.1(+)) does not have a c-Myc tag or any other tag to distinguish empty vector transfected cells from untransfected cells. An empty vector expression construct engineered to contain a c-Myc tag is required to validate these findings.

In summary, the main aim was to investigate a role for ms1 in cardiac hypertrophy and cardioprotection by transiently over-expressing ms1 *in vitro* and examining cell size and the ability of ms1 to protect against staurosporine-induced apoptotic cell death. ms1 appears to increase cell size and prevent staurosporine-induced apoptosis *in vitro*, suggesting that ms1 may promote hypertrophy and have a cardioprotective role. It was demonstrated in chapter 4 that ms1 affects hypertrophic and cardioprotective genes possibly via a MRTF-SRF signalling pathway thereby further supporting a role for ms1 in cardiac hypertrophy and cardioprotection.

Chapter 6

Construction and initial analysis of a transgenic with cardiac specific over-expression of ms1

6.1 Introduction

In vitro, ms1 appears to affect genes associated with cardiac hypertrophy and increase cell size. In addition, ms1 was found to affect anti-apoptotic genes and appears to inhibit apoptotic cell death *in vitro*. However, it remains uncertain as to whether ms1 causes cardiac hypertrophy and can be cardioprotective *in vivo*. To further elucidate a role for ms1, the aim of the work in this chapter was to investigate the physiological and pathophysiological consequences of increased ms1 expression *in vivo*. This was carried out by generating a transgenic strain over-expressing ms1 selectively in the heart to study the effects of increased cardiac expression of ms1 on cardiac size and physiology, in particular whether it leads to LVH and provides cardioprotection in response to acute ischaemia.

A powerful approach in order to examine gene function in cardiac development, physiology and disease is the use of transgenic mice (Petrich *et al.*, 2003; Sugden and Clerk, 1998). Genetic manipulation is a very useful approach to investigate the complex signalling pathways in cardiac development, function and pathology. However, conventional transgenic approaches using tissue specific promoters lack temporal specificity. Several problems can occur due to unregulated expression throughout cardiac development. One problem is where there is difficulty in establishing stable transgenic animal lines for functional studies when transgene expression leads to early lethality. Another problem is when developmental and pathological effects cannot be distinguished in the cardiac phenotype of adult animals leading to physiological studies being compromised (Petrich *et al.*, 2003). To overcome this, controlled expression can be obtained using conditional transgenesis. This involves using the Cre/*loxP* system to modulate gene expression in a temporal and spatial manner (Lakso *et al.*, 1992; Nagy, 2000; Orban *et al.*, 1992). The Cre/*loxP* system involves Cre, a member of the α integrase family of site-specific recombinases. Cre recombinase of the P1 bacteriophage is a 38 kD protein that catalyses the recombination between two of its recognition sites, called *loxP* (locus of crossover) (Hamilton and Abremski, 1984). This is a 34 bp consensus sequence comprising two

13 bp palindromes separated by an asymmetric 8 bp core. The asymmetric core sequence defines an orientation to the *loxP* site. A major advantage of this system is that no additional cellular factors are needed; the only requirements for DNA rearrangement are the integrase and the recombination sites. Recombination occurs within the spacer area of the *loxP* sites when a single recombinase molecule binds to each palindromic half of a *loxP* site, then the recombinase molecules form a tetramer, thus bringing the two *loxP* sites together (Nagy, 2000; Ryding *et al.*, 2001). *In vitro* cell culture experiments in the late 80's and early 90's were the first to show that Cre recombinase would work in eukaryotic cells (Sauer and Henderson, 1988; Sauer and Henderson, 1989; Sauer and Henderson, 1990). It was then discovered that the Cre recombinase worked in the mouse as well when expressed from a transgene (Lakso *et al.*, 1992; Orban *et al.*, 1992).

The Cre recombinase system can be added to excise or invert *loxP*-flanked DNA segments or create intermolecular recombination between different DNA molecules. Using the recombinase activity as a genetic activation or inactivation switch, conditional transgenesis or conditional knockouts become available (Nagy, 2000).

The mechanism for conditional transgene activation involves the promoter and the coding region for the gene of interest to be separated by a *loxP*-flanked STOP region. This does not allow any transcription initiated from the promoter to read through and include the gene. Expression of the gene occurs when the region is removed by Cre-mediated excision (Nagy, 2000) (figure 6.1).

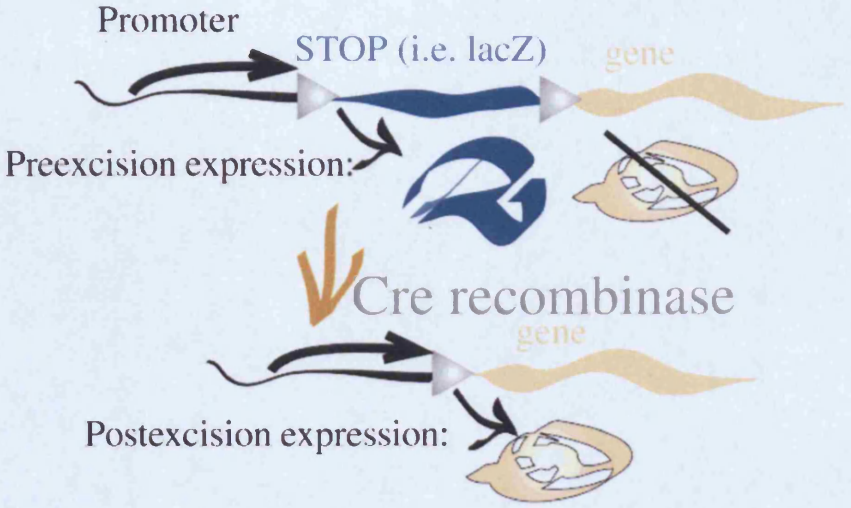

Figure 6.1. The structure of a conditional transgene (Nagy, 2000).
The conditional transgene consists of a promoter and the coding region for the gene of interest to be separated by a *loxP*-flanked lacZ (STOP) region. This does not allow any transcription initiated from the promoter to read through and include the gene prior to Cre excision. The addition of Cre recombinase removes the lacZ region and expression of the gene occurs.

In order to generate a transgenic strain over-expressing ms1 in a cardiac-specific manner, a transgene was first constructed. The transgenic vector PCCALL2-IRES-EGFP/anton (pi Z/EG) was kindly provided by C Lobe (University of Toronto, Canada) and is based on the Z/EG vector (Novak *et al.*, 2000) that has been previously used by other investigators (de Lange *et al.*, 2003; Guo *et al.*, 2002). The pi Z/EG vector is shown in appendix 1 of chapter 2 and was used because it allows controlled expression when using the Cre/*loxP* system that can be monitored in a double-reporter transgenic line. The advantage of using a pi Z/EG mouse line is that it provides a double-reporter system for Cre excision utilising lacZ and the enhanced green fluorescent protein (EGFP). Using this system it was discovered that lacZ was expressed throughout embryonic development and in adult stages and upon Cre excision, the lacZ gene was removed and the second reporter EGFP was activated (Lobe *et al.*, 1999; Novak *et al.*, 2000). Thus, this novel system is advantageous because Cre-mediated exicision can be monitored in live samples and it can importantly show which tissues have not undergone Cre excision.

The first aim of this study was to use the pi Z/EG vector and generate a ms1 transgene that consists of the ms1 coding sequence driven by a pCAGGS promoter comprising the CMV (cytomegalo virus) enhancer and chicken β actin promoter. Following the

chicken β actin promoter is a *loxP*-flanked lacZ/neomycin-resistance fusion gene and three SV40 polyadenylation sequences. Thus read-through transcription will not occur due to the presence of a strong transcription STOP sequence (the polyadenylation sequences) at the end of the lacZ gene. Following the second *loxP* site and at the 3' side of the ms1 gene are an internal ribosome entry site (IRES), the coding sequence of the EGFP protein and a rabbit β globin polyadenylation sequence (Novak *et al.*, 2000). The expression of Cre recombinase can remove the lacZ gene, thus, prior to Cre excision, the lacZ reporter and the neomycin resistance gene are expressed. After Cre excision the *loxP*-flanked lacZ/polyadenylation sequence is removed and the promoter is placed adjacent to the ms1 sequence and the EGFP reporter gene to direct ms1 and EGFP expression (Novak *et al.*, 2000), see figure 6.2. This approach therefore allows conditional over-expression of ms1 and GFP positive cells allow identification of cells over-expressing ms1.

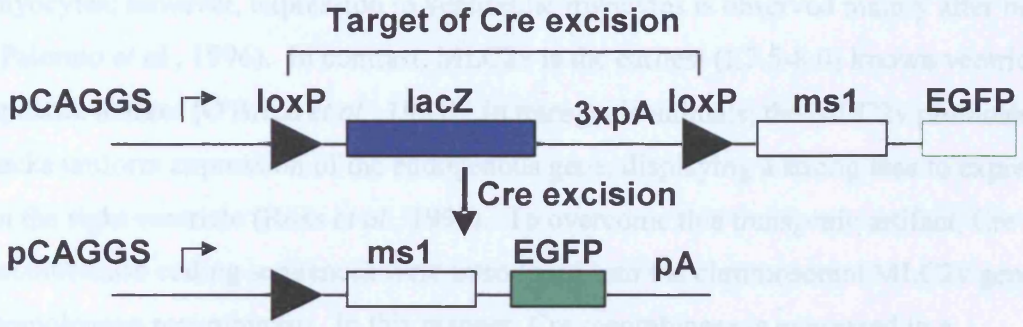

Figure 6.2. The mechanism of the ms1 conditional transgene.
The ms1 transgene consists of the ms1 and EGFP coding sequence driven by a pCAGGS promoter. Following the promoter is a *loxP*-flanked lacZ gene and three SV40 polyadenylation sequences. Thus read-through transcription will not occur due to the presence of a strong transcription STOP sequence (the polyadenylation sequences) at the end of the lacZ gene. Prior to Cre excision, only the lacZ reporter is expressed. The addition of Cre recombinase removes the lacZ gene, thus, ms1 and EGFP are expressed.

To confirm the ms1 transgene was functional, the transgene was transfected *in vitro*, in NIH3T3 cells to first check that lacZ was expressed and ms1/GFP was not over-expressed and then the ms1 transgene was co-transfected with a Cre recombinase expressing vector, pCre-Pac vector (Taniguchi *et al.*, 1998) (appendix 1 of chapter 2) to

confirm that Cre recombinase removed lacZ and hence produced no lacZ expression but resulted in ms1/GFP over-expression.

The second aim of this study was to generate ms1 transgenic mice that showed successful germ-line transmission of the ms1 transgene identified using PCR, Southern blotting and lacZ mRNA and protein analysis. Once ms1 transgenic mice were generated they were crossed with mice expressing Cre recombinase to create cardiac specific over-expression of ms1 identified by ms1/GFP expression in the heart by semi-quantitative RT-PCR and immunostaining. To over-express ms1 specifically in the heart, the mice used to cross with ms1 transgenic mice were MLC2v Cre mice that were already established at the University of Leicester transgenic unit and initially obtained from K R Chien (Chen *et al.*, 1998b). A knock-in of Cre recombinase into the MLC2v locus or the use of the α-myosin heavy chain (α-MHC) promoter are the most common models of cardiac-specific Cre transgene expression (Agah *et al.*, 1997; Chen *et al.*, 1998a). The α-MHC promoter drives expression in embryonic and adult atrial myocytes; however, expression in ventricular myocytes is observed mainly after birth (Palermo *et al.*, 1996). In contrast, MLC2v is the earliest (E7.5-8.0) known ventricular-specific marker (O'Brien *et al.*, 1993). In transgenic animals, the MLC2v promoter lacks uniform expression of the endogenous gene, displaying a strong bias to expression in the right ventricle (Ross *et al.*, 1996). To overcome this transgenic artifact, Cre recombinase coding sequences were introduced into the chromosomal MLC2v gene by homologous recombinase. In this manner, Cre recombinase is expressed in a temporally and spatially restricted manner that corresponds to the endogenous MLC2v gene (Chen *et al.*, 1998b). Mice that are heterozygous for this allele are normal, express normal levels of MLC2v protein, and have neither a molecular or physiological cardiac phenotype at base line or following hypertrophic stimuli (Chen *et al.*, 1998b; Minamisawa *et al.*, 1999). Thus the MLC2v Cre knock-in strategy is a valid approach for gene targeting and transgenesis to explore the molecular mechanisms of cardiac hypertrophy and heart development.

The endogenous MLC2v gene is expressed in ventricular cardiomyocytes and therefore so will Cre recombinase. When ms1 transgenic mice are crossed with MLC2v Cre mice, mice are generated that will over-express ms1/GFP in those cells that express Cre (ventricular cardiomyocytes).

In summary, the aim of the work presented in this chapter was to construct a msl transgene that was first confirmed to be functional by transiently over-expressing msl/GFP *in vitro* and then use the msl transgene to generate msl transgenic mice that over-express msl in a cardiac-specific manner when crossed with MLC2v Cre mice, in order to investigate whether increased cardiac expression of msl leads to LVH and provides cardioprotection.

6.2 Results

6.2.1 Construction of the msl transgene

The full-length mouse msl coding sequence was already cloned into the pGEM-T Easy vector as described in section 3.2.1 of chapter 3. The pGEM-T Easy vector was cut with the restriction enzymes *Bgl*II and *Xho*I and the full-length msl fragment (approximately 1.3 kb) was released. The transgenic vector pi Z/EG was also cut with the restriction enzymes *Bgl*II and *Xho*I and both the msl fragment and pi Z/EG vector (approximately 10.9 kb) were agarose gel extracted and ran on an agarose gel to check for DNA purity prior to ligation of msl into pi Z/EG.

msl was then cloned into the pi Z/EG vector and restriction digest confirmed that the pi Z/EG vector contained msl by producing the correct sized fragment for msl (approximately 1.3 kb) and the correct approximate 10.9 kb fragment for pi Z/EG which is shown in figure 6.3. msl was also confirmed by sequencing to be cloned into pi Z/EG.

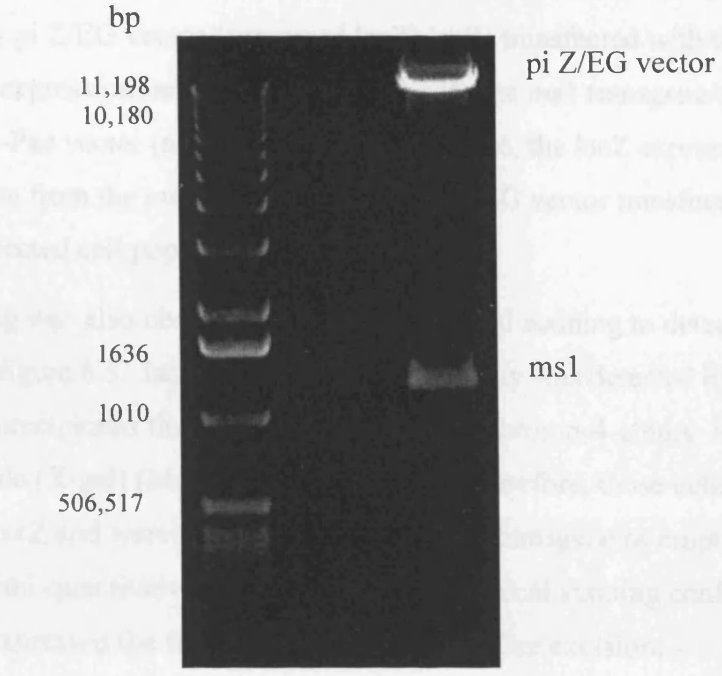

Figure 6.3. Agarose gel analysis following a restriction digest of the ms1 transgene using the enzymes *Bgl*II and *Xho*I confirmed that the ms1 transgene contained ms1.

6.2.2 Transient transfection of the ms1 transgene in vitro leads to over-expression of ms1

In order to determine that the constructed ms1 transgene was functional, NIH3T3 cells were left untransfected or transfected with various vectors for 48 hours as described in sections 2.4.5 and 2.4.6 of chapter 2 and analysed for lacZ and ms1/GFP expression by semi-quantitative RT-PCR, histochemical staining and fluorescence microscopy. NIH3T3 cells were used because this cell line is one of the easiest to transfect and monitor expression from a transgene.

As shown in figure 6.4 lacZ mRNA expression was observed for cells transfected with the ms1 transgene or empty pi Z/EG vector control and for cells co-transfected with the ms1 transgene and pCre-Pac vector or the empty pi Z/EG vector control and the pCre-Pac vector compared to untransfected cells and pCre-Pac vector transfected cells.

The addition of Cre removes the lacZ gene; however, lacZ expression was still observed when cells were co-transfected with the ms1 transgene and pCre-Pac vector or the empty pi Z/EG vector control and the pCre-Pac vector. This was probably because co-transfection of the ms1 transgene/empty pi Z/EG vector and pCre-Pac vector would

have given a mixed population of untransfected cells, cells transfected with the msl transgene/empty pi Z/EG vector (expressed lacZ), cells transfected with the pCre-Pac vector (no lacZ expression) and cells transfected with the msl transgene/empty pi Z/EG vector and pCre-Pac vector (no lacZ expression). Hence, the lacZ expression observed would have come from the msl transgene/empty pi Z/EG vector transfected cells within the mixed transfected cell population.

The same finding was also observed using histochemical staining to detect lacZ expression, see figure 6.5. lacZ (β-galactosidase) activity was detected by the formation of visible, blue precipitates through the hydrolysis of 5-bromo-4-chloro-3-indolyl-β-D-galactopyranoside (X-gal) (MacGregor *et al.*, 1987); therefore, those cells that appeared blue expressed lacZ and were transfected with the msl transgene or empty pi Z/EG vector. Thus, semi-quantitative RT-PCR and histochemical staining confirmed that the msl transgene expressed the first reporter lacZ prior to Cre excision.

msl mRNA over-expression was confirmed for cells co-transfected with the msl transgene and pCre-Pac vector (figure 6.4) by semi-quantitative RT-PCR. Therefore cells co-transfected with the msl transgene and pCre-Pac vector over-expressed msl (and hence GFP) due to expression of Cre recombinase from the pCre-Pac vector that removed the *loxP*-flanked lacZ/polyadenylation sequence resulting in msl/GFP expression. However, msl over-expression was also observed for cells transfected with the msl transgene and there should only be msl over-expression when Cre recombinase was present. This expression was not endogenous msl because NIH3T3 cells express very low levels of msl and if detected it would also be observed for the other samples. Also there was no msl expression detected when the RNA extracted from cells transfected with the msl transgene was DNase treated and the reverse transcription enzyme was excluded (-RT) during cDNA synthesis (figure 6.4), suggesting that the msl expression observed was msl mRNA and not from the plasmid DNA. It was therefore possible that the msl transgene was leaky and the polyadenylation sequences at the end of the lacZ gene allowed read-through transcription.

To examine this further the second reporter GFP was analysed by fluorescence microscopy, see figure 6.5. GFP expression was only observed for cells co-transfected with the msl transgene and pCre-Pac vector or the empty pi Z/EG vector control and the pCre-Pac vector. Therefore cells co-transfected with the msl transgene and pCre-Pac vector appeared green and over-expressed msl. As no GFP expression was

observed for cells transfected with the ms1 transgene but ms1 mRNA was detected this suggested that the ms1 transgene was possibly a little leaky and very low levels of ms1 transcript was detected because PCR is a highly sensitive technique.

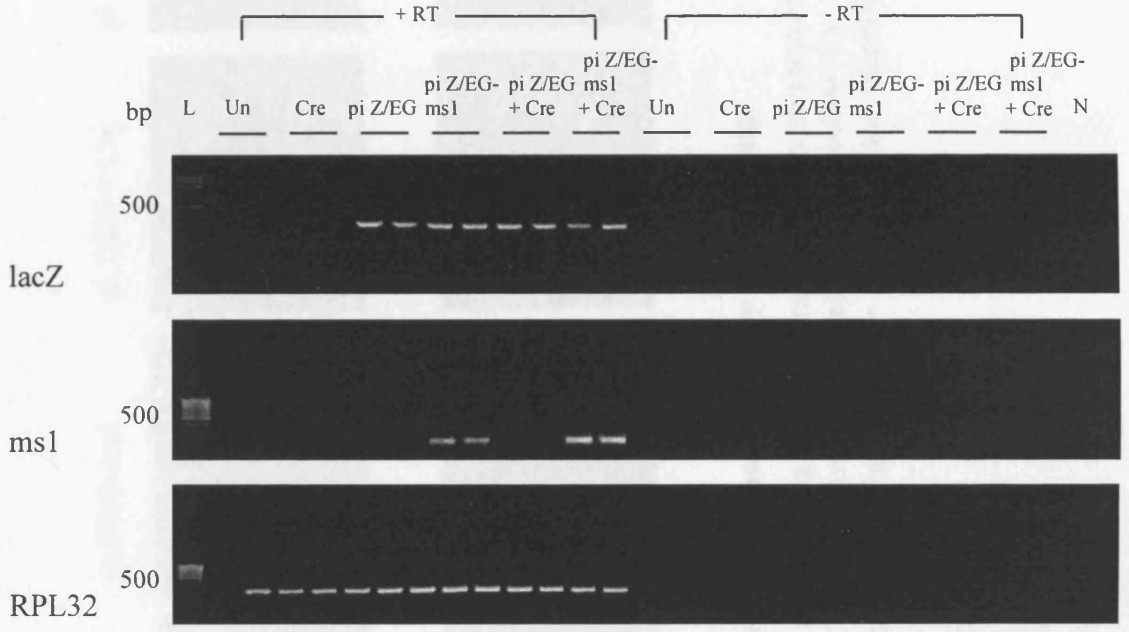

Figure 6.4. Transient transfection of the ms1 transgene leads to lacZ expression prior to Cre excision and ms1 over-expression following Cre exision.

NIH3T3 cells were left untransfected (Un) or transfected with the constructs pCre-Pac (Cre), pi Z/EG (empty vector control), pi Z/EG-ms1 (ms1 transgene) or co-transfected with the pi Z/EG-ms1 (ms1 transgene) and pCre-Pac vector or the empty pi Z/EG vector control and the pCre-Pac vector for 48 hours, n = 2. LacZ and ms1 mRNA expression was determined by semi-quantitative RT-PCR. RPL32 was used as an internal control for inaccuracies in initial RNA levels. N refers to the no template control, L refers to the 100 bp DNA ladder and the band sizes (bp) are given. + RT indicates that the RT enzyme was included during cDNA synthesis and –RT indicates that the RT enzyme was omitted.

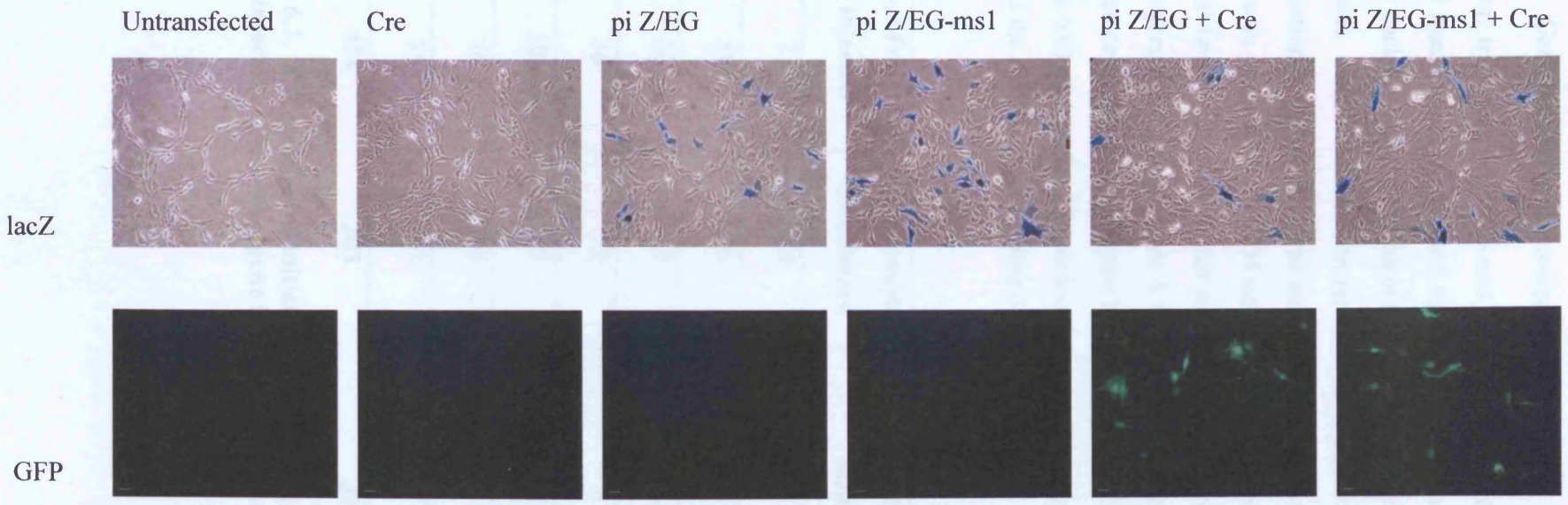

Figure 6.5. Transient transfection of the ms1 transgene leads to ms1 over-expression detected by GFP staining.

Light microscopy and fluorescence microscopy of X-gal staining (lacZ) and GFP staining following transient (48 hours) transfection of NIH3T3 cells with the constructs pCre-Pac (Cre), pi Z/EG (empty vector control), pi Z/EG-ms1 (ms1 transgene) or cotransfection of pi Z/EG-ms1 (ms1 transgene) with the pCre-Pac vector or the empty pi Z/EG vector control with the pCre-Pac vector, n = 3. Bar = 5μm. Magnification 20×.

6.2.3 Generation of ms1 transgenic mice

The ms1 transgene (pi Z/EG-ms1) was purified as described in section 2.7.1 of chapter 2) and linearised at the *Sfi*I and *Sca*I sites (see appendix 1 of chapter 2) to remove the vector backbone by S Munson at the Embryonic Stem Cell Facility, University of Leicester. The linearised transgene was then injected into the pronucleus of day 1 post-fertilisation oocytes. This was performed by J Brown at the University of Leicester transgenic unit. A total of 434 oocytes were injected in batches with the ms1 transgene and just under half of them that survived were re-implanted into the oviducts of pseudopregnant females (table 6.1). 37 mice were born and screened to assess inheritance of the ms1 transgene by PCR using lacZ and GFP vector specific primers (figure 6.6) as described in section 2.7.3.1 of chapter 2. Out of 37 newborn mice, 5 carried the ms1 transgene (table 6.1).

No. of oocytes injected	No. of oocytes transferred	No. Born (B6CBF1 Strain)	ms1 transgene positive
72	24	7	1
69	26	9	1
30	28	8	1
36	22	6	0
106	47	4	1
46	19	1	0
75	37	2	1
Total 434	**203**	**37**	**5**

Table 6.1. The number of initial offspring carrying the ms1 transgene following microinjection of the transgene into the pronucleus of oocytes.

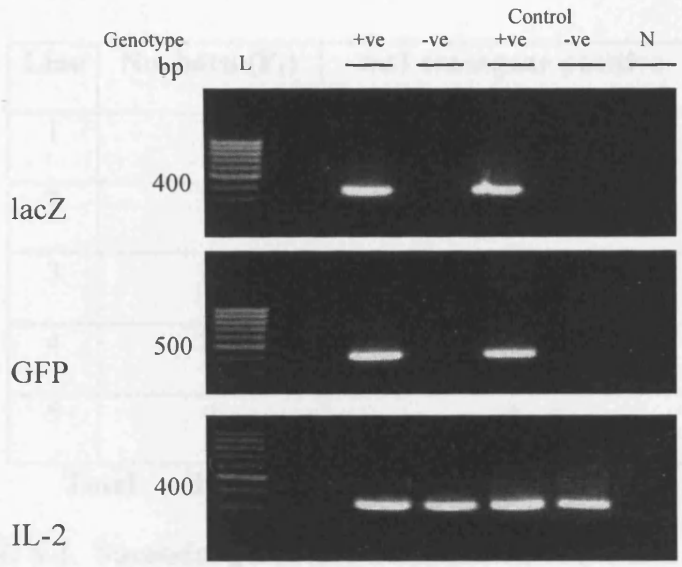

Figure 6.6. Inheritance of the ms1 transgene by PCR analysis

Founders were genotyped to identify inheritance of the ms1 transgene by PCR using lacZ and GFP vector specific primers. IL-2 was used as an internal control. N refers to the no template control, L refers to the 100 bp DNA ladder and the band sizes (bp) are given.

The 5 mice found positive for carrying the ms1 transgene were bred with C57BL6 mice to establish breeding lines. In total 104 mice were born and 25 of these were found to be positive by PCR for carrying the ms1 transgene (table 6.2). Line 2 did not show successful germ-line transmission of the ms1 transgene but the other lines were found to show successful germ-line transmission. Positive founder mice that were identified to have inherited the ms1 transgene (ms1 transgenic) from lines 3, 4 and 5 were taken forward and bred further to create more breeding lines.

Line	No. born (F_1)	msl transgene positive
1	38	8
2	34	0
3	13	1
4	15	12
5	4	4
Total	**104**	**25**

Table 6.2. Sucessful germ-line transmission of the msl transgene.

Two msl transgenic mice from each line were bred with C57BL6 mice to carry on the breeding line except for line 3 because there was only one founder that inherited the msl transgene and hence this one founder was bred to carry on line 3. Table 6.3 shows the total number of mice (F_2) carrying the msl transgene out of the total number born for each line. The total number of mice found to carry the msl transgene for all three lines was much higher than expected. Approximately 80%, 70% and 90% of founders for lines 3, 4 and 5, respectively, inherited the msl transgene which is higher than the expected amount of 50% according to mendelian inheritance, thus, these genotyping results suggests multiple integrations of the msl transgene for all three lines.

Line	Animal ID	Litter	No. Born (F_2)	No. +ve	No. -ve	
3	19.6	1	8	5	3	
	19.6	2	7	6	1	
	19.6	3	9	8	1	
			24	**19**	**5**	**Total**
4	32.1	1	Lost Litter			
	32.1	2	3	0	3	
	32.1	3	5	0	5	
	32.1	4	9	9	0	
	32.1	5	11	11	1	
			28	**19**	**9**	**Total**
	32.2	1	6	5	1	
	32.2	2	2	2	0	
	32.2	3	9	6	3	
	32.2	4	6	5	1	
			23	**18**	**5**	**Total**
5	37.1	1	5	5	0	
	37.1	2	2	2	0	
	37.1	3	Lost Litter			
	37.1	4	7	7	0	
			14	**14**	**0**	**Total**
	37.2	1	3	1	2	
	37.2	2	6	5	1	
	37.2	3	13	13	0	
			22	**19**	**3**	**Total**

Table 6.3. The total number of founders (F_2) carrying the ms1 transgene (no. +ve) out of the total number born for each line.

6.2.4 ms1 transgene integration and copy number

In order to determine transgene integration and copy number, Southern blot analysis was performed on total liver DNA (10 μg) digested with *Sst*I and hybridised with a ^{32}P-labelled probe (655 bp *Not*I-*Bam*HI fragment that includes the rabbit β-globin polyadenylation sequence of the pi Z/EG vector). The *Sst*I restriction endonuclease recognition site only occurs once in the transgene, thus if the transgene inserted in a head-to-tail concatemer, cutting with *Sst*I should result in one fragment the same size as the transgene (approximately 10.5 kb), and in the end fragments of the transgene array where they meet with genomic DNA that will be of unpredictable size (figure 6.7). This

insertion is known as tandem integration. The intensity of the hybridisation signal corresponds to the copy number of the transgene in the insertion site. If the transgene has integrated more than once (multiple integration sites), a Southern blot will show multiple end fragments of unknown length corresponding to the number of integration events (figure 6.7). If it is single copy integration, a Southern blot should show a single fragment of unknown length (figure 6.7).

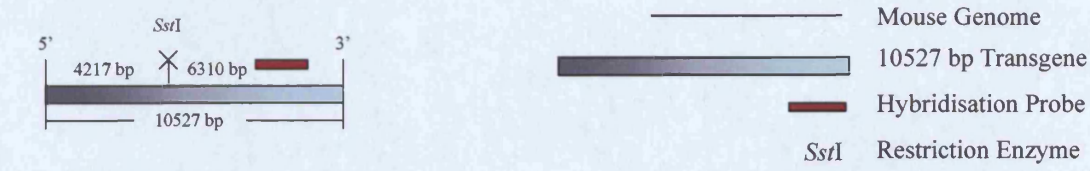

ms1 transgene

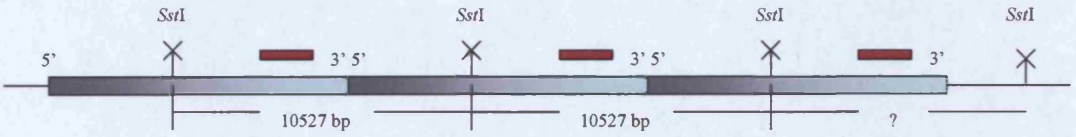

Tandem integration

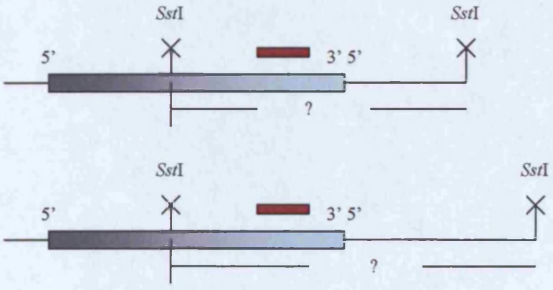

Multiple integration sites

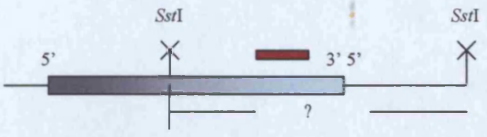

Single copy integration site

Figure 6.7. Predicted possible integrations of the ms1 transgene following a digest with a restriction enzyme that cuts once in the transgene.

Southern blot analysis of *Sst*I digested genomic DNA from mice (F_2) that were approximately 8 weeks old revealed a single fragment of approximately 10.5 kb (figure 6.8), suggesting tandem integration; however, there was no additional band (end fragment) present determined by the next *Sst*I restriction site in the mouse genome. This was observed for animals from all three lines. The intensity of the approximate 10.5 kb band was strong signifying multiple transgene copy numbers in the insertion site. Band intensity comparison suggests that the mouse from line 3 had more transgene copy numbers than the mouse from line 4 and line 5 and the mouse from line 4 had more copy numbers than the mouse from line 5.

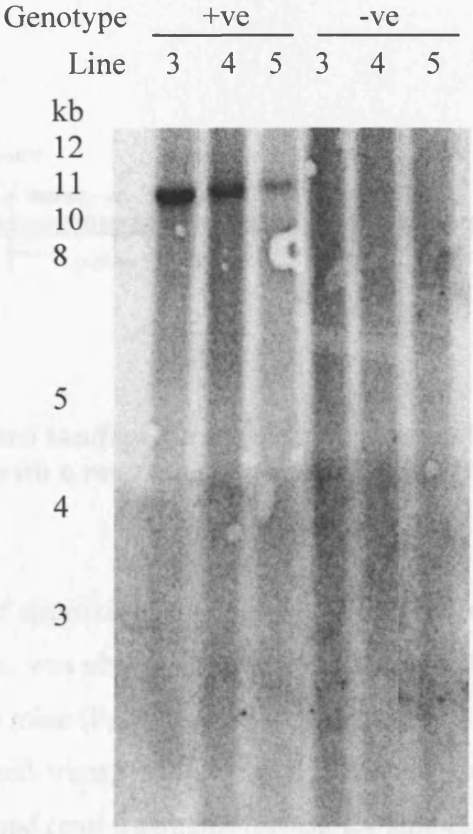

Figure 6.8. Southern blot analysis of *Sst*I digested genomic DNA isolated from mice (F_2) that was hybridised to radiolabeled probe.

Total liver DNA (10 μg) was isolated from approximately 8 week old F_2 mice from all three lines, digested with *Sst*I, Southern blotted and hybridised with a ^{32}P-labelled 655 bp *Not*I-*Bam*HI fragment that includes the rabbit β-globin polyadenylation sequence of the pi Z/EG vector. Southern blot analysis was performed on two animals identified to carry the ms1 transgene (+ve genotype) and two littermate animals identified not to inherit the ms1 transgene (-ve genotype) from each line. Shown is an example of a representative Southern blot.

To confirm this finding, total liver DNA (10 μg) was digested with a different restriction enzyme *Eco*RV and hybridised with a ^{32}P-labelled 655 bp *Not*I-*Bam*HI fragment that includes the rabbit β-globin polyadenylation sequence of the pi Z/EG vector. The *Eco*RV restriction cuts twice in the transgene, thus if the transgene inserted in a head-to-tail arrangement, cutting with *Eco*RV should result in two bands, one band of approximately 5.4 kb and a band of unknown length (figure 6.9).

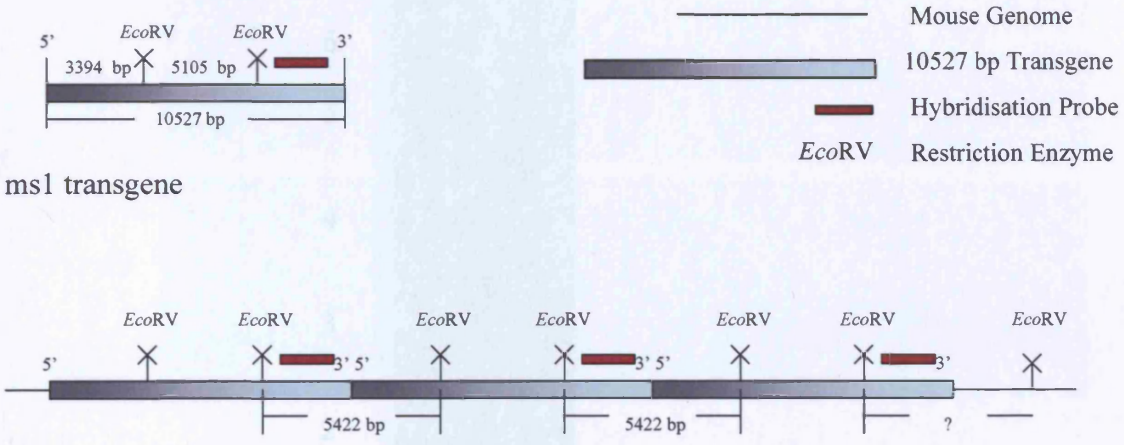

Figure 6.9. Predicted tandem arrangement of the ms1 transgene following following a digest with a restriction enzyme, *Eco*RV that cuts twice in the transgene.

A single fragment of approximately 5.4 kb (figure 6.10), suggesting tandem integration of the ms1 transgene, was observed following Southern blot analysis of *Eco*RV digested genomic DNA from mice (F_2) that were approximately 8 weeks old. This finding confirmed that the ms1 transgene integrated in a tandem arrangement; however, there was no additional band (end fragment) present for animals from all three lines as observed previously when genomic DNA from mice was digested with *Sst*I (figure 6.8). As shown in figure 6.10 the intensity of the approximate 5.4 kb band was strong indicative of multiple transgene copy numbers in the insertion site. As seen before in figure 6.8, the band intensity suggests that the mouse from line 3 contained more transgene copy numbers than the mouse from line 4 and line 5 and the mouse from line 4 had more copy numbers than the mouse from line 5. This finding confirms that the ms1 transgene integrated in a tandem arrangement in all three lines.

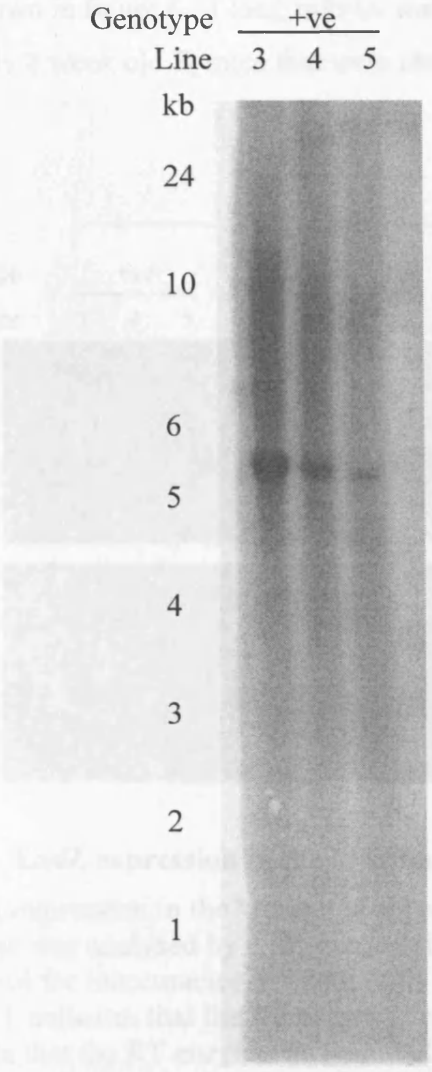

Figure 6.10. Southern blot analysis of total liver DNA digested with *Eco*RV and hybridised to radiolabeled probe confirmed tandem integration of the ms1 transgene.

Total liver DNA (10 µg) was isolated from approximately 8 week old F_2 mice from all three lines, digested with *Eco*RV, Southern blotted and hybridised with a ^{32}P-labelled 655 bp *Not*I-*Bam*HI fragment that includes the rabbit β-globin polyadenylation sequence of the pi Z/EG vector. Southern blot analysis was performed on two animals from each line. Shown is an example of a representative Southern blot.

6.2.5 Expression of the first reporter lacZ from the ms1 transgene

The ms1 transgene consists of a pCAGGS promoter comprising the CMV enhancer and chicken β actin promoter that drives lacZ expression ubiquitously prior to the addition of Cre recombinase. To determine that all three lines expressed lacZ and therefore the ms1 transgene, lacZ expression in the kidney was analysed by semi-quantitative RT-

PCR. As shown in figure 6.11 lacZ mRNA was not found in the kidneys of approximately 8 week old F_2 mice that were identified by genotyping to carry the ms1 transgene.

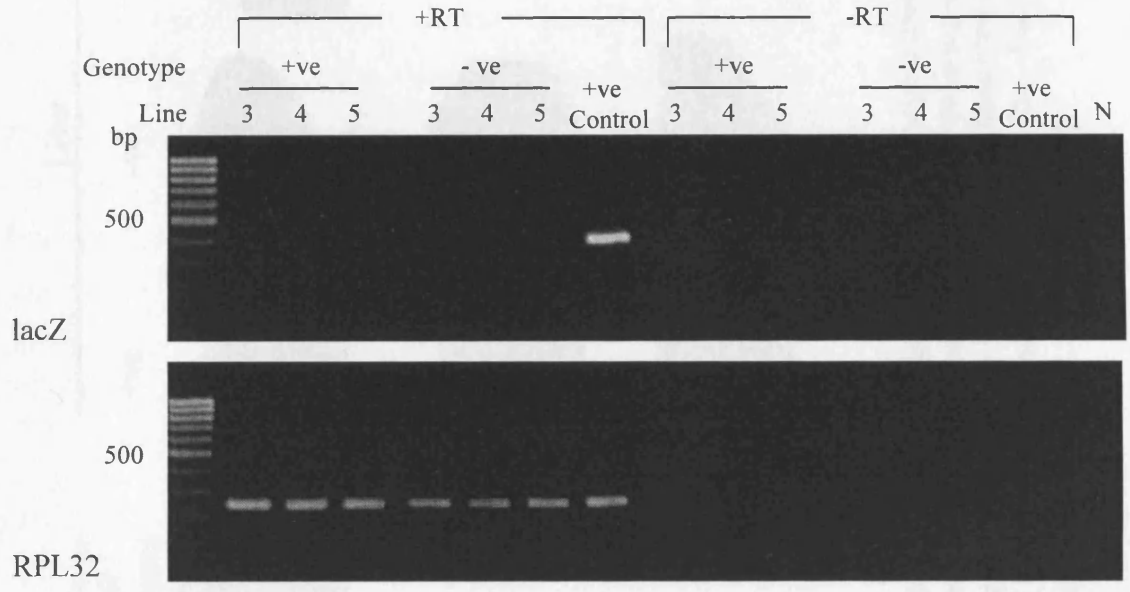

Figure 6.11. LacZ expression in the kidneys of F_2 mice.

LacZ mRNA expression in the kidneys of approximately 8 week old F_2 mice (n = 3) from each line was analysed by semi-quantitative RT-PCR. RPL32 was used as an internal control for inaccuracies in initial RNA levels. N refers to the no template control. + RT indicates that the RT enzyme was included during cDNA synthesis and –RT indicates that the RT enzyme was omitted. Shown is an example of lacZ expression in the kidney from one animal identified to carry the ms1 transgene (+ve genotype) and a littermate animal identified not to inherit the ms1 transgene (-ve genotype) from each line. LacZ expression in the kidney from an animal known to express lacZ was included as a positive control.

The same finding was also observed using histochemical staining to detect lacZ expression, see figure 6.12. In addition, the heart and liver were also stained for lacZ expression and as observed in the kidney there was no visible blue staining present in the heart and liver and hence no lacZ expression. Kidney, heart and liver tissues from a mouse known to carry the pi Z/EG vector and express lacZ was provided by L Shenje and included as a positive control. As shown in figures 6.11 and 6.12 these tissues expressed lacZ and therefore semi-quantitative RT-PCR and histochemical staining was performed correctly. These findings suggest that although the ms1 trangene was integrated it was not functional in mice that were approximately 8 weeks old from all three lines.

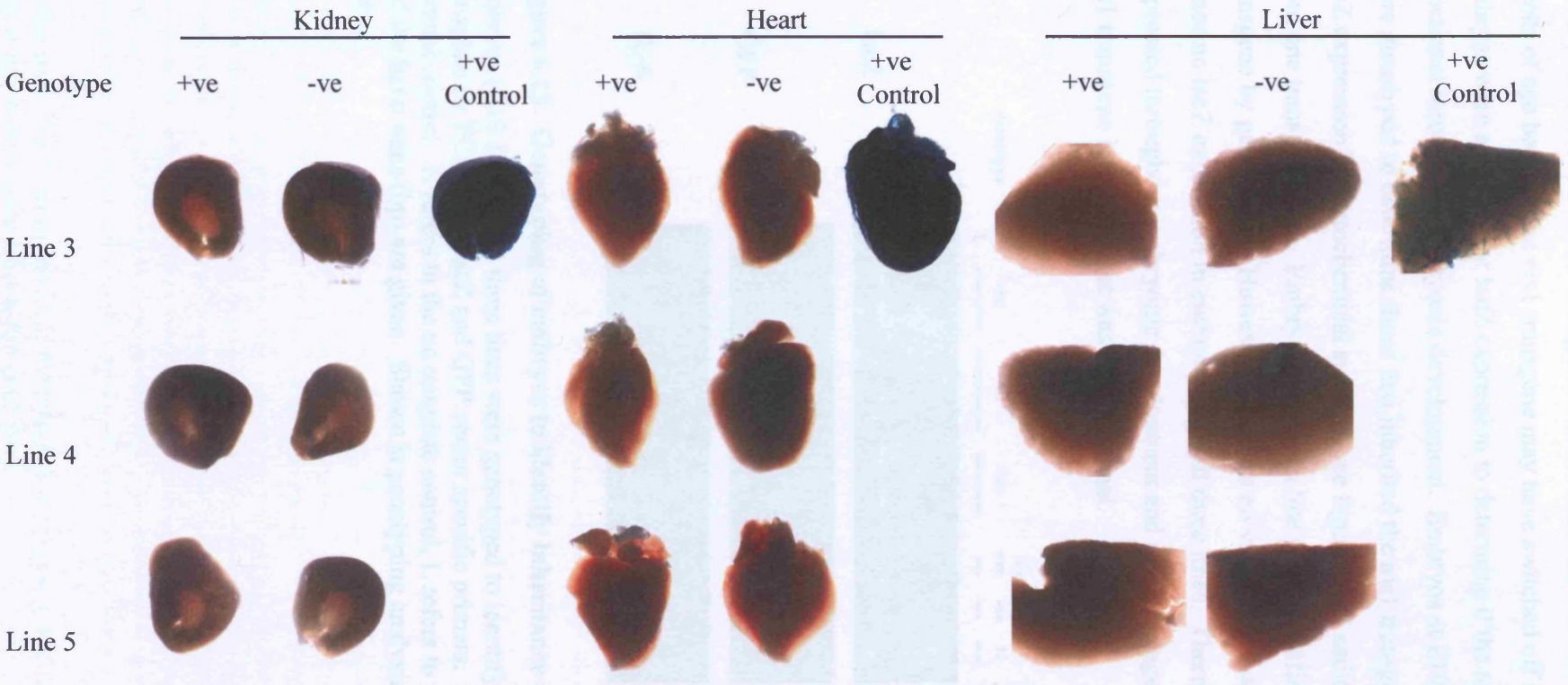

Figure 6.12. LacZ expression in tissues from three transgenic lines.

Histochemical staining using X-gal was performed to detect lacZ expression in tissues of ms1 transgenic mice (F_2) at approximately 8 weeks of age from each line compared to a littermate wild type control, n = 2. A cytoplasmic blue colour appeared in tissues expressing high levels of lacZ, see +ve control tissues. Shown is an example of lacZ expression in the kidney, heart and liver from one animal identified to carry the ms1 transgene (+ve genotype) and a littermate animal identified not to inherit the ms1 transgene (-ve genotype) from each line. LacZ expression in the kidney, heart and liver from an animal known to express lacZ was included as a positive control. Magnification 1×.

It was possible that the ms1 transgene was not functional in mice at approximately 8 weeks of age because the ms1 transgene may have switched off in the adult. Therefore, embryos were analysed for lacZ expression to determine if the ms1 transgene was functional throughout embryonic development. Embryos at E10.5 from all three lines were genotyped to determine those that inherited the ms1 transgene and analysed for lacZ expression by histochemical staining, see figures 6.13 and 6.14 for an example from one transgenic line. Embryos from each line were identified to carry the ms1 transgene by genotyping. However, there was no visible blue staining present and hence no lacZ expression in embryos from all three lines. Therefore, lacZ was not expressed throughout embryonic development and in adult stages, confirming that the ms1 transgene integrated but was not functional.

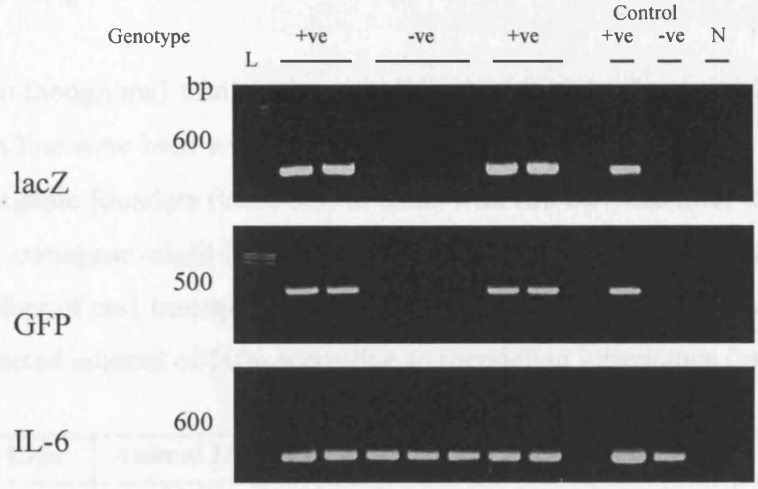

Figure 6.13. Genotyping of embryos to identify inheritance of the ms1 transgene.
Embryos (E10.5) from all three lines were genotyped to identify inheritance of the ms1 transgene by PCR using lacZ and GFP vector specific primers. IL-2 was used as an internal control. N refers to the no template control, L refers to the 100 bp DNA ladder and the band sizes (bp) are given. Shown is genotyping analysis of embryos from one line.

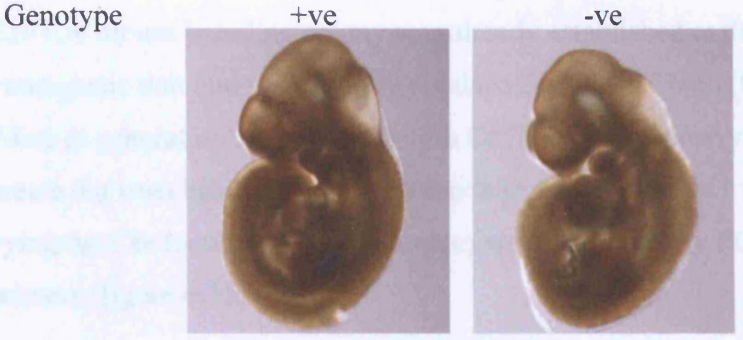

Figure 6.14. LacZ expression in embryos (E10.5).

Embryos (E10.5) from each line were stained for lacZ expression. Shown is an example of lacZ staining from one embryo identified to carry the ms1 transgene (+ve genotype) and one embryo not to inherit the ms1 transgene (-ve genotype) from one line. Magnification 1.6×.

Even though ms1 transgenic mice did not express lacZ, two ms1 transgenic mice from each line were bred with C57BL6 mice to carry on the breeding lines and generate ms1 transgenic founders (table 6.4) to cross with MLC2v Cre mice as it was possible that the ms1 transgene might function when Cre was present. As observed previously, the total number of ms1 transgenic founders from all three lines was much higher than the expected amount of 50% according to mendelian inheritance (table 6.4).

Line	Animal ID	Litter	No. Born (F_3)	No. +ve	No. -ve	
3	19.35	1	6	6	0	
		2	5	2	3	
		3	3	3	0	
			14	**11**	**3**	**Total**
	19.36	1	3	1	2	
			3	**1**	**2**	**Total**
4	32.32	1	4	3	1	
		2	Lost Litter			
			4	**3**	**1**	**Total**
	32.40	1	9	8	1	
			9	**8**	**1**	**Total**
5	37.35	1	11	9	2	
		2	7	5	2	
			18	**14**	**4**	**Total**
	37.6	1	5	4	1	
			5	**4**	**1**	**Total**

Table 6.4. The total number of founders (F_3) carrying the ms1 transgene (no. +ve) out of the total number born for each line.

6.2.6 Generation of MLC2v Cre mice

The MLC2v Cre mouse breeding colony was already established at the University of Leicester transgenic unit and was initially obtained from K R Chien (Chen *et al.*, 1998b). Mice at generation 18 were bred with C57BL6 mice to carry on the breeding line and create our own breeding colony to use to cross with the ms1 transgenic lines. Mice carrying the Cre locus (MLC2v Cre mice) were identified by PCR using Cre specific primers (figure 6.15)

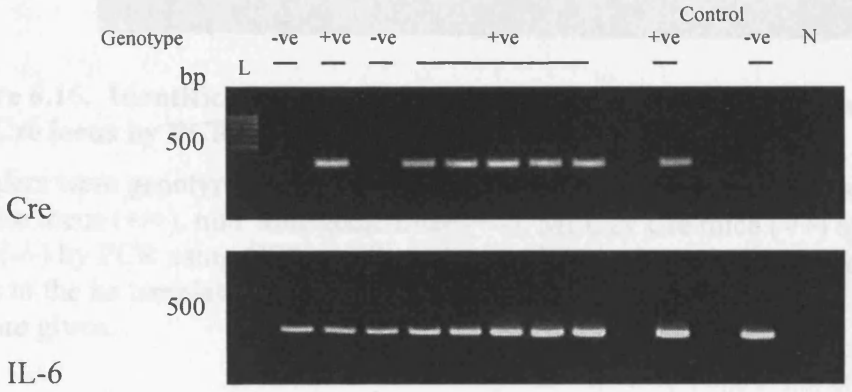

Figure 6.15. Identification of MLC2v Cre positive mice by PCR analysis.
Founders were genotyped to identify mice carrying the Cre locus by PCR using Cre primers. IL-2 was used as an internal control. N refers to the no template control, L refers to the 100 bp DNA ladder and the band sizes (bp) are given.

6.2.7 Generation of double transgenic mice carrying the ms1 transgene and Cre locus

MLC2v Cre mice were bred with two ms1 transgenic mice from each line to produce founders that carried both the ms1 transgene and the Cre locus (double transgenics) and therefore over-expressed ms1 specifically in the heart. As shown in figure 6.16 mice carrying the ms1 transgene and the Cre locus (double transgenics) were identified by PCR using GFP primers and Cre primers, respectively. The total number of double transgenics from all three lines was much higher than the expected amount of 1:4, see table 6.5. Approximately 72%, 36% and 44% of founders for lines AK1, AK2 and AK3, respectively, inherited the ms1 transgene and Cre locus.

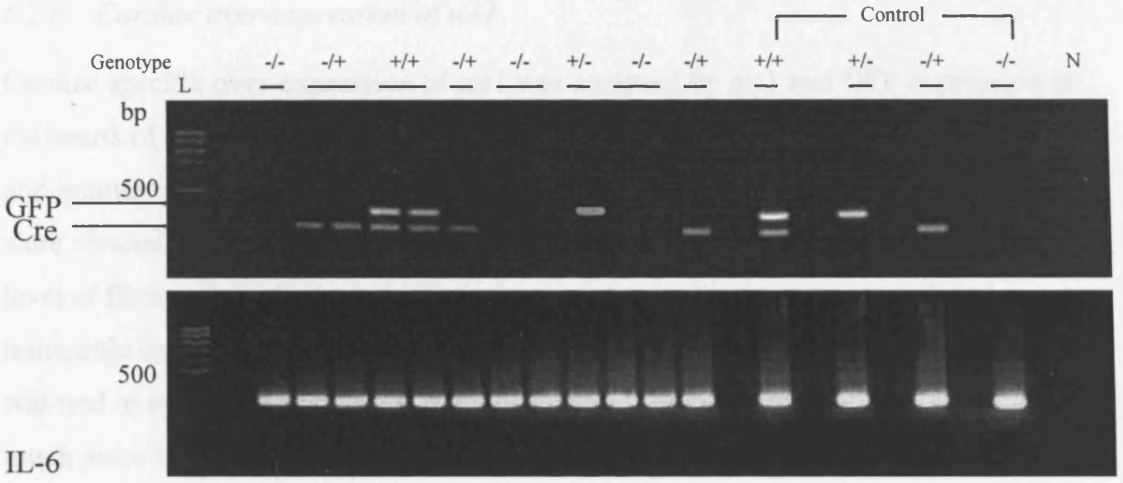

Figure 6.16. Identification of double transgenic mice carrying the ms1 transgene and Cre locus by PCR analysis.

Founders were genotyped to identify double transgenic mice carrying the ms1 transgene and Cre locus (+/+), ms1 transgenic mice (+/-), MLC2v Cre mice (-/+) and wild type mice (-/-) by PCR using GFP and Cre primers. IL-2 was used as an internal control. N refers to the no template control, L refers to the 100 bp DNA ladder and the band sizes (bp) are given.

Line	Animal ID (ms1 transgenic)	Litter	No. Born	+/+	+/-	-/+	-/-	
AK1	19.38	1	9	6	2	0	1	
			9	**6**	**2**	**0**	**1**	**Total**
	19.41	1	9	7	2	0	0	
			9	**7**	**2**	**0**	**0**	**Total**
AK2	32.34	1	8	4	3	0	1	
			8	**4**	**3**	**0**	**1**	**Total**
	32.41	1	5	3	2	0	0	
		2	12	2	1	4	5	
			17	**5**	**3**	**4**	**5**	**Total**
AK3	37.41	1	5	4	0	1	0	
		2	4	0	3	0	1	
			9	**4**	**3**	**1**	**1**	**Total**
	37.46	1	7	3	4	0	0	
			7	**3**	**4**	**0**	**0**	**Total**

Table 6.5. The total number of double transgenics (+/+), ms1 transgenics (+/-), MLC2v Cre mice (-/+) and wild type mice (-/-) identified by genotyping the total number born for each line.

6.2.8 Cardiac over-expression of ms1

Cardiac specific over-expression of ms1 was analysed by ms1 and GFP expression in the hearts of double transgenic mice from all three lines by semi-quantitative RT-PCR and immunostaining. The hearts from double transgenics and ms1 transgenic controls were viewed for green fluorescence and there was green fluorescence present but the level of fluorescence looked similar in hearts from double transgenics and ms1 transgenic controls. Also it was hard to distinguish if the green fluorescence observed was real or not. Therefore, GFP immunostaining was performed as this technique is much more sensitive. As shown in figure 6.17, ms1 mRNA over-expression was not observed in the hearts of approximately 8 week old double transgenic mice from all three lines. ms1 transcript levels in the hearts of double transgenic mice from all three lines were similar in expression levels when compared to levels in the hearts from a littermate ms1 transgenic or wild type control. There was also no GFP mRNA in the hearts of double transgenics.

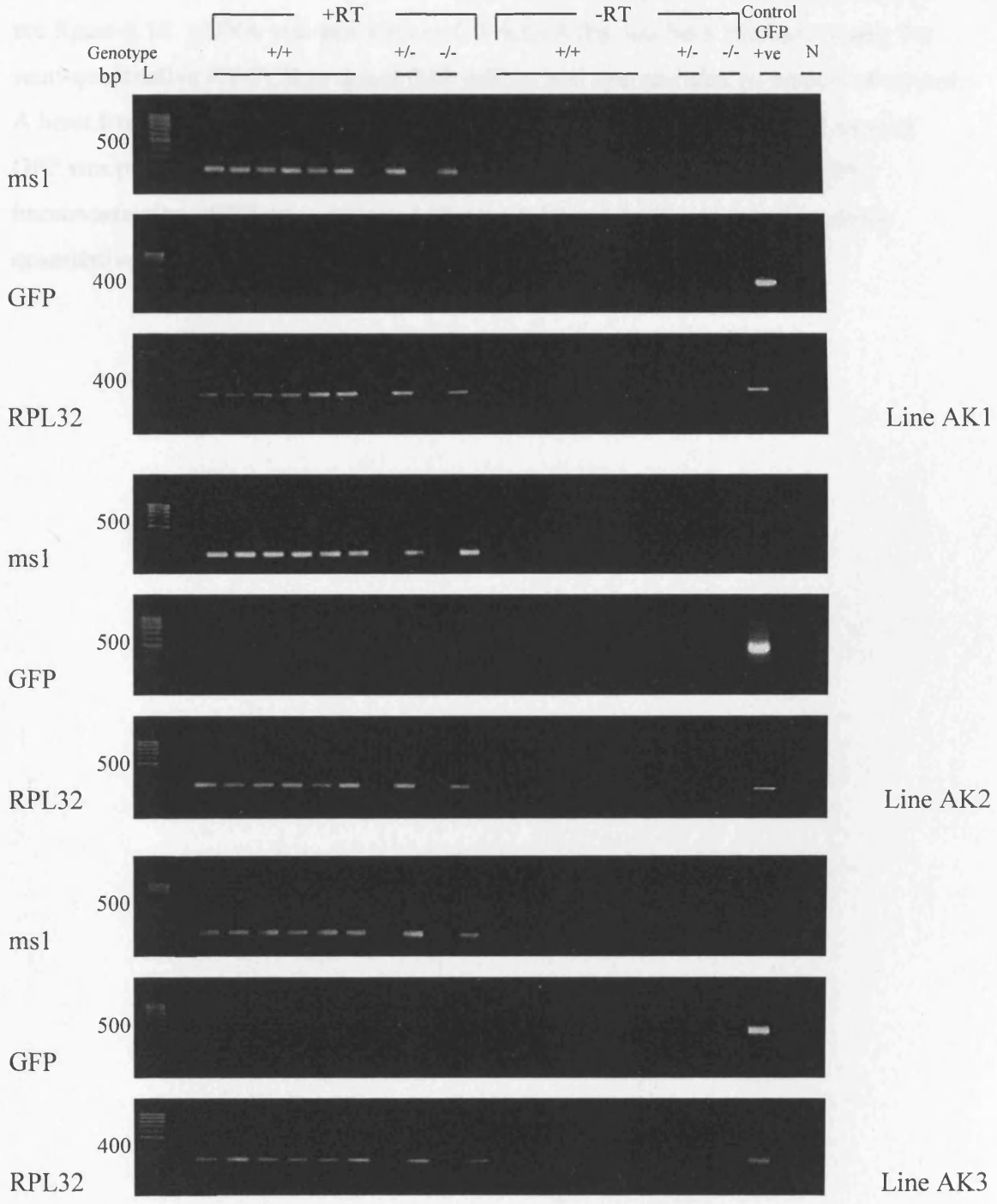

Figure 6.17. ms1/GFP expression in the hearts from three transgenic lines.

Semi-quantitative RT-PCR analysis of ms1 and GFP mRNA expression in the hearts of approximately 8 week old double transgenic mice (+/+), n = 6 compared to a littermate ms1 transgenic (+/-), n=1 and a littermate wild type control (-/-), n=1 from each line. RPL32 was used as an internal control for inaccuracies in initial RNA levels. N refers to the no template control, L refers to the 100 bp DNA ladder and the band sizes (bp) are given. + RT indicates that the RT enzyme was included during cDNA synthesis and –RT indicates that the RT enzyme was omitted.

The same finding was also observed using immunostaining to detect GFP expression, see figure 6.18. cDNA was provided by C Prichard that has been used previously for semi-quantitative RT-PCR to detect GFP mRNA and was included as a positive control. A heart from a mouse known to carry the pi Z/EG vector and Cre locus and express GFP was provided by L Shenje and was included as a positive control for GFP immunostaining. GFP was expressed (figures 6.17 and 6.18) and therefore semi-quantitative RT-PCR and immunostaining was performed accurately.

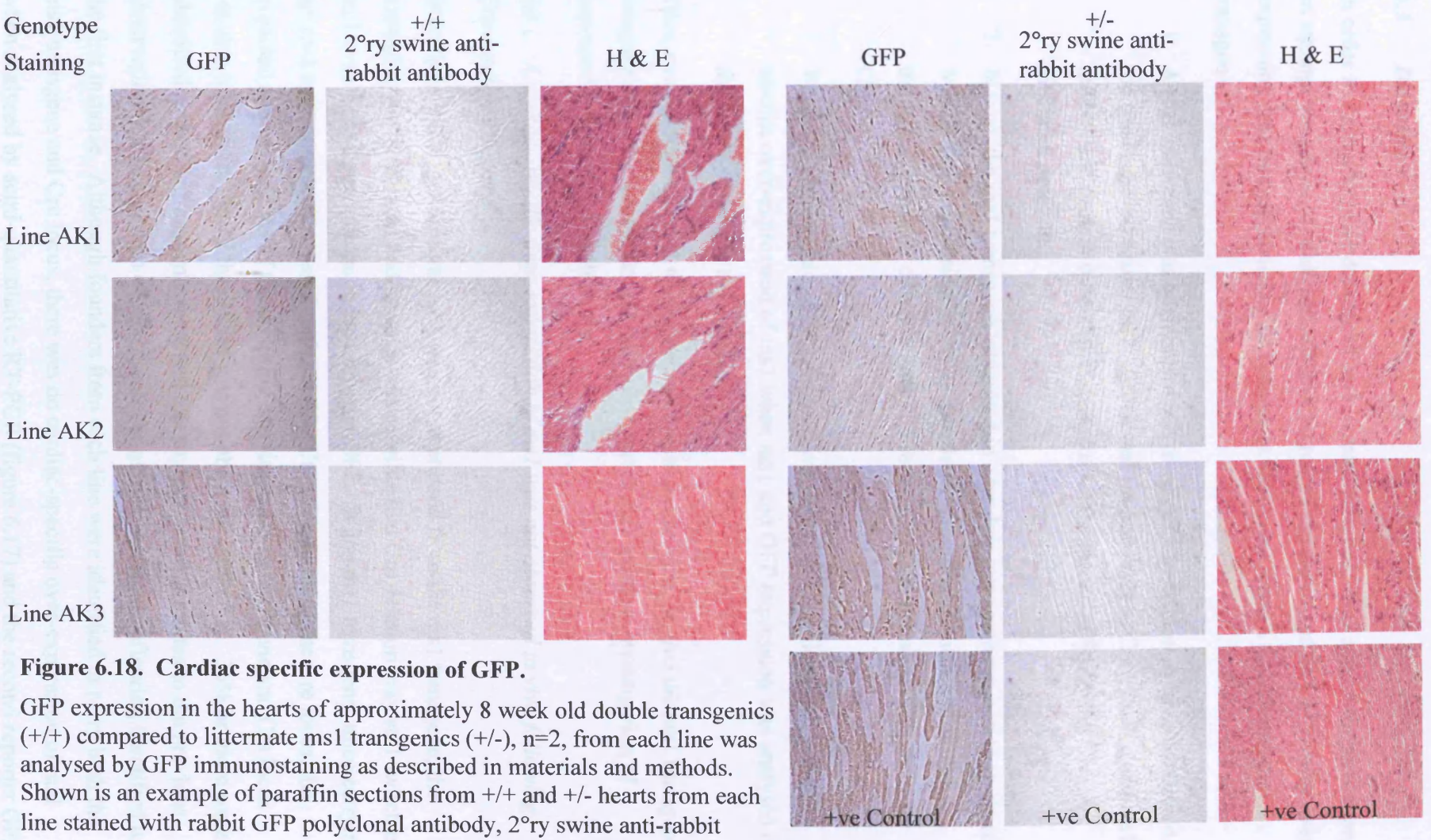

Figure 6.18. Cardiac specific expression of GFP.

GFP expression in the hearts of approximately 8 week old double transgenics (+/+) compared to littermate ms1 transgenics (+/-), n=2, from each line was analysed by GFP immunostaining as described in materials and methods. Shown is an example of paraffin sections from +/+ and +/- hearts from each line stained with rabbit GFP polyclonal antibody, 2°ry swine anti-rabbit antibody only or Haematoxylin and Eosin (H & E). Magnification 40×.

6.3 Discussion

In order to further explore the role of msl in cardiac hypertrophy and cardioprotection, an attempt was made to study the effect of increased expression of msl *in vivo* by over-expressing msl in a cardiac-specific manner in the mouse using a conditional msl transgene.

1. A msl transgene was constructed and transient transfection *in vitro* confirmed the transgene expressed lacZ mRNA and protein prior to Cre excision and msl mRNA and protein over-expression plus GFP expression following Cre-mediated deletion.
2. *In vivo*, the msl transgene integrated in a tandem arrangement; however, there was no lacZ expression in embryonic development or in the adult of msl transgenics prior to crossing with Cre recombinase expressing mice (MLC2v Cre).
3. When msl transgenic mice were bred with MLC2v Cre mice there was no cardiac over-expression of msl when msl and GFP expression was analysed in the hearts of double transgenics.

Thus, even though the msl transgene was functional *in vitro*, *in vivo* the msl transgene integrated into the mouse but did not over-express msl to allow investigation of increased levels of msl in the heart.

6.3.1 Cardiac-specific over-expression of msl was not observed in vivo following Cre-mediated excision

Even though the first reporter lacZ was not expressed from the msl transgene, the transgene was integrated and hence it was possible that Cre deletion may still switch on msl over-expression and the second reporter GFP. When msl transgenic mice carrying the msl transgene were crossed with MLC2v Cre mice carrying the Cre locus, the expected amount of 25% of the offspring carrying the msl transgene and Cre locus (double transgenics) in all three lines was not observed (table 6.5). 36% or more were identified as double transgenic mice and this finding possibly relates to the previous observation of a higher than expected number of msl transgenic offspring identified in the first instance. Although founders from each line were identified to carry both the msl transgene and Cre locus, there was no cardiac-specific over-expression of msl when analysed by semi-quantitative RT-PCR (figure 6.17) and the second reporter GFP

was not expressed either when analysed by both semi-quantitative RT-PCR (figure 6.17) and immunostaining (figure 6.18).

It appears that although mice from all three lines carried the ms1 transgene, when they were crossed with MLC2v Cre mice that expressed Cre recombinase, ms1 was not over-expressed in the heart suggesting that Cre-mediated deletion did not switch on ms1 over-expression or the second reporter GFP probably because the ms1 transgene was not expressed in the first instance prior to Cre excision. The physiological and pathophysiological consequences of increased ms1 expression *in vivo* were therefore not investigated.

The finding that the ms1 transgene was integrated but was not expressed is difficult to interpret. It is not known how common this is as it has not been reported in the literature. It is possible that there was a structural problem with the transgene as there was no expression of the ms1 transgene in all three lines. However, the transgene was expressed *in vitro* and therefore this was an unlikely explanation.

Expression of a transgene can be affected by position effects (Hammes and Schedl, 2000). Position effects can reduce or abolish transgene expression and one way this can occur is due to insertion of the transgene into a transcriptionally inactive region of the genome (Hammes and Schedl, 2000). Therefore, it is feasible that there was no ms1 transgene expression because the construct inserted into an inactive region. In addition, multiple copies within a concatameric array can inactivate transgene expression (Garrick *et al.*, 1998). Although poorly understood, it is believed to occur due to repeat-induced gene silencing where the repeat structure alters chromatin structure with the possibility that local heterochromatin formation may be responsible (Garrick *et al.*, 1998; Henikoff, 1998).

Southern blot analysis showed that in all three lines the transgene was found to possibly integrate in a tandem arrangement. However, there was no additional band present on the blot indicative of the end fragment of the transgene array (figures 6.8 and 6.9). It was possible that the end fragment was not observed because if it was a single copy it would appear as a very faint band that may be difficult to detect in comparison to the very intense approximate 10.5 kb and 5.4 kb bands. Another possibility was that the end fragment was too large in size to transfer efficiently to the Southern membrane.

The most likely explanation was that the transgene integration was defective and hence the end fragment was not readily observed.

Fluorescence in situ hybridization (FISH) can be used to identify sites of transgene integration (Hammes and Schedl, 2000). FISH is mainly used on metaphase chromosomes, because at this stage integration sites on the chromosome are more easily determined. Gene (and transgene) expression occurs mainly during interphase and FISH can also be used to visualise transgenes and their transcripts during interphase from tissues (Santos *et al.*, 2006). Due to time constraints transgene detection by FISH was not performed.

Recently a second attempt was made to make a transgenic mouse over-expressing ms1 using the same Cre/*loxP* system. This again was unsuccessful despite successful integration of the transgene.

Another approach to create transgenic mice is by transfection of the transgene into Embryonic Stem (ES) cells. The ES cells can be screened for lacZ expression by X-gal staining and those that express lacZ can then be analysed by Southern blotting to determine transgene integration. Those that have successfully integrated the transgene can undergo Cre deletion to monitor GFP expression. Candidate clones are injected back into a host blastocyst and re-implanted in a pseudopregnant mouse. This procedure is currently being performed as an alternative strategy to generate ms1 transgenic mice.

At the time of discovering that the transgenic mice did not over-express ms1, Kuwahara *et al.* (2007) generated transgenic mice using the α-MHC promoter to over-express STARS in the heart. Increased expression of STARS in the heart did not cause hypertrophy or any histological abnormalities of the heart. However, when STARS transgenic mice were subjected to pressure overload there was an exaggerated deterioration in cardiac function. This was also observed when STARS transgenic mice were crossed with calcineurin transgenic mice known to display hypertrophy. Kuwahara *et al.* (2007) suggest that increased expression of STARS in response to hypertrophic stimuli facilitates the transition to cardiac dysfunction implicating STARS in the transition from cardiac hypertrophy to heart failure. Kuwahara *et al.* (2007) also discovered that STARS is a cardiac-specific and stress-inducible target of MEF2 and activator of SRF target genes, suggesting that STARS modulates adverse cardiac

remodelling by functioning as a key mediator of MEF2 signalling and SRF activity. The implications of these findings along with findings from chapters 4 and 5 will be discussed in more detail in chapter 7.

Chapter 7

General Discussion

The novel gene ms1 is rapidly up-regulated following pressure-induced LVH and during ischaemia-reperfusion, suggesting that ms1 may be involved in the development of hypertrophy and provide cardioprotection. The function of ms1 in cardiac physiology and disease, in particular whether ms1 leads to hypertrophy and has a cardioprotective role was investigated by examining the effects of ms1 over-expression *in vitro* and *in vivo*.

The main findings to emerge were as follows:

1. ms1 over-expression colocalised with actin in H9c2 cells.
2. Transient over-expression of ms1 in H9c2 cells altered gene expression of known hypertrophic and cardioprotective markers that are MRTF-SRF target genes.
3. Transient over-expression of ms1 increases the size of H9c2 cells and protects H9c2 cells from apoptotic cell death.

These findings suggest that ms1 may mediate a hypertrophic response and provide cardioprotection via a MRTF-SRF signalling mechanism where ms1 binds to actin, promotes actin polymerisation causing MRTF translocation to the nucleus resulting in activation of SRF dependent transcription of hypertrophic and cardioprotective genes.

7.1 Other evidence to support a role for ms1 in cardiac physiology and disease via a MRTF-SRF pathway

During this investigation our group investigated the effects of adding SRF mRNA with knockdown of ms1 in the zebrafish in collaboration with S Shaw (Cardiovascular Research Center, Massachusetts General Hospital, USA). Knockdown of ms1 in the zebrafish caused decreased cardiac contractility, an enlarged atrium and curvature and shortening of the longitudinal axis (figure 7.1). Injection of SRF mRNA remarkably reversed these cardiac abnormalities (unpublished results). SRF itself and many of the SRF target genes are involved in cardiac development, structure and function and ms1 via the MRTF-SRF pathway may regulate SRF target genes (chapter 4) that maintain cardiac function. It is therefore feasible that knockdown of ms1 caused a loss of SRF activity via MRTFs resulting in a loss of cardiac function. The addition of SRF

possibly restored SRF activity and transcription of muscle-specific genes to rescue the cardiac abnormalities. These findings support the concept of ms1 involved in a MRTF-SRF signalling pathway to regulate expression of genes that are important in cardiac physiology and disease.

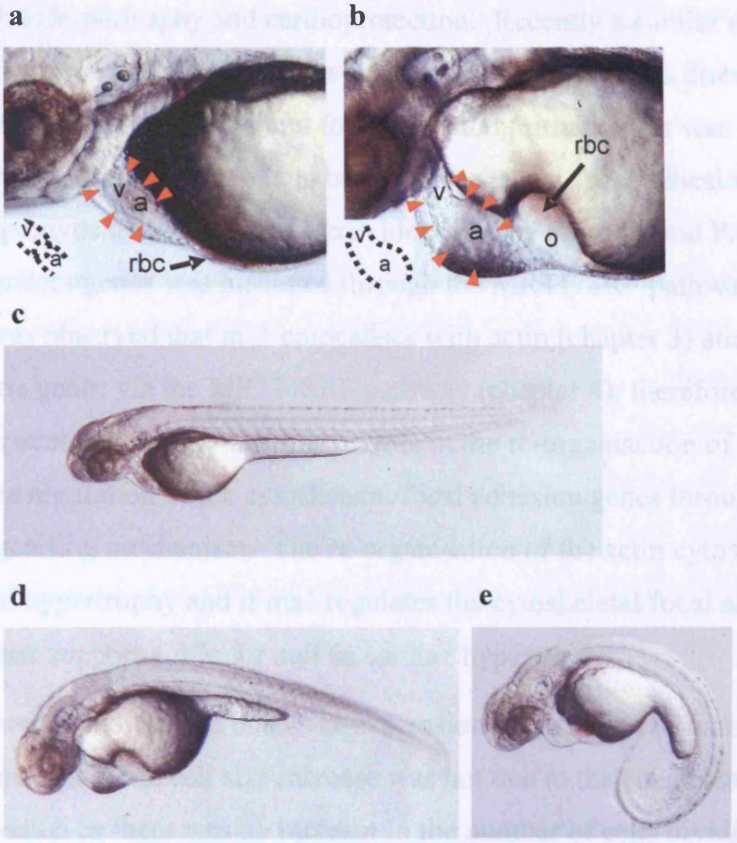

Figure 7.1. Developmental phenotype of morpholino-induced knockdown of ms1. Lateral views of 56 hpf embryos. (**a**) Embryo injected with control morpholino (with 5 mismatches). The cardiac silhouette is demarcated by arrowheads. The heart tube is looped so that the ventricle (v) and atrium (a) are closely apposed (inset). Circulating red blood cells (rbc) are visible in a thin rim along the inferior aspect of the yolk and within the heart. (**b**) Embryo injected with ms1 morpholino. The heart tube is unlooped so that the ventricle (v) and atrium (a) are co-linear, with atrial dilation (inset). There is significant oedema (o) in the pericardium and over the yolk, with stasis of red blood cells (rbc) over the yolk. (**c**) Lateral view of entire 56 hpf embryo following injection of control, mismatch morpholino. (**d**) and (**e**) 56 hpf embryos showing representative phenotypes of ms1 morpholino injection.

In addition, Kuwahara *et al.* (2005) showed that knockdown of ms1 reduced SRF activity and it was demonstrated that cardiac-specific deletion of SRF in the embryonic heart results in cardiac defects (Miano *et al.*, 2004) and deletion of SRF from the adult heart caused dilated cardiomyopathy (Parlakian *et al.*, 2005). Therefore, loss of

function of both msl and SRF are detrimental to cardiac function probably because msl and SRF work together (msl-MRTF-SRF pathway).

In chapter 4 it was investigated whether msl over-expression altered a subset of known MRTF-dependent genes involved in hypertrophy and cell survival to strengthen a role for msl in cardiac hypertrophy and cardioprotection. Recently a similar approach was undertaken by Morita *et al.* (2007) who were interested to discover a direct role for the MRTF-SRF pathway in stress fiber and focal adhesion formation. It was discovered that the transcriptional regulation of a subset of cytoskeletal/focal adhesion genes caldesmon, tropomyosin, vinculin and zyxin identified by Selvaraj and Prywes (2004) as MRTF-dependent genes was mediated through the MRTF/SRF pathway (Morita *et al.*, 2007). It was observed that msl colocalises with actin (chapter 3) and possibly regulates cardiac genes via the MRTF/SRF pathway (chapter 4); therefore, it is interesting to speculate that msl may play a role in the re-organisation of the actin cytoskeleton via regulation of the cytoskeletal/focal adhesion genes through a MRTF/SRF signalling mechanism. The re-organisation of the actin cytoskeleton is a characteristic of hypertrophy and if msl regulates the cytoskeletal/focal adhesion genes this would further support a role for msl in cardiac hypertrophy.

In chapter 5 it was demonstrated that over-expression of msl *in vitro* increases cell size and inhibits apoptosis. The cell size increase was not due to the cells increasing in size prior to cell division as there was no increase in the number of cells dividing following msl over-expression. The results imply that msl may regulate hypertrophic rather than general cellular growth. The finding that msl altered MRTF/SRF target genes involved in hypertrophy (chapter 4) strengthens a role for msl in hypertrophy via a MRTF-SRF signalling pathway. The involvement of msl in cardiac hypertrophy requires confirmation *in vivo*. The findings *in vitro* were achieved from a transient response of msl over-expression and the increase in levels of msl following pressure overload and ischaemia-reperfusion were transient. Hence, the increase in msl following pressure induced LVH and ischaemia-reperfusion could be a stress response and thus it is possible that in response to stress, msl is up-regulated, binds to actin and promotes actin polymerisation causing nuclear import of MRTFs and stimulation of SRF dependent gene transcription to mediate the hypertrophic response and provide cardioprotection as a compensatory response.

At the same time these observations were made, Kuwahara *et al.* (2007) discovered similar findings. STARS expression was up-regulated in mouse models of cardiac hypertrophy as initially observed by Mahadeva *et al.* (2002). STARS expression was also up-regulated in failing human hearts. The STARS promoter was found to be responsive to hypertrophic stress induced by crossing transgenic mice carrying the STARS promoter with calcineurin transgenic mice that display cardiac hypertrophy and induced by hypertrophic agonists in cardiomyocytes (Kuwahara *et al.*, 2007). In addition, the STARS promoter was found to contain an essential MEF2-binding site and MEF2C was observed to control cardiac-specific and stress-inducible expression of STARS. The fetal cardiac genes BNP and cardiac α-actin were up-regulated following msl over-expression *in vitro* (chapter 4) and Kuwahara *et al.* (2007) also showed that these fetal cardiac genes that are known SRF target genes were up-regulated following STARS over-expression *in vivo* by generating transgenic mice. However, increased expression of STARS in the heart did not cause cardiac hypertrophy and when STARS transgenic mice were subjected to pressure overload or crossed with calcineurin transgenic mice, there was an exaggerated deterioration in cardiac function. Thus, it appears that msl is up-regulated in response to stress and sustained increase in msl results in the transition to heart failure (Kuwahara *et al.*, 2007).

These observations along with findings from this work suggest that in response to stress stimuli, msl is up-regulated via MEF2 and msl binds to actin and sequesters actin monomers, thereby allowing MRTFs to translocate to the nucleus and activate SRF-dependent gene expression to mediate hypertrophy and provide cardioprotection initially as a compensatory response. Sustained increase in msl may result in an alteration of SRF target genes causing cardiac deterioration.

7.2 Future work

This study is the first to demonstrate that msl mediates hypertrophy and has an anti-apoptotic function and these novel findings require confirmation by the use of additional assays. Cell size and expression of known hypertrophic genes were used as a marker of hypertrophy. Hypertrophy is also characterised by an increase in protein synthesis and a re-organisation of the sarcomere, which could be examined following msl over-expression. In addition to analysing altered gene expression of known anti-apoptotic markers, the apoptotic assay employed was the use of a fluorescent dye to assess apoptosis on the basis of DNA fragmentation. Additional DNA fragmentation

assays include nucleosomal laddering of DNA fragments (Enari *et al.*, 1998; Gottlieb *et al.*, 1994; Wyllie, 1980) and the Terminal deoxynucleotidyl Transferase Biotin-dUTP Nick End Labelling (TUNEL) assay (Gavrieli *et al.*, 1992). Other assays to measure apoptosis could be performed such as those to assess poly(ADP-ribose) polymerase (PARP) cleavage (Lazebnik *et al.*, 1994), caspase activation (Bonavita *et al.*, 2003) and cytochrome c release (Green and Leeuwenburgh, 2002; Liu *et al.*, 1996; Reed, 1997). Morphological changes could be examined by the use of nuclear staining with the fluorescent dye bisbenzimide (Hoechst 33258) (Belloc *et al.*, 1994) or the use of M30 cytodeath antibody to look for nuclear cytokeratin cleavage (Caulin *et al.*, 1997; Leers *et al.*, 1999; Schutte *et al.*, 2004).

msl's hypertrophic and protective effects were demonstrated by over-expressing a c-Myc-msl fusion protein *in vitro*, another strategy to verify msl's role in hypertrophy and msl's anti-apoptotic function would be to inhibit expression of msl using RNA intereference (small interfering RNA (siRNA) of msl) *in vitro*, where knockdown of msl may not cause hypertrophy but cause apoptosis. The ability of msl to provide cardioprotection is currently being investigated *in vivo* by generating a transgenic mouse over-expressing msl specifically in the heart using an ES cell approach as discussed in chapter 6. This would also allow confirmation as to whether msl is involved in the development of cardiac hypertrophy.

To verify that msl regulates the hypertrophic and cardioprotective genes observed to increase following msl over-expression via the MRTF-SRF pathway, additional transfections to over-express msl with over-expression of MRTFs and SRF could be performed to examine if the same genes were up-regulated. Knockdown experiments using msl with and without knockdown of MRTFs/SRF could also be investigated to see if expression levels of hypertrophic and cardioprotective genes were reduced and hence indicate their regulation by msl via MRTF-SRF. To reveal the transcriptional regulation of hypertrophic and cardioprotective genes via msl-MRTF-SRF, luciferase reporter assays using the promoters of the genes involved in hypertrophic and cell survival pathways could be performed. Many of these genes have CArG boxes in their promoter regions (table 4.1 of chapter 4). Luciferase reporters containing the CArG boxes could be generated and co-transfected with the msl expression vector with and without MRTFs and SRF expression constructs to examine whether msl via MRTF-

SRF enhances promoter activities. In addition, the SRF binding sites may be mutated to see if promoter activities were abolished.

Once it is confirmed that msl is involved in the regulation of hypertrophic and anti-apoptotic genes, these genes could be over-expressed with msl to determine which genes with msl cause hypertrophy and which provide protection against apoptotic cell death. This would provide an important novel insight in to the downstream pathways of msl and allow a more detailed hypertrophic and cell survival signalling pathway to emerge.

7.3 Concluding remarks

At the outset of this work the aims were to identify target genes and downstream pathways of msl by over-expressing msl and to examine the biological consequences of msl over-expression. Taken together, the findings presented suggest that msl induces a hypertrophic response and provides cardioprotection via a MRTF-SRF signalling pathway. It is important to note that many of the identified downstream target genes of msl implicated in hypertrophy and cardioprotection are also implicated in other important roles such as cardiac, skeletal and smooth muscle cell differentiation (SRF, GATA 4, MEF2C, myocardin and ARC) and cardiac development (SRF, GATA 4, MEF2C and myocardin). A role for msl in differentiation is supported by its developmental up-regulation (Mahadeva *et al.*, 2002) and msl was shown to have an important role in cardiac development (Mahadeva *et al.*, 2007). Thus, msl plays an important widespread role in cardiac development, differentiation, cardiac hypertrophy and cardioprotection and this may involve the MRTF-SRF signalling pathway.

Collectively, these findings may lead to further studies to explore the beneficial effects of the msl-MRTF-SRF pathway in cardiac development and function and as a therapeutic target for the treatment of cardiovascular disease.

References

Adiseshaiah,P., Peddakama,S., Zhang,Q., Kalvakolanu,D.V., Reddy,S.P. (2005) Mitogen regulated induction of FRA-1 proto-oncogene is controlled by the transcription factors binding to both serum and TPA response elements. *Oncogene* **24,** 4193-4205.

Agah,R., Frenkel,P.A., French,B.A., Michael,L.H., Overbeek,P.A., Schneider,M.D. (1997) Gene recombination in postmitotic cells. Targeted expression of Cre recombinase provokes cardiac-restricted, site-specific rearrangement in adult ventricular muscle in vivo. *J.Clin.Invest* **100,** 169-179.

Ancey,C., Corbi,P., Froger,J., Delwail,A., Wijdenes,J., Gascan,H., Potreau,D., Lecron,J.C. (2002) Secretion of IL-6, IL-11 and LIF by human cardiomyocytes in primary culture. *Cytokine* **18,** 199-205.

Andersson,M.B., Ketterman,A.J., Bogoyevitch,M.A. (1998) Differential regulation of parallel mitogen-activated protein kinases in cardiac myocytes revealed by phosphatase inhibition. *Biochem.Biophys.Res.Commun.* **251,** 328-333.

Antos,C.L., McKinsey,T.A., Frey,N., Kutschke,W., McAnally,J., Shelton,J.M., Richardson,J.A., Hill,J.A., Olson,E.N. (2002) Activated glycogen synthase-3 beta suppresses cardiac hypertrophy in vivo. *Proc.Natl.Acad.Sci.U.S.A* **99,** 907-912.

Arai,A., Spencer,J.A., Olson,E.N. (2002) STARS, a striated muscle activator of Rho signaling and serum response factor-dependent transcription. *J.Biol.Chem.* **277,** 24453-24459.

Arceci,R.J., King,A.A., Simon,M.C., Orkin,S.H., Wilson,D.B. (1993) Mouse GATA-4: a retinoic acid-inducible GATA-binding transcription factor expressed in endodermally derived tissues and heart. *Mol.Cell Biol.* **13,** 2235-2246.

Arends,M.J., Wyllie,A.H. (1991) Apoptosis: mechanisms and roles in pathology. *Int.Rev.Exp.Pathol.* **32,** 223-254.

Autelitano,D.J., Ridings,R., Tang,F. (2001) Adrenomedullin is a regulated modulator of neonatal cardiomyocyte hypertrophy in vitro. *Cardiovasc.Res.* **51,** 255-264.

Baines,C.P., Molkentin,J.D. (2005) STRESS signaling pathways that modulate cardiac myocyte apoptosis. *J.Mol.Cell Cardiol.* **38,** 47-62.

Barrientos,T., Frank,D., Kuwahara,K., Bezprozvannaya,S., Pipes,G.C., Bassel-Duby,R., Richardson,J.A., Katus,H.A., Olson,E.N., Frey,N. (2007) Two novel members of the ABLIM protein family, ABLIM-2 and -3, associate with STARS and directly bind F-actin. *J.Biol.Chem* **282,** 8393-8403.

Belaguli,N.S., Schildmeyer,L.A., Schwartz,R.J. (1997) Organization and myogenic restricted expression of the murine serum response factor gene. A role for autoregulation. *J.Biol.Chem* **272,** 18222-18231.

Belaguli,N.S., Sepulveda,J.L., Nigam,V., Charron,F., Nemer,M., Schwartz,R.J. (2000) Cardiac tissue enriched factors serum response factor and GATA-4 are mutual coregulators. *Mol.Cell Biol.* **20,** 7550-7558.

Belloc,F., Dumain,P., Boisseau,M.R., Jalloustre,C., Reiffers,J., Bernard,P., Lacombe,F. (1994) A flow cytometric method using Hoechst 33342 and propidium iodide for simultaneous cell cycle analysis and apoptosis determination in unfixed cells. *Cytometry* **17,** 59-65.

Bertrand,R., Solary,E., O'Connor,P., Kohn,K.W., Pommier,Y. (1994) Induction of a common pathway of apoptosis by staurosporine. *Exp.Cell Res.* **211,** 314-321.

Bisping,E., Ikeda,S., Kong,S.W., Tarnavski,O., Bodyak,N., McMullen,J.R., Rajagopal,S., Son,J.K., Ma,Q., Springer,Z., Kang,P.M., Izumo,S., Pu,W.T. (2006) Gata4 is required for maintenance of postnatal cardiac function and protection from pressure overload-induced heart failure. *Proc.Natl.Acad.Sci.U.S.A* **103,** 14471-14476.

Black,B.L., Olson,E.N. (1998) Transcriptional control of muscle development by myocyte enhancer factor-2 (MEF2) proteins. *Annu.Rev.Cell Dev.Biol.* **14,** 167-196.

Black,E.J., Walker,M., Clark,W., MacLaren,A., Gillespie,D.A. (2002) Cell transformation by v-Jun deactivates ERK MAP kinase signalling. *Oncogene* **21,** 6540-6548.

Bogoyevitch,M.A., Gillespie-Brown,J., Ketterman,A.J., Fuller,S.J., Ben Levy,R., Ashworth,A., Marshall,C.J., Sugden,P.H. (1996) Stimulation of the stress-activated mitogen-activated protein kinase subfamilies in perfused heart. p38/RK mitogen-activated protein kinases and c-Jun N-terminal kinases are activated by ischemia/reperfusion. *Circ.Res.* **79,** 162-173.

Bollag,D.M., Rozycki,M.D., Edelstein,S.J. (1996) Gel Electrophoresis Under Denaturing Conditions. In: *Protein Methods*, pp. 107-125. Wiley-Liss, Inc.

Bonavita,F., Stefanelli,C., Giordano,E., Columbaro,M., Facchini,A., Bonafe,F., Caldarera,C.M., Guarnieri,C. (2003) H9c2 cardiac myoblasts undergo apoptosis in a model of ischemia consisting of serum deprivation and hypoxia: inhibition by PMA. *FEBS Lett.* **536,** 85-91.

Brand,T., Sharma,H.S., Fleischmann,K.E., Duncker,D.J., McFalls,E.O., Verdouw,P.D., Schaper,W. (1992) Proto-oncogene expression in porcine myocardium subjected to ischemia and reperfusion. *Circ.Res.* **71,** 1351-1360.

Braylan,R.C., Diamond,L.W., Powell,M.L., Harty-Golder,B. (1980) Percentage of cells in the S phase of the cell cycle in human lymphoma determined by flow cytometry. *Cytometry* **1,** 171-174.

Brostrom,M.A., Reilly,B.A., Wilson,F.J., Brostrom,C.O. (2000) Vasopressin-induced hypertrophy in H9c2 heart-derived myocytes. *Int.J.Biochem.Cell Biol.* **32,** 993-1006.

Brown,M., Wittwer,C. (2000) Flow cytometry: principles and clinical applications in hematology. *Clin.Chem* **46,** 1221-1229.

Bueno,O.F., De Windt,L.J., Lim,H.W., Tymitz,K.M., Witt,S.A., Kimball,T.R., Molkentin,J.D. (2001) The dual-specificity phosphatase MKP-1 limits the cardiac hypertrophic response in vitro and in vivo. *Circ.Res.* **88,** 88-96.

Bueno,O.F., Lips,D.J., Kaiser,R.A., Wilkins,B.J., Dai,Y.S., Glascock,B.J., Klevitsky,R., Hewett,T.E., Kimball,T.R., Aronow,B.J., Doevendans,P.A., Molkentin,J.D. (2004) Calcineurin Abeta gene targeting predisposes the myocardium to acute ischemia-induced apoptosis and dysfunction. *Circ.Res.* **94,** 91-99.

Bueno,O.F., Molkentin,J.D. (2002) Involvement of extracellular signal-regulated kinases 1/2 in cardiac hypertrophy and cell death. *Circ.Res.* **91,** 776-781.

Burgering,B.M., Coffer,P.J. (1995) Protein kinase B (c-Akt) in phosphatidylinositol-3-OH kinase signal transduction. *Nature* **376,** 599-602.

Casey,T.M., Arthur,P.G., Bogoyevitch,M.A. (2005) Proteomic analysis reveals different protein changes during endothelin-1- or leukemic inhibitory factor-induced hypertrophy of cardiomyocytes in vitro. *Mol.Cell Proteomics.* **4,** 651-661.

Caulin,C., Salvesen,G.S., Oshima,R.G. (1997) Caspase cleavage of keratin 18 and reorganization of intermediate filaments during epithelial cell apoptosis. *J.Cell Biol.* **138,** 1379-1394.

Cen,B., Selvaraj,A., Burgess,R.C., Hitzler,J.K., Ma,Z., Morris,S.W., Prywes,R. (2003) Megakaryoblastic leukemia 1, a potent transcriptional coactivator for serum response factor (SRF), is required for serum induction of SRF target genes. *Mol.Cell Biol.* **23,** 6597-6608.

Cen,B., Selvaraj,A., Prywes,R. (2004) Myocardin/MKL family of SRF coactivators: key regulators of immediate early and muscle specific gene expression. *J.Cell Biochem.* **93(1),** 74-82.

Charron,F., Tsimiklis,G., Arcand,M., Robitaille,L., Liang,Q., Molkentin,J.D., Meloche,S., Nemer,M. (2001) Tissue-specific GATA factors are transcriptional effectors of the small GTPase RhoA. *Genes Dev.* **15,** 2702-2719.

Chen,J., Kubalak,S.W., Chien,K.R. (1998a) Ventricular muscle-restricted targeting of the RXRalpha gene reveals a non-cell-autonomous requirement in cardiac chamber morphogenesis. *Development* **125,** 1943-1949.

Chen,J., Kubalak,S.W., Minamisawa,S., Price,R.L., Becker,K.D., Hickey,R., Ross,J., Jr., Chien,K.R. (1998b) Selective requirement of myosin light chain 2v in embryonic heart function. *J.Biol.Chem.* **273,** 1252-1256.

Chen,Q.M., Tu,V.C., Wu,Y., Bahl,J.J. (2000) Hydrogen peroxide dose dependent induction of cell death or hypertrophy in cardiomyocytes. *Arch.Biochem.Biophys.* **373,** 242-248.

Chien,K.R., Knowlton,K.U., Zhu,H., Chien,S. (1991) Regulation of cardiac gene expression during myocardial growth and hypertrophy: molecular studies of an adaptive physiologic response. *FASEB J.* **5,** 3037-3046.

Chien,K.R., Olson,E.N. (2002) Converging pathways and principles in heart development and disease: CV@CSH. *Cell* **110,** 153-162.

Chong,A.J., Pohlman,T.H., Hampton,C.R., Shimamoto,A., Mackman,N., Verrier,E.D. (2003) Tissue factor and thrombin mediate myocardial ischemia-reperfusion injury. *Ann.Thorac.Surg.* **75,** S649-S655.

Clerk,A., Cole,S.M., Cullingford,T.E., Harrison,J.G., Jormakka,M., Valks,D.M. (2003) Regulation of cardiac myocyte cell death. *Pharmacol Ther.* **97(3),** 223-261.

Clerk,A., Sugden,P.H. (2000) Small guanine nucleotide-binding proteins and myocardial hypertrophy. *Circ.Res.* **86,** 1019-1023.

de Lange,F.J., Moorman,A.F., Christoffels,V.M. (2003) Atrial cardiomyocyte-specific expression of Cre recombinase driven by an Nppa gene fragment. *Genesis.* **37,** 1-4.

De Windt,L.J., Lim,H.W., Bueno,O.F., Liang,Q., Delling,U., Braz,J.C., Glascock,B.J., Kimball,T.F., del Monte,F., Hajjar,R.J., Molkentin,J.D. (2001) Targeted inhibition of calcineurin attenuates cardiac hypertrophy in vivo. *Proc.Natl.Acad.Sci.U.S.A* **98,** 3322-3327.

De Windt,L.J., Lim,H.W., Taigen,T., Wencker,D., Condorelli,G., Dorn,G.W., Kitsis,R.N., Molkentin,J.D. (2000) Calcineurin-mediated hypertrophy protects cardiomyocytes from apoptosis in vitro and in vivo: An apoptosis-independent model of dilated heart failure. *Circ.Res.* **86,** 255-263.

Dean,P.N., Dolbeare,F., Gratzner,H., Rice,G.C., Gray,J.W. (1984) Cell-cycle analysis using a monoclonal antibody to BrdUrd. *Cell Tissue Kinet.* **17,** 427-436.

Ding,B., Price,R.L., Borg,T.K., Weinberg,E.O., Halloran,P.F., Lorell,B.H. (1999) Pressure overload induces severe hypertrophy in mice treated with cyclosporine, an inhibitor of calcineurin. *Circ.Res.* **84,** 729-734.

Doetschman,T.C., Eistetter,H., Katz,M., Schmidt,W., Kemler,R. (1985) The in vitro development of blastocyst-derived embryonic stem cell lines: formation of visceral yolk sac, blood islands and myocardium. *J.Embryol.Exp.Morphol.* **87,** 27-45.

Dolbeare,F., Gratzner,H., Pallavicini,M.G., Gray,J.W. (1983) Flow cytometric measurement of total DNA content and incorporated bromodeoxyuridine. *Proc.Natl.Acad.Sci.U.S.A* **80,** 5573-5577.

Donath,S., Li,P., Willenbockel,C., Al Saadi,N., Gross,V., Willnow,T., Bader,M., Martin,U., Bauersachs,J., Wollert,K.C., Dietz,R., von Harsdorf,R. (2006) Apoptosis repressor with caspase recruitment domain is required for cardioprotection in response to biomechanical and ischemic stress. *Circulation* **113,** 1203-1212.

Draetta,G., Beach,D. (1988) Activation of cdc2 protein kinase during mitosis in human cells: cell cycle-dependent phosphorylation and subunit rearrangement. *Cell* **54,** 17-26.

Draetta,G., Piwnica-Worms,H., Morrison,D., Druker,B., Roberts,T., Beach,D. (1988) Human cdc2 protein kinase is a major cell-cycle regulated tyrosine kinase substrate. *Nature* **336,** 738-744.

Du,K.L., Ip,H.S., Li,J., Chen,M., Dandre,F., Yu,W., Lu,M.M., Owens,G.K., Parmacek,M.S. (2003) Myocardin is a critical serum response factor cofactor in the transcriptional program regulating smooth muscle cell differentiation. *Mol.Cell Biol.* **23,** 2425-2437.

Edwards,M.K., Harris,J.F., McBurney,M.W. (1983) Induced muscle differentiation in an embryonal carcinoma cell line. *Mol.Cell Biol.* **3,** 2280-2286.

Ekhterae,D., Lin,Z., Lundberg,M.S., Crow,M.T., Brosius,F.C., III, Nunez,G. (1999) ARC inhibits cytochrome c release from mitochondria and protects against hypoxia-induced apoptosis in heart-derived H9c2 cells. *Circ.Res.* **85,** e70-e77.

Ekhterae,D., Platoshyn,O., Zhang,S., Remillard,C.V., Yuan,J.X. (2003) Apoptosis repressor with caspase domain inhibits cardiomyocyte apoptosis by reducing K+ currents. *Am.J.Physiol Cell Physiol* **284,** C1405-C1410.

Enari,M., Sakahira,H., Yokoyama,H., Okawa,K., Iwamatsu,A., Nagata,S. (1998) A caspase-activated DNase that degrades DNA during apoptosis, and its inhibitor ICAD. *Nature* **391,** 43-50.

Erlich,J.H., Boyle,E.M., Labriola,J., Kovacich,J.C., Santucci,R.A., Fearns,C., Morgan,E.N., Yun,W., Luther,T., Kojikawa,O., Martin,T.R., Pohlman,T.H., Verrier,E.D., Mackman,N. (2000) Inhibition of the tissue factor-thrombin pathway limits infarct size after myocardial ischemia-reperfusion injury by reducing inflammation. *Am.J.Pathol.* **157,** 1849-1862.

Eto,Y., Yonekura,K., Sonoda,M., Arai,N., Sata,M., Sugiura,S., Takenaka,K., Gualberto,A., Hixon,M.L., Wagner,M.W., Aoyagi,T. (2000) Calcineurin is activated in rat hearts with physiological left ventricular hypertrophy induced by voluntary exercise training. *Circulation* **101,** 2134-2137.

Falciani,M., Gori,A.M., Fedi,S., Chiarugi,L., Simonetti,I., Dabizzi,R.P., Prisco,D., Pepe,G., Abbate,R., Gensini,G.F., Neri Serneri,G.G. (1998) Elevated tissue factor and tissue factor pathway inhibitor circulating levels in ischaemic heart disease patients. *Thromb.Haemost.* **79,** 495-499.

Finn,S.G., Plonk,S.G., Fuller,S.J. (1999) G alpha 13 stimulates gene expression and increases cell size in cultured neonatal rat ventricular myocytes. *Cardiovasc.Res.* **42,** 140-148.

Fischer,T.A., Ludwig,S., Flory,E., Gambaryan,S., Singh,K., Finn,P., Pfeffer,M.A., Kelly,R.A., Pfeffer,J.M. (2001) Activation of cardiac c-Jun NH(2)-terminal kinases and p38-mitogen-activated protein kinases with abrupt changes in hemodynamic load. *Hypertension* **37,** 1222-1228.

Franke,T.F., Yang,S.I., Chan,T.O., Datta,K., Kazlauskas,A., Morrison,D.K., Kaplan,D.R., Tsichlis,P.N. (1995) The protein kinase encoded by the Akt proto-oncogene is a target of the PDGF-activated phosphatidylinositol 3-kinase. *Cell* **81,** 727-736.

Fredj,S., Bescond,J., Louault,C., Delwail,A., Lecron,J.C., Potreau,D. (2005) Role of interleukin-6 in cardiomyocyte/cardiac fibroblast interactions during myocyte hypertrophy and fibroblast proliferation. *J.Cell Physiol* **204,** 428-436.

Frey,N., Katus,H.A., Olson,E.N., Hill,J.A. (2004) Hypertrophy of the heart: a new therapeutic target? *Circulation* **109,** 1580-1589.

Frey,N., Olson,E.N. (2003) Cardiac hypertrophy: the good, the bad, and the ugly. *Annu.Rev.Physiol* **65,** 45-79.

Garrick,D., Fiering,S., Martin,D.I., Whitelaw,E. (1998) Repeat-induced gene silencing in mammals. *Nat.Genet.* **18,** 56-59.

Gauthier-Rouviere,C., Vandromme,M., Tuil,D., Lautredou,N., Morris,M., Soulez,M., Kahn,A., Fernandez,A., Lamb,N. (1996) Expression and activity of serum response factor is required for expression of the muscle-determining factor MyoD in both dividing and differentiating mouse C2C12 myoblasts. *Mol.Biol.Cell* **7,** 719-729.

Gavrieli,Y., Sherman,Y., Ben Sasson,S.A. (1992) Identification of programmed cell death in situ via specific labeling of nuclear DNA fragmentation. *J.Cell Biol.* **119,** 493-501.

Gerdes,J., Lemke,H., Baisch,H., Wacker,H.H., Schwab,U., Stein,H. (1984) Cell cycle analysis of a cell proliferation-associated human nuclear antigen defined by the monoclonal antibody Ki-67. *J.Immunol.* **133,** 1710-1715.

Gerdes,J., Schwab,U., Lemke,H., Stein,H. (1983) Production of a mouse monoclonal antibody reactive with a human nuclear antigen associated with cell proliferation. *Int.J.Cancer* **31,** 13-20.

Gillespie-Brown,J., Fuller,S.J., Bogoyevitch,M.A., Cowley,S., Sugden,P.H. (1995) The mitogen-activated protein kinase kinase MEK1 stimulates a pattern of gene expression typical of the hypertrophic phenotype in rat ventricular cardiomyocytes. *J.Biol.Chem* **270,** 28092-28096.

Golino,P., Ragni,M., Cirillo,P., Avvedimento,V.E., Feliciello,A., Esposito,N., Scognamiglio,A., Trimarco,B., Iaccarino,G., Condorelli,M., Chiariello,M., Ambrosio,G. (1996) Effects of tissue factor induced by oxygen free radicals on coronary flow during reperfusion. *Nat.Med.* **2,** 35-40.

Gottlieb,R.A., Burleson,K.O., Kloner,R.A., Babior,B.M., Engler,R.L. (1994) Reperfusion injury induces apoptosis in rabbit cardiomyocytes. *J.Clin.Invest* **94,** 1621-1628.

Gratzner,H.G. (1982) Monoclonal antibody to 5-bromo- and 5-iododeoxyuridine: A new reagent for detection of DNA replication. *Science* **218,** 474-475.

Green,P.S., Leeuwenburgh,C. (2002) Mitochondrial dysfunction is an early indicator of doxorubicin-induced apoptosis. *Biochim.Biophys.Acta* **1588,** 94-101.

Guo,C., Yang,W., Lobe,C.G. (2002) A Cre recombinase transgene with mosaic, widespread tamoxifen-inducible action. *Genesis.* **32,** 8-18.

Gupta,M.K., Neelakantan,T.V., Sanghamitra,M., Tyagi,R.K., Dinda,A., Maulik,S., Mukhopadhyay,C.K., Goswami,S.K. (2006) An assessment of the role of reactive oxygen species and redox signaling in norepinephrine-induced apoptosis and hypertrophy of H9c2 cardiac myoblasts. *Antioxid.Redox.Signal.* **8,** 1081-1093.

Gustafsson,A.B., Tsai,J.G., Logue,S.E., Crow,M.T., Gottlieb,R.A. (2004) Apoptosis repressor with caspase recruitment domain protects against cell death by interfering with Bax activation. *J.Biol.Chem.* **279(20),** 21233-8.

Gustafsson,A.B., Sayen,M.R., Williams,S.D., Crow,M.T., Gottlieb,R.A. (2002) TAT protein transduction into isolated perfused hearts: TAT-apoptosis repressor with caspase recruitment domain is cardioprotective. *Circulation* **106,** 735-739.

Hall,P.A., Levison,D.A. (1990) Review: assessment of cell proliferation in histological material. *J.Clin.Pathol.* **43,** 184-192.

Hamilton,D.L., Abremski,K. (1984) Site-specific recombination by the bacteriophage P1 lox-Cre system. Cre-mediated synapsis of two lox sites. *J.Mol.Biol.* **178,** 481-486.

Hammes,A., Schedl,A. (2000) Generation of transgenic mice from plasmids, BACs and YACs. In: Jackson IJ, Abbot CM (eds) *Mouse Genetics and Transgenics. A practical approach*, pp. 217-245. Oxford University Press.

Han,H., Long,H., Wang,H., Wang,J., Zhang,Y., Wang,Z. (2004) Progressive apoptotic cell death triggered by transient oxidative insult in H9c2 rat ventricular cells: a novel pattern of apoptosis and the mechanisms. *Am.J.Physiol Heart Circ.Physiol* **286,** H2169-H2182.

Hardt,S.E., Sadoshima,J. (2004) Negative regulators of cardiac hypertrophy. *Cardiovasc Res.* **63(3),** 500-509.

Heikinheimo,M., Scandrett,J.M., Wilson,D.B. (1994) Localization of transcription factor GATA-4 to regions of the mouse embryo involved in cardiac development. *Dev.Biol.* **164,** 361-373.

Henikoff,S. (1998) Conspiracy of silence among repeated transgenes. *Bioessays* **20,** 532-535.

Hill,C.S., Wynne,J., Treisman,R. (1995) The Rho family GTPases RhoA, Rac1, and CDC42Hs regulate transcriptional activation by SRF. *Cell* **81,** 1159-1170.

Hiraoka,E., Kawashima,S., Takahashi,T., Rikitake,Y., Hirase,T., Yokoyama,M. (2003) PI 3-kinase-Akt-p70 S6 kinase in hypertrophic responses to leukemia inhibitory factor in cardiac myocytes. *Kobe J.Med.Sci.* **49,** 25-37.

Hirota,H., Yoshida,K., Kishimoto,T., Taga,T. (1995) Continuous activation of gp130, a signal-transducing receptor component for interleukin 6-related cytokines, causes myocardial hypertrophy in mice. *Proc.Natl.Acad.Sci.U.S.A* **92,** 4862-4866.

Hoshijima,M., Chien,K.R. (2002) Mixed signals in heart failure: cancer rules. *J.Clin.Invest* **109,** 849-855.

Hoshijima,M., Sah,V.P., Wang,Y., Chien,K.R., Brown,J.H. (1998) The low molecular weight GTPase Rho regulates myofibril formation and organization in neonatal rat ventricular myocytes. Involvement of Rho kinase. *J.Biol.Chem.* **273,** 7725-7730.

Hou,Q., Hsu,Y.T. (2005) Bax translocates from cytosol to mitochondria in cardiac cells during apoptosis: development of a GFP-Bax-stable H9c2 cell line for apoptosis analysis. *Am.J.Physiol Heart Circ.Physiol* **289,** H477-H487.

Howard,A., Pelc,SR. (1951) Nuclear incorporation of 32P as demonstrated by autoradiographs. *Exp.Cell Res.* **2,** 178-187.

Howard,A., Pelc,SR. (1953) Synthesis of desoxyribonucleic acid in normal and irradiated cells and its relation to chromosome breakage. *Heredity* 173-261.

Huang,C.Y., Kuo,W.W., Chueh,P.J., Tseng,C.T., Chou,M.Y., Yang,J.J. (2004) Transforming growth factor-beta induces the expression of ANF and hypertrophic growth in cultured cardiomyoblast cells through ZAK. *Biochem.Biophys.Res.Commun.* **324,** 424-431.

Hunter,A.L., Zhang,J., Chen,S.C., Si,X., Wong,B., Ekhterae,D., Luo,H., Granville,D.J. (2007) Apoptosis repressor with caspase recruitment domain (ARC) inhibits myogenic differentiation. *FEBS Lett.* **581,** 879-884.

Hunter,J.J., Chien,K.R. (1999) Signaling pathways for cardiac hypertrophy and failure. *N.Engl.J.Med.* **341,** 1276-1283.

Hunter,J.J., Tanaka,N., Rockman,H.A., Ross,J., Jr., Chien,K.R. (1995) Ventricular expression of a MLC-2v-ras fusion gene induces cardiac hypertrophy and selective diastolic dysfunction in transgenic mice. *J.Biol.Chem* **270,** 23173-23178.

Hwang,G.S., Oh,K.S., Koo,H.N., Seo,H.W., You,K.H., Lee,B.H. (2006) Effects of KR-31378, a novel ATP-sensitive potassium channel activator, on hypertrophy of H9c2 cells and on cardiac dysfunction in rats with congestive heart failure. *Eur.J.Pharmacol.* **540,** 131-138.

Ishiyama,Y., Kitamura,K., Kato,J., Sakata,J., Kangawa,K., Eto,T. (1997) Changes in cardiac adrenomedullin concentration in renovascular hypertensive rats. *Hypertens.Res.* **20,** 113-117.

Jacobsen,M.D., Weil,M., Raff,M.C. (1996) Role of Ced-3/ICE-family proteases in staurosporine-induced programmed cell death. *J.Cell Biol.* **133,** 1041-1051.

Jacobson,M.D., Burne,J.F., Raff,M.C. (1994) Programmed cell death and Bcl-2 protection in the absence of a nucleus. *EMBO J.* **13,** 1899-1910.

Janknecht,R., Ernst,W.H., Pingoud,V., Nordheim,A. (1993) Activation of ternary complex factor Elk-1 by MAP kinases. *EMBO J.* **12,** 5097-5104.

Jougasaki,M., Rodeheffer,R.J., Redfield,M.M., Yamamoto,K., Wei,C.M., McKinley,L.J., Burnett,J.C., Jr. (1996) Cardiac secretion of adrenomedullin in human heart failure. *J.Clin.Invest* **97,** 2370-2376.

Jougasaki,M., Wei,C.M., McKinley,L.J., Burnett,J.C., Jr. (1995) Elevation of circulating and ventricular adrenomedullin in human congestive heart failure. *Circulation* **92,** 286-289.

Kageyama,K., Ihara,Y., Goto,S., Urata,Y., Toda,G., Yano,K., Kondo,T. (2002) Overexpression of calreticulin modulates protein kinase B/Akt signaling to promote apoptosis during cardiac differentiation of cardiomyoblast H9c2 cells. *J.Biol.Chem* **277,** 19255-19264.

Kaiser,M., Kahr,O., Shimada,Y., Smith,P., Kelly,M., Mahadeva,H., Adams,M., Lodwick,D., Aalkjaer,C., Avkiran,M., Samani,N.J. (1998) Differential regulation of ventricular adrenomedullin and atrial natriuretic peptide gene expression in pressure and volume overload in the rat. *Clin.Sci.(Lond)* **94,** 359-365.

Kakita,T., Hasegawa,K., Iwai-Kanai,E., Adachi,S., Morimoto,T., Wada,H., Kawamura,T., Yanazume,T., Sasayama,S. (2001) Calcineurin pathway is required for endothelin-1-mediated protection against oxidant stress-induced apoptosis in cardiac myocytes. *Circ.Res.* **88,** 1239-1246.

Kelly,R.G., Buckingham,M.E. (2002) The anterior heart-forming field: voyage to the arterial pole of the heart. *Trends Genet.* **18,** 210-216.

Kerr,J.F., Wyllie,A.H., Currie,A.R. (1972) Apoptosis: a basic biological phenomenon with wide-ranging implications in tissue kinetics. *Br.J.Cancer* **26,** 239-257.

Kimes,B.W., Brandt,B.L. (1976) Properties of a clonal muscle cell line from rat heart. *Experimental Cell Research.* **98(2),** 367-81.

Klumpp,S., Krieglstein,J. (2002) Serine/threonine protein phosphatases in apoptosis. *Curr.Opin.Pharmacol.* **2,** 458-462.

Kodama,H., Fukuda,K., Pan,J., Makino,S., Baba,A., Hori,S., Ogawa,S. (1997) Leukemia inhibitory factor, a potent cardiac hypertrophic cytokine, activates the JAK/STAT pathway in rat cardiomyocytes. *Circ.Res.* **81,** 656-663.

Kolodziejczyk,S.M., Wang,L., Balazsi,K., DeRepentigny,Y., Kothary,R., Megeney,L.A. (1999) MEF2 is upregulated during cardiac hypertrophy and is required for normal post-natal growth of the myocardium. *Curr.Biol.* **9,** 1203-1206.

Koseki,T., Inohara,N., Chen,S., Nunez,G. (1998) ARC, an inhibitor of apoptosis expressed in skeletal muscle and heart that interacts selectively with caspases. *Proc.Natl.Acad.Sci.U.S.A* **95,** 5156-5160.

Kunisada,K., Hirota,H., Fujio,Y., Matsui,H., Tani,Y., Yamauchi-Takihara,K., Kishimoto,T. (1996) Activation of JAK-STAT and MAP kinases by leukemia inhibitory factor through gp130 in cardiac myocytes. *Circulation* **94,** 2626-2632.

Kunisada,K., Tone,E., Fujio,Y., Matsui,H., Yamauchi-Takihara,K., Kishimoto,T. (1998) Activation of gp130 transduces hypertrophic signals via STAT3 in cardiac myocytes. *Circulation* **98,** 346-352.

Kuo,C.T., Morrisey,E.E., Anandappa,R., Sigrist,K., Lu,M.M., Parmacek,M.S., Soudais,C., Leiden,J.M. (1997) GATA4 transcription factor is required for ventral morphogenesis and heart tube formation. *Genes Dev.* **11,** 1048-1060.

Kuwahara,K., Barrientos,T., Pipes,G.C., Li,S., Olson,E.N. (2005) Muscle-specific signaling mechanism that links actin dynamics to serum response factor. *Mol Cell Biol.* **25(8),** 3173-81.

Kuwahara,K., Pipes,G.C., McAnally,J., Richardson,J.A., Hill,J.A., Bassel-Duby,R., Olson,E.N. (2007) Modulation of adverse cardiac remodeling by STARS, a mediator of MEF2 signaling and SRF activity. *J.Clin.Invest.* **117,** 1324-1334.

Kvaloy,S., Godal,T., Marton,P.F., Steen,H., Brenhovd,I.O., Abrahamsen,A.F. (1981) Spontaneous (H)-thymidine uptake in histological subgroups of human B-cell lymphomas. *Scand.J.Haematol.* **26,** 221-234.

Kvaloy,S., Marton,P.F., Kaalhus,O., Hoie,J., Foss-Abrahamsen,A., Godal,T. (1985) 3H-thymidine uptake in B cell lymphomas--relationship to treatment response and survival. *Scand.J.Haematol.* **34,** 429-435.

Lakso,M., Sauer,B., Mosinger,B., Jr., Lee,E.J., Manning,R.W., Yu,S.H., Mulder,K.L., Westphal,H. (1992) Targeted oncogene activation by site-specific recombination in transgenic mice. *Proc.Natl.Acad.Sci.U.S.A* **89,** 6232-6236.

Laufs,U., Kilter,H., Konkol,C., Wassmann,S., Bohm,M., Nickenig,G. (2002) Impact of HMG CoA reductase inhibition on small GTPases in the heart. *Cardiovasc.Res.* **53,** 911-920.

Laverriere,A.C., MacNeill,C., Mueller,C., Poelmann,R.E., Burch,J.B., Evans,T. (1994) GATA-4/5/6, a subfamily of three transcription factors transcribed in developing heart and gut. *J.Biol.Chem* **269,** 23177-23184.

Lazebnik,Y.A., Kaufmann,S.H., Desnoyers,S., Poirier,G.G., Earnshaw,W.C. (1994) Cleavage of poly(ADP-ribose) polymerase by a proteinase with properties like ICE. *Nature* **371,** 346-347.

Lee,A.K., Wiley,B., Dugan,J.M., Hamilton,W.H., Loda,M., Heatley,G.J., Cook,L., Silverman,M.L. (1992) Quantitative DNA analysis and proliferation in breast carcinomas. A comparison between image analysis and flow cytometry. *Pathol.Res.Pract.* **188,** 428-432.

Lee,S.D., Chu,C.H., Huang,E.J., Lu,M.C., Liu,J.Y., Liu,C.J., Hsu,H.H., Lin,J.A., Kuo,W.W., Huang,C.Y. (2006) Roles of insulin-like growth factor II in cardiomyoblast apoptosis and in hypertensive rat heart with abdominal aorta ligation. *Am.J.Physiol Endocrinol.Metab* **291,** E306-E314.

Leers,M.P., Kolgen,W., Bjorklund,V., Bergman,T., Tribbick,G., Persson,B., Bjorklund,P., Ramaekers,F.C., Bjorklund,B., Nap,M., Jornvall,H., Schutte,B. (1999) Immunocytochemical detection and mapping of a cytokeratin 18 neo-epitope exposed during early apoptosis. *J.Pathol.* **187,** 567-572.

Levy,D., Murabito,J.M., Anderson,K.M., Christiansen,J.C., Castelli,W.P. (1992) Echocardiographic left ventricular hypertrophy: clinical characteristics. The Framingham Heart Study. *Clin.Exp.Hypertens.A* **14,** 85-97.

Levy,D., Savage,D.D., Garrison,R.J., Anderson,K.M., Kannel,W.B., Castelli,W.P. (1987) Echocardiographic criteria for left ventricular hypertrophy: the Framingham Heart Study. *Am.J.Cardiol.* **59,** 956-960.

Li,P., Nijhawan,D., Budihardjo,I., Srinivasula,S.M., Ahmad,M., Alnemri,E.S., Wang,X. (1997a) Cytochrome c and dATP-dependent formation of Apaf-1/caspase-9 complex initiates an apoptotic protease cascade. *Cell* **91,** 479-489.

Li,S., Wang,D.Z., Wang,Z., Richardson,J.A., Olson,E.N. (2003) The serum response factor coactivator myocardin is required for vascular smooth muscle development. *Proc.Natl.Acad.Sci.U.S.A* **100,** 9366-9370.

Li,Z., Bing,O.H., Long,X., Robinson,K.G., Lakatta,E.G. (1997b) Increased cardiomyocyte apoptosis during the transition to heart failure in the spontaneously hypertensive rat. *Am.J.Physiol* **272,** H2313-H2319.

Liang,Q., De Windt,L.J., Witt,S.A., Kimball,T.R., Markham,B.E., Molkentin,J.D. (2001) The transcription factors GATA4 and GATA6 regulate cardiomyocyte hypertrophy in vitro and in vivo. *J.Biol.Chem* **276,** 30245-30253.

Liang,Q., Molkentin,J.D. (2003) Redefining the roles of p38 and JNK signaling in cardiac hypertrophy: dichotomy between cultured myocytes and animal models. *J.Mol.Cell Cardiol.* **35,** 1385-1394.

Liao,P., Georgakopoulos,D., Kovacs,A., Zheng,M., Lerner,D., Pu,H., Saffitz,J., Chien,K., Xiao,R.P., Kass,D.A., Wang,Y. (2001) The in vivo role of p38 MAP kinases in cardiac remodeling and restrictive cardiomyopathy. *Proc.Natl.Acad.Sci.U.S.A* **98,** 12283-12288.

Lim,H.W., De Windt,L.J., Steinberg,L., Taigen,T., Witt,S.A., Kimball,T.R., Molkentin,J.D. (2000) Calcineurin expression, activation, and function in cardiac pressure-overload hypertrophy. *Circulation* **101,** 2431-2437.

Lin,Q., Schwarz,J., Bucana,C., Olson,E.N. (1997) Control of mouse cardiac morphogenesis and myogenesis by transcription factor MEF2C. *Science* **276,** 1404-1407.

Liu,C.J., Cheng,Y.C., Lee,K.W., Hsu,H.H., Chu,C.H., Tsai,F.J., Tsai,C.H., Chu,C.Y., Liu,J.Y., Kuo,W.W., Huang,C.Y. (2008) Lipopolysaccharide induces cellular hypertrophy through calcineurin/NFAT-3 signaling pathway in H9c2 myocardiac cells. *Mol.Cell Biochem.* **313,** 167-178.

Liu,X., Kim,C.N., Yang,J., Jemmerson,R., Wang,X. (1996) Induction of apoptotic program in cell-free extracts: requirement for dATP and cytochrome c. *Cell* **86,** 147-157.

Livak,K.J., Schmittgen,T.D. (2001) Analysis of relative gene expression data using real-time quantitative PCR and the 2(-Delta Delta C(T)) Method. *Methods* **25,** 402-408.

Lobe,C.G., Koop,K.E., Kreppner,W., Lomeli,H., Gertsenstein,M., Nagy,A. (1999) Z/AP, a double reporter for cre-mediated recombination. *Dev.Biol.* **208,** 281-292.

Lorell,B.H., Carabello,B.A. (2000) Left ventricular hypertrophy: pathogenesis, detection, and prognosis. *Circulation* **102,** 470-479.

Luther,T., Dittert,D.D., Kotzsch,M., Erlich,J., Albrecht,S., Mackman,N., Muller,M. (2000) Functional implications of tissue factor localization to cell-cell contacts in myocardium. *J.Pathol.* **192,** 121-130.

MacGregor,G.R., Mogg,A.E., Burke,J.F., Caskey,C.T. (1987) Histochemical staining of clonal mammalian cell lines expressing E. coli beta galactosidase indicates heterogeneous expression of the bacterial gene. *Somat.Cell Mol.Genet.* **13,** 253-265.

Mahadeva,H., Brooks,G., Lodwick,D., Chong,N.W., Samani,N.J. (2002) ms1, a novel stress-responsive, muscle-specific gene that is up-regulated in the early stages of pressure overload-induced left ventricular hypertrophy. *FEBS Lett.* **521,** 100-104.

Mahadeva,H., Mason,A., Chong,N., Shaw S., Samani,N.J. (2007) Knockdown in zebrafish supports important role for myocyte stress 1 in cardiac development and function. *Heart* **93,** A82.

Mahadeva,H., Starkey,M.P., Sheikh,F.N., Mundy,C.R., Samani,N.J. (1998) A simple and efficient method for the isolation of differentially expressed genes. *J.Mol.Biol.* **284,** 1391-1398.

Makino,S., Fukuda,K., Miyoshi,S., Konishi,F., Kodama,H., Pan,J., Sano,M., Takahashi,T., Hori,S., Abe,H., Hata,J., Umezawa,A., Ogawa,S. (1999) Cardiomyocytes can be generated from marrow stromal cells in vitro. *J.Clin.Invest* **103,** 697-705.

Mann,M., Jensen,O.N. (2003) Proteomic analysis of post-translational modifications. *Nature Biotechnology* **21(3),** 255-261.

Manon,S., Chaudhuri,B., Guerin,M. (1997) Release of cytochrome c and decrease of cytochrome c oxidase in Bax-expressing yeast cells, and prevention of these effects by coexpression of Bcl-xL. *FEBS Lett.* **415,** 29-32.

Mao,Y.W., Liu,J.P., Xiang,H., Li,D.W. (2004) Human alphaA- and alphaB-crystallins bind to Bax and Bcl-X(S) to sequester their translocation during staurosporine-induced apoptosis. *Cell Death.Differ.* **11,** 512-526.

Matsui,H., Fujio,Y., Kunisada,K., Hirota,H., Yamauchi-Takihara,K. (1996) Leukemia inhibitory factor induces a hypertrophic response mediated by gp130 in murine cardiac myocytes. *Res.Commun.Mol.Pathol.Pharmacol.* **93,** 149-162.

Matsushita,K., Iwanaga,S., Oda,T., Kimura,K., Shimada,M., Sano,M., Umezawa,A., Hata,J., Ogawa,S. (2005) Interleukin-6/soluble interleukin-6 receptor complex reduces infarct size via inhibiting myocardial apoptosis. *Lab Invest* **85,** 1210-1223.

Menard,C., Pupier,S., Mornet,D., Kitzmann,M., Nargeot,J., Lory,P. (1999) Modulation of L-type calcium channel expression during retinoic acid-induced differentiation of H9C2 cardiac cells. *J.Biol.Chem* **274,** 29063-29070.

Miano,J.M. (2003) Serum response factor: toggling between disparate programs of gene expression. *J.Mol.Cell Cardiol.* **35,** 577-593.

Miano,J.M., Ramanan,N., Georger,M.A., Mesy Bentley,K.L., Emerson,R.L., Balza,R.O., Jr., Xiao,Q., Weiler,H., Ginty,D.D., Misra,R.P. (2004) Restricted inactivation of serum response factor to the cardiovascular system. *Proc.Natl.Acad.Sci.U.S.A* **101,** 17132-17137.

Minamisawa,S., Gu,Y., Ross,J., Jr., Chien,K.R., Chen,J. (1999) A post-transcriptional compensatory pathway in heterozygous ventricular myosin light chain 2-deficient mice results in lack of gene dosage effect during normal cardiac growth or hypertrophy. *J.Biol.Chem* **274,** 10066-10070.

Minty,A., Kedes,L. (1986) Upstream regions of the human cardiac actin gene that modulate its transcription in muscle cells: presence of an evolutionarily conserved repeated motif. *Mol.Cell Biol.* **6,** 2125-2136.

Miralles,F., Posern,G., Zaromytidou,A.I., Treisman,R. (2003) Actin dynamics control SRF activity by regulation of its coactivator MAL. *Cell* **113,** 329-342.

Miwa,T., Kedes,L. (1987) Duplicated CArG box domains have positive and mutually dependent regulatory roles in expression of the human alpha-cardiac actin gene. *Mol.Cell Biol.* **7,** 2803-2813.

Miyamoto,T., Takeishi,Y., Takahashi,H., Shishido,T., Arimoto,T., Tomoike,H., Kubota,I. (2004) Activation of distinct signal transduction pathways in hypertrophied hearts by pressure and volume overload. *Basic Res Cardiol.* **99(5),** 328-337.

Miyazaki,H., Oka,N., Koga,A., Ohmura,H., Ueda,T., Imaizumi,T. (2006) Comparison of gene expression profiling in pressure and volume overload-induced myocardial hypertrophies in rats. *Hypertens.Res.* **29,** 1029-1045.

Molkentin,J.D. (2000) The zinc finger-containing transcription factors GATA-4, -5, and -6. Ubiquitously expressed regulators of tissue-specific gene expression. *J.Biol.Chem* **275,** 38949-38952.

Molkentin,J.D. (2004) Calcineurin-NFAT signaling regulates the cardiac hypertrophic response in coordination with the MAPKs. *Cardiovasc.Res.* **63,** 467-475.

Molkentin,J.D., Dorn II,G.W. (2001) Cytoplasmic signaling pathways that regulate cardiac hypertrophy. *Annu.Rev.Physiol* **63,** 391-426.

Molkentin,J.D., Lin,Q., Duncan,S.A., Olson,E.N. (1997) Requirement of the transcription factor GATA4 for heart tube formation and ventral morphogenesis. *Genes Dev.* **11,** 1061-1072.

Molkentin,J.D., Lu,J.R., Antos,C.L., Markham,B., Richardson,J., Robbins,J., Grant,S.R., Olson,E.N. (1998) A calcineurin-dependent transcriptional pathway for cardiac hypertrophy. *Cell* **93,** 215-228.

Morimoto,A., Nishikimi,T., Yoshihara,F., Horio,T., Nagaya,N., Matsuo,H., Dohi,K., Kangawa,K. (1999) Ventricular adrenomedullin levels correlate with the extent of cardiac hypertrophy in rats. *Hypertension* **33,** 1146-1152.

Morita,T., Mayanagi,T., Sobue,K. (2007) Reorganization of the actin cytoskeleton via transcriptional regulation of cytoskeletal/focal adhesion genes by myocardin-related transcription factors (MRTFs/MAL/MKLs). *Exp.Cell Res.* **313,** 3432-3445.

Nagy,A. (2000) Cre recombinase: the universal reagent for genome tailoring. *Genesis.* **26,** 99-109.

Narula,J., Haider,N., Virmani,R., DiSalvo,T.G., Kolodgie,F.D., Hajjar,R.J., Schmidt,U., Semigran,M.J., Dec,G.W., Khaw,B.A. (1996) Apoptosis in myocytes in end-stage heart failure. *N.Engl.J.Med.* **335,** 1182-1189.

Nelson,T.J., Balza,R., Jr., Xiao,Q., Misra,R.P. (2005) SRF-dependent gene expression in isolated cardiomyocytes: Regulation of genes involved in cardiac hypertrophy. *J.Mol.Cell Cardiol.* **39,** 479-489.

Neuss,M., Monticone,R., Lundberg,M.S., Chesley,A.T., Fleck,E., Crow,M.T. (2001) The apoptotic regulatory protein ARC (apoptosis repressor with caspase recruitment domain) prevents oxidant stress-mediated cell death by preserving mitochondrial function. *J.Biol.Chem.* **276,** 33915-33922.

Nicoletti,I., Migliorati,G., Pagliacci,M.C., Grignani,F., Riccardi,C. (1991) A rapid and simple method for measuring thymocyte apoptosis by propidium iodide staining and flow cytometry. *Journal of Immunological Methods* **139,** 271-279.

Nishida,K., Yamaguchi,O., Hirotani,S., Hikoso,S., Higuchi,Y., Watanabe,T., Takeda,T., Osuka,S., Morita,T., Kondoh,G., Uno,Y., Kashiwase,K., Taniike,M., Nakai,A., Matsumura,Y., Miyazaki,J., Sudo,T., Hongo,K., Kusakari,Y., Kurihara,S., Chien,K.R., Takeda,J., Hori,M., Otsu,K. (2004) p38alpha mitogen-activated protein kinase plays a critical role in cardiomyocyte survival but not in cardiac hypertrophic growth in response to pressure overload. *Mol.Cell Biol.* **24(24),** 10611-10620.

Nishikimi,T., Horio,T., Sasaki,T., Yoshihara,F., Takishita,S., Miyata,A., Matsuo,H., Kangawa,K. (1997) Cardiac production and secretion of adrenomedullin are increased in heart failure. *Hypertension* **30,** 1369-1375.

Nishikimi,T., Yoshihara,F., Mori,Y., Kangawa,K., Matsuoka,H. (2003) Cardioprotective effect of adrenomedullin in heart failure. *Hypertens.Res.* **26 Suppl,** S121-S127.

Niu,P., Shindo,T., Iwata,H., Iimuro,S., Takeda,N., Zhang,Y., Ebihara,A., Suematsu,Y., Kangawa,K., Hirata,Y., Nagai,R. (2004) Protective effects of endogenous adrenomedullin on cardiac hypertrophy, fibrosis, and renal damage. *Circulation* **109,** 1789-1794.

Novak,A., Guo,C., Yang,W., Nagy,A., Lobe,C.G. (2000) Z/EG, a double reporter mouse line that expresses enhanced green fluorescent protein upon Cre-mediated excision. *Genesis.* **28,** 147-155.

O'Brien,T.X., Lee,K.J., Chien,K.R. (1993) Positional specification of ventricular myosin light chain 2 expression in the primitive murine heart tube. *Proc.Natl.Acad.Sci.U.S.A* **90,** 5157-5161.

Oie,E., Vinge,L.E., Yndestad,A., Sandberg,C., Grogaard,H.K., Attramadal,H. (2000) Induction of a myocardial adrenomedullin signaling system during ischemic heart failure in rats. *Circulation* **101,** 415-422.

Oka,T., Dai,Y.S., Molkentin,J.D. (2005) Regulation of calcineurin through transcriptional induction of the calcineurin A beta promoter in vitro and in vivo. *Mol.Cell Biol.* **25,** 6649-6659.

Oka,T., Maillet,M., Watt,A.J., Schwartz,R.J., Aronow,B.J., Duncan,S.A., Molkentin,J.D. (2006) Cardiac-Specific Deletion of Gata4 Reveals Its Requirement for Hypertrophy, Compensation, and Myocyte Viability. *Circ.Res.* **98(6),** 837-845.

Okumura,H., Nagaya,N., Itoh,T., Okano,I., Hino,J., Mori,K., Tsukamoto,Y., Ishibashi-Ueda,H., Miwa,S., Tambara,K., Toyokuni,S., Yutani,C., Kangawa,K. (2004) Adrenomedullin infusion attenuates myocardial ischemia/reperfusion injury through the phosphatidylinositol 3-kinase/Akt-dependent pathway. *Circulation* **109,** 242-248.

Okumura,H., Nagaya,N., Kangawa,K. (2003) Adrenomedullin infusion during ischemia/reperfusion attenuates left ventricular remodeling and myocardial fibrosis in rats. *Hypertens.Res.* **26 Suppl,** S99-104.

Olson,E.N. (2004) A decade of discoveries in cardiac biology. *Nat.Med.* **10,** 467-474.

Olson,E.N., Schneider,M.D. (2003) Sizing up the heart: development redux in disease. *Genes Dev.* **17,** 1937-1956.

Oltvai,Z.N., Milliman,C.L., Korsmeyer,S.J. (1993) Bcl-2 heterodimerizes in vivo with a conserved homolog, Bax, that accelerates programmed cell death. *Cell* **74,** 609-619.

Orban,P.C., Chui,D., Marth,J.D. (1992) Tissue- and site-specific DNA recombination in transgenic mice. *Proc.Natl.Acad.Sci.U.S.A* **89,** 6861-6865.

Palermo,J., Gulick,J., Colbert,M., Fewell,J., Robbins,J. (1996) Transgenic remodeling of the contractile apparatus in the mammalian heart. *Circ.Res.* **78,** 504-509.

Parker,T.G., Schneider,M.D. (1991) Growth factors, proto-oncogenes, and plasticity of the cardiac phenotype. *Annu.Rev.Physiol* **53,** 179-200.

Parlakian,A., Charvet,C., Escoubet,B., Mericskay,M., Molkentin,J.D., Gary-Bobo,G., De Windt,L.J., Ludosky,M.A., Paulin,D., Daegelen,D., Tuil,D., Li,Z. (2005) Temporally controlled onset of dilated cardiomyopathy through disruption of the SRF gene in adult heart. *Circulation* **112,** 2930-2939.

Pesant,M., Sueur,S., Dutartre,P., Tallandier,M., Grimaldi,P.A., Rochette,L., Connat,J.L. (2006) Peroxisome proliferator-activated receptor delta (PPARdelta) activation protects H9c2 cardiomyoblasts from oxidative stress-induced apoptosis. *Cardiovasc.Res.* **69,** 440-449.

Petrich,B.G., Molkentin,J.D., Wang,Y. (2003) Temporal activation of c-Jun N-terminal kinase in adult transgenic heart via cre-loxP-mediated DNA recombination. *FASEB J.* **17,** 749-751.

Pfaffl,M.W. (2001) A new mathematical model for relative quantification in real-time RT-PCR. *Nucleic Acids Res.* **29,** e45.

Pikkarainen,S., Tokola,H., Kerkela,R., Ruskoaho,H. (2004) GATA transcription factors in the developing and adult heart. *Cardiovasc Res.* **63(2),** 196-207

Pokharel,S., Sharma,U.C., Pinto,Y.M. (2003) Left ventricular hypertrophy: virtuous intentions, malign consequences. *Int.J.Biochem.Cell Biol.* **35,** 802-806.

Raff,M.C. (1992) Social controls on cell survival and cell death. *Nature* **356,** 397-400.

Ramirez,M.T., Sah,V.P., Zhao,X.L., Hunter,J.J., Chien,K.R., Brown,J.H. (1997) The MEKK-JNK pathway is stimulated by alpha1-adrenergic receptor and ras activation and is associated with in vitro and in vivo cardiac hypertrophy. *J.Biol.Chem.* **272,** 14057-14061.

Reed,J.C. (1997) Cytochrome c: can't live with it--can't live without it. *Cell* **91,** 559-562.

Reichek,N., Devereux,R.B. (1981) Left ventricular hypertrophy: relationship of anatomic, echocardiographic and electrocardiographic findings. *Circulation* **63,** 1391-1398.

Ricci,R., Eriksson,U., Oudit,G.Y., Eferl,R., Akhmedov,A., Sumara,I., Sumara,G., Kassiri,Z., David,J.P., Bakiri,L., Sasse,B., Idarraga,M.H., Rath,M., Kurz,D., Theussl,H.C., Perriard,J.C., Backx,P., Penninger,J.M., Wagner,E.F. (2005) Distinct functions of junD in cardiac hypertrophy and heart failure. *Genes Dev.* **19,** 208-213.

Ritter,O., Hack,S., Schuh,K., Rothlein,N., Perrot,A., Osterziel,K.J., Schulte,H.D., Neyses,L. (2002) Calcineurin in human heart hypertrophy. *Circulation* **105(19),** 2265-9.

Rockman,H.A., Ross,R.S., Harris,A.N., Knowlton,K.U., Steinhelper,M.E., Field,L.J., Ross,J., Jr., Chien,K.R. (1991) Segregation of atrial-specific and inducible expression of an atrial natriuretic factor transgene in an in vivo murine model of cardiac hypertrophy. *Proc.Natl.Acad.Sci.U.S.A* **88,** 8277-8281.

Romppanen,H., Marttila,M., Magga,J., Vuolteenaho,O., Kinnunen,P., Szokodi,I., Ruskoaho,H. (1997) Adrenomedullin gene expression in the rat heart is stimulated by acute pressure overload: blunted effect in experimental hypertension. *Endocrinology* **138,** 2636-2639.

Ross,R.S., Navankasattusas,S., Harvey,R.P., Chien,K.R. (1996) An HF-1a/HF-1b/MEF-2 combinatorial element confers cardiac ventricular specificity and established an anterior-posterior gradient of expression. *Development* **122,** 1799-1809.

Rybkin,I.I., Markham,D.W., Yan,Z., Bassel-Duby,R., Williams,R.S., Olson,E.N. (2003) Conditional expression of SV40 T-antigen in mouse cardiomyocytes facilitates an inducible switch from proliferation to differentiation. *J.Biol.Chem.* **278,** 15927-15934.

Ryding,A.D., Sharp,M.G., Mullins,J.J. (2001) Conditional transgenic technologies. *J.Endocrinol.* **171,** 1-14.

Saito,S., Hiroi,Y., Zou,Y., Aikawa,R., Toko,H., Shibasaki,F., Yazaki,Y., Nagai,R., Komuro,I. (2000) beta-Adrenergic pathway induces apoptosis through calcineurin activation in cardiac myocytes. *J.Biol.Chem* **275,** 34528-34533.

Saito,T., Fukuzawa,J., Osaki,J., Sakuragi,H., Yao,N., Haneda,T., Fujino,T., Wakamiya,N., Kikuchi,K., Hasebe,N. (2003) Roles of calcineurin and calcium/calmodulin-dependent protein kinase II in pressure overload-induced cardiac hypertrophy. *J.Mol.Cell Cardiol.* **35,** 1153-1160.

Sambrook,J., Fritsch,E.F., Maniatis,T. (1989) Detection and Analysis of Proteins Expressed from Cloned Genes. In: *Molecular Cloning A Laboratory Manual*, pp. 18.47-18.66. Cold Springer Harbor Laboratory Press.

Sanna,B., Bueno,O.F., Dai,Y.S., Wilkins,B.J., Molkentin,J.D. (2005) Direct and indirect interactions between calcineurin-NFAT and MEK1-extracellular signal-regulated kinase 1/2 signaling pathways regulate cardiac gene expression and cellular growth. *Mol.Cell Biol.* **25,** 865-878.

Sano,M., Fukuda,K., Kodama,H., Pan,J., Saito,M., Matsuzaki,J., Takahashi,T., Makino,S., Kato,T., Ogawa,S. (2000) Interleukin-6 family of cytokines mediate angiotensin II-induced cardiac hypertrophy in rodent cardiomyocytes. *J.Biol.Chem* **275,** 29717-29723.

Santos,A.P., Wegel,E., Allen,G.C., Thompson,W.F., Stoger,E., Shaw,P., Abranches,R. (2006) In situ methods to localize transgenes and transcripts in interphase nuclei: a tool for transgenic plant research. *Plant Methods* **2,** 18.

Saraste,A., Pulkki,K., Kallajoki,M., Henriksen,K., Parvinen,M., Voipio-Pulkki,L.M. (1997) Apoptosis in human acute myocardial infarction. *Circulation* **95,** 320-323.

Sasazuki,T., Sawada,T., Sakon,S., Kitamura,T., Kishi,T., Okazaki,T., Katano,M., Tanaka,M., Watanabe,M., Yagita,H., Okumura,K., Nakano,H. (2002) Identification of a novel transcriptional activator, BSAC, by a functional cloning to inhibit tumor necrosis factor-induced cell death. *J.Biol.Chem* **277,** 28853-60.

Sauer,B., Henderson,N. (1988) Site-specific DNA recombination in mammalian cells by the Cre recombinase of bacteriophage P1. *Proc.Natl.Acad.Sci.U.S.A* **85,** 5166-5170.

Sauer,B., Henderson,N. (1989) Cre-stimulated recombination at loxP-containing DNA sequences placed into the mammalian genome. *Nucleic Acids Res.* **17,** 147-161.

Sauer,B., Henderson,N. (1990) Targeted insertion of exogenous DNA into the eukaryotic genome by the Cre recombinase. *New Biol.* **2,** 441-449.

Schiekofer,S., Shiojima,I., Sato,K., Galasso,G., Oshima,Y., Walsh,K. (2006) Microarray analysis of Akt1 activation in transgenic mouse hearts reveal transcript expression profiles associated with compensatory hypertrophy and failure. *Physiol Genomics.* **27,** 156-170.

Schutte,B., Henfling,M., Kolgen,W., Bouman,M., Meex,S., Leers,M.P., Nap,M., Bjorklund,V., Bjorklund,P., Bjorklund,B., Lane,E.B., Omary,M.B., Jornvall,H., Ramaekers,F.C. (2004) Keratin 8/18 breakdown and reorganization during apoptosis. *Exp.Cell Res.* **297,** 11-26.

Selvaraj,A., Prywes,R. (2004) Expression profiling of serum inducible genes identifies a subset of SRF target genes that are MKL dependent. *BMC Mol Biol.* **5(1),** 13.

Shibata,R., Ouchi,N., Ito,M., Kihara,S., Shiojima,I., Pimentel,D.R., Kumada,M., Sato,K., Schiekofer,S., Ohashi,K., Funahashi,T., Colucci,W.S., Walsh,K. (2004) Adiponectin-mediated modulation of hypertrophic signals in the heart. *Nat.Med.* **10,** 1384-1389.

Shimokubo,T., Sakata,J., Kitamura,K., Kangawa,K., Matsuo,H., Eto,T. (1995) Augmented adrenomedullin concentrations in right ventricle and plasma of experimental pulmonary hypertension. *Life Sci.* **57,** 1771-1779.

Shimokubo,T., Sakata,J., Kitamura,K., Kangawa,K., Matsuo,H., Eto,T. (1996) Adrenomedullin: changes in circulating and cardiac tissue concentration in Dahl salt-sensitive rats on a high-salt diet. *Clin.Exp.Hypertens.* **18,** 949-961.

Shimoyama,M., Hayashi,D., Takimoto,E., Zou,Y., Oka,T., Uozumi,H., Kudoh,S., Shibasaki,F., Yazaki,Y., Nagai,R., Komuro,I. (1999) Calcineurin plays a critical role in pressure overload-induced cardiac hypertrophy. *Circulation* **100,** 2449-2454.

Shioi,T., Kang,P.M., Douglas,P.S., Hampe,J., Yballe,C.M., Lawitts,J., Cantley,L.C., Izumo,S. (2000) The conserved phosphoinositide 3-kinase pathway determines heart size in mice. *EMBO J.* **19,** 2537-2548.

Smart,N., Mojet,M.H., Latchman,D.S., Marber,M.S., Duchen,M.R., Heads,R.J. (2006) IL-6 induces PI 3-kinase and nitric oxide-dependent protection and preserves mitochondrial function in cardiomyocytes. *Cardiovasc.Res.* **69,** 164-177.

Sotiropoulos,A., Gineitis,D., Copeland,J., Treisman,R. (1999) Signal-regulated activation of serum response factor is mediated by changes in actin dynamics. *Cell* **98,** 159-169.

Southern,E.M. (1975) Detection of specific sequences among DNA fragments separated by gel electrophoresis. *J.Mol.Biol.* **98,** 503-517.

Spencer,J.A., Misra,R.P. (1996) Expression of the serum response factor gene is regulated by serum response factor binding sites. *J.Biol.Chem* **271,** 16535-16543.

Spencer,J.A., Misra,R.P. (1999) Expression of the SRF gene occurs through a Ras/Sp/SRF-mediated-mechanism in response to serum growth signals. *Oncogene* **18,** 7319-7327.

Stepczynska,A., Lauber,K., Engels,I.H., Janssen,O., Kabelitz,D., Wesselborg,S., Schulze-Osthoff,K. (2001) Staurosporine and conventional anticancer drugs induce overlapping, yet distinct pathways of apoptosis and caspase activation. *Oncogene* **20,** 1193-1202.

Sugden,P.H. (2003) Ras, Akt, and Mechanotransduction in the Cardiac Myocyte. *Circ Res.* **93(12),** 1179-1192.

Sugden,P.H., Clerk,A. (1998) Cellular mechanisms of cardiac hypertrophy. *J.Mol.Med.* **76,** 725-746.

Sun,Q., Chen,G., Streb,J.W., Long,X., Yang,Y., Stoeckert,C.J., Jr., Miano,J.M. (2006) Defining the mammalian CArGome. *Genome Res.* **16,** 197-207.

Takahashi,A., Hirata,H., Yonehara,S., Imai,Y., Lee,K.K., Moyer,R.W., Turner,P.C., Mesner,P.W., Okazaki,T., Sawai,H., Kishi,S., Yamamoto,K., Okuma,M., Sasada,M. (1997) Affinity labeling displays the stepwise activation of ICE-related proteases by Fas, staurosporine, and CrmA-sensitive caspase-8. *Oncogene* **14,** 2741-2752.

Takahashi,N., Saito,Y., Kuwahara,K., Harada,M., Kishimoto,I., Ogawa,Y., Kawakami,R., Nakagawa,Y., Nakanishi,M., Nakao,K. (2003) Angiotensin II-induced ventricular hypertrophy and extracellular signal-regulated kinase activation are suppressed in mice overexpressing brain natriuretic peptide in circulation. *Hypertens.Res.* **26,** 847-853.

Tanaka,H., Sakurai,K., Takahashi,K., Fujimoto,Y. (2003) Requirement of intracellular free thiols for hydrogen peroxide-induced hypertrophy in cardiomyocytes. *J.Cell Biochem.* **89,** 944-955.

Taniguchi,M., Sanbo,M., Watanabe,S., Naruse,I., Mishina,M., Yagi,T. (1998) Efficient production of Cre-mediated site-directed recombinants through the utilization of the puromycin resistance gene, pac: a transient gene-integration marker for ES cells. *Nucleic Acids Res.* **26,** 679-680.

Teiger,E., Than,V.D., Richard,L., Wisnewsky,C., Tea,B.S., Gaboury,L., Tremblay,J., Schwartz,K., Hamet,P. (1996) Apoptosis in pressure overload-induced heart hypertrophy in the rat. *J.Clin.Invest* **97,** 2891-2897.

Telford,W.G., King,L.E., Fraker,P.J. (1991) Evaluation of glucocorticoid-induced DNA fragmentation in mouse thymocytes by flow cytometry. *Cell Proliferation* **24,** 447-459.

Telford,W.G., King,L.E., Fraker,P.J. (1992) Comparative evaluation of several DNA binding dyes in the detection of apoptosis-associated chromatin degradation by flow cytometry. *Cytometry* **13,** 137-143.

Thompson,C.B. (1995) Apoptosis in the pathogenesis and treatment of disease. *Science* **267,** 1456-1462.

Thorburn,J., Xu,S., Thorburn,A. (1997) MAP kinase- and Rho-dependent signals interact to regulate gene expression but not actin morphology in cardiac muscle cells. *EMBO J.* **16,** 1888-1900.

Timm,M., Kimlinger,T.K., Hanson,C., Witzig,T.E. (1998) Measurement of the cell proliferation rate of bone marrow erythroid precursors by flow cytometry: initial applications to multiple myeloma. *Leuk.Lymphoma* **30,** 353-359.

Tokudome,T., Horio,T., Yoshihara,F., Suga,S., Kawano,Y., Kohno,M., Kangawa,K. (2002) Adrenomedullin inhibits doxorubicin-induced cultured rat cardiac myocyte apoptosis via a cAMP-dependent mechanism. *Endocrinology* **143,** 3515-3521.

Tsujita,Y., Muraski,J., Shiraishi,I., Kato,T., Kajstura,J., Anversa,P., Sussman,M.A. (2006) Nuclear targeting of Akt antagonizes aspects of cardiomyocyte hypertrophy. *Proc.Natl.Acad.Sci.U.S.A* **103,** 11946-11951.

Turner,N.A., Xia,F., Azhar,G., Zhang,X., Liu,L., Wei,J.Y. (1998) Oxidative stress induces DNA fragmentation and caspase activation via the c-Jun NH2-terminal kinase pathway in H9c2 cardiac muscle cells. *J.Mol.Cell Cardiol.* **30,** 1789-1801.

Van Empel,V.P.M., De Windt,L.J. (2004) Myocyte hypertrophy and apoptosis: A balancing act. *Cardiovasc Res.* **63(2),** 487-499.

van Wamel,J.E., Ruwhof,C., van der Valk-Kokshoorn EJ, Schrier,P.I., van der,L.A. (2000) Rapid gene transcription induced by stretch in cardiac myocytes and fibroblasts and their paracrine influence on stationary myocytes and fibroblasts. *Pflugers Arch.* **439,** 781-788.

Verheijen,R., Kuijpers,H.J., Schlingemann,R.O., Boehmer,A.L., van Driel,R., Brakenhoff,G.J., Ramaekers,F.C. (1989a) Ki-67 detects a nuclear matrix-associated proliferation-related antigen. I. Intracellular localization during interphase. *J.Cell Sci.* **92 (Pt 1),** 123-130.

Verheijen,R., Kuijpers,H.J., van Driel,R., Beck,J.L., van Dierendonck,J.H., Brakenhoff,G.J., Ramaekers,F.C. (1989b) Ki-67 detects a nuclear matrix-associated proliferation-related antigen. II. Localization in mitotic cells and association with chromosomes. *J.Cell Sci.* **92 (Pt 4),** 531-540.

Wang,C., Dobrzynski,E., Chao,J., Chao,L. (2001a) Adrenomedullin gene delivery attenuates renal damage and cardiac hypertrophy in Goldblatt hypertensive rats. *Am.J.Physiol Renal Physiol* **280,** F964-F971.

Wang,D., Chang,P.S., Wang,Z., Sutherland,L., Richardson,J.A., Small,E., Krieg,P.A., Olson,E.N. (2001b) Activation of cardiac gene expression by myocardin, a transcriptional cofactor for serum response factor. *Cell* **105,** 851-862.

Wang,D.Z., Li,S., Hockemeyer,D., Sutherland,L., Wang,Z., Schratt,G., Richardson,J.A., Nordheim,A., Olson,E.N. (2002) Potentiation of serum response factor activity by a family of myocardin-related transcription factors. *Proc.Natl.Acad.Sci.U.S.A* **99,** 14855-14860.

Wang,Y., Huang,S., Sah,V.P., Ross,J., Jr., Brown,J.H., Han,J., Chien,K.R. (1998a) Cardiac muscle cell hypertrophy and apoptosis induced by distinct members of the p38 mitogen-activated protein kinase family. *J.Biol.Chem.* **273,** 2161-2168.

Wang,Y., Su,B., Sah,V.P., Brown,J.H., Han,J., Chien,K.R. (1998b) Cardiac hypertrophy induced by mitogen-activated protein kinase kinase 7, a specific activator for c-Jun NH2-terminal kinase in ventricular muscle cells. *J.Biol.Chem.* **273,** 5423-5426.

Wang,Z., Wang,D.Z., Hockemeyer,D., McAnally,J., Nordheim,A., Olson,E.N. (2004) Myocardin and ternary complex factors compete for SRF to control smooth muscle gene expression. *Nature.* **428,** 185-9.

Wang,Z., Wang,D.Z., Pipes,G.C., Olson,E.N. (2003) Myocardin is a master regulator of smooth muscle gene expression. *Proc.Natl.Acad.Sci.U.S.A* **100,** 7129-7134.

Webster,K.A., Discher,D.J., Bishopric,N.H. (1993) Induction and nuclear accumulation of fos and jun proto-oncogenes in hypoxic cardiac myocytes. *J.Biol.Chem* **268,** 16852-16858.

Wyllie,A.H. (1980) Glucocorticoid-induced thymocyte apoptosis is associated with endogenous endonuclease activation. *Nature* **284,** 555-556.

Xin,M., Davis,C.A., Molkentin,J.D., Lien,C.L., Duncan,S.A., Richardson,J.A., Olson,E.N. (2006) A threshold of GATA4 and GATA6 expression is required for cardiovascular development. *Proc.Natl.Acad.Sci.U.S.A* **103,** 11189-11194.

Yanazume,T., Hasegawa,K., Wada,H., Morimoto,T., Abe,M., Kawamura,T., Sasayama,S. (2002) Rho/ROCK pathway contributes to the activation of extracellular signal-regulated kinase/GATA-4 during myocardial cell hypertrophy. *J.Biol.Chem.* **277,** 8618-8625.

Yasukawa,H., Hoshijima,M., Gu,Y., Nakamura,T., Pradervand,S., Hanada,T., Hanakawa,Y., Yoshimura,A., Ross,J., Jr., Chien,K.R. (2001) Suppressor of cytokine signaling-3 is a biomechanical stress-inducible gene that suppresses gp130-mediated cardiac myocyte hypertrophy and survival pathways. *J.Clin.Invest* **108,** 1459-1467.

Yasuoka,C., Ihara,Y., Ikeda,S., Miyahara,Y., Kondo,T., Kohno,S. (2004) Antiapoptotic activity of Akt is down-regulated by Ca2+ in myocardiac H9c2 cells. Evidence of Ca(2+)-dependent regulation of protein phosphatase 2Ac. *J.Biol.Chem* **279,** 51182-51192.

Yin,H., Chao,L., Chao,J. (2004) Adrenomedullin protects against myocardial apoptosis after ischemia/reperfusion through activation of Akt-GSK signaling. *Hypertension* **43,** 109-116.

Yue,T.L., Wang,C., Romanic,A.M., Kikly,K., Keller,P., DeWolf,W.E., Jr., Hart,T.K., Thomas,H.C., Storer,B., Gu,J.L., Wang,X., Feuerstein,G.Z. (1998) Staurosporine-induced apoptosis in cardiomyocytes: A potential role of caspase-3. *J.Mol.Cell Cardiol.* **30,** 495-507.

Zechner,D., Thuerauf,D.J., Hanford,D.S., McDonough,P.M., Glembotski,C.C. (1997) A role for the p38 mitogen-activated protein kinase pathway in myocardial cell growth, sarcomeric organization, and cardiac-specific gene expression. *J.Cell Biol.* **139,** 115-127.

Zhang,C.L., McKinsey,T.A., Chang,S., Antos,C.L., Hill,J.A., Olson,E.N. (2002) Class II histone deacetylases act as signal-responsive repressors of cardiac hypertrophy. *Cell* **110,** 479-488.

Zhang,J.J., Yoshida,H., Chao,L., Chao,J. (2000) Human adrenomedullin gene delivery protects against cardiac hypertrophy, fibrosis, and renal damage in hypertensive dahl salt-sensitive rats. *Hum.Gene Ther.* **11,** 1817-1827.

Zhang,W., Kowal,R.C., Rusnak,F., Sikkink,R.A., Olson,E.N., Victor,R.G. (1999) Failure of calcineurin inhibitors to prevent pressure-overload left ventricular hypertrophy in rats. *Circ.Res.* **84,** 722-728.

Zhang,X., Azhar,G., Chai,J., Sheridan,P., Nagano,K., Brown,T., Yang,J., Khrapko,K., Borras,A.M., Lawitts,J., Misra,R.P., Wei,J.Y. (2001) Cardiomyopathy in transgenic mice with cardiac-specific overexpression of serum response factor. *Am.J.Physiol Heart Circ.Physiol* **280,** H1782-H1792.

Zhang,Y.Q., Herman,B. (2006) ARC protects rat cardiomyocytes against oxidative stress through inhibition of caspase-2 mediated mitochondrial pathway. *J.Cell Biochem.* **99(2),** 575-88.

Zou,Y., Hiroi,Y., Uozumi,H., Takimoto,E., Toko,H., Zhu,W., Kudoh,S., Mizukami,M., Shimoyama,M., Shibasaki,F., Nagai,R., Yazaki,Y., Komuro,I. (2001) Calcineurin plays a critical role in the development of pressure overload-induced cardiac hypertrophy. *Circulation* **104,** 97-101.